Evaluation of Kinetic and Mechanistic Data for Modeling of Photochemical Smog

Roger Atkinson

Statewide Air Pollution Research Center, University of California, Riverside, California 92521

and

Alan C. Lloyd

Environmental Research & Technology, Inc., Newbury Park, California 91320

This review is a critical evaluation of the rate constants, mechanisms, and products of selected atmospheric reactions of hydrocarbons, nitrogen oxides, and sulfur oxides in air. The evaluation considers eight hydrocarbons (*n*-butane, 2,3-dimethylbutane, ethene, propene, 1-butene, *trans*-2-butene, toluene, and *m*-xylene) for which smog chamber irradiations have been carried out under carefully controlled conditions and which have been the subject of computer modeling studies by more than one research group. The reactions involved are treated in the following categories: inorganic reactions in organic-NO_x-air irradiations; organic reactions of the formaldehyde-NO_x-air system; organic reactions of the acetaldehyde-NO_x-air system; organic reactions of the alkene-NO_x-air systems; organic reactions of the alkane-NO_x-air systems; organic reactions of selected carbonyl-NO_x-air systems; organic reactions of the aromatic-NO_x-air systems; combination reactions of peroxy radicals, and homogeneous gas phase SO_2 reactions. This report considers literature through early 1983.

Key words: air pollution; atmospheric chemistry; chemical kinetics; data evaluation; gas phase; photoabsorption cross section; photochemistry; photochemical smog; quantum yield; rate coefficient.

Contents

1. Introduction

It is essentially only in the past decade that intensive investigations into the atmospheric chemistry of polluted urban atmospheres and of the lower troposphere have been carried out. While a vast amount of experimental work has been amassed, the complexity of the polluted troposphere is such that there remain large areas of uncertainty [1] (figures in brackets indicate literature references at the end of this paper).

One of the ultimate goals of air pollution research is to be able to accurately computer model the secondary manifestations of photochemical smog formation, such as ozone (O_3), nitrogen dioxide (NO_2), peroxyacetyl nitrate (PAN), nitric acid (HNO_3) and other products (which may, for instance, be toxic), and hydrocarbon (or organic) depletion in order to formulate more effective control strategies. Indeed, computer models are becoming everyday tools to assess the impact of emissions changes associated with specific point or area sources, or with urban areas or the regional scale. Thus, the reliability and limitations of these urban airshed models must be well understood and the chemical module is one component of these models.

The accuracy of such chemical modules is, however, constrained by the accuracy of the input data, i.e., the rate constants and products of the many hundreds of elementary gas phase reactions which occur in photochemical air pollution systems.

It is evident that, along with laboratory investigations, ambient atmospheric measurements, and computer modeling development, there must also be a continuing effort to critically evaluate the rates, mechanisms, and products of

the relevant chemical reactions and to update these evaluations as new experimental data become available. Such a continuing evaluation for stratospheric reactions has been very successfully carried out mainly through the National Bureau of Standards (e.g., the latest NBS special publication 513 [2]) and, more recently via the National Atmospheric and Space Administration (as exemplified by the most recent 1982 NASA evaluation [3]). However, such evaluations, although dealing very thoroughly with the inorganic reaction systems, generally consider only the relatively few organics of specific interest to stratospheric problems, i.e., typically C_1 or C_2 organics.

CODATA has also recently carried out a critical evaluation [4] of the reactions involved in the troposphere, but again, since the primary emphasis for the evaluation was on the clean troposphere, for the organics this evaluation deals mainly with the reactions stemming from the methane oxidation cycle. The polluted troposphere, however, contains hundreds of different hydrocarbons from C_2 to C_{20} and beyond, including heteroatom (O, S, N, and halogen) substituted organics.

There is thus a critical need for a comprehensive evaluation of the gas phase chemistry associated with the more complex organics encountered in photochemical air pollution systems. However, because of the very large number of organic compounds encountered, it is necessary to limit the number considered and to select those organics which serve as useful surrogates for their chemical classes and which are important constituents of anthropogenic emissions in urban atmospheres.

In this review, the evaluation is confined to eight hydrocarbons (*n*-butane, 2, 3-dimethylbutane, ethene, propene, 1-butene, *trans*-2-butene, toluene and *m*-xylene) for which, under EPA funding, smog chamber irradiations have been carried out under carefully controlled conditions [5] and which have been the subject of computer modeling studies by more than one research group [6–12]. The results of this evaluation are intended to aid modelers in developing chemical mechanisms to describe smog chamber experiments and to ensure that the best available data are used in the modeling study and to limit any tendency to "curve fit" the data. While we consider this report to be as current as possible (the literature through early 1983 has been evaluated), we believe it is very important that the report be updated at regular intervals and expanded to other chemical compounds so that maximum benefit to model development is provided.

In order to most logically discuss the chemistry involved, a systematic classification has been made of the reactions to be evaluated. The reactions evaluated in this report are subdivided into the following sections:

(2) inorganic reactions in organic-NO_x-air irradiations;

(3) organic reactions of the formaldehyde-NO_x-air system,

(4) organic reactions of the acetaldehyde-NO_x-air system,

(5) organic reactions of the alkene-NO_x-air systems,

(6) organic reactions of the alkane-NO_x-air systems,

(7) organic reactions of selected carbonyl-NO_x-air systems,

(8) organic reactions of the aromatic-NO_x-air systems,

(9) combination reactions of peroxy radicals, and

(10) homogeneous gas phase SO_2 reactions.

It should be emphasized that in order to facilitate the acquisition of data for the user and make a large amount of data available in one place, there is, in certain of these sections, a significant amount of overlap with previous evaluations. Thus the inorganic reactions, Sec. 2, have previously been critically evaluated by the NBS [2], NASA [3], and the CODATA [4] reviews, and certain portions of Secs. 3 and 4 dealing with formaldehyde and other C_1 species (e.g., CH_3O and CH_3O_2) have been evaluated by these publications [2–4]. This is especially so for the C_1 species by the NASA and CODATA evaluations [3,4].

It is not the intention of this evaluation to reevaluate this body of work, but since it is of obvious and great utility to the reader to have the data available in one place for all the reactions involved in these NO_x-organic-air photooxidations, these previously evaluated reactions have been included. However, the previous recommendations (especially those of the most recent NASA evaluation [3]) have been used for these reactions unless more recent experimental or theoretical work has superceded them, and, in almost all cases the changes, if any, are minor. For these reactions a brief discussion of the data base behind the NBS, NASA, or CODATA evaluations has generally been given in order to provide relevant information for the reader.

However, the majority of this report deals with reactions which have not been previously covered, but which are critical for model development. In some cases there is much less certainty about the rates and mechanisms of the reactions than for the inorganics or simple organics. However, estimates are needed if the modeling technology is to improve. Thus, in the more complex chemistry dealt with in Secs. 4–8, much use has been made of thermochemical arguments and analogies with other related systems, since in many cases no unambiguous experimental data are available. Hence in such cases only discussions of related chemistry and suggested reaction rates, pathways, and mechanisms can be presented, rather than firm recommendations. These suggested rates and mechanisms should be regularly evaluated and upgraded as new experimental data becomes available. For those rate constants for which recommendations are made, the error limits cited are of necessity subjective. However, these error limits are generally dependent on the number of studies conducted on the particular reaction and the agreement of the results from these studies. Additionally, the error limits may be estimated by analogy with the status of knowledge of similar reactions.

The rate constants used in this evaluation are those of cm molecule s units, these being the most widely used among chemical kineticists. A conversion table is given (Table 1) to facilitate the use of the data given here for specific cases, e.g., to ppm min units as commonly used by urban airshed modelers.

2. Inorganic Reactions

$$NO_2 + h\nu \rightarrow NO + O(^3P) \quad (1)$$

The rate constant, expressed as the photodissociation rate k_1, for this reaction is normally experimentally measured for each individual environmental chamber. However, the quantum yields and absorption cross-sections for this photodissociative process are necessary in order to derive other photolysis rate constants. The absorption cross-sections recommended by NASA [3] are those of Bass et al. [13], which are also in good agreement with the more recent, longer wavelength (λ>375 nm) data of Harker et al. [14]. Table 2 gives the NASA [3] recommended absorption cross-sections at 298 K (the cross-sections are temperature dependent) for the wavelength region 280-410 nm.

Absolute quantum yields for the photodissociation of NO_2 have been determined by Pitts et al. [15], Gaedtke and Troe [16] and by Harker et al. [14]. These reported quantum yields are shown in figure 1 as a function of wavelength, and it can be seen that, at least for λ>375 nm, the photodissociation quantum yield is significantly less than unity. The extensive quantum yield data of Harker et al. [14] for $\lambda \geq 375$ nm, which has been confirmed by more recent measurements of Davenport [17], are recommended by NASA [3].

The quantum yields at shorter wavelengths (i.e., $295 \leq \lambda < 375$ nm) are not accurately known (figure 1), but are also apparently less than unity [18]. No definitive recommendation can be made for the actinic wavelength region $295 \leq \lambda < 375$ nm, but we tentatively recommend that for this region (with λ in nm):

$$\phi = 1.00 - 0.0025\ (\lambda - 295) \text{ nm}$$

as shown in figure 1. (Note that this is somewhat different from the NASA evaluation [3].) For λ>375 nm, we recommend the quantum yield data of Harker et al. [14], which are also recommended by NASA [3], as given in table 3.

The error limits on the absorption cross-sections are judged, on the basis of the agreement between the data of Bass et al. [13] and Harker et al. [14], to be ±10-15%, while the error limits on the quantum yields are ~±10% for λ>375 nm, and (tentatively) ±10-15% for $295 \leq \lambda \leq 375$ nm.

$$O(^3P) + O_2 + M \rightarrow O_3 + M \ (M=air) \quad (2)$$

The most recent NASA evaluation [3] recommends:

$$k_2 = (6.0 \pm 0.5) \times 10^{-34}\ (T/300)^{-(2.3 \pm 0.5)}\ cm^6\ molecule^{-2}\ s^{-1},$$

$$k_2 = (6.1 \pm 0.5) \times 10^{-34}\ cm^6\ molecule^{-2}\ s^{-1}$$

at 298 K, based upon the recent data of Klais et al. [19] and of Lin and Leu [20]. This recommendation is in good agreement with previous data and with the earlier NBS recommendation [2].

Since this reaction is fast and is the major reaction pathway for $O(^3P)$ atoms under atmospheric conditions, model predictions are not too sensitive to this rate constant.

$$O(^3P) + NO_2 \rightarrow NO + O_2 \quad (a) \quad (3)$$

$$\xrightarrow{M} NO_3 \quad (b)$$

The NASA [3] evaluation recommends

$$k_{3a} = 9.3 \times 10^{-12}\ cm^3\ molecule^{-1}\ s^{-1},$$

independent of temperature, with an uncertainty in the 298 K value of ±10%. This recommendation supersedes, but is in close agreement with, the NBS [2] recommendation of

$$k_{3a} = 9.1 \times 10^{-12}\ cm^3\ molecule^{-1}\ s^{-1},$$

independent of temperature, which was taken from the study of Davis et al. [21].

At atmospheric pressure, the reaction of $O(^3P)$ atoms with NO_2 to yield NO_3:

$$O(^3P) + NO_2 + M \rightarrow NO_3 + M \quad (3b)$$

has a second-order rate constant [2,3] of

$$\simeq 2.0 \times 10^{-12}\ cm^3\ molecule^{-1}\ s^{-1} \text{ at } 298 \text{ K}.$$

NASA [3] recommends

$$k_{3b} = (9 \pm 1) \times 10^{-32}\ (T/300)^{-(2 \pm 1)}\ cm^6\ molecule^{-2}\ s^{-1}$$

as the third-order rate constant, which is applicable, to within ~±20%, up to atmospheric pressure.

Since reaction (3) (i.e., both 3a and 3b) has a limited importance for sub-ppm concentrations of NO_2, the three-body reaction to yield NO_3 can probably be neglected for photochemical air pollution modeling studies.

$$NO + O_3 \rightarrow NO_2 + O_2 \quad (4)$$

The NASA [3] evaluation of k_4 yields

$$k_4 = 2.2 \times 10^{-12}\ e^{-(1430 \pm 200)/T}\ cm^3\ molecule^{-1}\ s^{-1},$$

$$k_4 = 1.8 \times 10^{-14} \text{ cm}^3 \text{ molecule}^{-1} \text{ s}^{-1}$$

at 298 K, with an uncertainty of ±20% at 298 K. This agrees well with the earlier NBS [2] recommended value.

$$O_3 + NO_2 \rightarrow NO_3 + O_2 \quad (5)$$

Both NBS [2] and NASA [3] recommend that:

$$k_5 = 1.2 \times 10^{-13} e^{-(2450\pm140)/T} \text{ cm}^3 \text{ molecule}^{-1} \text{ s}^{-1},$$

$$k_5 = 3.2 \times 10^{-17} \text{ cm}^3 \text{ molecule}^{-1} \text{ s}^{-1}$$

at 298 K, with an uncertainty of ±15% at 298 K.

$$NO + NO_3 \rightarrow 2\ NO_2 \quad (6)$$

The most recent data available for this reaction are those of Graham and Johnston [22], who derived

$$k_6 = 1.9 \times 10^{-11} \text{ cm}^3 \text{ molecule}^{-1} \text{ s}^{-1}$$

at 298 K. This value is recommended by NASA [3] with an uncertainty of a factor of 3. Because of the high value of this rate constant at room temperature, any temperature dependence is expected to be small, and probably slightly negative. By analogy with HO_2 + NO [23,24]

Table 1. Conversion Tables (From Hampson and Garvin, 1978)
A. Equivalent Second Order Rate Constants

A \ B	$cm^3mol^{-1}s^{-1}$	$dm^3mol^{-1}s^{-1}$	$m^3mol^{-1}s^{-1}$	$cm^3molecule^{-1}s^{-1}$	$(mm\ Hg)^{-1}s^{-1}$	$atm^{-1}s^{-1}$	$ppm^{-1}min^{-1}$	$m^2kN^{-1}s^{-1}$
1 $cm^3mol^{-1}s^{-1}$ =	1	10^{-3}	10^{-6}	1.66×10^{-24}	$1.604 \times 10^{-5}T^{-1}$	$1.219 \times 10^{-2}T^{-1}$	2.453×10^{-9}	$1.203 \times 10^{-4}T^{-1}$
1 $dm^3mol^{-1}s^{-1}$ =	10^3	1	10^{-3}	1.66×10^{-21}	$1.604 \times 10^{-2}T^{-1}$	$12.19\ T^{-1}$	2.453×10^{-6}	$1.203 \times 10^{-1}T^{-1}$
1 $m^3mol^{-1}s^{-1}$ =	10^6	10^3	1	1.66×10^{-18}	$16.04\ T^{-1}$	$1.219 \times 10^{4}T^{-1}$	2.453×10^{-3}	$120.3\ T^{-1}$
1 $cm^3molecule^{-1}s^{-1}$ =	6.023×10^{23}	6.023×10^{20}	6.023×10^{17}	1	$9.658 \times 10^{18}T^{-1}$	$7.34 \times 10^{21}T^{-1}$	1.478×10^{15}	$7.244 \times 10^{19}T^{-1}$
1 $(mm\ Hg)^{-1}s^{-1}$ =	$6.236 \times 10^{4}T$	$62.36\ T$	$6.236 \times 10^{-2}T$	$1.035 \times 10^{-19}T$	1	760	4.56×10^{-2}	7.500
1 $atm^{-1}s^{-1}$ =	$82.06\ T$	$8.206 \times 10^{-2}T$	$8.206 \times 10^{-5}T$	$1.362 \times 10^{-22}T$	1.316×10^{-3}	1	6×10^{-5}	9.869×10^{-3}
1 $ppm^{-1}min^{-1}$ = at 298K, 1 atm. total pressure	4.077×10^{8}	4.077×10^{5}	407.7	6.76×10^{-16}	21.93	1.667×10^{4}	1	164.5
1 $m^2kN^{-1}s^{-1}$ =	$8314\ T$	$8.314\ T$	$8.314 \times 10^{-3}T$	$1.38 \times 10^{-20}T$	0.1333	101.325	6.079×10^{-3}	1

To convert a rate constant from one set of units A to a new set B find the conversion factor for the row A under Column B and multiply the old value by it, e.g. to convert $cm^3molecule^{-1}s^{-1}$ to $m^3mol^{-1}s^{-1}$ multiply by 6.023×10^{17}.

Table adapted from Evaluated Kinetic Data for High Temperature Reactions, Volume 1: Homogeneous Gas Phase Reactions of the H_2-O_2 System, Butterworths, London, 1972.

Table 1. Conversion Tables (From Hampson and Garvin, 1978)

B. Equivalent Third Order Rate Constants

A \ B	$cm^6 mol^{-2} s^{-1}$	$dm^6 mol^{-2} s^{-1}$	$m^6 mol^{-2} s^{-1}$	$cm^6 molecule^{-2} s^{-1}$	$(mm\ Hg)^{-2} s^{-1}$	$atm^{-2} s^{-1}$	$ppm^{-2} min^{-1}$	$m^4 kN^{-2} s^{-1}$
1 $cm^6 mol^{-2} s^{-1}$ =	1	10^{-6}	10^{-12}	2.76×10^{-48}	$2.57 \times 10^{-10} T^{-2}$	$1.48 \times 10^{-4} T^{-2}$	1.003×10^{-19}	$1.447 \times 10^{-8} T^{-2}$
1 $dm^6 mol^{-2} s^{-1}$ =	10^6	1	10^{-6}	2.76×10^{-42}	$2.57 \times 10^{-4} T^{-2}$	$148\ T^{-2}$	1.003×10^{-13}	$1.447 \times 10^{-2} T^{-2}$
1 $m^6 mol^{-2} s^{-1}$ =	10^{12}	10^6	1	2.76×10^{-36}	$257\ T^{-2}$	$1.48 \times 10^{8} T^{-2}$	1.003×10^{-7}	$1.447 \times 10^{4} T^{-2}$
1 $cm^6 molecule^{-2} s^{-1}$ =	3.628×10^{47}	3.628×10^{41}	3.628×10^{35}	1	$9.328 \times 10^{37} T^{-2}$	$5.388 \times 10^{43} T^{-2}$	3.64×10^{28}	$5.248 \times 10^{39} T^{-2}$
1 $(mm\ Hg)^{-2} s^{-1}$ =	$3.89 \times 10^{9} T^2$	$3.89 \times 10^{3} T^2$	$3.89 \times 10^{-3} T^2$	$1.07 \times 10^{-38} T^2$	1	5.776×10^{5}	3.46×10^{-5}	56.25
1 $atm^{-2} s^{-1}$ =	$6.733 \times 10^{3} T^2$	$6.733 \times 10^{-3} T^2$	$6.733 \times 10^{-9} T^2$	$1.86 \times 10^{-44} T^2$	1.73×10^{-6}	1	6×10^{-11}	9.74×10^{-5}
1 $ppm^{-2} min^{-1}$ = at 298K, 1 atm. total pressure	9.97×10^{18}	9.97×10^{12}	9.97×10^{6}	2.75×10^{-29}	2.89×10^{4}	1.667×10^{10}	1	1.623×10^{6}
1 $m^4 kN^{-2} s^{-1}$ =	$6.91 \times 10^{7} T^2$	$69.1\ T^2$	$6.91 \times 10^{-5} T^2$	$1.904 \times 10^{-40} T^2$	0.0178	1.027×10^{4}	6.16×10^{-7}	1

See note to Table for Second Order Rate Constants

Table 1. Conversion Tables (From Hampson and Garvin, 1978)

C. Conversion Factors for Units of Optical Absorption Coefficients

A \ B	(cross section σ) $cm^2 molecule^{-1}$ base e	$(atm\ at\ 273)^{-1} cm^{-1}$ base e	$dm^3 mol^{-1} cm^{-1}$ base 10	$cm^2 mol^{-1}$ base 10
1 $(atm\ at\ 298)^{-1} cm^{-1}$ base e =	4.06×10^{-20}	1.09	10.6	1.06×10^{4}
1 $(atm\ at\ 298)^{-1} cm^{-1}$ base 10 =	9.35×10^{-20}	2.51	24.4	2.44×10^{4}
1 $(mm\ Hg\ at\ 298)^{-1} cm^{-1}$ base 10 =	7.11×10^{-17}	1.91×10^{3}	1.86×10^{4}	1.86×10^{7}
1 $(atm\ at\ 273)^{-1} cm^{-1}$ base e =	3.72×10^{-20}	1	9.73	9.73×10^{3}
1 $(atm\ at\ 273)^{-1} cm^{-1}$ base 10 =	8.57×10^{-20}	2.303	22.4	2.24×10^{4}
1 $dm^3\ mol^{-1} cm^{-1}$ base 10 =	3.82×10^{-21}	0.103	1	10^{3}
1 $cm^2\ mol^{-1}$ base 10 =	3.82×10^{-24}	1.03×10^{-4}	10^{-3}	1
1 cm^2 molecule^{-1} base e =	1	2.69×10^{19}	2.62×10^{20}	2.62×10^{23}

To convert an absorption coefficient from one set of units A to a new set B, multiply by the value tabulated for row A under column B, e.g. to convert the value of the absorption coefficient expressed in $dm^3\ mol^{-1} cm^{-1}$ base 10 to $(atm\ at\ 273)^{-1} cm^{-1}$ base e, multiply by 0.103.

Table 2. NO_2 Absorption Cross-Sections at 298 K, as Recommended by NASA [3]

Wavelength (nm)	10^{19} x σ (cm^2)	Wavelength (nm)	10^{19} x σ (cm^2)
280	0.554	350	4.10
285	0.699	355	5.13
290	0.818	360	4.51
295	0.967	365	5.78
300	1.17	370	5.42
305	1.66	375	5.35
310	1.76	380	5.99
315	2.25	385	5.94
320	2.54	390	6.00
325	2.79	395	5.89
330	2.99	400	6.76
335	3.45	405	6.32
340	3.88	410	5.77
345	4.07		

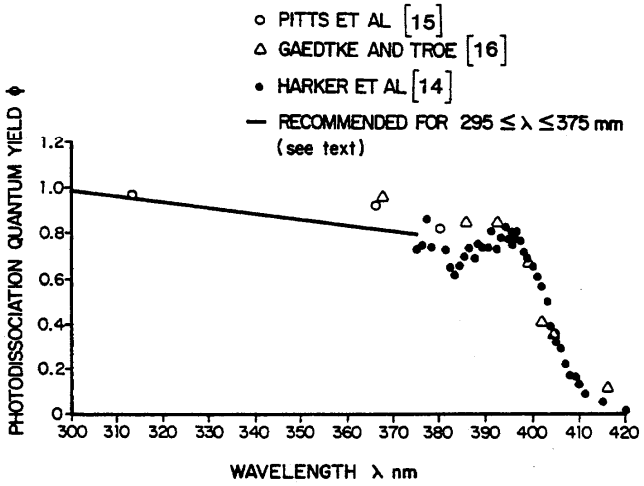

Figure 1. Absolute Quantum Yield for the Photodissociation of NO_2.

Table 3. Quantum Yields φ for NO_2 Photodissociation, from Harker et al. [14], as Recommended by NASA [3]

λ (nm)	φ	λ (nm)	φ	λ (nm)	φ
375	0.73	389	0.74	400	0.65
376	0.75	390	0.74	401	0.62
377	0.86	391	0.81	402	0.57
378	0.74	392	0.73	403	0.50
379	0.83	393	0.78	404	0.40
380	0.81	394	0.83	405	0.32
381	0.73	394.5	0.78	406	0.30
382	0.65	395	0.81	407	0.23
383	0.62	395.5	0.75	408	0.18
384	0.66	396	0.78	409	0.17
385	0.70	396.5	0.81	410	0.14
386	0.74	397	0.77	411	0.10
387	0.69	398	0.72	415	0.067
388	0.76	399	0.70	420	0.023

and other related reactions, an estimated rate constant expression of

$$k_6 = 8 \times 10^{-12}\ e^{250/T}\ cm^3\ molecule^{-1}\ s^{-1},$$

is tentatively recommended, which yields the Graham and Johnston [22] 298 K value.

$$NO_2 + NO_3 \xrightarrow{M} N_2O_5 \qquad (7)$$

and

$$N_2O_5 \xrightarrow{M} NO_2 + NO_3 \qquad (8)$$

The most recent NASA evaluation [3] for these reactions is based on the data of Connell and Johnston [25] and Viggiano et al. [26] for the thermal decomposition of N_2O_5. That evaluation [3] used the general "fall-off" relationship

$$k = \left\{ \frac{k_o(T)[M]}{1+k_o(T)[M]/k_\infty(T)} \right\} x$$

$$0.6^{\{1+[\log_{10}(k_o(T)[M]/k_\infty(T))]^2\}^{-1}}$$

$$cm^3\ molecule^{-1}\ s^{-1}$$

(where [M] is the concentration of air in molecule cm^{-3})

with $k_o(T) = (2.2\pm1.1) \times 10^{-30}$

$$(T/300)^{-(2.8\pm1.0)}\ cm^6\ molecule^{-2}\ s^{-1}$$

and

$$k_\infty(T) = (1.0\pm0.8) \times 10^{-12}\ (T/300)^{0\pm1}$$

$$cm^3\ molecule^{-1}\ s^{-1}$$

for reaction (7), and the equilibrium constant

$$k_8/k_7 = 5.65 \times 10^{26}\ e^{-11001/T}\ molecule\ cm^{-3}.$$

At 760 torr[2] total pressure, these expressions yield rate constants of

$$k_7 = 8.65 \times 10^{-13}\ cm^3\ molecule^{-1}\ s^{-1}$$

at 298 K,

$$= 6.7 \times 10^{-13}\ e^{74/T}\ cm^3\ molecule^{-1}\ s^{-1}\ (268 \le T \le 330\ K)$$

$$k_8 = 0.045\ s^{-1} \text{ at } 298\ K$$

$$= 0.031\ s^{-1} \text{ at } 295\ K.$$

A recent thorough evaluation by Malko and Troe [27] yields rate constants at 760 torr **a factor of ~1.1 higher:**

$$k_7 = 9.6 \times 10^{-13}\ cm^3\ molecule^{-1}\ s^{-1}$$

at 295 K

$$= 4.2 \times 10^{-13}\ e^{226/T}\ cm^3\ molecule^{-1}\ s^{-1}\ (268 \le T \le 330\ K)$$

$$k_8 = 0.034\ s^{-1} \text{ at } 295\ K$$

$$= 1.56 \times 10^{14}\ e^{-10655/T}\ s^{-1}\ (268 \le T \le 330\ K).$$

These two evaluations yield data which agree within the stated uncertainties. However, the rate constants obtained for reaction (7) are lower than may be expected (the k_∞ values being 1.0×10^{-12} [3] and $1.6 \times 10^{-12}\ (T/300)^{0.2}$ [27] $cm^3\ molecule^{-1}\ s^{-1}$) by analogy with other radical-NO_2 reactions. We thus recommend the evaluation of Malko and Troe [27]; for pressures other than 760 torr their article should be consulted. Further work is, we believe, necessary on reaction (7) and/or the equilibrium constant for this reaction pair before k_7 can be placed on a firm basis.

$$NO_3 + NO_2 \rightarrow NO + NO_2 + O_2 \qquad (9)$$

The most recent data available for this reaction are those of Graham and Johnston [22], who obtained the expression

$$k_9 = (2.5\pm0.5) \times 10^{-14}\ e^{-(1230\pm100)/T}\ cm^3\ molecule^{-1}\ s^{-1},$$

yielding

$$k_9 = 4.0 \times 10^{-16}\ cm^3\ molecule^{-1}\ s^{-1}$$

at 298 K.

In the absence of other data, we recommend these expressions, with an estimated uncertainty at 298 K of a factor of 2.

$$NO_3 + h\nu \rightarrow NO + O_2 \qquad (10)$$

and

$$NO_3 + h\nu \rightarrow NO_2 + O(^3P) \qquad (11)$$

Absorption cross-sections for NO_3 have been reported by Johnston and Graham [28], Graham and Johnston [22], Mitchell et al.

[2] 1 torr = 133.3 Newtons m^{-2}.

[29], and Marinelli et al. [30]. The discrepancies between the peak absorption cross-sections determined by Graham and Johnston [22] and Mitchell et al. [29] have been shown [30] to be due to differences in instrumental resolution. The recommended cross-sections given in table 4, which are also recommended by NASA [3], are those of Graham and Johnston [22]. The distribution between the two pathways, i.e., reactions (10) and (11), was determined by Graham and Johnston [22] to be $\phi_{11} \sim 1.0$ for $\lambda < 580$ nm, ~ 0.0 for $\lambda > 640$ nm; $\phi_{10} + \phi_{11} \simeq 0.0$ for $\lambda > 650$ nm, using broadband lamp distributions. The more recent study of Magnotta and Johnston [31] has determined, using laser excitation, the quantum yield distributions given in figure 2.

Specifically, it can be seen from figure 2 that absorption at the strong bands at 623 and 662 nm leads to very low photodissociation quantum yields and that the photodissociation pathway into $NO_2 + O(^3P)$ is the predominant pathway [31]. It should be noted that the observation that the total quantum yield exceeds unity at $\sim$590 nm indicates that there is some systematic error, most probably in the quantum yields [3].

$$NO + NO + O_2 \rightarrow 2\ NO_2 \qquad (12)$$

The rate constant evaluated by NBS [2] is recommended, i.e.,

$$k_{12} = 3.3 \times 10^{-39}\ e^{530/T}\ cm^6\ molecule^{-2}\ s^{-1}$$

and

$$k_{12} = 2.0 \times 10^{-38}\ cm^6\ molecule^{-2}\ s^{-1}$$

at 298 K, with an uncertainty of $\pm$25% at 298 K.

This reaction is reasonably unimportant at sub-ppm levels of NO under atmospheric conditions but can be important in the initial stages of plume chemistry.

$$O_3 + h\nu \rightarrow O_2 + O(^3P) \qquad (a) \qquad (13)$$

$$\rightarrow O_2(^1\Delta_g) + O(^1D) \qquad (b)$$

Absorption cross-sections have been measured in numerous studies (see, for example [32-35]). The cross-sections are all in good agreement, and have been tabulated by Moortgat and Warneck [34] for $297.5 \leq \lambda \leq 330.0$ nm and by Arnold et al. [35] for $295 \leq \lambda \leq 320$ nm; the maximum deviations between these two sets of data being $\sim$7%.

The quantum yield of $O(^1D)$ production, ϕ_b, can be best considered in the two wavelength regions $\lambda \leq 300$ nm and $\lambda \geq 300$ nm. Despite two absolute quantum yields determinations below 300 nm which showed that ϕ_b was unity [36,37], recent data [38-43] show that ϕ_b is significantly less than unity for $248 < \lambda < 300$ nm. The two molecular beam-photofragment spectroscopic studies of Fairchild et al. [38] and Sparks et al. [39] show that $\phi_b \sim 0.90$ at 266 nm [39] and 274 nm [38], (with ϕ_b possibly increasing somewhat over the wavelength range 274-300 nm [38]). Brock and Watson [40] have determined that $\phi_b = 0.88 \pm 0.02$ at 266 nm, while Amimoto et al. [41] have reinvestigated this system and now obtain $\phi_b = 0.85 \pm 0.02$ at 248 nm. More recently, Wine and Ravishankara [42] and Greenblatt and Wiesenfeld [43] have obtained $\phi_b = 0.91 \pm 0.03$ and 0.94 ± 0.01 at 248 nm, respectively.

The quantum yield determinations for $\lambda > 300$ nm have generally been relative to $\phi_b = 1.00$ at 300 nm. The value of ϕ_b decreases rapidly for $\lambda > 305$ nm, and the recent data of Moortgat and Warneck [34], Arnold et al. [35] and Brock and Watson [44] as a function of wavelength and temperature at 298 K (the quantum yields are temperature dependent, with lower quantum yields at lower temperatures [45]) are in good agreement.

Since it is now evident that ϕ_b is less than unity for $\lambda \leq 300$ nm, we recommend that for $248 \leq \lambda \leq 300$ nm,

$$\phi_b = 0.90$$

For $\lambda \geq 300$ nm, NASA [3] have recommended the value of ϕ_b, as a function of wavelength and temperature, derived from the mathematical expression of Moortgat and Kudszus [46], scaled by a factor of 0.9. Thus

$$\lambda \geq 300 \text{ nm};\ \phi_b(\lambda,T) =$$

$$[A(\tau)\arctan [B(\tau)(\lambda - \lambda_o(\tau))] + C(\tau)]$$

where $\tau = T - 230$ K; λ is in nm, and arctan is in radians, with

$$A(\tau) = 0.332 + 2.565 \times 10^{-4}\ \tau + 1.152 \times 10^{-5}\ \tau^2 + 2.313 \times 10^{-8}\ \tau^3$$

$$B(\tau) = -0.575 + 5.59 \times 10^{-3}\ \tau - 1.439 \times 10^{-5}\ \tau^2 - 3.27 \times 10^{-8}\ \tau^3$$

$$\lambda_o(\tau) = 308.20 + 4.4871 \times 10^{-2}\ \tau + 6.9380 \times 10^{-5}\ \tau^2 - 2.5452 \times 10^{-6}\ \tau^3$$

$$C(\tau) = 0.466 + 8.883 \times 10^{-4}\ \tau - 3.546 \times 10^{-5}\ \tau^2 + 3.519 \times 10^{-7}\ \tau^3$$

and, in the limits where $\phi_b(\lambda,T) > 0.90$, the quantum yield is set at $\phi_b = 0.90$, and similarly, for $\phi_b(\lambda,T) < 0$, the quantum yield is set at $\phi_b = 0$.

The uncertainties in the above recommendations are expected to be less than $\pm$0.05

Table 4. Absorption Cross Sections (cm^2 $molecule^{-1}$, base e), Averaged Over Each nm, for NO_3 [22]

λ (nm)	10^{19} x σ (cm^2)	λ (nm)	10^{19} x σ (cm^2)	λ (nm)	10^{19} x σ (cm^2)	λ (nm)	10^{19} x σ (cm^2)	λ (nm)	10^{19} x σ (cm^2)
400	0.0	461	3.6	522	17.2	583	26.8	644	7.1
401	0.1	462	3.5	523	16.6	584	24.7	645	6.7
402	0.1	463	3.8	524	15.0	585	24.6	646	5.6
403	0.3	464	4.1	525	13.8	586	27.5	647	4.9
404	0.2	465	4.5	526	13.7	587	34.8	648	4.8
405	0.5	466	4.5	527	15.1	588	44.8	649	3.7
406	0.3	467	4.8	528	17.9	589	55.2	650	3.2
407	0.1	468	5.0	529	21.0	590	56.7	651	3.3
408	0.3	469	5.2	530	20.9	591	51.9	652	3.9
409	0.5	470	4.9	531	19.1	592	48.3	653	4.7
410	0.6	471	5.0	532	18.1	593	43.2	654	5.7
411	0.5	472	5.4	533	17.3	594	39.2	655	6.9
412	0.3	473	5.5	534	17.7	595	39.1	656	8.9
413	0.7	474	5.6	535	20.2	596	41.6	657	11.8
414	0.7	475	5.9	536	23.2	597	40.9	658	16.8
415	0.6	476	6.4	537	23.8	598	35.4	659	27.6
416	0.3	477	6.8	538	21.1	599	28.9	660	51.2
417	0.4	478	6.6	539	18.8	600	24.5	661	101.5
418	0.6	479	6.4	540	18.1	601	24.5	662	170.8
419	0.9	480	6.4	541	16.8	602	28.4	663	170.4
420	0.9	481	6.5	542	16.8	603	33.9	664	115.4
421	0.9	482	6.3	543	14.3	604	40.0	665	73.5
422	0.8	483	6.1	544	13.9	605	41.8	666	48.6
423	1.0	484	6.2	545	16.2	606	33.8	667	29.7
424	1.2	485	6.6	546	20.4	607	23.2	668	17.5
425	1.3	486	7.4	547	25.6	608	15.9	669	10.7
426	0.9	487	8.0	548	27.5	609	13.3	670	7.5
427	0.8	488	8.0	549	24.9	610	13.5	671	6.0
428	1.2	489	8.6	550	22.4	611	14.3	672	5.7
429	1.2	490	9.3	551	21.4	612	16.9	673	4.7
430	1.2	491	9.2	552	21.6	613	21.7	674	3.6
431	1.5	492	8.9	553	22.2	614	22.4	675	3.0
432	1.4	493	8.9	554	24.5	615	19.9	676	3.1
433	1.5	494	8.8	555	27.8	616	17.4	677	4.0
434	1.7	495	9.1	556	29.5	617	16.7	678	5.5
435	2.1	496	10.4	557	30.0	618	18.3	679	5.9
436	2.1	497	11.2	558	31.7	619	20.2	680	4.9
437	1.8	498	10.8	559	34.3	620	24.7	681	3.5
438	1.8	499	10.3	560	32.3	621	39.8	682	2.5
439	2.1	500	9.8	561	28.5	622	76.1	683	1.6
440	1.9	501	9.4	562	26.8	623	120.4	684	0.9
441	1.9	502	9.1	563	25.9	624	116.6	685	0.5
442	2.0	503	9.5	564	24.8	625	86.5	686	0.3
443	1.9	504	10.5	565	24.7	626	70.0	687	0.2
444	2.1	505	11.6	566	25.8	627	69.0	688	0.4
445	2.3	506	11.9	567	25.5	628	68.9	689	0.2
446	2.3	507	11.4	568	25.7	629	67.0	690	0.1
447	2.5	508	10.6	569	26.3	630	64.1	691	0.0
448	2.8	509	11.2	570	25.3	631	50.2	692	0.0
449	2.8	510	13.0	571	25.1	632	32.7	693	0.1
450	2.7	511	15.1	572	24.8	633	19.9	694	0.1
451	2.8	512	16.1	573	24.7	634	13.2	695	0.2
452	3.1	513	15.1	574	25.5	635	10.6	696	0.4
453	3.2	514	14.1	575	27.0	636	12.3	697	0.4
454	3.4	515	14.0	576	29.2	637	16.4	698	0.4
455	3.5	516	14.0	577	30.5	638	17.6	699	0.4
456	3.2	517	13.0	578	30.3	639	13.4	700	0.3
457	3.4	518	12.1	579	29.4	640	9.8	701	0.2
458	3.7	519	12.8	580	29.9	641	7.8	702	0.2
459	3.9	520	14.4	581	32.0	642	6.8	703	0.1
460	3.9	521	15.8	582	31.0	643	6.9	704	0.0

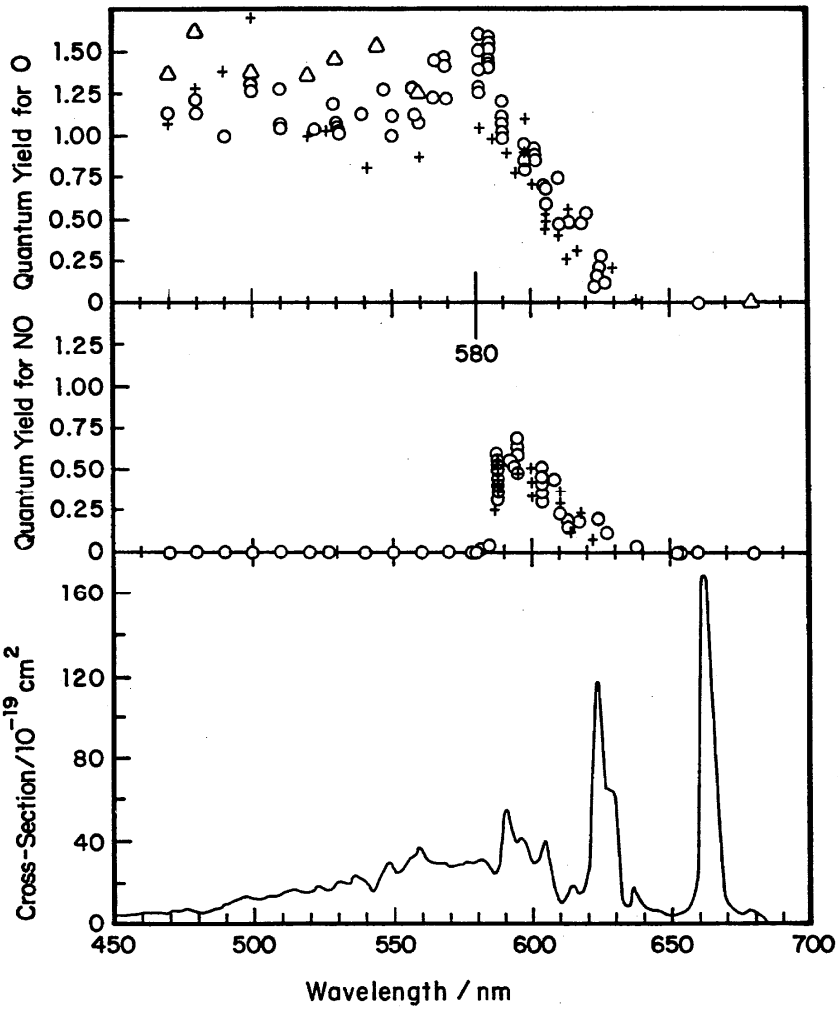

Figure 2. Observed NO_3 Radical Absorption Cross-Sections and NO and $O(^3P)$ Atom Formation Quantum Yields from the Photodissociation of the NO_3 Radical (adapted from [31]).

in absolute units in ϕ_b for $266<\lambda<320$ nm. For this wavelength region, $266\lesssim\lambda\lesssim350$ nm, $(\phi_a + \phi_b)$ is unity [2].

$$O(^1D) + M\ (M=air) \rightarrow O(^3P) + M \qquad (14)$$

$$O(^1D) + H_2O \rightarrow 2\ OH \qquad (15)$$

We recommend the use of the NASA [3] evaluation with

$$k_{14}\ (M=air) = 2.9 \times 10^{-11}\ cm^3\ molecule^{-1}\ s^{-1}$$

at 298 K, with an uncertainty of a factor of 1.2 at 298 K, and being essentially independent of temperature over the range 273-320 K; and

$$k_{15} = 2.2 \times 10^{-10}\ cm^3\ molecule^{-1}\ s^{-1}$$

independent of temperature, with an uncertainty at 298 K of a factor of 1.2.

The reactions of $O(^1D)$ atoms with N_2 and O_2 proceed via deactivation to $O(^3P)$ atoms [47] while the reaction of $O(^1D)$ atoms with H_2O leads essentially entirely to two OH radicals [42,48]:

$$O(^1D) + N_2 \rightarrow O(^3P) + N_2$$

$$O(^1D) + O_2 \rightarrow O(^3P) + O_2$$

$$O(^1D) + H_2O \rightarrow 2\ OH$$

$$OH + NO + M \rightarrow HONO + M \qquad (16)$$

This reaction is in the fall-off region between second- and third-order kinetics at atmospheric pressure and room temperature. The two most relevant studies are those of Overend et al. [49] and of Anastasi and Smith [50], both for M=N_2. These studies result in bimolecular rate constants of

$$k_{16}\ (M=N_2) = 7.0 \times 10^{-12}\ cm^3\ molecule^{-1}\ s^{-1}\ \text{at 636 torr } N_2,$$

and

$$k_{16}\ (M=N_2) = 6.9 \times 10^{-12}\ cm^3\ molecule^{-1}\ s^{-1}$$

at 770 torr N_2 and 295 K [49], and

$$k_{16}\ (M=N_2) = 6.7 \times 10^{-12}\ cm^3\ molecule^{-1}\ s^{-1}$$

at 298 K and 1 atmosphere (presumably 760 torr) total pressure by a short extrapolation [50].

These values are further substantiated by the earlier work of Atkinson et al. [51] for M=Ar and N_2. Thus, there is good agreement for M=Ar at ~700 torr between the data of Atkinson et al. [51] and Overend et al. [49], and the Atkinson et al. [51] extrapolated atmospheric pressure value of

$$k_{16}\ (M=N_2) = (6.1\pm1.0) \times 10^{-12}\ cm^3\ molecule^{-1}\ s^{-1}$$

at room temperature agrees well with the above values. Assuming (reasonably) that O_2 and N_2 have essentially identical third-body efficiencies, then

$$k_{16} = 6.8 \times 10^{-12}\ cm^3\ molecule^{-1}\ s^{-1},$$

(M = air, room temperature, atmospheric pressure), with an estimated uncertainty of ±20%.

However, the most recent NASA evaluation [3] derives a value of

$$k_{16} = 4.7 \times 10^{-12}\ cm^3\ molecule^{-1}\ s^{-1}$$

at 300 K and 760 torr total pressure.

This rate constant is clearly inconsistent with the above cited data, and we recommend the earlier 1979 NASA evaluation [52], which yielded:

$$k_{16} = 6.6 \times 10^{-12}\ cm^3\ molecule^{-1}\ s^{-1}$$

at 300 K and 760 torr air from the expression:

$$k_{16} = \left\{\frac{k_o(T)[M]}{1+k_o(T)[M]/k_\infty(T)}\right\} \times 0.6^{\{1+[\log_{10}(k_o(T)[M]/k_\infty(T))]^2\}^{-1}}\ cm^3\ molecule^{-1}\ s^{-1}$$

where

$$k_o(T) = 6.7 \times 10^{-31}\ (T/300)^{-3.3}\ cm^6\ molecule^{-2}\ s^{-1},$$

$$k_\infty(T) = 3.0 \times 10^{-11}\ (T/300)^{-1.0}\ cm^3\ molecule^{-1}\ s^{-1}$$

and [M] = concentration of air in molecule cm^{-3}.

$$OH + NO_2 + M \rightarrow HNO_3 + M \quad (17)$$

The rate date for this reaction has been extensively evaluated by NBS [2] and NASA [3], resulting in, for M=N_2, [2]:

$$\log_{10} k_{17} (M=N_2) = - AT/B+T - 0.5 \log_{10} (T/280)$$

where

$$A = A_1 + A_2Z + A_3Z^2 + A_4Z^3$$

$$B = B_1 + B_2Z + B_3Z^2$$

and

$$Z = \log_{10} [N_2], ([N_2] \text{ in molecule cm}^{-3})$$

$A_1 = 31.62273$

$A_2 = -0.258304$

$A_3 = -0.0889287$

$A_4 = 0.002520173$

$B_1 = -327.372$

$B_2 = 44.5586$

$B_3 = -1.38092$

This equation is applicable for 200 < T < 350 K, 16.3 < $\log_{10}$ [N_2] < 19.5 (~1-1000 torr at 300 K).

Since k_{16} (M=air) = 0.94 k_{17} (M=N_2) [2], then at 298 K and 1 atmosphere air,

$$k_{17} = 1.1 \times 10^{-11} \text{ cm}^3 \text{ molecule}^{-1} \text{ s}^{-1} .$$

This evaluation is based primarily on the extensive pressure and temperature rate constant data of Anastasi and Smith [53]. Recent work of Wine et al. [54] for M=N_2 yields rate constants in excellent agreement with those of Anastasi and Smith [53]. The NASA [3] evaluation also yields

$$k_{17} = 1.1 \times 10^{-11} \text{ cm}^3 \text{ molecule}^{-1} \text{ s}^{-1}$$

for atmospheric pressure and 300 K using the expression

$$k_{17} = \left\{ \frac{k_o(T)[M]}{1+k_o(T)[M]/k_\infty(T)} \right\} \times 0.6^{\{1+[\log_{10}(k_o(T)[M]/k_\infty(T))]^2\}^{-1}}$$

cm^3 molecule^{-1} s^{-1} with

$$k_o(T) = 2.6 \times 10^{-30} (T/300)^{-2.9} \text{ cm}^6 \text{ molecule}^{-2} \text{ s}^{-1},$$

$$k_\infty(T) = 2.4 \times 10^{-11} (T/300)^{-1.3} \text{ cm}^3 \text{ molecule}^{-1} \text{ s}^{-1}$$

$$HONO + h\nu \rightarrow OH + NO \quad (18)$$

The quantum yield for this process is taken as unity since Cox [55] concluded that the alternative photodissociation pathway

$$HONO + h\nu \rightarrow H + NO_2$$

accounts for ≤3% of the total photodissociative pathways. The major uncertainty lies in the absorption cross-sections of HONO, the two latest studies being those of Cox and Derwent [56] and Stockwell and Calvert [57]. The discussion by Stockwell and Calvert [57] of the discrepancies and their probable origins should be consulted for details; in essence, the earlier Johnston and Graham [28] study gave low absorption cross-sections due to lower-than-assumed equilibrium HONO concentrations, while Cox and Derwent [56] may have undercorrected for the NO_2 absorption present. Furthermore, the data of Stockwell and Calvert [57] are consistent with the relative rates of photolysis of HONO and NO_2 in their environmental chamber. Hence, in agreement with NASA [3], the absorption cross-section data of Stockwell and Calvert [57] are recommended (table 5), with a photodissociation quantum yield of unity for the process

$$HONO + h\nu \rightarrow OH + NO$$

$$HNO_3 + h\nu \rightarrow OH + NO_2 \quad (19)$$

This process is generally regarded to be unimportant in environmental chamber modeling studies. The NASA [3] recommended absorption cross-sections are those of Molina and Molina [58], which are in excellent agreement with the data of Johnston and Graham [59] and Biaume [60], and table 6 tabulates these absorption cross-sections at 5 nm intervals for the wavelength region 250-330 nm. The quantum yield is unity [61].

Table 5. HONO Absorption Cross-Sections [57], as Recommended by NASA [3]

λ (nm)	10^{20} x σ (cm^2)	λ (nm)	10^{20} x σ (cm^2)	λ (nm)	10^{20} x σ (cm^2)
310	0.0	339	16.3	368	45.0
311	0.0	340	10.5	369	29.3
312	0.2	341	8.70	370	11.9
313	0.42	342	33.5	371	9.46
314	0.46	343	20.1	372	8.85
315	0.42	344	10.2	373	7.44
316	0.3	345	8.54	374	4.77
317	0.46	346	8.32	375	2.7
318	3.6	347	8.20	376	1.9
319	6.10	348	7.49	377	1.5
320	2.1	349	7.13	378	1.9
321	4.27	350	6.83	379	5.8
322	4.01	351	17.4	380	7.78
323	3.93	352	11.4	381	11.4
324	4.01	353	37.1	382	14.0
325	4.04	354	49.6	383	17.2
326	3.13	355	24.6	384	19.9
327	4.12	356	11.9	385	19.0
328	7.55	357	9.35	386	11.9
329	6.64	358	7.78	387	5.65
330	7.29	359	7.29	388	3.2
331	8.70	360	6.83	389	1.9
332	13.8	361	6.90	390	1.2
333	5.91	362	7.32	391	0.5
334	5.91	363	9.00	392	0.0
335	6.45	364	12.1	393	0.0
336	5.91	365	13.3	394	0.0
337	4.58	366	21.3	395	0.0
338	19.1	367	35.2	396	0.0

Table 6. Absorption Cross-Sections, σ, for HNO_3 Over the Wavelength Region 250-330 nm (From NASA [3])

λ (nm)	10^{20} x σ (cm^2)
250	1.91
255	1.90
260	1.88
265	1.71
270	1.59
275	1.35
280	1.10
285	0.848
290	0.607
295	0.409
300	0.241
305	0.146
310	0.071
315	0.032
320	0.012
325	0.005
330	0.002

$$OH + HNO_3 \rightarrow \text{Products} \qquad (20)$$

This reaction is relatively unimportant for environmental chamber modeling studies. NASA [3] recommends

$$k_{20} = 9.4 \times 10^{-15}\, e^{(778\pm100)/T}\ cm^3\ molecule^{-1}\ s^{-1}$$

$$= 1.3 \times 10^{-13}\ cm^3\ molecule^{-1}\ s^{-1}$$

at 298 K, with an uncertainty of a factor of 1.3 at 298 K.

There are still some uncertainties regarding this rate constant [3]. The yield of NO_3 per OH radical removed is unity, within the experimental errors, at 298 K [62-64].

$$OH + HONO \rightarrow H_2O + NO_2 \qquad (21)$$

This reaction is again reasonably unimportant in environmental chamber modeling studies due to the rapid photolysis rate of HONO (reaction 18). The sole data for this reaction are from Cox [55] and Cox et al. [65]. In both cases, relative rate constants were obtained at ∿296 K and atmospheric pressure; relative to

$$k(OH + CO) = 1.5 \times 10^{-13}\ cm^3\ molecule^{-1}\ s^{-1}$$

in the earlier work [55], and relative to

$$k(OH + H_2) = 7.0 \times 10^{-15}\ cm^3\ molecule^{-1}\ s^{-1}$$

(which agrees well with the evaluations of this reaction by NBS [2], NASA [3], and by Cohen and Westberg [66]) in the later work [65], where the pressure dependence of k(OH + CO) became evident. Using these more reliable later data, a rate constant for reaction (21) of

$$k_{21} = 6.6 \times 10^{-12}\ cm^3\ molecule^{-1}\ s^{-1}$$

was obtained at 296 K [65]. No temperature dependence is available, but it would be expected to be zero or small. We recommend for modeling of polluted urban atmospheres that

$$k_{21} = 6.6 \times 10^{-12}\ cm^3\ molecule^{-1}\ s^{-1},$$

independent of temperature, with an estimated uncertainty of a factor of 2.

$$NO + NO_2 + H_2O \underset{23}{\overset{22}{\rightleftharpoons}} 2\ HONO \qquad (22,23)$$

Recently, three measurements of the kinetics of this system have been reported. Chan et al. [67,68] obtained

$$k_{23} = 1 \times 10^{-18}\ cm^3\ molecule^{-1}\ s^{-1}$$

and

$$k_{22} = 6 \times 10^{-38}\ cm^6\ molecule^{-2}\ s^{-1},$$

in agreement with earlier data. This agreement for different surface-to-volume ratios then suggested that these data were for the homogeneous reaction. However, Cox and Derwent [56] reported that reaction (23) was ∿200 times slower than expected from the data of Chan et al. [67,68]. More recently, Kaiser and Wu [69] have determined that these reactions are heterogeneous in their system, with upper limits to the rate constants of

$$k_{23} \leq 1 \times 10^{-20}\ cm^3\ molecule^{-1}\ s^{-1}$$

and

$$k_{22} \leq 4.4 \times 10^{-40}\ cm^6\ molecule^{-2}\ s^{-1}$$

at 300 K. The equilibrium constant at 300 K is

$$k_{22,23} = 4.4 \times 10^{-20}\ cm^3\ molecule^{-1}\ [70].$$

We make no explicit recommendation since this reaction should be experimentally, investigated for each particular environmental chamber. However, at present the evidence is that for sub-ppm concentrations of NO and NO_2, these reactions are unimportant for daytime chemistry; the situation may be different for nighttime chemistry.

$$N_2O_5 + H_2O \rightarrow 2\ HNO_3 \qquad (24)$$

The laboratory study of Morris and Niki [71] showed that the homogeneous rate constant k_{24} at 298 K was:

$$k_{24} \leq 1.3 \times 10^{-20}\ cm^3\ molecule^{-1}\ s^{-1}$$

and that although the observations (changing the total pressure from 200 to 650 torr and the wall materials from Pyrex to aluminum or Teflon having only small effects on the measured value of k_{24}) were consistent with a homogeneous reaction, a heterogeneous reaction could not be ruled out. Environmental chamber modeling studies [7,72] suggest lower values, indicating that this reaction may be heterogeneous and hence chamber specific, and a recent study in which N_2O_5 was monitored by FT-IR spectroscopy in two environmental chambers at 298 ± 1 K yielded a rate constant of

$$k_{24} \leq 1.3 \times 10^{-21}\ cm^3\ molecule^{-1}\ s^{-1}\ [73].$$

$$OH + CO \xrightarrow{O_2} HO_2 + CO \qquad (25)$$

Recently this reaction has been shown to have a pressure dependent rate constant at room temperature [65,74-79]. At present, it is reasonably evident that for M=air at room temperature, the rate constant increases from

$$k_{25} = 1.5 \times 10^{-13} \text{ cm}^3 \text{ molecule}^{-1} \text{ s}^{-1}$$

at low pressure ($\lesssim$25 torr total pressure) to

$$k_{25} \gtrsim (2.7\text{-}3.0) \times 10^{-13} \text{ cm}^3 \text{ molecule}^{-1} \text{ s}^{-1}$$

at atmospheric pressure [65,75,79]. NBS [2] recommends

$$k_{25} = 3.0 \times 10^{-13} \text{ cm}^3 \text{ molecule}^{-1} \text{ s}^{-1}$$

at 300 K and 1 atmosphere of air; while NASA [3] recommends

$$k_{25} = 1.35 \times 10^{-13} (1 + P_{atm}) \text{ cm}^3 \text{ molecule}^{-1} \text{ s}^{-1},$$

independent of temperature.

Perry et al. [77] proposed, based on their data for M=SF_6 and the atmospheric pressure data of Cox et al. [65] and Chan et al. [75], the following expression for k_{25} (M=air) of (with P in atmospheres):

$$k_{25} \text{ (M=air)} = \frac{6.0 \times 10^{-13} (0.25+0.456P)}{(1+0.456P)} \text{ cm}^3 \text{ molecule}^{-1} \text{ s}^{-1}$$

at 298 K. This leads to

$$k_{25} = 2.9 \times 10^{-13} \text{ cm}^3 \text{ molecule}^{-1} \text{ s}^{-1}$$

at 1 atmosphere (760 torr) of air and 298 K.

For modeling purposes at atmospheric pressure these three "recommendations" are essentially equivalent--differences between those of NASA [3] and of Perry et al. [77] occur for intermediate pressures less than 1 atmosphere. We recommend

$$k_{25} = 2.9 \times 10^{-13} \text{ cm}^3 \text{ molecule}^{-1} \text{ s}^{-1}$$

at one atmosphere of air, independent of temperature over the small temperature ranges associated with modeling studies of polluted atmospheres, with an uncertainty of $\pm$25%.

$$OH + O_3 \rightarrow HO_2 + O_2 \qquad (26)$$

This reaction, which is of minor importance in modeling studies, has recently been evaluated by NASA [3], who recommend:

$$k_{26} = 1.6 \times 10^{-12} e^{-(940\pm300)/T} \text{ cm}^3 \text{ molecule}^{-1} \text{ s}^{-1}$$

and

$$k_{26} = 6.8 \times 10^{-14} \text{ cm}^3 \text{ molecule}^{-1} \text{ s}^{-1}$$

at 298 K, with an uncertainty of a factor of 1.3.

$$HO_2 + NO \rightarrow OH + NO_2 \qquad (27)$$

The most recent NASA evaluation [3] recommends the rate constant

$$k_{27} = 3.7 \times 10^{-12} e^{(240\pm80)/T} \text{ cm}^3 \text{ molecule}^{-1} \text{ s}^{-1},$$

$$k_{27} = 8.3 \times 10^{-12} \text{ cm}^3 \text{ molecule}^{-1} \text{ s}^{-1}$$

at 298 K with an estimated uncertainty at 298 K of a factor of 1.2.

The temperature dependence is obtained from the studies of Howard [24] and Leu [23].

$$HO_2 + NO_2 \xrightarrow{M} HO_2NO_2 \qquad (28)$$

The reaction of HO_2 radicals with NO_2 has been shown to proceed essentially exclusively to form HO_2NO_2 [80-82]. Howard [82] has determined rate constants for M=He, N_2, O_2 and NO_2 at low pressures and 296 K, but since this reaction is in the fall-off region between third- and second-order kinetics at atmospheric pressure and room temperature [83], these data are not directly relevant for atmospheric purposes. Three rate constants for reaction (28) have been reported at around atmospheric pressure.

Graham et al. [83] utilized their HO_2NO_2 thermal decomposition rate data together with Howard's [82] low pressure values of k_{28} to yield

$$k_{28} \text{ (M=air)} = \frac{6.9 \times 10^{-33} e^{1007/T} [M]}{(1 + 4.86 \times 10^{-12} [M]^{0.61})} \text{ cm}^3 \text{ molecule}^{-1} \text{ s}^{-1}$$

This yields

$$k_{28} \text{ (M=air)} = 1.14 \times 10^{-12} \text{ cm}^3 \text{ molecule}^{-1} \text{ s}^{-1}$$

at 760 torr of air and 300 K.

Simonaitis and Heicklen [84] reported a lower value of k_{28} derived from photolyses of N_2O, H_2, O_2, NO and NO_2 mixtures. Because of complications in their system, their cited rate constants are almost certainly not correct. Simonaitis and Heicklen [84] derived

$$k_{28}/k_{27} = 0.61\pm0.15$$

at 245 K which leads, using the recommended values of k_{27}, to

$$k_{28} = (6.0\pm1.5) \times 10^{-12} \text{ cm}^3 \text{ molecule}^{-1} \text{ s}^{-1}$$

at 245 K, which, with an assumed Arrhenius activation energy of -2000 cal mol^{-1} for reaction (28) [83] yields

$$k_{28} \text{ (298 K)} \simeq 2.9 \times 10^{-12} \text{ cm}^3 \text{ molecule}^{-1} \text{ s}^{-1}$$

subject to relatively large error limits.

More recently, Cox and Patrick [85] determined, by a short extrapolation from their absolute rate constant data at total pressures of 40-600 torr, that

$$k_{28} \text{ (M=}N_2+O_2\text{)} \simeq 1.0 \times 10^{-12} \text{ cm}^3 \text{ molecule}^{-1} \text{ s}^{-1}$$

at atmospheric pressure and 284 K.

Additionally, NASA [3] has estimated that

$$k_{28} = 1.45 \times 10^{-12} \text{ cm}^3 \text{ molecule}^{-1} \text{ s}^{-1}$$

at 300 K and 760 torr of air from the expression

$$k_{28} = \left\{ \frac{k_o(T)[M]}{1+k_o(T)[M]/k_\infty(T)} \right\} \times 0.6^{\{1+[\log_{10}(k_o(T)[M]/k_\infty(T))]^2\}^{-1}} \text{ cm}^3 \text{ molecule}^{-1} \text{ s}^{-1}$$

where

$$k_o(T) = 2.3 \times 10^{-31} (T/300)^{-4.6} \text{ cm}^6 \text{ molecule}^{-2} \text{ s}^{-1},$$

$$k_\infty(T) = 4.2 \times 10^{-12} \text{ cm}^3 \text{ molecule}^{-1} \text{ s}^{-1}$$

Since this estimate [3] at atmospheric pressure and room temperature appears to be somewhat higher than the available experimental data, we would recommend for lower tropospheric modeling purposes that the expression of Graham et al. [83] be used, i.e.,

$$k_{28} = 1.1 \times 10^{-12} \text{ cm}^3 \text{ molecule}^{-1} \text{ s}^{-1}$$

at 760 torr and 298 K, with an estimated uncertainty of a factor of 2.

The possible alternative reaction pathway to form HONO + O_2:

$$HO_2 + NO_2 \rightarrow HONO + O_2 \qquad (28b)$$

has been shown [81,82] to be of essentially negligible importance at atmospheric pressure and ~298 K, with

$$k_{28b} < 3 \times 10^{-15} \text{ cm}^3 \text{ molecule}^{-1} \text{ s}^{-1}$$

[82] and

$$\lesssim 1 \times 10^{-15} \text{ cm}^3 \text{ molecule}^{-1} \text{ s}^{-1}$$

[81,83].

$$HO_2NO_2 \xrightarrow{M} HO_2 + NO_2 \qquad (29)$$

Of the studies carried out [81,83,84,86], the most extensive is that of Graham et al. [83]. Since that study was the most direct, we recommend the rate constant obtained in that study, i.e., that for M=air,

$$k_{29} = 4.9 \times 10^{-6} e^{-10015/T} \times \{[M]/[1+4.86 \times 10^{-17}[M]^{0.61}]\} \text{ s}^{-1}$$

for atmospheric pressure and below. For atmospheric pressure, in their earlier study Graham et al. [81] obtained

$$k_{29} \text{ (M=air)} = 1.3 \times 10^{14} e^{-10418/T} \text{ s}^{-1},$$

in good agreement at around room temperature with

$$k_{29} = 1.26 \times 10^{16} e^{-11700/T} \text{ s}^{-1}$$

determined by Cox et al. [86]. For 760 torr of air at 298 K, these expressions yield

$k_{29} = 0.076\ s^{-1}$ [83],

$= 0.085\ s^{-1}$ [81], and

$= 0.112\ s^{-1}$ [86].

Since the study of Graham et al. [81] extended to higher pressures and temperatures than their later study, for atmospheric modeling purposes

$$k_{29}\ (M=air) = 1.3 \times 10^{14}\ e^{-10418/T}\ s^{-1}$$

is recommended. For lower pressures, the alternative expression of Graham et al. [83] should be used. At atmospheric pressure and room temperature, the uncertainties should be of the order of ±25%.

$$HO_2 + O_3 \rightarrow OH + O_2 + O_2 \qquad (30)$$

NASA [3] recommends:

$$k_{30} = 1.4 \times 10^{-14}\ e^{-580/T}\ cm^3\ molecule^{-1}\ s^{-1},$$

$$k_{30} = 2.0 \times 10^{-15}\ cm^3\ molecule^{-1}\ s^{-1}$$

at 298 K, with an uncertainty of a factor of 1.5.

This recommendation is based on the sole direct study of Zahniser and Howard [87].

$$HO_2 + HO_2 \rightarrow H_2O_2 + O_2 \qquad (31)$$

The status of temperature-dependent rate constant data for this reaction is still in a state of uncertainty.

The rate constant for this reaction has been shown to be temperature and pressure dependent, and to depend on the concentration of water vapor. The temperature and/or pressure dependencies have been investigated by Cox and Burrows [88], Lii et al. [89,90], Thrush and Wilkinson [91], Sander et al. [92], Simonaitis and Heicklen [93], Thrush and Tyndall [94,95] and Patrick and Pilling [96]. The effect of water vapor on the rate constant has been observed by Hamilton and Lii [97], Cox and Burrows [88], Sander et al. [92], and Lii et al. [90]. In the absence of water vapor, the data from Sander et al. [92], Simonaitis and Heicklen [93], and Thrush and Tyndall [94,95] show that at ∿300 K the rate constant has a limiting low pressure value of

$$k_{31} \sim 1.6 \times 10^{-12}\ cm^3\ molecule^{-1}\ s^{-1}$$

and that the rate constant increases with increasing pressure [92,93] to ∿(2.5-3.0) x 10^{-12} cm^3 $molecule^{-1}$ s^{-1} at 760 torr of air.

NASA [3] recommends

$$k_{31} = (1.6 + 1.2\ P_{atm}) \times 10^{-12}\ cm^3\ molecule^{-1}\ s^{-1}$$

at 298 K with an uncertainty of a factor of 1.5

$$= (3.4 + 2.5\ P_{atm}) \times 10^{-14}\ e^{(1150\pm600)/T}\ cm^3\ molecule^{-1}\ s^{-1},$$

based on the temperature dependencies of Cox and Burrows [88] and Lii et al. [89].

However, it should be noted that more recently Thrush and Tyndall [95] and Patrick and Pilling [96] have determined significantly lower negative Arrhenius activation energies of -1.11 kcal mol^{-1} at 7-20 torr total pressure [95] and -(1.25 ± 0.23) kcal mol^{-1} at 700 torr total pressure of N_2 [96]. Hence the temperature dependence of this reaction may be less than that recommended by NASA [3].

$$HO_2 + HO_2 + H_2O \rightarrow H_2O_2 + O_2 + H_2O \qquad (32)$$

The effect of water vapor on reaction (31), i.e., the occurrence of reaction (32), has been investigated by Hamilton and Lii [97], Cox and Burrows [88], Lii et al. [90], and Sander et al. [92]. Hamilton and Lii [97] obtained

$$k_{32} = 6.25 \times 10^{-30}\ cm^6\ molecule^{-2}\ s^{-1}$$

at 295 K, Cox and Burrows [88] determined k_{32} to be:

$$k_{32} = 3.2 \times 10^{-30}\ cm^6\ molecule^{-2}\ s^{-1}$$

at 298 K, with an Arrhenius activation energy of -(11.5±2.4) kcal mol^{-1}, while Sander et al. [92] and Lii et al. [90] determined

$$k_{32} \sim 6 \times 10^{-30}\ cm^6\ molecule^{-2}\ s^{-1}$$

at 298 K.

We recommend that:

$$k_{32} = 6 \times 10^{-30}\ cm^6\ molecule^{-2}\ s^{-1}$$

at 298 K, with an uncertainty of a factor of 3, and with an Arrhenius activation energy of ∿-11.5 kcal mol^{-1}, i.e.,

$$k_{32} = 2.2 \times 10^{-38}\ e^{5800/T}\ cm^6\ molecule^{-2}\ s^{-1}$$

This temperature-dependent rate constant k_{32} must be viewed with caution and is applic-

able, with the available experimental data, over the narrow temperature range 278-318 K. Obviously, much further work is necessary on this reaction. This reaction proceeds via complex formation, i.e.,

$$HO_2 + H_2O \rightleftharpoons (HO_2 \cdot H_2O)$$

(equilibrium constant K)

$$HO_2 + (HO_2 \cdot H_2O) \xrightarrow{k_a} (H_2O_4) + H_2O$$

$$(H_2O_4) \rightarrow H_2O_2 + O_2$$

and hence $k_{32} = k_a K$.

$$H_2O_2 + h\nu \rightarrow 2\ OH \qquad (33)$$

The recommended absorption cross-sections are those recommended by NASA [3] (table 7), based on the mean of the data of Molina and Molina [58] and of Lin et al. [98], which are in excellent agreement over the 210-350 nm wavelength region. The quantum yield for photodissociation is taken as unity.

$$OH + H_2O_2 \rightarrow HO_2 + H_2O \qquad (34)$$

This reaction is apparently unimportant for computer modeling of photochemical air pollution.

Based upon the recent data of Sridharan et al. [99], Keyser [100], Wine et al. [101], and Kurylo et al. [102], NASA [3] recommends

$$k_{34} = 3.1 \times 10^{-12}\ e^{-(187\pm100)/T}\ cm^3\ molecule^{-1}\ s^{-1}$$

$$= 1.7 \times 10^{-12}\ cm^3\ molecule^{-1}\ s^{-1}$$

at 298 K, with an uncertainty of a factor of 1.3 at 298 K.

Effect of H_2O Vapor on HO_2 Reactions. (35)

While it is now evident that H_2O vapor significantly increases the recombination rate of HO_2 radicals via complex formation, [88,90, 92,97] i.e.,

$$HO_2 + H_2O \rightleftharpoons (HO_2 \cdot H_2O)$$

$$HO_2 + (HO_2 \cdot H_2O) \rightarrow\!\!\rightarrow H_2O_2 + O_2 + H_2O$$

there is, at present, no evidence for or against an H_2O vapor effect on other HO_2 reactions. This obviously depends on the relative rate constants for

$$HO_2 + X \xrightarrow{k_a} \text{products}$$

and

$$(HO_2 \cdot H_2O) + X \xrightarrow{k_b} \text{products}$$

If K is the equilibrium constant for

$$HO_2 + H_2O \underset{d}{\overset{c}{\rightleftharpoons}} (HO_2 \cdot H_2O).\ \text{i.e.,}$$

$$K = \frac{k_c}{k_d}$$

Then, k^{obs} (i.e., where $-d[HO_2]/dt = k^{obs}[HO_2][X]$)

is given by:

$$k^{obs} = k_a + \frac{k_b\ k_c\ [H_2O]}{(k_d + k_b\ [X])}$$

Presuming that $k_d >> k_b\ [X]$, then

$$k^{obs} \approx k_a + k_b\ K[H_2O].$$

Since $K \approx 1 \times 10^{-19}$ cm^3 molecule^{-1} at 298 K [88,97] then for 50% relative humidity (RH) ($\sim 5 \times 10^{17}$ molecule cm^{-3}) $K[H_2O] \sim 5 \times 10^{-2}$ and $k_b/k_a < 2$ for no observable (10%) effect at 50% RH. Obviously, data concerning this possible H_2O vapor effect are urgently needed.

3. Formaldehyde Chemistry

$$O(^3P) + HCHO \rightarrow \text{Products} \qquad (36)$$

This reaction is of minimal importance as a loss process for HCHO under atmospheric conditions, photolysis and reaction with OH radicals being the primary sinks.

Three recent temperature dependent rate constant determinations have been carried out for this reaction [103-105], with the data being in excellent agreement; values of $10^{13} \times k_{36}$ at 298 K (cm^3 molecule^{-1} s^{-1}) and E/T (K) being: 1.7±0.2, 1583±73 [103]; 1.61±0.17, 1525±40 [104]; and 1.50±0.10, 1554±126 [105].

We agree with the NASA [3] recommendation of

$$k_{36} = 3.0 \times 10^{-11}\ e^{-(1550\pm250)/T}\ cm^3\ molecule^{-1}\ s^{-1}$$

$$= 1.6 \times 10^{-13}\ cm^3\ molecule^{-1}\ s^{-1}$$

at 298 K, with an estimated uncertainty of a factor of 1.25.

Earlier product studies [106-108] concluded that the reaction proceeds via

$$O(^3P) + HCHO \rightarrow OH + HCO$$

However, Chang and Barker [103] have suggested from the observed CO_2 yield and its invariance on the O_2 concentration [which rules out the reaction

$$O(^3P) + HCO \rightarrow H + CO_2$$

as the CO_2 source since

$$O_2 + HCO \rightarrow HO_2 + CO$$

is fast] that the overall reaction may proceed via $O(^3P)$ atom addition to HCHO to ultimately form a triplet HCOOH which decomposes to HCO + OH and CO_2 + 2 H.

Since the number of radicals ultimately formed (HO_2 + OH or 2 HO_2) are the same and this reaction is of minimal importance under atmospheric conditions, we recommend that the reaction sequence

$$O(^3P) + HCHO \rightarrow OH + HCO$$

be used.

$$HCHO + h\nu \rightarrow H + HCO \qquad a \qquad (37)$$

$$\rightarrow H_2 + CO \qquad b$$

The absorption cross-sections of HCHO have been recently determined by Bass et al. [109] and Moortgat et al. [110], the latter data being ~30% higher for $\lambda \gtrsim 300$ nm. The NASA recommended cross-section values [3] are the mean of the two sets of data, and are given in table 8 averaged over 10 nm intervals at 220 K and 290 K (the temperature dependence is small).

The quantum yield measurements of Horowitz and Calvert [111], Clark et al. [112], Moortgat and Warneck [113], Tang et al. [114], and Moortgat et al. [110,115] are in good agreement (figure 3). The NASA [3] recommended quantum yields ϕ_a and ϕ_b at 760 torr total pressure of air, averaged over 10 nm intervals, are given in table 9. For $\lambda \gtrsim 330$ nm the overall photodissociation quantum yield ($\phi_a + \phi_b$) is less than unity.

$$OH + HCHO \rightarrow H_2O + HCO \qquad (38)$$

Rate constant data for this reaction through 1978 have been reviewed by Atkinson et al. [116]. The rate constants obtained by Morris and Niki [117] and Niki et al. [118], using discharge flow-mass spectrometry and a relative rate technique, respectively, are in very good agreement with

$$k_{38} = 1.4 \times 10^{-11} \text{ cm}^3 \text{ molecule}^{-1} \text{ s}^{-1}$$

at 298 K [116].

However, the two recent flash photolysis-resonance fluorescence temperature dependence studies of Atkinson and Pitts [119] and of Stief et al. [120] obtained values of

$$k_{38} \ (9.4 \pm 1.0) \times 10^{-12} \text{ cm}^3 \text{ molecule}^{-1} \text{ s}^{-1}$$

and

$$k_{38} \ (9.9 \pm 1.1) \times 10^{-12} \text{ cm}^3 \text{ molecule}^{-1} \text{ s}^{-1}$$

at 298 K, respectively, with a zero or near zero temperature dependence.

The rate constants k_{38} determined by Smith [121], derived relative to the rate constant for the combination reaction of OH radicals, are significantly lower than the other literature data, and must be regarded as being of low accuracy. As shown in figure 4, the rate constants obtained by Atkinson and Pitts [119] and Stief et al. [120] are in excellent agreement over the temperature range common to both studies, and combining these data, we recommend (as does NASA [3]) that:

$$k_{38} = 1.01 \times 10^{-11} \text{ cm}^3 \text{ molecule}^{-1} \text{ s}^{-1}$$

independent of temperature, with an estimated uncertainty of ±25%.

It has been suggested [103,122] that this reaction proceeds, at least in part, via OH radical addition, initially forming $HOCH_2O$ which could decompose to HCOOH + H or react with O_2 to yield HCOOH + HO_2. However, Niki [123] and Morrison and Heicklen [124] reported data which indicate that this pathway is unimportant.

$$HO_2 + HCHO \rightarrow HO_2CH_2O \qquad (39)$$

Recent work [125-128] has shown that the reaction of HO_2 radicals with HCHO proceeds via addition to initially form the HO_2CH_2O radical (reaction 39). Two distinct chemical schemes have been used to study this reaction. Su et al. [125,126] and Niki et al. [128] have used Fourier transform infrared absorption spectroscopy to investigate the photolysis of Cl_2-HCHO-O_2-N_2 and Cl_2-HCHO-H_2-O_2-N_2 mixtures, and have identified the metastable compound HO_2CH_2OH. In this system the reaction sequence was postulated to be [126]:

$$HO_2 + HCHO \rightleftarrows (HO_2CH_2O) \rightleftarrows O_2CH_2OH \quad (39,-39)$$

$$HO_2 + O_2CH_2OH \rightarrow HO_2CH_2OH + O_2$$

$$2\ O_2CH_2OH \rightarrow 2\ OCH_2OH + O_2$$

Table 7. Absorption Cross-Sections of H_2O_2 Vapor, As Recommended by NASA [3], for the Wavelength Region 250-350 nm

λ (nm)	10^{20} x σ (cm^2)
250	8.3
255	6.7
260	5.2
265	4.2
270	3.2
275	2.5
280	2.0
285	1.5
290	1.13
295	0.87
300	0.66
305	0.49
310	0.37
315	0.28
320	0.20
325	0.15
330	0.12
335	0.09
340	0.07
345	0.05
350	0.03

Table 8. Absorption Cross Sections of CH_2O (From NASA [3])

λ (nm)	10^{20} x σ (cm^2) 290 K	220 K
240	0.03	0.08
250	0.13	0.08
260	0.47	0.47
270	0.86	0.85
280	1.86	1.93
290	2.51	2.47
300	2.62	2.58
310	2.45	2.40
320	1.85	1.71
330	1.76	1.54
340	1.18	1.10
350	0.42	0.39
360	0.06	0.02

Note: The values are averaged for 10 nm intervals centered on the indicated wavelength.

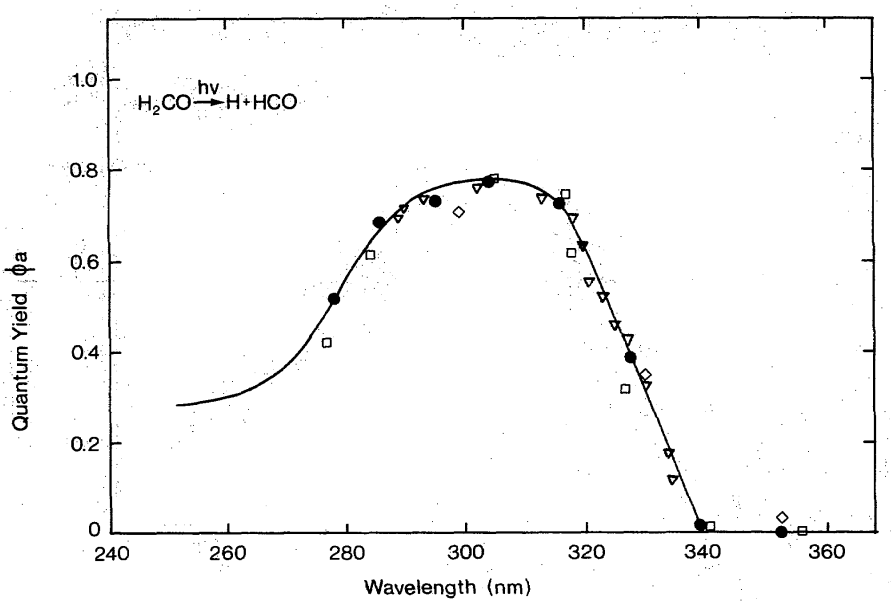

Figure 3. Quantum yield ϕa for the photodissociation of HCHO. ● Data of Moortgat et al. [110, 115] at 300 K; □ Data of Moortgat and Warneck [113] as corrected by Moortgat et al. [115]; ▽ Data of Horowitz and Calvert [111]; ◊ Data of Clark et al [112]. (Adapted from [115].)

Table 9. Quantum Yields ϕ_a and ϕ_b for the Photodissociation of HCHO at 760 Torr Total Pressure of Air (From NASA [3])

λ (nm)	ϕ_1 (H + HCO)	ϕ_2 (H_2 + CO)
240	0.21	0.42
250	0.24	0.46
260	0.30	0.48
270	0.40	0.46
280	0.59	0.35
290	0.71	0.26
300	0.78	0.22
310	0.77	0.23
320	0.62	0.38
330	0.17	0.80
340	0	0.69[a]
350	0	0.40[a]
360	0	0.12[a]

Note: The values are averaged for 10 nm intervals centered on the indicated wavelength.

[a]: At p = 760 torr, pressure dependent.

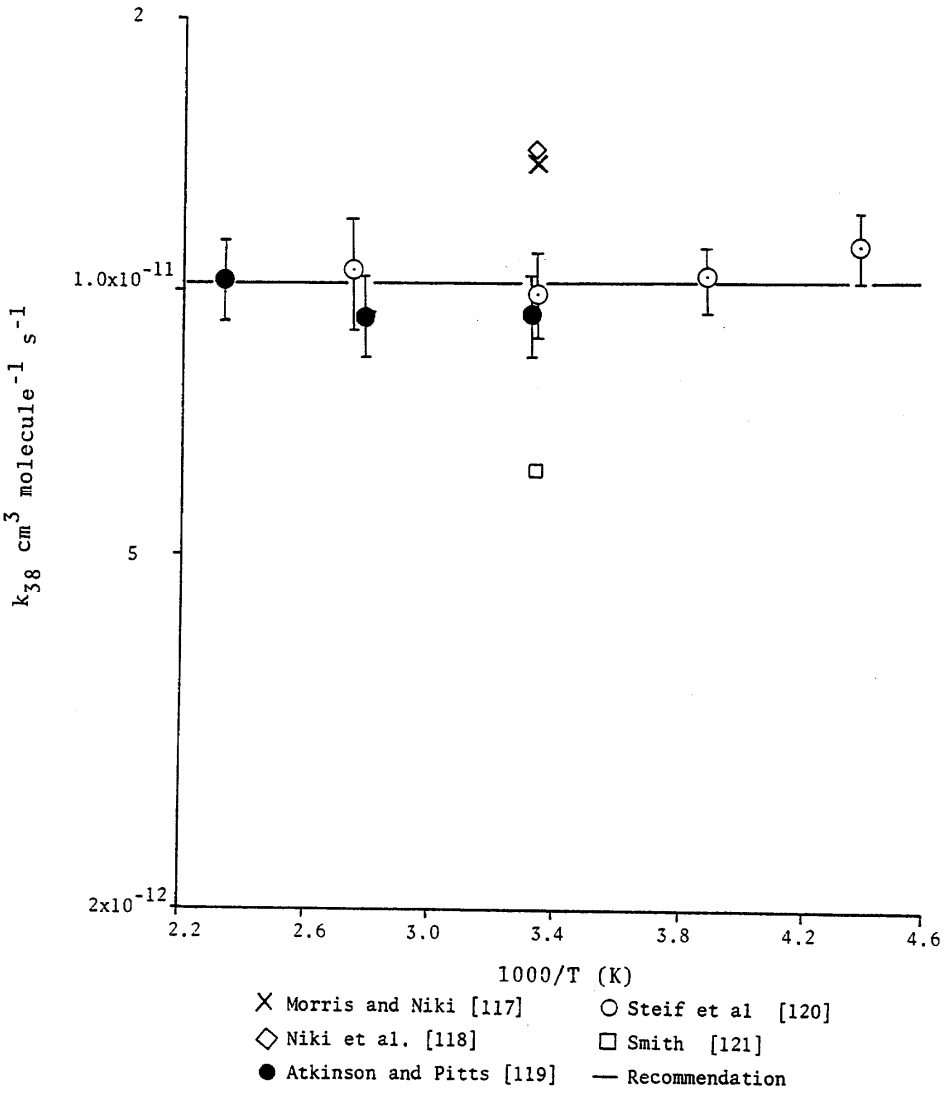

Figure 4. Rate Constants for k_{38} for the Reaction of OH Radicals with HCHO.

$$OCH_2OH + O_2 \rightarrow HCO_2H + HO_2 \quad (40)$$

$$HO_2CH_2OH \xrightarrow{\text{(wall)}} HCO_2H + H_2O$$

$$HO_2CH_2OH + h\nu \rightarrow HCO_2H + H_2O$$

From a kinetic computer analysis of the data, assuming that the O_2CH_2OH radical behaves analogously to the CH_3O_2 radical with respect to self-combination and reaction with O_2, Su et al. [125,126] derived

$$k(HO_2 + HCHO) = k_{39}$$

$$= 1.0 \times 10^{-14} \text{ cm}^3 \text{ molecule}^{-1} \text{ s}^{-1}$$

and

$$k_{-39} \approx 1.5 \text{ s}^{-1}$$

both at 298 K and 700 torr total pressure.

Su et al. [126] further reported that the HO_2CH_2OH species decayed in the dark, and more rapidly in the light, to yield formic acid, with a photolysis rate constant of ~ 0.039 s^{-1} in their system for photolysis conditions apparently reasonably similar to noontime summer conditions [$k(NO_2 + h\nu) = 0.01$ s^{-1}]. Under atmospheric conditions in the presence of NO_x, the reactions subsequent to the initial addition of HO_2 to HCHO are, however, expected to be:

$$HO_2 + HCHO \rightarrow (HOOCH_2O) \rightarrow OOCH_2OH$$

This peroxy radical can, in the presence of NO_x, react via:

$$OOCH_2OH + NO \rightarrow NO_2 + OCH_2OH \quad (41)$$

and

$$OOCH_2OH + NO_2 \rightleftarrows HOCH_2OONO_2$$

The latter reaction product ($HOCH_2OONO_2$) has been observed by Niki et al. [129], but, analogous to other alkyl peroxynitrates, it is expected (see reaction 51) to thermally back-decompose rapidly to reactants. The reaction with NO is expected, analogous to other peroxy radicals, to have a rate constant

$$k_{41} \sim 7 \times 10^{-12} \text{ cm}^3 \text{ molecule}^{-1} \text{ s}^{-1}$$

at room temperature (see acetaldehyde chemistry section below). Hence, for NO concentrations $\gtrsim 2 \times 10^{11}$ molecule cm^{-3} ($\sim$10 ppb), the reaction with NO will predominate. The alkoxy radical is then expected [125,127] to react with O_2 to yield formic acid:

$$OCH_2OH + O_2 \rightarrow HCO_2H + HO_2$$

Indeed, in the most recent study of flashed HCHO-O_2-NO mixtures, Veyret et al. [127], by monitoring NO_2 formation, postulated this same reaction sequence:

$$HO_2 + HCHO \rightarrow HOOCH_2O \rightarrow O_2CH_2OH \quad (39)$$

$$O_2CH_2OH + NO \rightarrow OCH_2OH + NO_2 \quad (41)$$

$$OCH_2OH + O_2 \rightarrow HCO_2H + HO_2 \quad (40)$$

$$OCH_2OH + NO \rightarrow \text{products} \quad (42)$$

Using a rate constant of

$$k_{41} = 7.5 \times 10^{-12} \text{ cm}^3 \text{ molecule}^{-1} \text{ s}^{-1}$$

the data at room temperature were fit [127] by

$$k_{39} = (7.5 \pm 3.5) \times 10^{-14} \text{ cm}^3 \text{ molecule}^{-1} \text{ s}^{-1}$$

$$k_{40} = (3.5 \pm 1.6) \times 10^{-14} \text{ cm}^3 \text{ molecule}^{-1} \text{ s}^{-1}$$

(a factor of $\sim$30 higher than for $CH_3O + O_2$ [reaction (57)])

and

$$k_{42} = (4.0 \pm 1.9) \times 10^{-11} \text{ cm}^3 \text{ molecule}^{-1} \text{ s}^{-1}$$

Obviously further work as to the rate constants in these systems is needed. However, at the present time we recommend that the rate data of Veyret et al. [127] be used, subject to confirmation.

Hence for NO concentrations >10 ppb, we anticipate that the reaction of HO_2 radicals with HCHO will ultimately yield HCOOH. For lower NO levels, i.e. [NO] <10 ppb, decomposition of the $OOCH_2OH$ species back to the reactants is expected [126]. It must, of course, be noted that only when NO concentrations decrease do HO_2 concentrations increase, and it is possible that under atmospheric conditions this reaction is of little importance. However, it resolves the apparent conflict of previous observations of formic acid formation in HCHO photooxidations and the fact that HCO radicals react with O_2 to yield HO_2 + CO, and not HCO_3 (see later).

As to whether the higher aldehydes react with HO_2 by analogous reaction pathways is, at present, unknown; and again, further work on these systems is obviously needed.

$$NO_3 + HCHO \rightarrow HNO_3 + HCO \quad (43)$$

The sole study of this reaction to date is that recently carried out by Atkinson et al. [130]. From the enhanced decay rates of N_2O_5 in N_2O_5-NO_2-HCHO-air mixtures, a value of

$k_{43} = (3.23 \pm 0.26) \times 10^{-16}$ cm^3 molecule^{-1} s^{-1}

at 298±1 K was derived, using the equilibrium constant $K_{7,8}$ of Malko and Troe [27]. In the absence of further experimental data, we recommend this value of k_{43}, with an estimated uncertainty of a factor of ∿2, i.e.,

$$k_{43} = 3.2 \times 10^{-16} \text{ cm}^3 \text{ molecule}^{-1} \text{ s}^{-1}$$

$$HCO + O_2 \rightarrow HO_2 + CO \qquad (44)$$

The reaction of HCO with O_2 is, under atmospheric conditions, effectively the sole loss process of HCO, and hence the precise value of its rate constant, since it is rapid, is of little concern. The evidence to date shows conclusively that the reaction proceeds as shown [116]. Thus, Hunziker and Wendt [131] observed that the addition of CO to the H + O_2 reaction in an amount sufficient to intercept >90% of the H atoms by the reaction:

$$H + CO + M \rightarrow HCO + M$$

had no observable effect on the observed HO_2 absorption, showing conclusively that HO_2 formation from the reaction of HCO radicals with O_2 is the only important pathway at 313 K and atmospheric pressure. In addition, no new absorption bands associated with HCO_3 were observed [131]. This reaction pathway has also been confirmed by the detection of HO_2NO_2 from the irradiation of HCHO-Cl_2-NO_2-O_2 mixtures [132], by the lack of a pressure dependence on the rate constant for reaction (44) [133], and by the laser magnetic resonance detection of HO_2 from the reaction of HCO radicals with O_2 [134]. Furthermore, the evidence for HCO_3 formation was mainly based upon observation of HCOOH in irradiated Cl_2-HCHO-O_2 mixtures [135,136]. This is now known to be due to the addition reaction of HO_2 with HCHO.

NASA [3] has recommended:

$$k_{44} = 5.5 \times 10^{-12} \text{ cm}^3 \text{ molecule}^{-1} \text{ s}^{-1}$$

at 298 K, with an uncertainty of a factor of 1.3.

$$= 3.5 \times 10^{-12} \, e^{(140 \pm 140)/T} \text{ cm}^3 \text{ molecule}^{-1} \text{ s}^{-1}$$

with the rate constant at 298 K and the temperature dependence being essentially identical to those measured by Veyret and Lesclaux [137].

4. Acetaldehyde Chemistry

$$O(^3P) + CH_3CHO \rightarrow CH_3CO + OH \qquad (45)$$

The most recent rate constant determination for this reaction is that of Singleton et al. [138], who obtained

$$k_{45} = 1.2 \times 10^{-11} \, e^{-(986 \pm 77)/T} \text{ cm}^3 \text{ molecule}^{-1} \text{ s}^{-1}$$

$$= 4.3 \times 10^{-13} \text{ cm}^3 \text{ molecule}^{-1} \text{ s}^{-1}$$

at 298 K, the data being in good agreement with previous rate constant data of Mack and Thrush [139], Cadle and Powers [140] and Cvetanovic [141].

The reaction has been shown to proceed via H atom abstraction from the aldehydic C-H group [139,142], with H atom abstraction from the CH_3 group accounting for ∿0.1% of the total reaction pathway at 298 K [138].

We recommend the data of Singleton et al. [138], i.e.,

$$k_{45} = 1.2 \times 10^{-11} \, e^{-986/T} \text{ cm}^3 \text{ molecule}^{-1} \text{ s}^{-1}$$

$$= 4.3 \times 10^{-13} \text{ cm}^3 \text{ molecule}^{-1} \text{ s}^{-1}$$

at 298 K, with an estimated uncertainty of a factor of 1.25.

$$CH_3CHO + h\nu \rightarrow CH_3 + HCO \qquad a \qquad (46)$$

$$\rightarrow CH_4 + CO \qquad b$$

$$\rightarrow H + CH_3CHO \qquad c$$

$$\rightarrow H_2 + CH_2CO \qquad d$$

The very recent data of Calvert and coworkers [143,144] and Moortgat and coworkers [145] have greatly clarified the position regarding the primary processes occurring in the photolysis of acetaldehyde. As discussed by Calvert and coworkers [143,144], the possible primary processes are:

$$CH_3CHO + h\nu \rightarrow CH_3CHO^*$$

$$CH_3CHO^* \rightarrow CH_3 + HCO \qquad \phi_a$$

$$\rightarrow CH_4 + CO \qquad \phi_b$$

$$\rightarrow H + CH_3CO \qquad \phi_c$$

$$\rightarrow H_2 + CH_2CO \qquad \phi_d$$

It was concluded [143,144] for $\lambda \geq 290$ nm at 298 K that ϕ_d is negligible. The quantum yields ϕ_a and ϕ_b determined by these two groups at 760 torr total pressure of air are in generally excellent agreement, and the quantum yields ϕ_a, ϕ_b and ϕ_c are given in table 10. These quantum yields are applicable only at 760 torr of air, since they are pressure dependent [143-145], and reference 144 should be consulted for further details. These data show that radical formation from CH_3CHO photolysis in the lower troposphere is far less than radical formation from HCHO photolysis [144].

The quantum yields for ϕ_a and ϕ_b given in table 10 are plotted against wavelength in figure 5, and our recommendation is shown as the solid curve. Our recommended values of ϕ_a and ϕ_b taken from this figure are also given in table 10.

$$OH + CH_3CHO \rightarrow H_2O + CH_3CO \qquad (47)$$

Rate constants for this reaction have been measured by Niki and coworkers [118,146] and by Atkinson and Pitts [119]. The data from these studies are in very good agreement [116], with the recommended rate constant being that of Atkinson and Pitts [119], that study being the only one carried out over a range of temperature, to give the expression:

$$k_{47} = 6.9 \times 10^{-12} e^{(250\pm150)/T} \text{ cm}^3 \text{ molecule}^{-1} \text{ s}^{-1}$$

$$= 1.6 \times 10^{-11} \text{ cm}^3 \text{ molecule}^{-1} \text{ s}^{-1}$$

at 298 K, with an estimated uncertainty of $\pm 25\%$.

Evidence that the reaction proceeds predominately as shown is obtained from product formation studies carried out in smog chambers (i.e., PAN formation).

$$CH_3CO + O_2 \rightarrow CH_3\overset{O}{\overset{\|}{C}}OO \cdot \qquad (48)$$

This reaction is expected to be fast, by analogy with alkyl radicals, and the infrared electronic spectrum attributed to CH_3CO_3 has been observed in the wavelength regions 1.2-1.8 μ by Hunziker and Wendt [131,147], following the Hg-photosensitized decomposition of CH_3CHO, $CH_3COCOCH_3$ or CH_3COCH_3 in the presence of O_2, and 210-250 nm by Addison et al. [148] following the modulated photolysis of CH_3COCH_3 and $CH_3COCOCH_3$ in the presence of O_2, or of Cl_2-CH_3CHO-O_2 mixtures. Under atmospheric conditions, this reaction is anticipated to be the sole reaction of CH_3CO radicals.

$$CH_3CO_3NO_2(PAN) \rightarrow CH_3CO_3 + NO_2 \qquad (49)$$

It has been shown that PAN thermally decomposes as shown, and that this reaction is in equilibrium with the reverse reaction [149-151]. Thermal decomposition rate constants, k_{49}, have been measured in four studies, mainly by using excess NO which perturbs the equilibrium via the reaction

$$CH_3CO_3 + NO \rightarrow CH_3CO_2 + NO_2$$

The rate constant data reported to date are given in table 11.

The data of Pate et al. [149], Hendry and Kenley [150] and of Nieboer and Duyzer [152] were obtained from the thermal decomposition of PAN in the presence of excess NO, where:

$$-d \ln[PAN]/dt = k_{49}$$

The derivation of values of k_{49} from the data of Cox and Roffey [151] involves the knowledge of the number of NO molecules removed following reaction of CH_3CO_3 with NO, and hence is subject to larger uncertainties.

Figure 6 shows an Arrhenius plot of the available data--the data of Nieboer and Duyzer [152] were reported graphically; hence their Arrhenius line has been estimated from their figure. It can be seen that the data of Hendry and Kenley [150], Pate et al. [149] (possibly fortuitous in view of the ±1 K temperature and the ±30% error limits of that study) and Nieboer and Duyzer [152] are in excellent agreement. In the study of Cox and Roffey [151], the determination of the number of NO molecules removed per PAN decomposition (4.9 ± 1.7) was carried out in a static experiment at 296 K, and the value of k_{49} derived from that experiment [$(2.65 \pm 1.0) \times 10^{-4}$ s^{-1}] is also in excellent agreement with the other data [149,150,152]. The lower temperature ($T \leq 313$ K) rate constants derived from the dynamic experiments of Cox and Roffey [151] are somewhat higher than but, because of the much wider error limits, still within agreement with the other data. Hence, we recommend the Arrhenius expression of Hendry and Kenley [150] of

$$k_{49} = 1.95 \times 10^{16} e^{-13543/T} \text{ s}^{-1}$$

$$= 3.6 \times 10^{-4} \text{ s}^{-1}$$

at 298 K, with an estimated uncertainty of ±20% over the temperature range 280-320 K.

$$CH_3CO_3 + NO \rightarrow CH_3CO_2 + NO_2 \qquad (50)$$

No direct experimental data are available for this reaction. The only data available are for the rate constant ratio $k_{50}/k(CH_3CO_3 + NO_2)$ [150,151,153] in combination with thermochemical estimates of the entropy change associated with reaction (49), and with a recent absolute rate constant determination

Table 10. Quantum Yields of the Primary Photodissociation Processes for CH_3CHO at Various Wavelengths at 760 Torr Total Pressure and 298 K

(Obs = Observed Data of References 144, 145; Rec = Recommended Value)

λ nm	ϕ_a		ϕ_b		ϕ_c
	Obs	Rec	Obs	Rec	
260	0.31[a]	0.31	0.47[a]	0.47	
270	0.38[a]	0.38	0.33[a]	0.33	
280	0.59[a]	0.59	0.06[a]	0.06	
290	0.54[a]; 0.56[b]	0.55	0.00[a]; 0.01[b]	0.01	0.026[b]
300	0.44[a]; 0.37[b]	0.415	0.00[a]; 0.00[b]	0.00	0.009[b]
310	0.29[a]	0.235	0.00[a]	0.00	
313	0.14[b]		0.01[b]		0.002[b]
320	0.10[a]; 0.053[b]	0.08	0.00[a]; 0.01[b]	0.00	0.00[b]
330	0.00[a]	0.00	0.00[a]	0.00	
331-2	0.01[b]		0.01[b]		0.00[b]

[a] From [145], values taken at 10 nm intervals from the figures in that presentation.

[b] From [144], estimated for 760 torr of air.

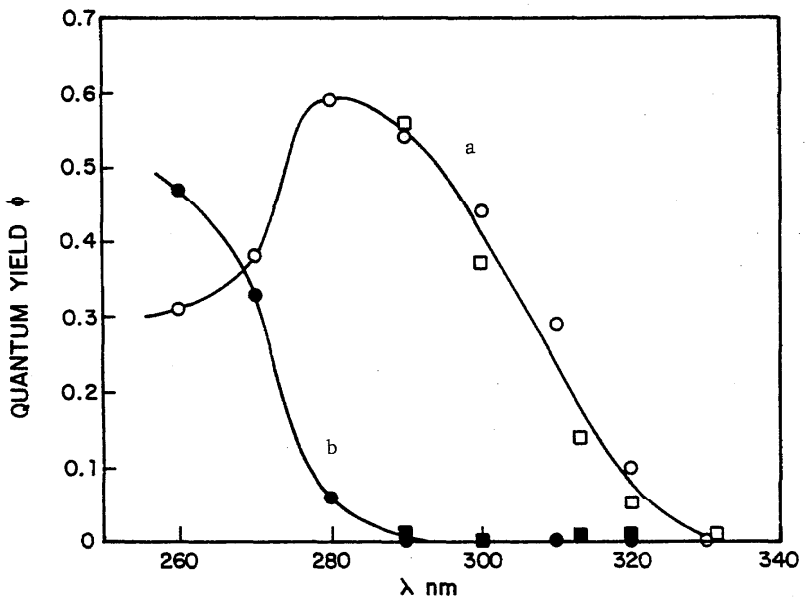

Figure 5. Quantum yields ϕ_a and ϕ_b for photodissociation of CH_3CHO. □, ■ - reference 144, O, ● - reference 145, — recommended.

Table 11. Rate Constants k_{49} at Room Temperature and Arrhenius Parameters for the Thermal Decomposition of PAN

A s^{-1}	E/T (K)	$10^4 \times k_{49}$ s^{-1}	T K	Reference
		2.8 ± 0.8	296 ± 1	149
1.95×10^{16}	13543 ± 453	3.70 ± 0.37	298	150
7.94×10^{14}	12510 ± 385	4.7	298	151
1×10^{18}	14595 ± 1007	4.0 ± 1.5	298	152

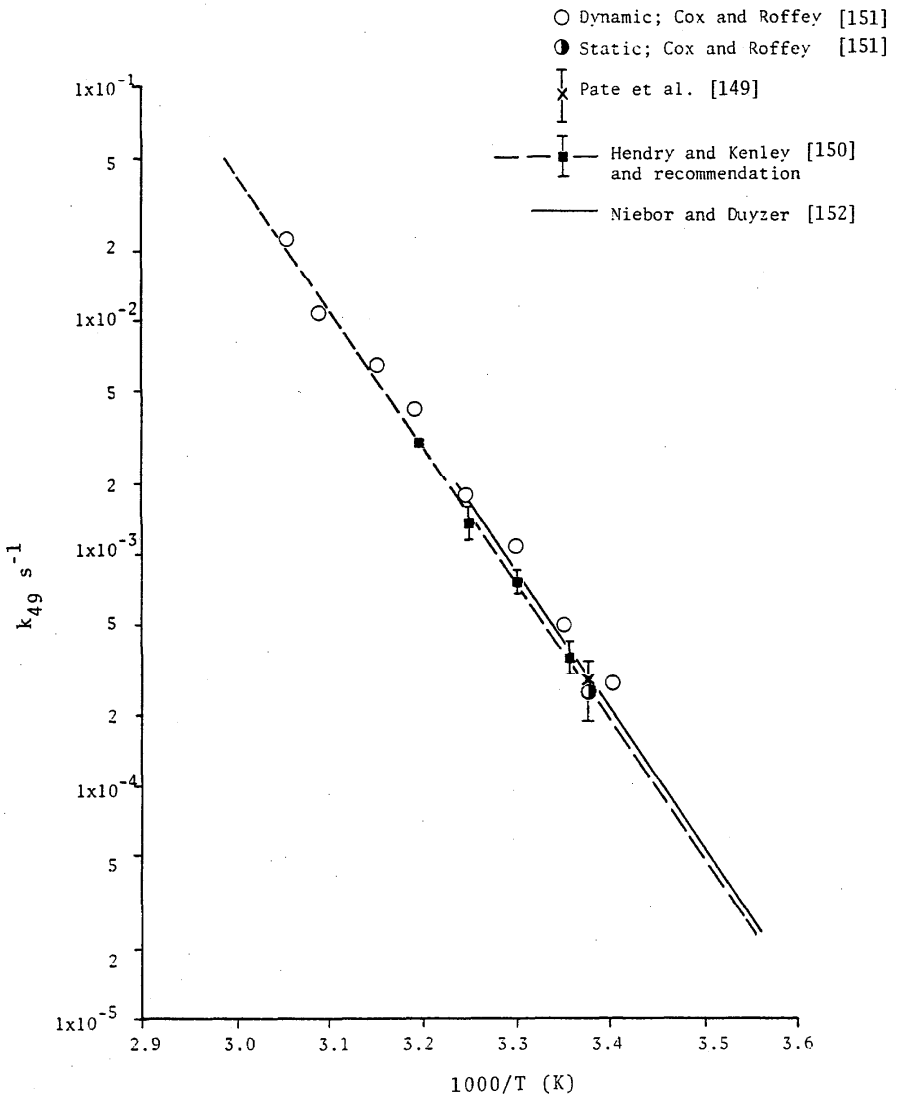

Figure 6. Literature Data For the Thermal Decomposition of PAN.

of the rate constant for the reaction CH_3CO_3 + NO_2 [148]. These thermochemical estimates assume that both reaction (50) and the reaction CH_3CO_3 + NO_2 → PAN have zero temperature dependencies, and hence they are realistically good to an order of magnitude only, predicting [150,151] that $k_{50} \approx 3 \times 10^{-12}$ cm^3 molecule^{-1} s^{-1} at room temperature, while the large uncertainties in the rate constant ratio $k_{50}/k(CH_3CO_3 + NO_2)$ and in the recent determination [148] of the rate constant for the reaction of CH_3CO_3 + NO_2 also leads to large (factors of 2 or 3) uncertainties in k_{50}.

We take the approach of considering RO_2 + NO reactions as a class, and derive/estimate a rate constant which, in the absence of further data, we assume applies to all RO_2 + NO and RCO_3 + NO reactions. We then proceed to do the same for the RO_2 + NO_2 reactions:

$$CH_3O_2 + NO \rightarrow CH_3O + NO_2 \qquad (50)$$

$$RO_2 + NO \rightarrow \text{Products}$$

$$RCO_3 + NO \rightarrow \text{Products}$$

Table 12 gives the rate constants obtained for the reaction of RO_2 radicals with NO, by both absolute and relative rate techniques. It can be seen that there is a discrepancy of a factor of 2-3 in the rate constant data for both methylperoxy and ethylperoxy radicals.

The recent studies of Cox and Tyndall [158,159], Sander and Watson [161], Ravishankara et al. [162], Simonaitis and Heicklen [163] and Plumb et al. [164] concerning the CH_3O_2 + NO reaction appear to be free of possible experimental problems, and are seen to be in good agreement as to the magnitude of the rate constant k_{50} at room temperature. No significant pressure dependence has been observed [161-163]. From these studies NASA recommends [3] a rate constant of

$$k_{50} = 7.6 \times 10^{-12} \text{ cm}^3 \text{ molecule}^{-1} \text{ s}^{-1}$$

at 298 K, with an uncertainty of a factor of 1.2.

The two temperature dependent studies [162,163] show that the rate constant k_{50} (CH_3O_2 + NO) has a small negative temperature dependence, and based upon these two studies [162,163] NASA [3] recommends

$$k_{50} = 4.2 \times 10^{-12} \, e^{(180 \pm 180)/T} \text{ cm}^3 \text{ molecule}^{-1} \text{ s}^{-1}$$

with

$$k_{50} = 7.6 \times 10^{-12} \text{ cm}^3 \text{ molecule}^{-1} \text{ s}^{-1}$$

at 298 K, as stated above.

The datum of Plumb et al. [166] for the reaction of $C_2H_5O_2$ with NO also appears to be free from experimental problems. Since this rate constant is, within the experimental uncertainties, identical to those for the reactions of HO_2 and CH_3O_2 radicals with NO, we further recommend that

$$k_{50} = 7.6 \times 10^{-12} \text{ cm}^3 \text{ molecule}^{-1} \text{ s}^{-1}$$

$$= 4.2 \times 10^{-12} \, e^{180/T} \text{ cm}^3 \text{ molecule}^{-1} \text{ s}^{-1}$$

for all RO_2 and RCO_3 radical reactions with NO.

The reaction of CH_3O_2 radicals with NO has been shown, from product studies [154, 162,167,168], to proceed primarily via the reaction:

$$CH_3O_2 + NO \rightarrow CH_3O + NO_2$$

while Plumb et al. [166] have shown that the reaction of $C_2H_5O_2$ radicals with NO produces NO_2 ≥80% of the time.

For the larger RO2 radicals, however, the data of Darnall et al. [169], Carter et al. [7], and Atkinson et al. [170] show that the reaction

$$RO_2 + NO \rightarrow [RO_2NO] \rightarrow RONO_2 \qquad (50a)$$

becomes increasingly important as the size of the alkyl peroxy (at least for the straight chain series) radical increases. The alkyl nitrate yields, which can be equated to the rate constant ratios k_{50a}/k_{50}, determined for the C_2 through C_8 n-alkane series by Atkinson et al. [170] at 299±2 K and 735 torr total pressure of air are given in table 13. For alkyl peroxy radicals other than those derived from the n-alkanes, the available data indicate that k_{50a}/k_{50} ≈0.045 for cyclopentyl peroxy radicals, ≈0.09 for cyclohexyl peroxy radicals and ≈0.05 for cycloheptyl peroxy radicals [171] at room temperature and atmospheric pressure. These rate constant ratios are significantly lower than those for the alkyl peroxy radicals derived from the n-alkanes, suggesting that the alkyl nitrate yields may be very dependent on the structure of the alkyl peroxy radical. Hence it is possible that generalizations based, for instance, on the carbon number cannot be made.

Atkinson et al. [170] suggest that the reaction of RO_2 radicals with NO proceeds via the pathways:

Table 12. Room Temperature Rate Constants, k_{50}, for the Reaction of RO_2 Radicals With NO

R	$10^{12} \times k_{50}$ cm^3 molecule^{-1} s^{-1}	Technique[a]	Reference
CH_3	>1.2	Relative Rate	[154]
	>1	FP-KS	[155]
	8.0 ± 2.0	DF-MS	[156]
	3.0 ± 0.2	FP-KS	[157]
	6.5 ± 2.0	MMS	[158, 159]
	$3.3^{+1.8}_{-1.2}$	Relative Rate	[160]
	7.1 ± 1.4	FP-KS	[161]
	7.8 ± 1.2	FP-KS	[162]
	7.7 ± 0.9	FP-KS	[163]
	8.6 ± 2.0	DF-MS	[164]
C_2H_5	2.7 ± 0.2	FP-KS	[165]
	8.9 ± 3.0	DF-MS	[166]
$(CH_3)_3C$	>1	FP-KS	[155]

[a] FP-KS: flash photolysis - kinetic spectroscopy.
DF-MS: discharge flow - mass spectrometry.
MMS: molecular modulation spectroscopy.

Table 13. Rate Constant Ratios k_{50a}/k_{50} for the C_2 through C_8 n-alkanes at 299 ± 2 K and 735 Torr Total Pressure, From [170]

n-Alkane	k_{50a}/k_{50}[a]
Ethane	≤0.014
Propane	0.036 ± 0.005
n-Butane	0.077 ± 0.009
n-Pentane	0.117 ± 0.013[b]
n-Hexane	0.208 ± 0.027[b]
n-Heptane	0.293 ± 0.042[b]
n-Octane	0.318 ± 0.027[b]

[a] Indicated error limits are two standard deviations.
[b] Secondary alkyl nitrate yields only (see [170]).

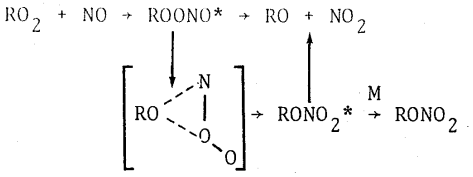

where the asterisk denotes vibrational excitation. Such a reaction sequence suggests that the alkyl nitrate yields should be pressure dependent. Indeed, the most recent study of Atkinson et al. [172] shows that for n-pentane and n-heptane the alkyl nitrate yields are pressure and temperature dependent, with the yields decreasing with decreasing pressure and increasing temperature. These data, and those obtained at 299 K and 735 torr total pressure for propane through n-octane, were shown to be fit with an expression similar to the generalized fall-off expression:

$$Y_P^T = \left[\frac{Y_o^{300}\ P\ (T/300)^{-m_o}}{1 + \left\{\frac{Y_o^{300}\ P\ (T/300)^{-m_o}}{Y_\infty^{300}\ (T/300)^{-m_\infty}}\right\}}\right] x$$

$$F\left\{1 + \left[\log_{10}\left(\frac{Y_o^{300}\ P\ (T/300)^{-m_o}}{Y_\infty^{300}\ (T/300)^{-m_\infty}}\right)\right]^2\right\}^{-1}$$

where:

Y_T^P is the alkyl nitrate yield at pressure P (in torr) and temperature T (K)

$Y_o^{300} = 4.15 \times 10^{-6}\ e^{1.079\ n}$

and n is the number of carbon atoms in the n-alkane

$Y_\infty^{300} = 0.384$

$m_o = 5.05$

$m_\infty = 4.17$

and $F = 0.467$

We recommend use of this expression for calculation of the alkyl nitrate yields from the n-alkanes propane through n-octane over the temperature and pressure ranges ∿280-340 K and ∿50-740 torr total pressure, respectively.

$$CH_3O_2 + NO_2 \rightarrow CH_3O_2NO_2 \qquad (51)$$

and

$$RO_2 + NO_2 \rightarrow RO_2NO_2$$

There are few direct experimental data for the rate constants for these reactions, the data being for R = CH_3 and C_2H_5.

For CH_3O_2 radicals, the two recent flash photolysis-kinetic spectroscopy studies of Sander and Watson [161] and Ravishankara et al. [173] have shown that these reactions are in the fall-off region below atmospheric pressure. Data were obtained for the diluent gases He, N_2 and SF_6 over the pressure range 50-700 torr at 298 K [161] and for N_2 over the pressure and temperature ranges 76-722 torr and 253-353 K [173]. The data for N_2 as the diluent gas at 298 K from both studies are in excellent agreement and Ravishankara et al. [173] have fit the data from both studies with N_2 as the diluent gas by

$$k_{51}\ (R=CH_3) = \left\{\frac{k_o(T)[M]}{1 + k_o(T)[M]/k_\infty(T)}\right\} x$$

$$0.4^{\{1+[\log_{10}\ (k_o(T)[M]/k_\infty(T))]^2\}^{-1}}$$

$cm^3\ molecule^{-1}\ s^{-1}$

where

$$k_o(T) = 2.2 \times 10^{-30}\ (T/298)^{-2.5}\ cm^6\ molecule^{-2}\ s^{-1}$$

$$k_\infty(T) = 7 \times 10^{-12}\ (T/298)^{-3.5}\ cm^3\ molecule^{-1}\ s^{-1}$$

This expression, which we recommend, is slightly different from that recommended by NASA [3], but gives a better fit to the experimental data [3].

For $\geq C_2$ alkyl peroxy radicals we recommend that

$$k_{51} = 7 \times 10^{-12}\ cm^3\ molecule^{-1}\ s^{-1}$$

at 298 K and 760 torr, uncertain to a factor of 2. This value, i.e., the limiting high pressure value, is taken as the k_{51} ($p \rightarrow \infty$) value given above for $CH_3O_2 + NO_2$.

For the case of $C_2H_5O_2$ it is expected that k_{51} will be pressure dependent at total pressures below atmospheric, but it is likely that the rate constant at 298 K will be at or close to the high pressure second-order limit at 760 torr of air, while for the higher homologues the fall-off region will obviously move to progressively lower pressures.

$$RCO_3 + NO_2 \rightarrow RCO_3NO_2 \qquad (51b)$$

For the acyl peroxy radical reactions with NO_2, i.e.,

$$RCO_3 + NO_2 \rightarrow RCO_3NO_2$$

the only available experiment data to date are the rate constant ratios k_{50}/k_{51b} from studies of PAN and PBzN thermal decompositions in the presence of NO and NO_2 [150,151,153,174], and a recent determination of the absolute rate constant for the reaction of CH_3CO_3 radicals with NO_2 [148]. For PAN, the experimental rate constant ratios

$$k(CH_3CO_3 + NO)/k(CH_3CO_3 + NO_2)$$

i.e., k_{50}/k_{51b}, at room temperature are:

3.1 ± 0.5 (Hendry and Kenley [150]);

1.7 (Cox et al. [153]);

and

$1.85^{+0.85}_{-0.41}$ (Cox and Roffey [151]);

while for PBzN, Kenley and Hendry [174] have determined a rate constant ratio of

$$k_{50}/k_{51b} = 1.52 \pm 0.12 \text{ at } 303 \text{ K},$$

Hence it appears that at room temperature the rate constants for the reaction of RCO_3 radicals with NO_2 are lower than those for reaction with NO.

The recent determination of $k_{51b}(R=CH_3)$ by Addison et al. [148] using molecular-modulation spectroscopy yielded values (at 302 ± 1 K) of

$$k_{51b} = (2.1 \pm 0.1) \times 10^{-12} \text{ cm}^3 \text{ molecule}^{-1} \text{ s}^{-1}$$

at 28 torr (mainly O_2) and

$$k_{51b} = (4.7 \pm 0.3) \times 10^{-12} \text{ cm}^3 \text{ molecule}^{-1} \text{ s}^{-1}$$

at 715 torr (mainly O_2). There thus appears to be a pressure effect on the rate constant for this reaction. Because of the experimental complications caused by the high value of the rate constant, Addison et al. [148] recommended that at 715 torr and 302 ± 1 K

$$k_{51b}(R=CH_3) = (6.0 \pm 2.0) \times 10^{-12} \text{ cm}^3 \text{ molecule}^{-1} \text{ s}^{-1}$$

The modeling study of NO_x photooxidations of n-butane-propene-air mixtures of Carter et al. [7] concluded that the best fit for calculated and experimental PAN profiles occurs for $k_{50}/k_{51b} = 1.5$, somewhat lower than the experimental rate constant ratio data [150, 151,153] for PAN, but consistent with our recommended value of k_{50} and the recent determination of k_{51b} [148]. Obviously, further work is necessary to refine this rate constant ratio, but based mainly on the modeling study of Carter et al. [7], we recommend that

$$k_{50}/k_{51b} = 1.5, \text{ independent of temperature},$$

at atmospheric pressure (it is possible that the datum of Hendry and Kenley [150] was obtained at lower total pressures in the fall-off region), and hence

$$k_{51b}(RCO_3) = 4.7 \times 10^{-12} \text{ cm}^3 \text{ molecule}^{-1} \text{ s}^{-1}$$

at 298 K and atmospheric pressure with an uncertainty of a factor of 2. This recommended value is consistent with the recent value of k_{51b} (R=CH_3) determined by Addison et al. [148].

The available experimental data show conclusively that the reactions of RO_2 and RCO_3 radicals with NO_2 proceed via formation of peroxynitrates as shown above [148-151,153, 174-180].

$$CH_3O_2NO_2 \rightarrow CH_3O_2 + NO_2 \qquad (52)$$

and $RO_2NO_2 \rightarrow RO_2 + NO_2$

Only recently have the alkyl peroxynitrates (RO_2NO_2) been characterized and studied [176-181]. Table 14 gives the available thermal decomposition rate constant data for these compounds, along with rate constant data for HO_2NO_2 as a comparison. It can be seen that the Arrhenius activation energies for the thermal decomposition of HO_2NO_2, $CH_3O_2NO_2$ and $C_3H_7O_2NO_2$ are $\sim$20 kcal mol^{-1}. While the HO_2NO_2 and $CH_3O_2NO_2$ decompositions are not at the high pressure limit at atmospheric pressure, the Arrhenius activation energy for HO_2NO_2 decomposition at the high pressure limit will be only slightly higher, and Baldwin and Golden [182] have derived (from RRKM calculations) the high pressure rate constant

$$k(HO_2NO_2 \rightarrow HO_2 + NO_2) = 2.7 \times 10^{16} e^{-11575/T} \text{ s}^{-1}$$

(i.e., E = 23.0 kcal mol^{-1}).

It is anticipated that the preexponential factor will be very similar for other alkyl peroxynitrate decompositions

(as it is for PAN, where $A = 1.95 \times 10^{16}$ s^{-1}).

Hence the data of Edney et al. [179,180], Hendry and Kenley [178] and of Bahta et al. [181] indicate that the activation energy for thermal decomposition of the alkyl peroxynitrates is $\leq$22.0 kcal mol^{-1}, very similar to that estimated by Hendry and Kenley [178] from thermochemical arguments. For $CH_3O_2NO_2$ the thermal decomposition rate constant at 760 torr is a factor of $\sim$1.5-2 lower than the high pressure first order limit [161,173,181] (the rate constant for HO_2NO_2 is a factor of $\sim$3-4 off the high pressure limit at atmospheric pressure and 298 K [83,182]). For the $\geq C_2$ alkyl peroxynitrates the limiting high pressure region should be attained at $\leq$1 atmosphere, and hence, for all the alkyl peroxynitrates their thermal decomposition lifetimes are expected to be <1 s at 298 K, and $\leq$1 min at 273 K. Hence we consider that for lower tropospheric modeling studies, T $\geq$285 K, the role of alkyl peroxynitrates will be negligible.

$$CH_3CO_2 \rightarrow CH_3 + CO_2 \qquad (53)$$

This reaction is considered, based on the thermochemistry, to be fast, such that it is the sole reaction pathway of the CH_3CO_2 radical under atmospheric conditions [7]. Therefore, the precise value of the rate constant is not important for atmospheric modeling studies.

$$CH_3 + O_2 \rightarrow CH_3O_2 \qquad (54)$$

and $R + O_2 \rightarrow RO_2$

At atmospheric pressure and 298 K, the reaction of CH_3 and higher alkyl radicals with O_2 have rate constants of

$$k_{54} \gtrsim 1 \times 10^{-12} \text{ cm}^3 \text{ molecule}^{-1} \text{ s}^{-1}$$

[2,3,184-186] and with the high atmospheric O_2 concentration is the sole reaction pathway for these radicals. Thus Hunziker and Wendt [147] have observed the electronic infrared spectra of CH_3O_2, $C_2H_5O_2$ and $(CH_3)_2CHO_2$, while Parkes and coworkers have observed the spectra of these peroxy radicals and of $(CH_3)_3CO_2$ in the ultraviolet [155,187-189].

The subsequent reactions leading to methoxy radical production have been discussed above, i.e.,

$$CH_3O_2 + NO \rightarrow CH_3O + NO_2 \qquad (50)$$

$$CH_3O_2 + NO_2 \rightleftarrows CH_3O_2NO_2 \qquad (51)$$

$$CH_3O + NO \rightarrow CH_3ONO \quad (a) \qquad (55)$$

$$\rightarrow HCHO + HNO \quad (b)$$

and

$$RO + NO \rightarrow RONO \quad (a)$$

$$\rightarrow R'R''CO + HONO \quad (b)$$

Except for a single very recent absolute rate constant determination of k_{55} for R=CH_3 [190], no other direct rate constant data are available for these reactions. The available information has been derived from the thermal decomposition rates of alkyl nitrites (-55a) and thermochemical data [191-203]. The Arrhenius activation energies for alkyl nitrite decomposition are observed to be identical, within the experimental errors ($\sim\pm$1 kcal mol^{-1}), with the heat of reaction, ΔH_{55a}. From the entropy of reaction, ΔS_{55a}, values of the preexponential factors A_{55a} were derived, as given in table 15. These preexponential factors are in the range

$$(1\text{-}5) \times 10^{-11} \text{ cm}^3 \text{ molecule}^{-1} \text{ s}^{-1},$$

with no clear-cut trend with the alkoxy radical size or structure. In view of the lack of further information, we estimate a mean preexponential factor of

$$A_{55a} = 3 \times 10^{-11} \text{ cm}^3 \text{ molecule}^{-1} \text{ s}^{-1},$$

independent of the alkoxy radical and with an uncertainty of a factor of 3. Using a zero Arrhenius activation energy for these reactions [192] leads to

$$k_{55a} = 3 \times 10^{-11} \text{ cm}^3 \text{ molecule}^{-1} \text{ s}^{-1},$$

independent of temperature, with an uncertainty of a factor of 3. We should point out, however, by analogy with other NO recombination reactions [3,23,24] a slightly negative Arrhenius activation energy of $\sim-(200 \pm 200)/T$ may be expected for these reactions.

For R = CH_3, the CH_3ONO thermal decomposition rate is pressure dependent below $\sim$100 torr total pressure for CF_4 as the bath gas [201-203] and has not reached the high pressure second-order limit at 700 torr total pressure of N_2:

$k_{55a}/k_{55a}^{\infty} \sim 0.8$ at one atmosphere of N_2 [202].

Hence for air, this reaction and the reverse, i.e.,

$$CH_3O + NO \rightarrow CH_3ONO$$

will be somewhat in the fall-off region at around atmospheric pressure [203]. Recently Sanders et al. [190] have determined, by monitoring CH_3O by laser induced fluorescence, that

$$k_{55a}\ (R=CH_3) = (2.08 \pm 0.12) \times 10^{-11}\ cm^3\ molecule^{-1}\ s^{-1}$$

at room temperature. Since this determination was carried out at a total pressure of 10-15 torr of diluent gas (Ar or N_2) [190] it is hence expected to be in the fall-off region. Although this rate constant is in the range expected from the above discussion, further studies are obviously necessary as a function of the total pressure.

Since the alkyl nitrites RONO photolyse rapidly, uncertainties in their formation rate constants k_{55a} have a minimal impact on modeling calculations. However, since alkyl nitrites, like HONO, do photolyse rapidly to yield radical species, their presence at the commencement of irradiations is of importance.

For reaction (55b), various studies have been carried out to determine the rate constant ratios k_{55b}/k_{55a}. The values for this ratio are given in table 16.

In evaluating these rate constant ratios k_{55b}/k_{55a} care must be exercised since these ratios will be upper limits if the combination reactions k_{55a} are in the fall-off region, i.e., below their limiting second-order kinetic values. This is especially so for the case of CH_3O where the combination reaction (55a) is in the fall-off region at atmospheric pressure. From the most recent, approximately atmospheric pressure, work of Batt and Rattray [203]

$$k_{55b}\ (R=CH_3) = \lesssim 1.3 \times 10^{-12}\ cm^3\ molecule^{-1}\ s^{-1},$$

approximately independent of temperature.

For the higher alkoxy radicals, the abstraction reaction apparently becomes more important, as may be anticipated because of the higher exothermicities of the reaction, and we recommend using

$$k_{55b}/k_{55a}\ (R \geq C_2\ \text{alkoxy}) = 0.22 \pm 0.05,$$

independent of temperature, i.e.,

$$k_{55b} = 6.6 \times 10^{-12}\ cm^3\ molecule^{-1}\ s^{-1},$$

independent of temperature.

$$CH_3O + NO_2 \rightarrow CH_3ONO_2 \quad a \qquad (56)$$

$$\rightarrow HONO + HCHO \quad b$$

$$RO + NO_2 \rightarrow RONO_2 \quad a$$

$$\rightarrow R'R''CO + HONO \quad b$$

No direct determinations of the rate constants for these reactions are available, and the data come solely from relative rate studies. For the rate constant ratios k_{55a}/k_{56a}, the available data are given in table 17. There appears to be no trend with R, and a simple average yields $k_{55a}/k_{56a} = 2 \pm 1$, independent of temperature (also arrived at by Barker et al. [219]), in agreement with the data cited by Batt [202] and with the recent study of Batt and Rattray [203] for $R = CH_3$. This leads to our recommended value of

$$k_{56a} = 1.5 \times 10^{-11}\ cm^3\ molecule^{-1}\ s^{-1},$$

independent of temperature, with an uncertainty of a factor of $\sim$3 at 298 K.

From a study of the thermal decomposition of CH_3ONO_2, Batt and Alvarado-Salinas [220] have, from the thermochemistry of the overall reaction, derived a rate constant

$$k_{56a}\ (R=CH_3) = 1.0 \times 10^{-11}\ cm^3\ molecule^{-1}\ s^{-1}$$

(to within a factor of 4), independent of temperature, while Mendenhall et al. [191], using their very low pressure pyrolysis (VLPP) technique, derived the high pressure rate constant for the thermal decomposition of n-propyl nitrate and, from the calculated entropy of the reaction, obtained an estimate of k_{56a} for R = n-propyl of

$$k_{56a} = 5.3 \times 10^{-12}\ cm^3\ molecule^{-1}\ s^{-1}$$

at 300 K. While this value is lower by a factor of $\sim$3 than those derived above, the ratio k_{55a} (R = t-butyl)/k_{56a} (R = n-propyl) = 2 from the VLPP work of Mendenhall et al. [191] again implies that the ratio of $k_{55a}/k_{56a} = 2$ is much more accurately known than the absolute values of k_{55a} or k_{56a}.

There are few data available for the rate constant ratio k_{56b}/k_{56a} (table 18). Batt and Robinson [221] point out that the value used by Barker et al. [219] for $R=CH_3$ is high because of the pressure dependence of reaction (56a) (i.e., in the fall-off region at the lower total pressures used by Barker et al. [219]).

More recently, the data of Batt and Rattray [203] indicate that for $R=CH_3$, $0 \leq k_{56b}/k_{56a} \leq 0.05$ with a most probable value of $\sim$0.01. This, together with the value quoted by Batt [202] for isopropoxy suggests that the abstraction pathway can be neglected.

$$CH_3O + O_2 \rightarrow HCHO + HO_2 \qquad (57)$$

and

Table 14. Rate Constants k_{52} for the Thermal Decomposition of Alkyl Peroxynitrates RO_2NO_2 and of HO_2NO_2

R	A s^{-1}	E kcal mol^{-1}	Lifetime, (s), at 298 K	Lifetime, (s), at 273 K	Reference
CH_3	6×10^{15}[a]	21.1 ± 1.5[a]	0.5[a]	13[a]	[181]
C_3H_7 (n- and iso- mixture)	1.2×10^{15}	19.8	0.3[b]	6[b]	[179, 180]
t-$(CH_3)_3C$			<<2.3		[178, 183]
H	1.3×10^{14}	20.7	12	290	[81, 83][c]
H	2.7×10^{16}	23.0	2.7	96	[182][d]

[a]At a total concentration of 1.3×10^{19} molecule cm^{-3} (401 torr at 298 K).

[b]Recalculated using a ratio of $k(RO_2+NO)/k(RO_2+NO_2) = 1.0$ instead of 2.4 as used by Edney et al. [179, 180].

[c]At atmospheric pressure.

[d]Calculated high pressure limit.

Table 15. Preexponential Factors A_{55a} for the Reaction RO + NO → RONO

R	$10^{11} \times A_{55a}$ cm^3 $molecule^{-1}$ s^{-1}	Uncertainty Factor	Reference
$CH_3\cdot$	2.1	4.0	[197]
	2.6	2.5	[203]
$C_2H_5\cdot$	3.3	2.5	[196]
$(CH_3)_2CH\cdot$	5.3	2.5	[195]
$CH_3\dot{C}HC_2H_5$	4.2	2.5	[194]
$(CH_3)_3C\cdot$	4.2	1.6	[193]
	1.05		[191]
$(CH_3)_2\dot{C}C_2H_5$	5.3	1.6	[198]
$CH_3CH_2CH_2CH_2\cdot$	4.2		[199]

Table 16. Rate Constant Ratios k_{55b}/k_{55a} for RO Reactions

R	k_{55b}/k_{55a} at T K	Reference
$CH_3\cdot$	0.13 at 298	[204]
	0.17 at 298-423	[205]
	0.18 ± 0.02 at 373-473	[192]
	0.01 - 0.05 at 383-423	[203]
$C_2H_5\cdot$	0.3 at 298	[206]
	0.30 ± 0.05 at 368-408	[207]
	0.34 at 473	[208]
	0.20 at 298	[209]
$CH_3CH_2\dot{C}H_2$	0.42 at 373-423	[210]
$(CH_3)_2\dot{C}H$	0.16 at 299	[211]
	0.20 at 350	[211]
	0.22 at 377-422	[212]
	0.17 at 299-453	[213]
	0.15 at 394-432	[214]
$CH_3\dot{C}HCH_2CH_3$	0.2 at 413	[215]
	0.26 at 373-413	[216]

$$RR'CHO + O_2 \rightarrow RR'CO + HO_2$$

The sole direct determination of rate constants k_{57} for the reaction of alkoxy radicals with O_2 is that of Gutman et al. [222]. Using a flash photolysis-laser induced fluorescence technique, rate constants for the reaction of CH_3O radicals with O_2 were determined over the temperature range 413-608 K, and for the reaction of C_2H_5O radicals with O_2 at 296 and 353 K. Based upon these data for $R=CH_3$ and the value of

$$k_{57} = 1.32 \times 10^{-15} \text{ cm}^3 \text{ molecule}^{-1} \text{ s}^{-1}$$

at 298 K derived by Cox et al. [223] from the photolysis of CH_3ONO in the presence of O_2 and NO_2, Gutman et al. [222] derived

$$k_{57} (R=CH_3) = 1.0 \times 10^{-13} e^{-1300/T} \text{ cm}^3 \text{ molecule}^{-1} \text{ s}^{-1}$$

$$= 1.3 \times 10^{-15} \text{ cm}^3 \text{ molecule}^{-1} \text{ s}^{-1}$$

at 298 K.

We recommend this rate expression, which is consistent with the upper limit of

$$k_{57} (R=CH_3) < 2 \times 10^{-15} \text{ cm}^3 \text{ molecule}^{-1} \text{ s}^{-1}$$

at room temperature derived by Sanders et al. [190] using a technique similar to that used by Gutman et al. [222]. This value of k_{57} at 298 K is judged to be uncertain by a factor of ~ 3.

For the higher alkoxy radicals, Gutman et al. [222] have, based upon their data for CH_3O and C_2H_5O and the procedures of Baldwin et al. [224], estimated Arrhenius parameters and rate constants k_{57} at 300 K for several alkoxy radicals. Their estimated data are given in table 19. The limited data in table 19 suggests that for primary alkoxy radicals (other than CH_3O), the rate constant k_{57} is given by

$$k_{57} \text{ (primary alkoxy)} \approx 7 \times 10^{-14} e^{-690/T} \text{ cm}^3 \text{ molecule}^{-1} \text{ s}^{-1}$$

$$\approx 7 \times 10^{-15} \text{ cm}^3 \text{ molecule}^{-1} \text{ s}^{-1}$$

at 298 K, while for secondary alkoxy radicals

$$k_{57} \text{ (secondary alkoxy)} \approx 3 \times 10^{-14} \text{ cm}^3 \text{ molecule}^{-1} \text{ s}^{-1},$$

independent of temperature.

We recommend these expressions, while emphasizing that much further work is required.

$$OH + CH_3ONO_2 \rightarrow \text{products} \qquad (58)$$

No rate constant for this reaction has been determined. However, from the rate constants for the reaction of OH radicals with a series of alkyl nitrates recently determined by Atkinson et al. [225], it is apparent that

$$k_{58} \lesssim 3 \times 10^{-13} \text{ cm}^3 \text{ molecule}^{-1} \text{ s}^{-1}$$

at 298 K, and hence this reaction can be neglected for modeling purposes.

For the rate constants k_{58} for selected primary (1-butyl) and secondary (2-propyl, 2-butyl, 2- and 3-pentyl, 2- and 3-hexyl, 3-heptyl and 3-octyl) nitrates, reference 225 should be consulted.

$$OH + CH_3ONO \rightarrow \text{products} \qquad (59)$$

The rate constant for this reaction has been determined in three studies [226-228], all using relative rate techniques. Campbell and Goodman [226] and Audley et al. [227], using the heterogeneous NO_2/H_2O_2 reaction to generate OH radicals, have obtained rate constants of

$$1.6 \times 10^{-12} \text{ cm}^3 \text{ molecule}^{-1} \text{ s}^{-1} \text{ [116,226]}$$

and

$$1.2 \times 10^{-12} \text{ cm}^3 \text{ molecule}^{-1} \text{ s}^{-1} \text{ [227]}$$

at around room temperature. However, more recently Tuazon et al. [228] have, using the $N_2H_4 + O_3$ reaction as a dark source of OH radicals, determined that

$$k_{59} \approx 2 \times 10^{-13} \text{ cm}^3 \text{ molecule}^{-1} \text{ s}^{-1}$$

at 300 K.

Since this latter value of k_{59} is consistent with the upper limit for the rate constant for the reaction of OH radicals with CH_3ONO_2, which is expected to proceed by a similar reaction pathway (i.e., H-atom reaction), we recommend this value, which makes this reaction totally negligible for computer modeling purposes (see also reaction (60) below).

$$CH_3ONO + h\nu \rightarrow CH_3O + NO \qquad (60)$$

$$RONO + h\nu \rightarrow RO + NO$$

This photodissociation is by far the major loss process of alkyl nitrites under

Table 17. Rate Constant Ratios $k(RO + NO \rightarrow RONO)/k(RO + NO_2 \rightarrow RONO_2)$

R	k_{55a}/k_{56a}	T K	Reference
CH_3	1.1		[205]
	2.7	403	[217]
	1.8	363	[218]
	2.0 ± 0.5		[203]
C_2H_5	2.5	403	[217]
$(CH_3)_3C$	1.7 ± 0.25	403	[217]

Table 18. Rate Constant Ratios k_{56b}/k_{56a} for the Reaction of RO Radicals With NO_2

R	k_{56b}/k_{56a}	T (K)	Reference
CH_3·	0.11	403	[217]
	0.30 ± 0.05	391-432	[219]
	∿0.05	383-433	[221]
	0.00-0.05	383-423	[203]
	∿0.01		
C_2H_5·	0.46	403	[217]
$(CH_3)_2CH$.	∿0.01		[202]

Table 19. Arrhenius Parameters and Rate Constants k_{57} at 300 K for Selected Alkoxy Radicals, as Estimated by Gutman et al. [222]

Alkoxy Radical	$10^{14} \times A$ (cm^3 $molecule^{-1}$ s^{-1})	E (kcal mol^{-1})	$10^{15} \times k_{57}$[a] (cm^3 $molecule^{-1}$ s^{-1})
CH_3O	10	2.6	1.3
C_2H_5O	7	1.3	7
n-C_3H_7O	7	1.3	7
i-C_3H_7O	3	0.0	30
n-C_4H_9O	7	1.4	7
i-C_4H_9O	7	1.1	10
s-C_4H_9O	3	-0.2	50

[a]At 300 K.

daytime atmospheric conditions [229]. In the actinic region, absorption coefficients are given by Calvert and Pitts [230], and for CH_3ONO, by Taylor et al. [229]. The photodissociation quantum yields are high [230], that for photodissociation of methyl nitrite to CH_3O + NO being unity within experimental error [223].

$$NO_3 + CH_3CHO \rightarrow \text{products} \qquad (61)$$

$$NO_3 + RCHO \rightarrow \text{products}$$

Rate constant determinations have been carried out for the reaction of NO_3 radicals with CH_3CHO by Morris and Niki [231] and by Atkinson et al. [130]. Both studies monitored the decay of N_2O_5 in N_2O_5-NO_2-CH_3CHO-air mixtures and derived k_{61} from a knowledge of the equilibrium constant $K_{7,8}$ for the reactions

$$N_2O_5 \rightleftarrows NO_2 + NO_3$$

Using the value of $K_{7,8}$ commended by Malko and Troe [27], values of

$$k_{61}\ (CH_3CHO) = 1.4 \times 10^{-15}\ cm^3\ molecule^{-1}\ s^{-1}$$

at 300 K [231], and

$$k_{61}\ (CH_3CHO) = 1.34 \times 10^{-15}\ cm^3\ molecule^{-1}\ s^{-1}$$

at 298 ± 1 K [130] were obtained.

These rate constants are in excellent agreement, and we recommend:

$$k_{61}\ (CH_3CHO) = 1.4 \times 10^{-15}\ cm^3\ molecule^{-1}\ s^{-1}$$

at 298 K, with an estimated uncertainty of a factor of 1.5. By analogy with the reactions of HCHO, CH_3CHO and the higher aldehydes with $O(^3P)$ atoms and OH radicals [116] we expect that the higher aldehydes will react somewhat more rapidly with NO_3 than does CH_3CHO, i.e.,

$$k_{61}\ (RCHO,\ R \geq C_3) \gtrsim 1.5 \times 10^{-15}\ cm^3\ molecule^{-1}\ s^{-1}$$

at 298 K. No temperature dependences can be recommended.

The reaction pathway appears [231] to be one of H atom abstraction.

$$NO_3 + CH_3CHO \rightarrow CH_3CO + HNO_3$$

$$NO_3 + RCHO \rightarrow RCO + HNO_3$$

5. Alkene Chemistry

In the following section the atmospheric chemistry of the alkenes ethene, propene, 1-butene and trans-2-butene is evaluated. Because of their similarities, we treat the reaction steps as a group with the differing rate constants/products noted.

$$O(^3P) + \text{Alkenes} \rightarrow \text{products} \qquad (62)$$

Absolute rate constants for these reactions have been determined in numerous studies utilizing a variety of experimental techniques [232,233, and references therein]. The two most recent and extensive rate constant determinations are those of Singleton and Cvetanovic [232] using a modulation-phase shift technique, and Atkinson and Pitts [233] using a flash photolysis - NO_2 chemiluminescence method. Nicovich et al. [234] and Sato and coworkers [235,236] have also recently determined absolute rate constants for the reactions of $O(^3P)$ atoms with ethene and a series of alkenes, respectively. Table 20 gives the room temperature rate constants k_{62} and Arrhenius activation energies obtained, together with the earlier relative rate constant data of Cvetanovic [237]. These recent absolute rate constant determinations are in generally excellent agreement and are totally consistent with the relative rate constant data of Cvetanovic [237] and with earlier absolute rate constant data (see reference 233). We recommend taking a least squares mean of the data of Singleton and Cvetanovic [232] and Atkinson and Pitts [233] for ethene, propene and 1-butene, and since the study of Atkinson and Pitts [233] is the only absolute rate constant determination for trans-2-butene carried out as a function of temperature, we recommend that as is. Figures 7 and 8 show Arrhenius plots of the data of Singleton and Cvetanovic [232] and Atkinson and Pitts [233] for ethene, propene and 1-butene, along with the recommended Arrhenius lines.

Recommendations

ethene: $k_{62} = 1.04 \times 10^{-11}\ e^{-792/T}\ cm^3\ molecule^{-1}\ s^{-1}$

$= 7.3 \times 10^{-13}\ cm^3\ molecule^{-1}\ s^{-1}$

at 298 K with an estimated uncertainty of ±15%.

Table 20. Recent Room Temperature Rate Constants k_{62} and Arrhenius Activation Energies E (cal mol^{-1}) for the Reaction of $O(^3P)$ Atoms With Alkenes

Alkene	$10^{12} \times k_{62}$ (cm^3 $molecule^{-1}$ s^{-1})	E (cal mol^{-1})	Reference
Ethene	0.75[a]		[237]
	0.702 ± 0.017	1679 ± 94	[232]
	0.761 ± 0.076	1475 ± 200	[233]
	0.694 ± 0.058	1794 ± 362	[234]
	1.0 ± 0.2		[235]
	0.87	1564	[236]
Propene	4.33[a]		[237]
	3.79	722 ± 40	[232]
	4.47 ± 0.45	515 ± 200	[233]
	4.7 ± 0.3		[235]
1-Butene	4.33[a]		[237]
	4.01	659 ± 45	[232]
	4.54 ± 0.46	665 ± 200	[233]
	4.7 ± 0.5		[235]
trans-2-Butene	21.3[a]		[237]
	23.5 ± 2.4	-20 ± 200	[233]
	23 ± 3		[235]

[a]Relative rate constants placed on an absolute basis using k_{62} [$O(^3P)$ + cis-2-butene] = 1.79×10^{-11} cm^3 $molecule^{-1}$ s^{-1} at 298 ± 1 K; mean of 1.81×10^{-11} cm^3 $molecule^{-1}$ s^{-1} [233] and 1.77×10^{-11} cm^3 $molecule^{-1}$ s^{-1} [232].

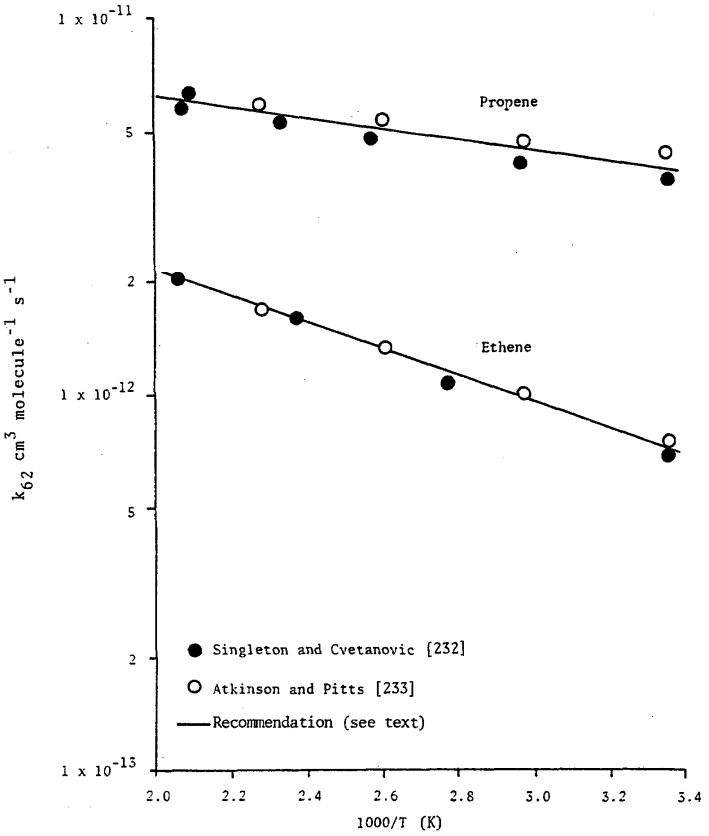

Figure 7. Arrhenius Plots for the Reaction of $O(^3P)$ Atoms with Ethene and Propene.

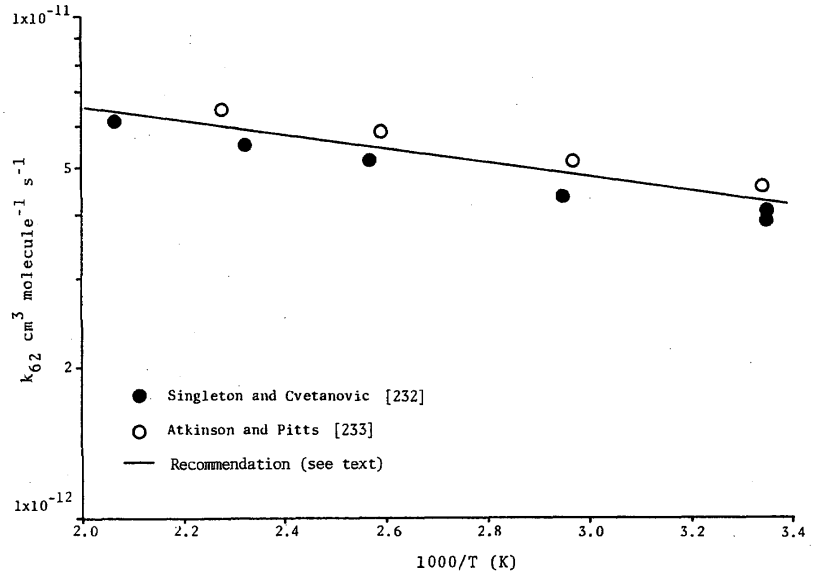

Figure 8. Arrhenius Plot for the Reaction of $O(^3P)$ Atoms with 1-Butene.

propene: $k_{62} = 1.18 \times 10^{-11} e^{-324/T}$ cm^3 molecule^{-1} s^{-1}

$= 4.0 \times 10^{-12}$ cm^3 molecule^{-1} s^{-1}

at 298 K with an uncertainty of ±20%.

1-butene: $k_{62} = 1.25 \times 10^{-11} e^{-326/T}$ cm^3 molecule^{-1} s^{-1}

$= 4.2 \times 10^{-12}$ cm^3 molecule^{-1} s^{-1}

at 298 K with an uncertainty of ±20%.

trans-2-butene: $k_{62} = 2.26 \times 10^{-11} e^{10/T}$ cm^3 molecule^{-1} s^{-1}

$= 2.3 \times 10^{-11}$ cm^3 molecule^{-1} s^{-1}

at 298 K with an uncertainty of ±20%.

While the mechanism for the reactions of $O(^3P)$ atoms with alkenes has been studied extensively by both "conventional" product studies [237,238] as well as by molecular beam and low pressure flow tube studies ([239, 240], for example), the recent molecular beam and spectroscopic studies of Inoue and Akimoto [241], Kleinermanns and Luntz [242], Hunziker et al. [243] and Buss et al. [244] concerning the formation of the vinoxy radical, C_2H_3O, have radically changed the previously accepted viewpoint of these reaction mechanisms. While the reaction mechanism is not totally understood [243], the present data show that the following product schemes appear to be applicable:

Ethene

Fragmentation totally dominates at atmospheric pressure and below, with three fragmentation pathways being operable:

$$O(^3P) + C_2H_4 \rightarrow CH_3 + HCO \quad a$$

$$\rightarrow C_2H_3O + H \quad b$$

$$\rightarrow CH_2CO + H_2 \quad c$$

The product studies of Cvetanovic [245], Pruss et al. [240] and Blumenberg et al. [246] have shown that pathway (62c) accounts for 4-5% of the overall reaction. While previously reaction (62a) was supposed to account for the remainder of the reaction, the recent data, especially that of Hunziker et al. [243], shows that this is not the case. The definitive data of Hunziker et al. [243] yield the rate constant ratios $k_{62b}/k_{62} = 0.36 \pm 0.04$ and $k_{62a}/k_{62} = 0.55$, independent of pressure (between 80 and 760 torr total pressure).

Within the experimental errors the fractional yield of these three pathways add up to unity at both pressures, and we recommend use of these data.

Propene

From the data of Cvetanovic [238], Blumenberg et al. [246] and Hunziker et al. [243], we recommend that at atmospheric pressure:

$$O(^3P) + \text{propene} \rightarrow 0.30\ CH_3CH\text{—}\overset{O}{\diagdown\diagup}CH_2$$

$$+ 0.30\ CH_3CH_2CHO$$

$$+ 0.20\ (C_2H_3O + CH_3)$$

$$+ 0.20\ (HCO + C_2H_5)$$

where C_2H_3O is the vinoxy radical.

The fragmentation/stabilization ratio is pressure dependent, increasing with decreasing pressure [238,243], with the yield of the vinoxy radical being ∿0.3 at 80 torr total pressure [243].

1-Butene

Based on the data of Cvetanovic [238] and Hunziker et al. [243] (H atom abstraction being negligible [232,247]) we recommend:

$$O(^3P) + \text{1-butene} \rightarrow 0.44\ CH_3CH_2CH\text{—}\overset{O}{\diagdown\diagup}CH_2$$

$$+ 0.39\ CH_3CH_2CH_2CHO$$

$$+ 0.17\ (C_2H_3O + C_2H_5)$$

with C_2H_3O being the vinoxy radical [243]. These yields are independent of pressure over the range ∿80-760 torr total pressure [238, 243]. It is possible that other reaction pathways are operable at the level of up to ∿10-20% [246].

trans-2-Butene

Since none of the more recent molecular beam [244] or spectroscopic [242,243] studies have investigated trans-2-butene, there is less relevant information available for this alkene. Based upon the data of Cvetanovic [238], Kanofsky et al. [239] and Blumenberg et al. [246], and by analogy with the above discussion, we tentatively recommend:

$$O(^3P) + \text{trans-2-butene} \rightarrow 0.40\ CH_3CH\text{—}CHCH_3\ (\text{cis + trans})$$
$$+ 0.19\ (CH_3)_2CHCHO$$
$$+ 0.21\ CH_3COCH_2CH_3$$
$$+ 0.20\ (CH_3CH{=}CHO\cdot + CH_3)$$

although other fragmentation pathways cannot be excluded.

The atmospheric reactions of the vinoxy radical, CH_2CHO, are not known with any certainty. The sole data concerning their reactions are those of Nelson and Gutman [248], who observed that the reactions of O_2 and NO with CH_2CHO are pressure dependent. The kinetics of the reaction of CH_2CHO with NO indicated that this reaction is an addition reaction, with a second order rate constant of

$$\sim 2 \times 10^{-11}\ cm^3\ molecule^{-1}\ s^{-1}$$

at room temperature and 400 torr total pressure of N_2 [248]. However, the reaction with O_2 appears to have a limiting low pressure rate constant of

$$\sim 1 \times 10^{-13}\ cm^3\ molecule^{-1}\ s^{-1}$$

at room temperature, attributed to the reaction pathway:

$$CH_2CHO + O_2 \rightarrow HCHO + CO + OH$$

At higher pressures, the second order rate constant tends towards a value of

$$\sim 3 \times 10^{-13}\ cm^3\ molecule^{-1}\ s^{-1}$$

at room temperature [248], indicating the involvement of an addition reaction:

$$CH_2CHO + O_2 \rightarrow OOCH_2CHO$$

which under atmospheric conditions is presumably followed by

$$OOCH_2CHO + NO \rightarrow OCH_2CHO + NO_2$$
$$OCH_2CHO \rightarrow HCHO + HCO$$
$$HCO + O_2 \rightarrow HO_2$$

In the absence of further information, we recommend the use of these reaction pathways, with the reaction of vinoxy with O_2 being totally dominant over reaction with NO (and presumably NO_2) under atmospheric conditions.

The epoxides, i.e. $CH_3CH(O)CH_2$, $CH_3CH_2CH(O)CH_2$ and $CH_3CH(O)CHCH_3$, appear to be relatively unreactive under atmospheric conditions [116]. From the disappearance rates of epoxypropane and 1,2-epoxybutane in irradiated NO_x-organic-air mixtures, Winer et al. [249] obtained the following OH radical rate constants at 300 ± 1 K:

$CH_3CH(O)CH_2$ (1,2-epoxypropane);

$$(1.3 \pm 0.8) \times 10^{-12}\ cm^3\ molecule^{-1}\ s^{-1}$$

and

$CH_3CH_2CH(O)CH_2$ (1,2-epoxybutane);

$$(2.4 \pm 0.7) \times 10^{-12}\ cm^3\ molecule^{-1}\ s^{-1}$$

Thus, in view of the low reactivities of those epoxides and the low importance of $O(^3P)$ atom reactions with the alkenes under realistic atmospheric conditions, the epoxides may, as a first approximation, be regarded as stable products.

$$OH + \text{Alkenes} \rightarrow \text{Products} \qquad (63)$$

The rate constants for the reaction of OH radicals with the alkenes ethene, propene, 1-butene and trans-2-butene have been evaluated by Atkinson et al. [116].

For ethene the rate constant is pressure dependent, being in the fall-off region between third- and second-order kinetics below ~225 torr total pressure of argon, and below ~300 torr pressure of helium [116]. For propene, the fall-off pressure would appear to be below ~20 torr helium [250]. Table 21 gives the available absolute rate constant data, that for ethene being obtained at the high-pressure limit.

It is obvious that the flash photolysis studies of Atkinson et al. [251,257], Ravishankara et al. [250], Paraskevopoulos and coworkers [252,258] and Tully [253] are in good or excellent agreement. Relative rate studies of Wu et al. [260], Lloyd et al. [261] and, more recently, of Atkinson et al. [262] are in agreement, within their experimental errors, with these flash photolysis studies [116,262]. The only studies carried out as a function of temperature in the high pressure second-order kinetic regime are those of Atkinson and Pitts [257], Atkinson et al. [251] and Tully [253].

Table 4. Absolute Rate Constants for the Reaction of OH Radicals With Ethene, Propene, 1-Butene and trans-2-Butene (At the High Pressure Limit for Ethene)

Alkene	$10^{12} \times A$ cm^3 $molecule^{-1}$ s^{-1}	E cal mol^{-1}	$10^{12} \times k_{63}$ cm^3 $molecule^{-1}$ s^{-1} at T K	Reference
Ethene	2.18	-770 ± 300	7.85 ± 0.79 at 299	[251]
			10.0 ± 1.7 at 296	[252]
	1.36[a]	-535 ± 82[a]	8.2[b] at 298	[253]
Propene			17 ± 4 at 300	[146]
			5.0 ± 1.7 at ∿300	[254]
			14.5 ± 2.2 at 298	[255]
			5 ± 1 at 300	[256]
	4.1	-1080 ± 300	25.1 ± 2.5 at 298	[257]
			25.6 ± 1.2[c] at 298	[250]
			24.6 ± 2.8 at 297	[258]
1-Butene			40.8 at 298	[259]
			15 ± 1 at 300	[256]
	7.6	-930 ± 300	35.3 ± 3.6 at 298	[257]
			29.4 ± 1.4[c] at 298	[250]
			33.4 ± 2.5 at 297	[258]
trans-2-Butene			71.4 at 298	[259]
			12 ± 10 at 300	[256]
	11.2	-1090 ± 300	69.9 ± 7.0 at 298	[257]

[a] Calculated from individual rate constants at 291, 361.5 and 438 K [253].

[b] Calculated from Arrhenius parameters for T = 298 K.

[c] Total pressure, 20 torr of helium, no pressure dependence noted over the total pressure ranges 20-200 torr helium for propene and 3-20 torr helium for 1-butene.

We recommend:

Ethene

$$k_{63} = 1.66 \times 10^{-12} e^{474/T} \text{ cm}^3 \text{ molecule}^{-1} \text{ s}^{-1}$$

$$= 8.1 \times 10^{-12} \text{ cm}^3 \text{ molecule}^{-1} \text{ s}^{-1}$$

at 298 K, with an uncertainty of ± 20%.

This expression is based upon a least squares analysis of the data of Atkinson et al. [251] and Tully [253].

Propene

A mean of the latest three flash photolysis studies [250,257,258] is recommended, namely:

$$k_{63} = 2.5 \times 10^{-11} \text{ cm}^3 \text{ molecule}^{-1} \text{ s}^{-1}$$

at 298 K, with an uncertainty of ± 20%.

The temperature dependent expression is that of Atkinson and Pitts [257], which also fits the mean 298 K datum:

$$k_{63} = 4.1 \times 10^{-12} e^{544/T} \text{ cm}^3 \text{ molecule}^{-1} \text{ s}^{-1}$$

It should also be noted that the recent room temperature relative rate constant data of Atkinson et al. [262] for ethene, propene and n-butane are in excellent agreement with the rate constants recommended here and in section 6.

1-Butene

A mean of the three flash photolysis studies [250,257,258] is recommended, i.e.:

$$k_{63} = 3.3 \times 10^{-11} \text{ cm}^3 \text{ molecule}^{-1} \text{ s}^{-1}$$

at 298 K, with an uncertainty of ± 20%.

The temperature dependence obtained by Atkinson and Pitts [257] for this reaction is used with this room temperature value; yielding

$$k_{63} = 6.9 \times 10^{-12} e^{468/T} \text{ cm}^3 \text{ molecule}^{-1} \text{ s}^{-1}$$

trans-2-Butene

In view of the above recommendations, we recommend the expression of Atkinson and Pitts [257], i.e.:

$$k_{63} = 1.12 \times 10^{-11} e^{549/T} \text{ cm}^3 \text{ molecule}^{-1} \text{ s}^{-1}$$

$$= 7.0 \times 10^{-11} \text{ cm}^3 \text{ molecule}^{-1} \text{ s}^{-1}$$

at 298 K, with an uncertainty of ± 25%.

As has been discussed in detail by Atkinson et al. [116], the preponderance of kinetic (i.e., the fall-off behavior of ethene) and mechanistic data, including the very recent mass spectrometric studies of Hoyermann and Sievert [263] and Biermann et al. [264], show that at around room temperature:

a) OH radical addition to ethene followed by, at atmospheric pressure, collisional stabilization of the adduct is the exclusive reaction pathway, and

b) OH radical addition is by far the predominant (≥95% of the total) reaction for propene [263-265] reaction pathway, with the OH radical adding ∿65% of the time to the terminal carbon atom, and ∿35% of the time to the internal carbon [265]. OH radical addition is also almost certainly by far the predominant reaction pathway for trans-2-butene and other methyl-substituted ethenes.

However, for alkenes with longer (≥C_2) sidechains containing weak allylic hydrogens, such as 1-butene, it has recently been shown [264], using a discharge flow system with photoionization mass spectrometric detection of radicals, that H-atom abstraction is a significant reaction pathway at ∿298 K.

$$OH + R_1R_2CHCH=CH_2 \rightarrow H_2O + R_1R_2CCH=CH_2 \quad (63a)$$

In the recent discharge flow-mass spectrometric study of Biermann et al. [264], the fraction of the reaction pathway for 1-butene proceeding via H-atom abstraction was determined to be 0.20 ± 0.06, which is in good agreement with the previous estimate, using linear free energy correlations, of Atkinson et al. [266]. For 1-butene, we thus recommend that k_{63a}/k_{63} = 0.20 ± 0.06 at room temperature and, from the evidence of Atkinson et al. [116, 266], that this ratio is independent of temperature over the small temperature ranges applicable to smog chamber modeling studies.

Hence, the recommended reaction mechanisms for the initial reaction of OH radicals with

the alkenes are:

Ethene

$$OH + CH_2 = CH_2 \rightarrow HOCH_2\dot{C}H_2 \quad k_{63} = 8.1 \times 10^{-12} \text{ cm}^3 \text{ molecule}^{-1} \text{ s}^{-1}$$

at 298 K.

Propene

$$OH + CH_3CH = CH_2 \begin{cases} \rightarrow CH_3\dot{C}HCH_2OH & k_{63} = 1.65 \times 10^{-11} \text{ cm}^3 \text{ molecule}^{-1} \text{ s}^{-1} \\ \rightarrow CH_3CHOHCH_2^{\cdot} & k_{63} = 8.5 \times 10^{-12} \text{ cm}^3 \text{ molecule}^{-1} \text{ s}^{-1}, \end{cases}$$

both at 298 K.

trans-2-Butene

$$OH + CH_3CH = CHCH_3 \rightarrow CH_3CHOHCHCH_3 \quad k_{63} = 7.0 \times 10^{-11} \text{ cm}^3 \text{ molecule}^{-1} \text{ s}^{-1}$$

at 298 K.

1-Butene

$$OH + CH_3CH_2CH = CH_2 \begin{cases} \rightarrow CH_3CH_2CHCH_2OH & k_{63} = 1.7 \times 10^{-11} \\ \rightarrow CH_3CH_2CHOHCH_2^{\cdot} & k_{63} = 9.4 \times 10^{-12} \\ \rightarrow CH_3CHCH = CH_2 + H_2O & k_{63a} = 6.6 \times 10^{-12} \end{cases}$$

at 298 K, (the partial rate constants being in cm^3 $molecule^{-1}$ s^{-1} units).

In the case of 1-butene we have used the same mode of addition as in propene, i.e., ∿65:35 terminal: non-terminal OH radical addition [265]. These hydroxy-alkyl radicals are then expected to react solely with O_2 under atmospheric conditions:

$$R + O_2 \rightarrow RO_2 \quad (54)$$

followed by reactions (50) and (51):

$$RO_2 + NO \rightarrow RO + NO_2 \quad (50b)$$

$$\xrightarrow{M} RONO_2 \quad (50a)$$

$$RO_2 + NO_2 \rightleftarrows RO_2NO_2 \quad (51,52)$$

Because of the short lifetimes of alkyl peroxy nitrates (RO_2NO_2) under atmospheric conditions, reaction (51) is of little or no consequence, and hence the species formed are:

Ethene

$$HOCH_2CH_2OO + NO \rightarrow HOCH_2CH_2O^{\cdot} + NO_2$$

Propene

$$CH_3\overset{OO}{\overset{|}{C}}HCH_2OH + NO \rightarrow CH_3\overset{O}{\overset{|}{C}}HCH_2OH + NO_2 \quad a$$

$$\rightarrow CH_3\overset{ONO_2}{\overset{|}{C}}HCH_2OH \quad b$$

and

$$CH_3CHOHCH_2OO + NO \rightarrow CH_3CHOHCH_2O + NO_2 \quad a$$

$$\rightarrow CH_3CHOHCH_2ONO_2 \quad b$$

with, at atmospheric pressure, $k_b/(k_a + k_b)$ ∿0.04, based upon the data of Carter et al. [7] and Atkinson et al. [170] for propane.

trans-2-Butene

$$CH_3\overset{OO}{\overset{|}{C}}HOHCHCH_3 + NO \begin{cases} \rightarrow CH_3\overset{O}{\overset{|}{C}}HOHCHCH_3 + NO_2 & a \\ \rightarrow CH_3CHOHCH(ONO_2)CH_3 & b \end{cases}$$

with, at atmospheric pressure, $k_b/(k_a + k_b)$ ∿0.08 based upon data for n-butane [7,169, 170].

1-Butene

$$CH_3CH_2\overset{OO}{\overset{|}{C}}HCH_2OH + NO \begin{cases} \rightarrow CH_3CH_2\overset{O}{\overset{|}{C}}HCH_2OH + NO_2 & a \\ \rightarrow CH_3CH_2CH(ONO_2)CH_2OH & b \end{cases}$$

$$CH_3CH_2CHOHCH_2OO + NO \begin{cases} \rightarrow CH_3CH_2CHOHCH_2O + NO_2 & a \\ \rightarrow CH_3CH_2CHOHCH_2ONO_2 & b \end{cases}$$

with, at atmospheric pressure, $k_b/(k_a + k_b)$ ∿0.08, as noted above for trans-2-butene.

However, the allylic radical formed after H atom abstraction from 1-butene, after adding O_2:

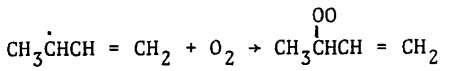

can either react with NO

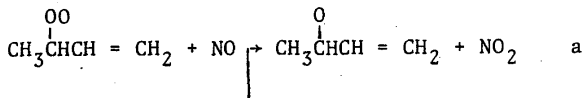

(with $k_b/(k_a + k_b)$ ∿0.08, at atmospheric pressure), or cyclise:

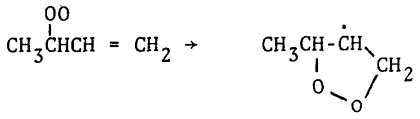

For the cyclisation reaction, Demerjian et al. [267] estimated a preexponential factor of $10^{11.5}$ s^{-1} and an activation energy of 11 kcal mol^{-1} (5 kcal mol^{-1} for the addition plus ∿6 kcal mol^{-1} for the resulting strain energy of a 5-membered ring). This then yields k (cyclization) ∿3 x 10^3 s^{-1}. Atkinson et al. [11] for analogous systems assumed a preexponential factor ≥10^{10} s^{-1} and an activation energy of [≤9 kcal mol^{-1} plus the reaction endothermicity (if any)]. Since the above cyclisation can be calculated from group additivity to be ∿6 kcal mol^{-1} exothermic, then k (cyclisation) ≳ 2.5 x 10^3 s^{-1} at 298 K.

Since the reaction with NO [reaction (50)] has a rate constant of

$$\sim 7 \times 10^{-12}\ cm^3\ molecule^{-1}\ s^{-1},$$

then for NO concentrations of 1 ppm (2.5 x 10^{13} molecule cm^{-3}) reaction (50) has a rate of ∿180 s^{-1}. Hence for sub-ppm concentrations of NO at > 298 K cyclisation is expected to dominate in agreement with Dermerjian et al. [267] and Atkinson et al. [11].

However, experimental data on analogous systems indicate that cyclisation of such radicals does not occur. Thus Arnts and Gay [268] observed the formation of methyl vinyl ketone and methacrolein during the early stages (before significant O_3 production had occurred) of NO_x-air photooxidations of isoprene, showing that the reaction of OH radicals with isoprene proceeds via

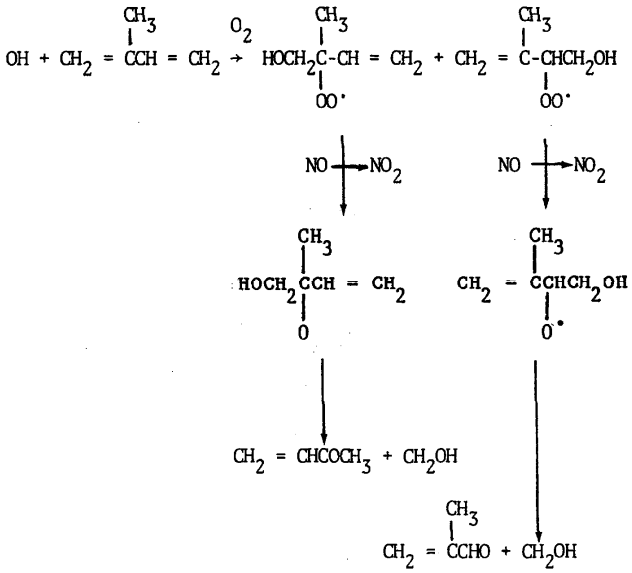

whereas peroxy radical cyclisation would have been expected to yield methylglyoxal and $HOCH_2CHO$ as two of the products.

Hence, it appears that cyclisation of peroxy radicals does not occur, and we thus neglect this pathway. The resulting alkoxy radicals from the respective alkenes at this stage are then:

Ethene

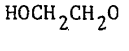

Propene

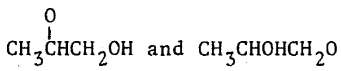

1-Butene

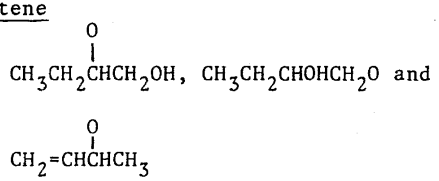

trans-2-Butene

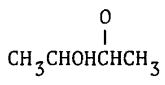

Alkoxy Radical Reactions

The alkoxy radicals (both those above and in general) can react via three routes.

a) React with O_2:

$$RR'CHO + O_2 \rightarrow RR'CO + HO_2$$

(reaction 57)

b) Unimolecularly decompose:

$$CH_3\overset{O}{\overset{|}{C}}HCH_2OH \rightarrow CH_3CHO + CH_2OH,$$

(reaction 64) or

c) Isomerise:

$$CHRR'CR''R'''O\cdot \rightarrow \cdot CRR'CR''R'''OH$$

(reaction 65).

These three pathways are illustrated for the following case:

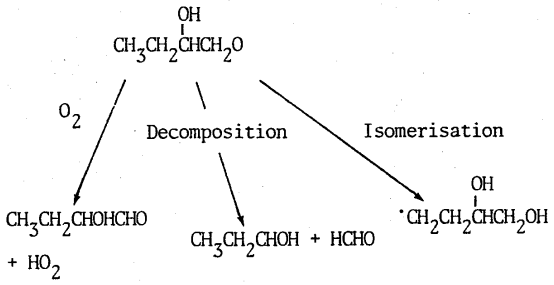

The rates of these general pathways have recently been theoretically discussed [6,7, 200-202,224,269,270], and experimental data exist for some of these reactions [7,200-202, 222,271,272]. The reactions of alkoxy radicals with O_2 have been discussed in section 4 (reaction 57). The conclusions of these theoretical and experimental studies are summarized below:

Alkoxy Radical Reactions With O_2 (57)

As discussed in section 4, the recent data and estimations of Gutman et al. [222] form the basis of the present recommendations. As discussed there, we recommend that at 298 K

$$k_{57}\ (CH_3O + O_2) = 1.3 \times 10^{-15}\ cm^3\ molecule^{-1}\ s^{-1}$$

$$k_{57}\ (\text{other primary alkoxy} + O_2) = 7 \times 10^{-15}\ cm^3\ molecule^{-1}\ s^{-1}$$

$$k_{57}\ (\text{secondary alkoxy} + O_2) \approx 3 \times 10^{-14}\ cm^3\ molecule^{-1}\ s^{-1}$$

Note that these recommendations do not extend to alkoxy radicals containing substituent groups such as -OH, -halogen, etc. (see reference [127], for example). Since many of the experimental data are obtained relative to k_{57}, these above values form the basis for comparison of experimental and theoretical data.

Isomerisation (65)

The available calculations (tables 22 and 23) were carried out in a similar manner by both groups [224,269] and the estimated isomerisation rates agree reasonably well (within a factor of 10 except for the 1.5-H shift from secondary C-H groups), when it is considered that Baldwin et al. [224] estimate that the uncertainties are of the order of a factor of ∿60.

The experimental data available, from n-butane-NO_x-air irradiations, concern only the 1-butoxy radical with rate constant ratios of

$$k_{65}/k_{57} = 1.65 \times 10^{19}\ \text{molecule cm}^{-3}$$

at 303 K [7];

$$= (1.5 \pm 0.5) \times 10^{19}\ \text{molecule cm}^{-3}$$

at 296 K [271];

$$= (1.9 \pm 0.2) \times 10^{19}\ \text{molecule cm}^{-3}$$

at 298 ± 2 K [272] having been derived. Taking the value of

$$k_{57} \sim 7 \times 10^{-15}\ cm^3\ molecule^{-1}\ s^{-1}$$

at 298 K given above, these data yield rate constants k_{65} of

$$\sim(1.0 - 1.4) \times 10^5\ s^{-1}$$

at ∿299 ± 3 K for the isomerisation of the 1-butoxy radical, in reasonably good agreement with the calculated data (table 23).

Alkoxy Radical Decomposition (64)

Some alkoxy radical decomposition rates have been determined experimentally [200-202] and others have been estimated by Baldwin et al. [224], Batt [200-202] and, from smog chamber data, by Carter et al. [7] and Cox et al. [271]. The data thus obtained are summarized in tables 24 and 25 for selected alkoxy and β-hydroxyalkoxy radicals of interest for this project.

The data shown in table 25 are obtained from the above discussions for selected alkoxy and β-hydroxyalkoxy radicals produced

Table 22. Estimation Procedures for Alkoxy Radical Isomerizations

Hydrogen Atom Abstracted	E (abstraction) kcal mol^{-1} [a]	
	Baldwin et al. [224] [b]	Carter et al. [269]
RCH_2-H	7.2	7.4
RCH(OH)-H	6.0	
R_1R_2CH-H	4.1	5.8
$R_1R_2R_3C$-H	4.1	4.1
$RC(OH)_2$-H	4.1	
	Strain Energy (kcal mol^{-1})	
5 membered ring	5.9	6.0
6 membered ring	0.5	1.5
	Log_{10}A Factor (per abstractable H atom) s^{-1}	
5 membered ring	11.2	12.0
6 membered ring	10.9	11.3

[a] These abstraction activation energies were, in both cases, derived by analogy with the experimental data for the H atom abstraction activation energies for alkoxy radical reactions.

[b] Uncertain to ± 2 kcal mol^{-1}.

Table 23. Rate Constants, k_{65}, at 298 K for Isomerization of Various Alkoxy Radicals

	Hydrogen Atom Abstracted	k_{65} s^{-1} per Abstractable H Atom	
		Baldwin et al. [224]	Carter et al. [269]
1.4-H Shift	RCH_2-H	39	1.5×10^2
	RCH(OH)-H	3.0×10^2	
	R_1R_2CH-H	7.3×10^3	2.2×10^3
	$R_1R_2R_3C$-H	7.3×10^3	3.9×10^3
	$RC(OH)_2$-H	7.3×10^3	
1.5-H Shift	RCH_2-H	1.8×10^5	5.9×10^4
	RCH(OH)-H	1.4×10^6	
	R_1R_2CH-H	3.4×10^7	8.8×10^5
	$R_1R_2R_3C$-H	3.4×10^7	1.6×10^7
	$RC(OH)_2$-H	3.4×10^7	

Table 24. Estimated Alkoxy Radical Decomposition Rates

Alkoxy Radicals	k_{64} s^{-1} (1 atmosphere air, 298 K) Baldwin et al. [224][a]	Batt [200-202]
CH_3-CH_2O	2×10^{-5}	<0.14
$CH_3CH_2CH_2-CH_2O$	0.3	
$CH_3CH_2-\dot{C}HCH_3$ (O)	3×10^3	5×10^3
$HOCH_2CH_2CH_2-CH_2O$	0.2	
$CH_3-\dot{C}O-CH_3$ (CH_3)	2×10^3	$\leq 1 \times 10^3$
β-Hydroxy Alkoxy Radicals		
$HOCH_2-CH_2O$	~0.2[b]	≲6
$CH_3CHOH-CH_2O$	3×10^{-2} to 2	
$CH_3\dot{C}H-CH_2OH$ (O)	30 to 2×10^3	
$CH_3CHOH-\dot{C}HCH_3$ (O)		≲2×10^2

[a] Recalculated from the A factor, activation energy and fall-off correction given by Baldwin et al. [224] in their Table II. Some of these recalculated values differ by a factor of 10 from those cited by Baldwin et al. [224] - reason unknown.

[b] Reference 270.

Table 25. Summary of Reaction Pathway Rates for Selected Alkoxy and β-Hydroxyalkoxy Radicals at 298 K and Atmospheric Pressure (760 Torr Total Pressure)

Alkoxy Radical	Reaction Rate (s^{-1}) Reaction with O_2	Decomposition	Isomerization
CH_3CH_2O	3.6×10^4	~2×10^{-5}	Negligible
$CH_3CH_2CH_2CH_2O$	3.6×10^4	0.3	2×10^5 - 6×10^5 (~1.2×10^5)[a]
$CH_3CH_2\dot{C}HCH_3$ (O)	1.6×10^5	5×10^3 (~8×10^4)[b]	120-450
β-Hydroxyalkoxy Radicals			
$HOCH_2CH_2O$	c	<6	Negligible
$CH_3CHOHCH_2O$	c	≲2	120-450
$CH_3\dot{C}HCH_2OH$ (O)	c	≲2×10^3	Negligible
$CH_3CH_2CHOHCH_2O$	c	d	2×10^5 - 6×10^5
$CH_3CH_2\dot{C}HCH_2OH$ (O)	c	d	120-450
$CH_3CHOH\dot{C}HCH_3$ (O)	c	~2×10^2	120-450

[a] Experimental value, relative to reaction with O_2, [7, 271, 272] at 296-303 K.

[b] Experimental value, relative to reaction with O_2, [7, 271] at 296-303 K.

[c] Not known; may be similar to those for primary or secondary alkoxy radicals given above (but see [127]).

[d] Not estimated.

in the alkane and alkene-NO_x-air photooxidations. Two points in table 25 need to be noted. The first is that, while there is good agreement between the calculated and experimental isomerisation rates for the 1-butoxy radical, the decomposition rate constant for the 2-butoxy radical obtained from environmental chamber data [7,271] is an order of magnitude higher than the experimental value of Batt and McCulloch [194]. Since these isomerisation and decomposition rates obtained from environmental chamber data [7,271,272] are based upon the RO + O_2 rate constants, it is obvious that further research as to the isomerisation, decomposition and reaction rates with O_2 are urgently needed. Secondly, although, as noted in table 25, no data are available for the rate constants for the reaction of the hydroxyalkoxy radicals with O_2, these reactions are expected to be as fast as, or possibly faster than [127], those for the corresponding alkoxy radicals, i.e. $\gtrsim 3 \times 10^4$ s^{-1} at 298 K and atmospheric pressure. Hence, for the β-hydroxyalkoxy radicals produced in the OH radical reactions with the alkenes of interest here, these data imply that reaction with O_2 should dominate, except for the $CH_3CH_2CHOHCH_2O$ radical derived from internal OH radical addition to 1-butene, where isomerisation may dominate.

However, in recent product studies of the ethene, propene and trans-2-butene-HONO-NO-air irradiation systems, Niki et al. [273, 274] monitored products by FT-IR (Fourier transform infrared) spectroscopy under conditions where photolyses of the product aldehydes were minimized, and from these definite studies [273,274] the following data were obtained:

Ethene

The most recent study of Niki et al. [274] has shown that the β-hydroxyalkoxy radical $HOCH_2CH_2O$ reacts via:

$$HOCH_2CH_2O \rightarrow HCHO + CH_2OH \quad (64)$$

$$HOCH_2CHO + O_2 \rightarrow HOCH_2CHO + HO_2 \quad (57)$$

with

$$k_{57}/k_{64} = (5.4 \pm 1.0) \times 10^{-20} \text{ cm}^3 \text{ molecule}^{-1}$$

at room temperature (the indicated uncertainty being one standard deviation), based on the observed glycolaldehyde and formaldehyde yields at varying O_2 concentrations. Thus, at 760 torr total pressure of air and 298 K, the fraction of $HOCH_2CHO$ radicals reacting with O_2 to yield glycolaldehyde is 0.22 ± 0.05, with the remainder decomposing to yield HCHO + CH_2OH. These data are in good agreement with the earlier study of Niki et al. [273] where 81% of the ethene reacting with OH radicals proceeded via reaction (64) at 700 torr total pressure of air and 300 K. Hence, we recommend the above rate constant ratio k_{57}/k_{64}.

Propene

The study of Niki et al. [273] showed that 8.1 ppm of propene reacting with OH radicals yielded 7.0 ppm of HCHO and 7.9 ppm of CH_3CHO. These data indicate that >86% of the propene reacted yields HCHO and CH_3CHO via decomposition of the β-hydroxyalkoxy radical. Since the (decomposition/reaction with O_2) ratio is expected to increase significantly in going from ethene to propene, we recommend that decomposition of the β-hydroxyalkoxy radicals be taken to be the sole reaction pathway at 300 K and 760 torr of air, i.e.,

$$CH_3CHOHCH_2O \rightarrow CH_3CHOH + HCHO$$

$$CH_3\overset{O}{\overset{|}{C}}HCH_2OH \rightarrow CH_3CHO + CH_2OH$$

trans-2-Butene

Again, the data of Niki et al. [273] show that the $CH_3\overset{O}{\overset{|}{C}}HCHOHCH_3$ radical reacts essentially solely by decomposition (6.1 ppm of trans-2-butene yielded 12.8 ppm of CH_3CHO):

$$CH_3\overset{O\cdot}{\overset{|}{C}}HCHOHCH_3 \rightarrow CH_3CHO + CH_3CHOH$$

We recommend these reaction pathways, and recommend that the β-hydroxyalkoxy radicals formed after terminal OH radical addition to 1-butene also react only via decomposition,

$$CH_3CH_2\overset{O}{\overset{|}{C}}HCH_2OH \rightarrow CH_3CH_2CHO + CH_2OH$$

followed by reaction of the α-hydroxy radicals (RR'CHOH) with O_2 to yield the aldehyde (see reaction (66) below).

However, (a) for the radical $CH_3CH_2CHOHCH_2O$; isomerisation

$$CH_3CH_2CHOHCH_2O\cdot \rightarrow \cdot CH_2CH_2CHOHCH_2OH \quad (65)$$

must also be considered as a possible pathway. From table 25, this isomerisation is estimated to have a rate at 298 K of 2×10^5 to 6×10^5 s^{-1}. From smog chamber data for the 1-butoxy radical [7,271,272], we recommend that

$$k_{65}\ (CH_3CH_2CH_2CH_2O\cdot) \sim 1.5 \times 10^{11} e^{-4200/T}\ s^{-1}$$

$$\sim 1.1 \times 10^5\ s^{-1}$$

at 298 K, which is in good agreement with the thermochemical estimates (table 22).

Since decomposition predominates over reaction with O_2 for the β-hydroxyalkoxy radicals derived from OH radical addition to ethene, propene and trans-2-butene [273,274], the decomposition rate constants k_{64} for the radicals $RCHOHCH_2O$ (including the radical $HOCH_2CH_2O$) are probably >1 x 10^5 s^{-1} at 298 K. Hence, it appears that, even for the $CH_3CH_2CHOHCH_2O$ radical, decomposition will be competitive with isomerisation and, until further evidence is forthcoming, we recommend that the $CH_3CH_2CHOHCH_2O$ radical be considered to only undergo decomposition under atmospheric conditions:

$$CH_3CH_2CHOHCH_2O\cdot \rightarrow CH_3CH_2CHOH + HCHO \quad (64)$$

(b) the $CH_3\overset{O}{\overset{|}{C}}HCH=CH_2$ radical, formed after initial H atom abstraction from 1-butene, can react via three pathways:

$$CH_3\overset{O}{\overset{|}{C}}HCH=CH_2 \rightarrow CH_3^{\cdot} + CH_2=CHCHO \quad a$$

$$\rightarrow CH_3CHO + \dot{C}H=CH_2 \quad b$$

$$CH_3\overset{O}{\overset{|}{C}}HCH=CH_2 + O_2 \rightarrow CH_3COCH=CH_2 + HO_2 \quad c$$

Of the decomposition pathways (a) and (b), (a) is thermochemically more favorable, but because of the weak allylic C-H bond, it is, a-priori, expected that reaction with O_2, i.e., pathway (c), should be the major reaction pathway to form methyl vinyl ketone. It should be noted that since the radical

$$CH_3\overset{O}{\overset{|}{C}}HCH=CH_2$$

is an alkoxy radical, albeit unsaturated, it should be more amenable to thermochemical estimates than the above discussed β-hydroxyalkoxy radicals.

$$RR_1\dot{C}OH + O_2 \rightarrow RCOR_1 + HO_2 \quad (66)$$

α-Hydroxy radicals are formed during NO_x-air-organic photooxidations from two major reaction paths; decomposition of β-hydroxyalkoxy radicals (as shown above), and from alkoxy radical isomerisations; an example of the latter process being:

Isomerisation

$$CH_3CH_2CH_2CH_2O\cdot \rightarrow \cdot CH_2CH_2CH_2CH_2OH$$

$$\cdot CH_2CH_2CH_2CH_2OH \xrightarrow{O_2,\ NO \rightarrow NO_2} \cdot OCH_2CH_2CH_2CH_2OH$$

$$\cdot OCH_2CH_2CH_2CH_2OH \xrightarrow{\text{Isomerisation}} HOCH_2CH_2\dot{C}HCH_2OH$$

The fates of such α-hydroxy radicals under atmospheric conditions have recently been investigated. Niki et al. [273], Carter et al. [275] and Ohta et al. [276] have concluded from product studies on irradiated HONO-NO-alcohol-air or Cl_2-NO-alcohol-air mixtures that α-hydroxy radicals, RCHOH, react essentially exclusively with O_2 by the reaction:

$$R\dot{C}HOH + O_2 \rightarrow RCHO + HO_2$$

since neither carboxylic acids, which could have resulted from

$$R\dot{C}HOH + O_2 \rightarrow \underset{OO\cdot}{\underset{|}{R}}CHOH \xrightarrow[NO_2]{NO} \underset{O\cdot}{\underset{|}{R}}CHOH \xrightarrow{O_2} RCOOH + HO_2$$

nor hydroxyalkyl peroxynitrates,

$$\underset{OONO_2}{\underset{|}{R}}CHOH$$

were detected.

These findings, while perhaps definitive for computer modeling purposes, are interesting, since the observation of $HOCH_2OONO_2$ from the HO_2 + HCHO system in the presence of NO_2 [129] indicates that the $HOCH_2OO$ specie is a stable radical. Thus, why the reaction of O_2 with CH_2OH appears to proceed via H-atom abstraction to yield HCHO + HO_2, and not via addition to yield the $HOCH_2OO$ radical, is not totally clear at the present time. Further work on these systems is obviously required.

Additionally, however, Radford [277], using the reaction of Cl atoms with methanol to generate exclusively CH_2OH radicals [278]

$$Cl + CH_3OH \rightarrow HCl + CH_2OH$$

in a discharge flow-laser magnetic resonance (LMR) system, obtained, by monitoring the HO_2 LMR signal as a function of the O_2 concentration, a rate constant of

$$k_{66} = (2^{+2}_{-1}) \times 10^{-12} \text{ cm}^3 \text{ molecule}^{-1} \text{ s}^{-1}$$

at 300 K for the reaction

$$CH_2OH + O_2 \rightarrow HCHO + HO_2$$

This reaction is thus rapid under atmospheric conditions, totally consistent with the above cited product data [273,275,276].

Hence, we recommend that the reaction of α-hydroxy radicals with O_2 proceeds via the pathway

$$RR_1\dot{C}OH + O_2 \rightarrow RCOR_1 + HO_2$$

with a rate constant at 300 K of

$$k_{66} \gtrsim 2 \times 10^{-12} \text{ cm}^3 \text{ molecule}^{-1} \text{ s}^{-1}$$

and that this reaction is the sole tropospheric fate of the α-hydroxy radicals. The OH radical reaction pathways for the four alkenes discussed above are shown schematically in figures 9 through 12.

$$NO_3 + \text{Alkenes} \rightarrow \text{Products} \qquad (67)$$

The reactions of NO_3 with alkenes in the gas phase have been studied by Morris and Niki [231], Japar and Niki [279], Hoshino et al. [280] and Atkinson et al. [130]. In the preliminary study of Morris and Niki [231] and in the much more extensive study of Japar and Niki [279] rate constants k_{67} were derived from the N_2O_5 decays in N_2O_5-NO_2-alkene mixtures. This technique and a relative rate technique were used by Atkinson et al. [130]. Both of these techniques yield rate constants which are linearly depend on the equilibrium constant for the reaction system.

$$NO_2 + NO_3 \rightleftarrows N_2O_5$$

With the recommended equilibrium constant $K_{7,8}$ of Malko and Troe [27], the rate constants k_{67} obtained at ~298 K for ethene, propene, 1-butene and trans-2-butene are:

Ethene

$$k_{67} = (1.09 \pm 0.12) \times 10^{-15} \text{ cm}^3 \text{ molecule}^{-1} \text{ s}^{-1} \text{ [279]}$$
$$= (6.1 \pm 2.6) \times 10^{-17} \text{ cm}^3 \text{ molecule}^{-1} \text{ s}^{-1} \text{ [130]}$$

Propene

$$k_{67} = (3.5 \pm 0.9) \times 10^{-15} \text{ cm}^3 \text{ molecule}^{-1} \text{ s}^{-1} \text{ [231]}$$
$$= (6.2 \pm 0.4) \times 10^{-15} \text{ cm}^3 \text{ molecule}^{-1} \text{ s}^{-1} \text{ [279]}$$
$$= (4.2 \pm 0.9) \times 10^{-15} \text{ cm}^3 \text{ molecule}^{-1} \text{ s}^{-1} \text{ [130]}$$

1-Butene

$$k_{67} = (9.1 \pm 1.0) \times 10^{-15} \text{ cm}^3 \text{ molecule}^{-1} \text{ s}^{-1} \text{ [279]}$$
$$= (5.4 \pm 1.2) \times 10^{-15} \text{ cm}^3 \text{ molecule}^{-1} \text{ s}^{-1} \text{ [130]}$$

trans-2-Butene

$$k_{67} = (1.6 \pm 0.12) \times 10^{-13} \text{ cm}^3 \text{ molecule}^{-1} \text{ s}^{-1} \text{ [279]}$$
$$= (2.11 \pm 0.24) \times 10^{-13} \text{ cm}^3 \text{ molecule}^{-1} \text{ s}^{-1} \text{ [130]}$$

Apart from ethene, these data are in general agreement and the recommended values of k_{67} are those of the most recent study of Atkinson et al. [130]:

Ethene

$$k_{67} = 6 \times 10^{-17} \text{ cm}^3 \text{ molecule}^{-1} \text{ s}^{-1}$$

at 298 K with an uncertainty of a factor of 3.

Propene

$$k_{67} = 4.2 \times 10^{-15} \text{ cm}^3 \text{ molecule}^{-1} \text{ s}^{-1}$$

at 298 K with an uncertainty of a factor of 2.

1-Butene

$$k_{67} = 5.4 \times 10^{-15} \text{ cm}^3 \text{ molecule}^{-1} \text{ s}^{-1}$$

at 298 K with an uncertainty of a factor of 2.

trans-2-Butene

$$k_{67} = 2.1 \times 10^{-13} \text{ cm}^3 \text{ molecule}^{-1} \text{ s}^{-1}$$

at 298 K with an uncertainty of a factor of 2.

In the studies of Morris and Niki [231] and of Japar and Niki [279], a product was observed which had an infrared absorption band at 1670 cm^{-1} for propene, and at similar frequencies for the other alkenes. This band was attributed to a nitrite. The marked increase in the rate constant with the degree of alkyl substitution (from

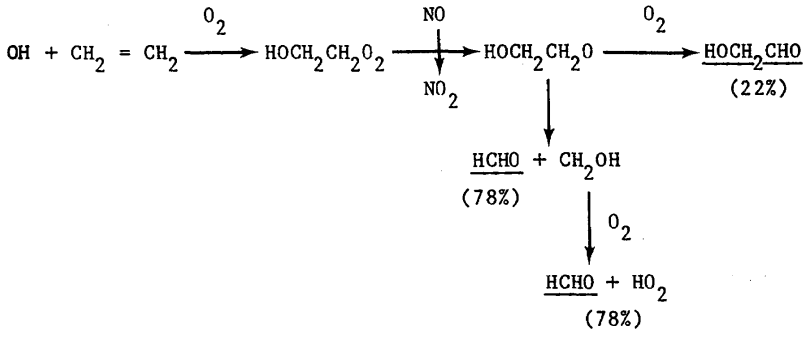

Figure 9. Recommended Reaction Pathways in the Irradiated NO_x-air-C_2H_4 System (Stable Products are Underlined).

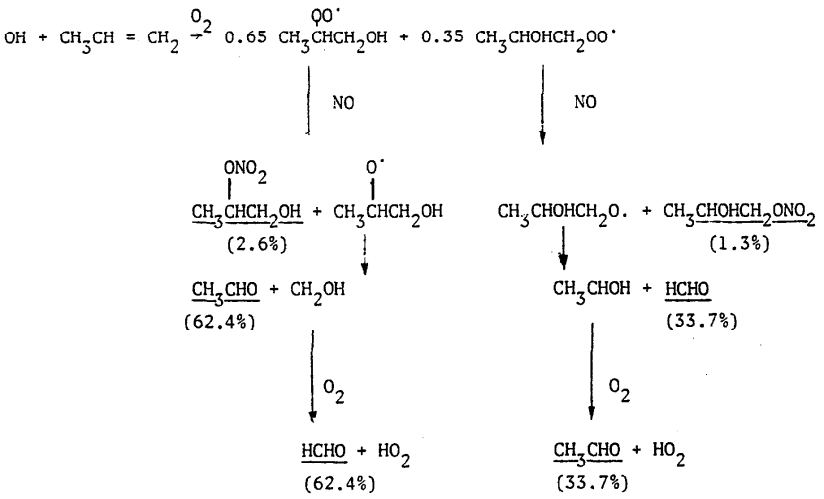

Total CH_3CHO yield 96%

HCHO yield 96%

$CH_3\underset{\displaystyle ONO_2}{\underset{|}{C}}HCH_2OH$ yield ∿2.6%

$CH_3CHOHCH_2ONO_2$ yield ∿1.3%

Figure 10. Recommended Reaction Pathways in the Irradiated NO_x-propene-air system.

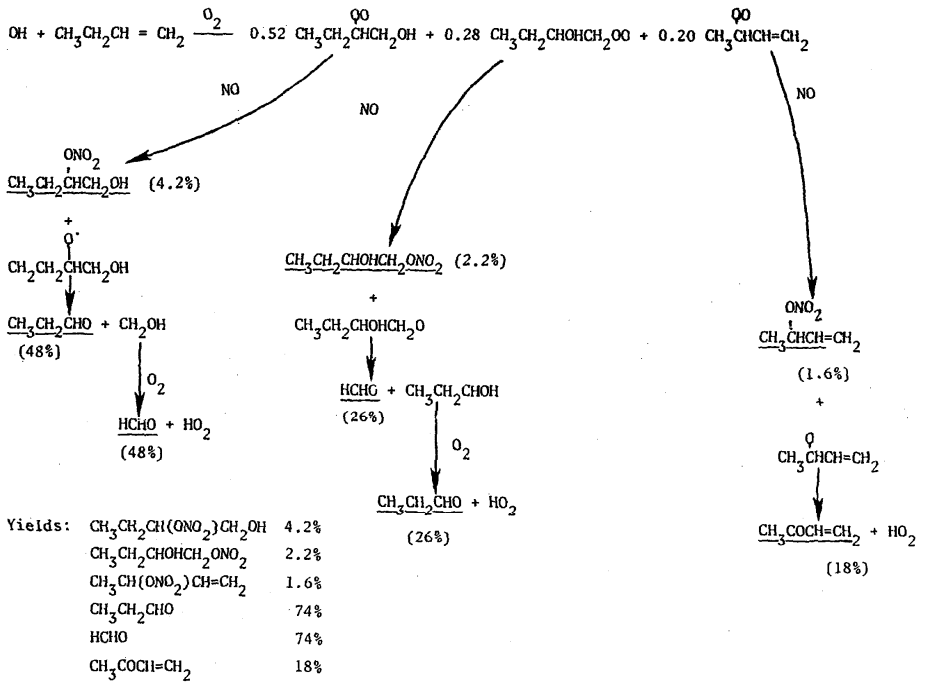

Figure 11. Recommended Reaction Pathways in the Irradiated NO_x-1-butene-air System.

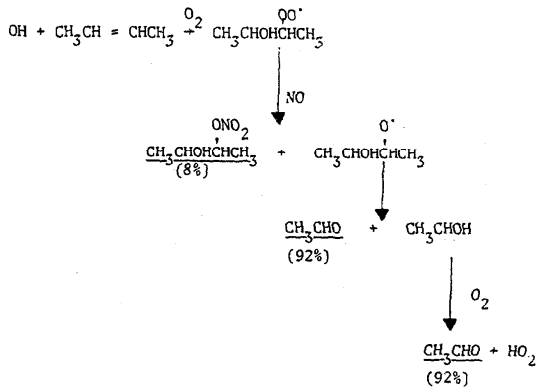

Total Products

CH_3CHO 184%

$CH_3CHOHCHCH_3$ (ONO2) 8%

Figure 12. Recommended reaction pathways in the irradiated NO_x-trans-2-butene-air system.

6×10^{-17} cm^3 $molecule^{-1}$ s^{-1}

for ethene to

3.1×10^{-11} cm^3 $molecule^{-1}$ s^{-1}

for 2,3-dimethyl-2-butene [130]) indicates [130,279] that the initial reaction is one of NO_3 addition to the alkene double bond (taking propene as an example):

$$NO_3 + CH_3CH{=}CH_2 \rightarrow CH_3\dot{C}HCH_2ONO_2 \text{ (major)} +$$

$$CH_3CH(ONO_2)\dot{C}H_2. \text{ (minor)}$$

Hoshino et al. [280] and Atkinson et al. [130] from an FT-IR study of the reaction of N_2O_5 with propene also observed a product with an IR absorption band at 1670 cm^{-1} (together with bands at 1280 and 840 cm^{-1}). These absorption bands were attributed by Hoshino et al. [280], by comparison to those of an authentic sample, to propylene glycol-1,2-dinitrate (PGDN):

$$CH_3CH(ONO_2)CH_2ONO_2$$

This assignment was confirmed by the observation of a peak at m/e = 167 by GC-CIMS (gas chromatography - chemical ionization mass spectrometry).

This product, i.e., PGDN, was also observed [281] in irradiated NO_x (1.5 ppm) - propene (3.0 ppm) - air mixtures at a level of ~0.10 ppm.

However, the mechanism of formation of such dinitrates is not immediately obvious in the presence of O_2. The initial reaction is expected to form mainly

$$CH_3\dot{C}HCH_2ONO_2, \text{ with } CH_3\dot{C}(ONO_2)CH_2.$$

formation being the minor pathway. Under atmospheric conditions, reaction with O_2 should then predominate:

$$CH_3\dot{C}HCH_2ONO_2 + O_2 \rightarrow CH_3CH(OO\cdot)CH_2ONO_2$$

$$CH_3CH(ONO_2)\dot{C}H_2 + O_2 \rightarrow CH_3CH(ONO_2)CH_2OO\cdot$$

Reaction with NO_2 should then yield the thermally short lived peroxynitrates

$$CH_3CH(OO\cdot)CH_2ONO_2 + NO_2 \rightleftarrows CH_3CH(OONO_2)CH_2ONO_2$$

$$CH_3CH(ONO_2)CH_2OO + NO_2 \rightleftarrows CH_3CH(ONO_2)CH_2OONO_2,$$

consistent with the observations of Bandow et al. [282].

In dark N_2O_5-propene-air mixtures, as studied by Bandow et al. [282], self-reaction of the peroxy radicals can lead to the corresponding alkoxy radicals

$$2\ CH_3CH(ONO_2)CH_2OO \rightarrow 2\ CH_3CH(ONO_2)CH_2O + O_2$$

$$2\ CH_3CH(OO)CH_2ONO_2 \rightarrow 2\ CH_3CH(O)CH_2ONO_2 + O_2$$

and Bandow et al. [282] derived a rate constant of $\sim 1.2 \times 10^{-12}$ cm^3 $molecule^{-1}$ s^{-1} for these self-reactions at room temperature. These alkoxy radicals can then combine with NO_2 to yield PGDN

$$CH_3CH(ONO_2)CH_2O + NO_2 \rightarrow CH_3CH(ONO_2)CH_2ONO_2$$

$$CH_3CH(O)CH_2ONO_2 + NO_2$$

or decompose to yield the other observed products CH_3CHO and HCHO [282].

$$CH_3CH(ONO_2)CH_2O \rightarrow CH_3\dot{C}HONO_2 + HCHO$$

$$\downarrow$$

$$CH_3CHO + NO_2$$

$$CH_3CH(O)CH_2ONO_2 \rightarrow CH_3CHO + \dot{C}H_2ONO_2$$

$$\downarrow$$

$$HCHO + NO_2$$

In irradiated systems, where if NO_x is present, NO is present (albeit sometimes in low concentrations) formation of PGDN may occur via, for example:

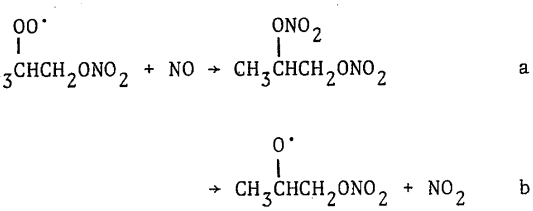

a

b

where the ratio k_a/k_b is not known, but is possibly of the order of 0.1 at atmospheric pressure.

$$O_3 + \text{Alkenes} \rightarrow \text{Products} \qquad (68)$$

The overall rate constants k_{68} have been measured for a variety of alkenes in numerous studies (see Niki [283] for a brief discussion covering the subject through mid-1978). The most extensive absolute rate constant studies for the alkenes have been those of Japar et al. [284], who measured the decay of O_3 in excess alkene with one atmosphere of air as diluent, and of Herron and Huie [285,286], who monitored the loss rate of O_3 in excess alkene at ∿3-4 torr total pressure of O_2. The absolute rate constant data for ethene, propene, 1-butene and trans-2-butene from these and other studies are shown in table 26.

As seen from table 26, and as discussed by Niki [283], the reported literature rate constants agree reasonably well for the terminal alkenes, but scatter far beyond the estimated experimental precision for the internal alkenes. While the recent data of Adeniji et al. [297] are in good agreement with the extensive study of Japar et al. [284], the recent studies of Atkinson et al. [298, 300], using techniques very similar to those used by references 284 and 297, yield lower rate constant data which are more in agreement with the rate constants obtained by Huie and Herron [286]. Since secondary reactions are known to occur in these systems [293,301,302], all O_3 + alkene rate constants must rigorously be regarded as upper limits. We recommend:

Ethene

From a unit-weighted least squares analysis of the data of DeMore [290], Stedman et al. [291], Herron and Huie [285], Japar et al. [284,293], Toby et al. [294], Su et al. [295], Kan et al. [296], Adeniji et al. [297] and Atkinson et al. [298], a rate constant of

$$k_{68} = 1.75 \times 10^{-18} \text{ cm}^3 \text{ molecule}^{-1} \text{ s}^{-1}$$

at 298 K, with an estimated uncertainty of ± 30%.

$$= 1.2 \times 10^{-14} e^{-2633/T} \text{ cm}^3 \text{ molecule}^{-1} \text{ s}^{-1}$$

is recommended.

Propene

From a unit-weighted least squares analysis of the data of Cox and Penkett [299], Stedman et al. [291], Herron and Huie [285], Japar et al. [284,293], Adeniji et al. [297] and Atkinson et al. [298], a rate constant of

$$k_{68} = 1.13 \times 10^{-17} \text{ cm}^3 \text{ molecule}^{-1} \text{ s}^{-1}$$

at 298 K, with an estimated uncertainty of ∿± 30%,

$$= 1.3 \times 10^{-14} e^{-2105/T} \text{ cm}^3 \text{ molecule}^{-1} \text{ s}^{-1}$$

is recommended.

1-Butene

From a unit-weighted least squares analysis of the data of Japar et al. [284], Huie and Herron [286] and Adeniji et al. [297], a rate constant of

$$k_{68} = 1.10 \times 10^{-17} \text{ cm}^3 \text{ molecule}^{-1} \text{ s}^{-1}$$

at 298 K, with an estimated uncertainty of ± 30%,

$$= 3.5 \times 10^{-15} e^{-1713/T} \text{ cm}^3 \text{ molecule}^{-1} \text{ s}^{-1}$$

is recommended.

trans-2-Butene

From a unit-weighted least squares analysis of the data of Cox and Penkett [299], Stedman et al. [291], Japar et al. [284,293], Huie and Herron [286] and Adeniji et al. [297], a rate constant of

$$k_{68} = 2.00 \times 10^{-16} \text{ cm}^3 \text{ molecule}^{-1} \text{ s}^{-1}$$

at 298 K, with an estimated uncertainty of ± 40%

$$= 9.1 \times 10^{-15} e^{-1136/T} \text{ cm}^3 \text{ molecule}^{-1} \text{ s}^{-1}$$

is recommended.

Table 26. Absolute Rate Constants (At Room Temperature) and Arrhenius Activation Energies for the Reaction of O_3 With Ethene, Propene, 1-Butene and trans-2-Butene

Alkene	$10^{18} \times k_{68}$ cm^3 $molecule^{-1}$ s^{-1}	at T K	E/R(K)	Reference
Ethene	3.6 ± 1.4	b		[287]
	1.35	b		[288]
	2.7 ± 0.3	303	2100 ± 200	[289]
	1.2[a]	298	2365 ± 101	[290]
	1.55 ± 0.15	299 ± 2		[291]
	≤2.8[c]	298	2491 ± 101	[292]
	1.9 ± 0.1	299 ± 2		[284,293]
	1.7[d]	298	2557 ± 167	[285]
	1.69 ± 0.13	303		[294]
	1.94[d]	298	2828 ± 181	[295,296]
	1.6	294 ± 2	∿2920	[297]
	1.43 ± 0.19	296 ± 2		[298]
Propene	6.2	b		[287]
	8.1	b		[288]
	12.6	296		[299]
	12.5 ± 1.0	299 ± 2		[291]
	14.5	298	1968 ± 101	[292]
	13.0 ± 0.1	299 ± 2		[284]
	10.6[d]	298	1897 ± 109	[285]
	13.2 ± 0.3	299		[293]
	12.6	294 ± 2	∿2010	[297]
	10.4 ± 1.4	296 ± 2		[298]
1-Butene	10.3	303		[289]
	12.3 ± 0.4	299 ± 2		[284]
	10.3[d]	298	1686 ± 20	[286]
	12.6	294 ± 2	∿1960	[297]
trans-2-Butene	432 ± 66	303	100 ± 150	[289]
	257	296		[299]
	275 ± 23	299 ± 2		[291]
	260 ± 9	299 ± 2		[284]
	176[d]	298	1051 ± 43	[286]
	256 ± 15	299		[293]
	288	294 ± 2		[297]

[a] Data obtained at 178-233 K. The room temperature rate constant requires a lengthy extrapolation of the Arrhenius expression and hence is not of high accuracy.

[b] Not reported, room temperature.

[c] Insufficient O_2 present to suppress secondary reactions, hence an upper limit [292].

[d] Calculated from Arrhenius expression.

While numerous product studies have been carried out, the most definitive mechanistic data have emerged from the studies of Cox and Penkett [299], Niki et al. [303-305], Herron and coworkers [301,302,306], Calvert and coworkers [295,296], and Dodge and Arnts [307]. These studies and the relevant data are summarized below.

It is now reasonably well established from these studies that the initial step in the O_3-alkene reaction is the formation of a "molozonide" which rapidly decomposes [308, 309] to a carbonyl and a biradical, which is also initially energy rich:

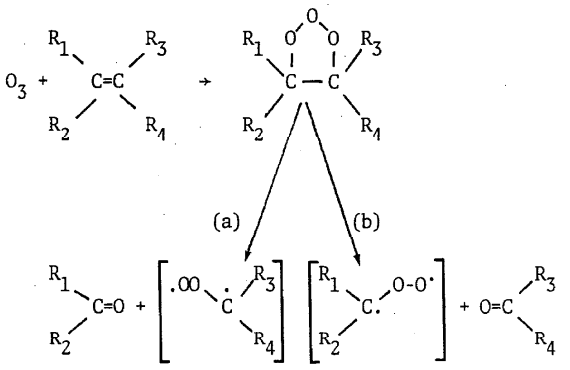

with [302], $k_a \simeq k_b$.

Hence, the major problem lies in the subsequent reactions of the "hot" biradicals $[R_1R_2\dot{C}O\dot{O}]$, and the information available is summarized below for increasing complexity of the biradical:

$[\dot{C}H_2\dot{O}_2]$

The most unambiguous data concerning the CH2OO biradical arise from studies of the O_3-ethene reaction. Herron and Huie [301] used photoionization-mass spectrometry to study the products and mechanisms of the O_3-ethene reaction at a total pressure of ∿4 torr.

Secondary reactions were observed to be very important, especially those involving OH radicals. By extrapolating their data back to zero reaction time, the initial stoichiometry observed was:

$$O_3 + C_2H_4 \rightarrow 1.0\ HCHO + 0.67\ H_2O$$

$$+ 0.27\ CO_2 + 0.06\ HCOOH + 0.03\ CH_3OH$$

and this was rationalized by the reaction sequence:

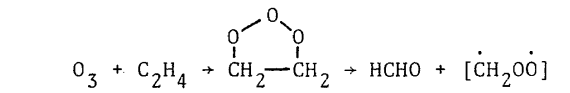

$$[\dot{C}H_2O\dot{O}] \rightarrow H_2C\begin{matrix}O\\|\\O\end{matrix} \rightarrow CH_2\begin{matrix}O\cdot\\O\cdot\end{matrix} \rightarrow [HCOOH]$$

where $[\dot{C}H_2O\dot{O}]$ denotes an energy rich biradical, while $\dot{C}H_2O\dot{O}$ denotes the thermalized biradical species.

The $H_2C\begin{matrix}O\\|\\O\end{matrix}$ species was observed by Lovas and Suenram [310] by microwave spectroscopy and by Martinez et al. [311] by mass spectrometry at low temperatures, and this sequence is in agreement with that postulated by Wadt and Goddard [312] and Harding and Goddard [308]. The highly energized acid was suggested [301,306] to decompose or be collisionally stabilized:

$$[HCOOH] \rightarrow CO_2 + H_2$$

$$\rightarrow CO + H_2O$$

$$\rightarrow H + HCO_2 \rightarrow H + CO_2$$

$$\xrightarrow{M} HCOOH$$

With these pathways, the amount of CO formed is equal to that of H_2O, and the amount of H_2 is equal to that of CO_2. This then yields an essentially 100% carbon and hydrogen balance.

Herron and Huie [301] thus deduced the following initial reaction scheme for their conditions:

$$O_3 + C_2H_4 \rightarrow HCHO + [\dot{C}H_2O\dot{O}]$$

$$[\dot{C}H_2O\dot{O}] \rightarrow [HCOOH] \rightarrow CO_2 + H_2 \qquad 18\%$$

$$\rightarrow CO + H_2O \qquad 67\%$$

$$\rightarrow H + H + CO_2 \qquad 9\%$$

$$\rightarrow HCOOH \qquad 6\%$$

with thermalized HCOOH being formed by wall collisions or by third-body interactions. This above reaction scheme for the $[\dot{C}H_2O\dot{O}]$ biradical has been used by Dodge and Arnts [307] to model the observed stoichiometries and products from the O_3-propene reaction. From this low pressure study [301] it appears that under their conditions the rearrangement of the energy-rich biradical via

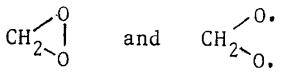

species, to hot HCOOH with subsequent decomposition, is so fast that bimolecular reactions of CH_2O_2 are unimportant.

Although secondary ozonide formation has not been observed in the gas phase O_3-ethene reaction [295,296,303-305,313], the recent FT-IR spectroscopic studies of Niki et al. [305] and Calvert and coworkers [295,296] have shown that at atmospheric pressure a substantial amount of thermalized $\dot{C}H_2\dot{O}_2$ biradicals are indeed formed and take part in bimolecular reactions with CO, HCHO, CH_3CHO and SO_2. Thus, addition of CH_3CHO to O_3-ethene-O_2-N_2 mixtures yielded propene ozonide [295],

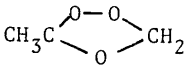

showing the presence of thermalized $\dot{C}H_2\dot{O}_2$ biradicals. From this and other observations it has been concluded [295,296,305] that ∿37% of the "hot" $[\dot{C}H_2\dot{O}_2]$ biradicals are thermalized at atmospheric pressure, while ∿63% fragment or rearrange in unimolecular steps, this latter fragmentation/rearrangement pattern being very similar to that estimated by Herron and Huie [301].

Thus, for atmospheric conditions, from the data of Herron and Huie [301], Niki et al. [305] and Calvert and coworkers [295,296], we recommend:

$$[\dot{C}H_2\dot{O}\dot{O}] \xrightarrow{M} \dot{C}H_2\dot{O}\dot{O} \text{ (thermalized)} \quad 40\%$$

$$[\dot{C}H_2\dot{O}\dot{O}] \rightarrow [HCOOH] \quad 60\%$$

followed by the decomposition reactions of [HCOOH] as proposed by Dodge and Arnts [307]

$$[HCOOH] \rightarrow CO_2 + H_2 \quad 20\%$$

$$\rightarrow CO + H_2O \quad 70\%$$

$$\rightarrow CO_2 + 2\,H \quad 10\%$$

The apparent discrepancy between the conclusions of Herron and Huie [301] and later work [295,296,305] regarding thermalized $\dot{C}H_2\dot{O}\dot{O}$ biradicals almost certainly arises because of the expected pressure dependent thermalization process

$$[\dot{C}H_2\dot{O}\dot{O}] + M \rightarrow \dot{C}H_2\dot{O}\dot{O} + M$$

Hence, under atmospheric conditions, the above reaction sequence leads to our recommended pathways for $[\dot{C}H_2\dot{O}_2]$ reactions:

$$[\dot{C}H_2\dot{O}\dot{O}] \xrightarrow{O_2} 0.40\ \dot{C}H_2\dot{O}\dot{O} + 0.18\ CO_2 + 0.42\ CO + 0.12\ H_2 + 0.42\ H_2O + 0.12\ HO_2 + [\dot{C}H_2CHO\dot{O}]$$

Information regarding this biradical comes mainly from the low pressure photoionization-mass spectrometry study of Herron and Huie [302], the FT-IR spectroscopic study of Niki et al. [304] and earlier work of Cox and Penkett [299].

For the O_3-propene reaction, carried out at ∿4 torr total pressure, the observed initial stoichiometry was [302]:

$$O_3 + CH_3CH = CH_2 \rightarrow 0.94\ HCHO + 0.45\ CH_3CHO + 0.04\ HCOOH + 0.24\ CO_2 + 0.38\ H_2O + 0.01\ CH_3COOH$$

and it was concluded that the initial reactions were:

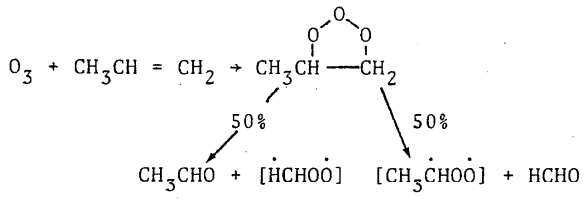

The subsequent reactions of $[\dot{H}CHO\dot{O}]$, as deduced from the previous study of the O_3-ethene reaction carried out at the same total pressure, which we believe to be applicable, were used to deduce the subsequent reactions of the $[\dot{C}H_2CHO\dot{O}]$ biradical. However, the fate of the $[\dot{C}H_2CHO\dot{O}]$ biradical could not, because of the greater complexity of the system, be unambiguously determined, but it appeared from computer modeling that [302];

$$[CH_3\dot{C}HO\dot{O}] \rightarrow [CH_3CO_2H] \rightarrow CH_3 + H + CO_2 \quad a$$

$$[CH_3\dot{C}HO\dot{O}] \rightarrow [CH_3CO_2H] \rightarrow CH_3 + CO + OH \quad b$$

or,

$$[CH_3\dot{C}HO\dot{O}] \rightarrow [HCOOCH_3] \begin{cases} \rightarrow CH_3 + H + CO_2 & c \\ \rightarrow CH_3O + HCO & d \end{cases}$$

Herron and Huie [302] concluded that these sets of pathways were of equal importance, i.e., $(k_a + k_c) = (k_b + k_d)$ and that the relative importance of $(k_a + k_b)/(k_c + k_d)$ could not be determined from their data.

Niki et al. [303,304] used FT-IR spectroscopy to study the gas phase products of the reactions of O_3 with a series of alkenes at ppm concentrations. Secondary ozonide formation has been observed [303] from alkenes as small as propene, contrary to the earlier LPIR (long path infrared) study of Hanst et al. [288]. For the reaction of O_3 (5 ppm) with cis-2-butene (10 ppm) in the presence of 10 ppm of HCHO, Niki et al. [304] obtained an 18% yield of propene ozonide, probably formed by the reaction sequence

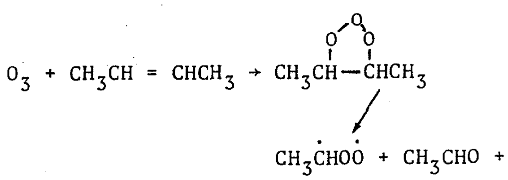

other products

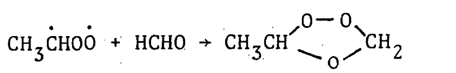

(propene ozonide)

Addition of 5 ppm SO_2 to this system completely quenched the ozonide formation, and SO_2 was consumed to an extent comparable to the ozonide yield observed in the absence of SO_2. This then indicates that

$$CH_3\dot{C}HO\dot{O} + SO_2 \rightarrow \text{products (possibly } SO_3 + CH_3CHO\text{, but see later)}$$

More recently, Dodge and Arnts [307] have used the data of Herron and Huie [301, 302] and of Niki and coworkers [303,304] to develop a mechanism for the O_3-propene reaction at atmospheric pressure which fitted experimental O_3-propene runs carried out at ppm concentration levels in air [307].

Dodge and Arnts [307] proposed that:

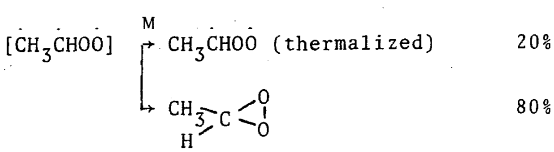

to account for the observed ~20% ozonide yields in the cis-2-butene-HCHO-O_3 system of Niki et al. [304]. Furthermore, since Niki et al. [304] observed a yield of ~14% CH_4 from the cis-2-butene-O_3-HCHO system, Dodge and Arnts [307], combining this observation with those of Herron and Huie [302], deduced that reasonable decomposition pathways of the dioxirane type compound are as follows:

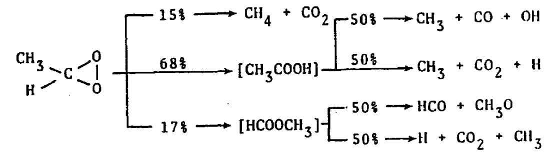

Under atmospheric conditions, i.e., in the presence of O_2, these reactions lead to [307]:

$$[CH_3\dot{C}HO\dot{O}] \rightarrow 0.20\ CH_3\dot{C}HO\dot{O}\ \text{(thermalized)} + 0.12\ CH_4 + 0.46\ CO_2 + 0.34\ CO + 0.41\ HO_2 + 0.27\ OH + 0.07\ CH_3O + 0.61\ CH_3O_2$$

Another set of data which shed light on the amount of thermalized biradicals formed at atmospheric pressure in O_3-alkene reactions comes from an earlier investigation of O_3-alkene-SO_2-H_2O-air systems at atmospheric pressure by Cox and Penkett [299]. They also showed that an intermediate was capable of oxidizing SO_2 to (ultimately) H_2SO_4 aerosols, and it was noted that aldehyde yields were increased in the presence of SO_2, indicating that this intermediate reacts with SO_2 to yield the aldehyde and (presumably) SO_3. A substantial effect of relative humidity was noted, with the conversion of SO_2 to H_2SO_4 aerosol (relative to the O_3 + alkene reaction rate) decreasing with increasing relative humidity (at constant temperature). Calvert et al. [314] have reviewed and reevaluated this data of Cox and Penkett [299] and, by a slight extension of Cox and Penkett's [299] suggested mechanism, postulated that (taking cis-2-butene as an example and simplifying the mechanism of Calvert et al. [314]):

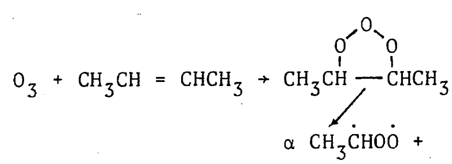

other products

(where α is the fraction of thermalized $CH_3\dot{C}HO\dot{O}$ radicals formed), followed by reactions of thermalized $CH_3\dot{C}HO\dot{O}$ biradicals:

$$CH_3\dot{C}HO\dot{O} + SO_2 \rightarrow CH_3CHO + SO_3 \qquad a$$

$$CH_3\dot{C}HO\dot{O} + H_2O \rightarrow CH_3COOH + H_2O \qquad b$$

$$CH_3\dot{C}HO\dot{O} \rightarrow \text{other products} \qquad c$$

Then,

$$\frac{-d[O_3]}{dt} \Big/ \frac{d[SO_3]}{dt} = \frac{1}{\alpha}\left\{1 + \frac{(k_b[H_2O]+k_c)}{k_a[SO_2]}\right\}$$

More recently, Martinez and Herron [315] have obtained essentially the same equation by postulating that the reaction of $R\dot{C}HO\dot{O}$ with SO_2 proceeds via:

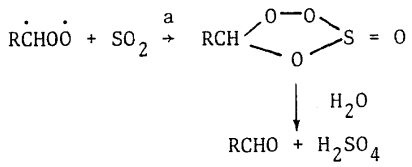

with (a) being the rate determining step. Although this reaction pathway better accounts for the observations of Cox and Penkett [299] (as discussed by Martinez and Herron [315]), it results in an identical expression to that given above.

Hence, as observed by Cox and Penkett [299] and Calvert et al. [314], a plot of $-d[O_3]/dt/d[SO_3]/dt$ against $1/[SO_2]$ yields a straight line with an intercept of $1/\alpha$ and a slope/intercept of $(k_b[H_2O]+k_c)/k_a$.

Table 27 gives the intercepts obtained by Cox and Penkett [299] for a variety of alkenes at 295 ± 2 K. For cis- and trans-2-butene, a weighted mean of the intercept yields $1/\alpha$ = 2.3, showing that for these alkenes reaction with O_3 leads to a yield of ∿43% thermalized $CH_3\dot{C}HO\dot{O}$ biradicals. Similar intercepts were obtained for the higher alkenes (table 27) cis-2-pentene and 2-methyl-1-pentene, also indicating an ∿40% yield of thermalized biradicals. While for cis-2-butene, this estimate of 43% is substantially higher than obtained from the more recent FT-IR investigation of Niki et al. [304], it is remarkably (perhaps fortuitously) similar to the ∿38% CH_2O_2 formation yield from the O_3-ethene reaction [295,296,305].

We recommend using a 40% yield of thermalized $CH_3\dot{C}HO\dot{O}$ biradicals from $[CH_3\dot{C}HO\dot{O}]$, and hence, based on Dodge and Arnts [307] mechanism; we recommend:

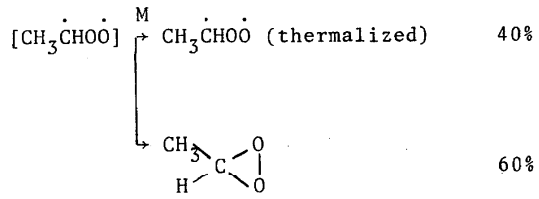

followed by

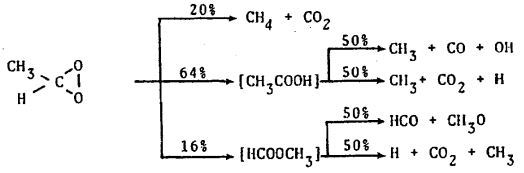

i.e., $[CH_3\dot{C}HO\dot{O}] \xrightarrow{O_2}$ 0.40 $CH_3\dot{C}HO\dot{O}$ + 0.12 CH_4 + 0.36 CO_2 + 0.24 CO + 0.29 HO_2 + 0.19 OH + 0.05 CH_3O + 0.43 CH_3O_2

Thus, based on these recommendations for the fates of the initially energy rich $[\dot{C}H_2O\dot{O}]$ and $[CH_3\dot{C}HO\dot{O}]$ biradicals, the *"initial" products* from the O_3-alkene reactions considered here are recommended to be:

Ethene

$$O_3 + \text{ethene} \rightarrow HCHO + 0.40\ \dot{C}H_2O\dot{O} + 0.18\ CO_2 + 0.42\ CO + 0.12\ H_2 + 0.42\ H_2O + 0.12\ HO_2$$

The radical yield from ethene is thus low, only 0.12 HO_2 radicals being formed per ethene reacted.

Propene

$$O_3 + \text{propene} \rightarrow 0.5\ HCHO + 0.5\ CH_3CHO + 0.5\ [\dot{C}H_2O\dot{O}] + 0.5\ [CH_3\dot{C}HO\dot{O}]$$

followed by the above recommended reactions of $[\dot{C}H_2O\dot{O}]$ and $[CH_3\dot{C}HO\dot{O}]$.

With respect to radical and biradical formation, the O_3-propene reaction forms:

$$O_3 + \text{propene} \rightarrow 0.20\ \dot{C}H_2O\dot{O} + 0.20\ CH_3\dot{C}HO\dot{O} + 0.205\ HO_2 + 0.095\ OH + 0.025\ CH_3O + 0.215\ CH_3O_2$$

and the radical yield is close to the estimate of ∿30% derived by Japar et al. [293] from the effect of O_2 on O_3-propene kinetics.

The lack of formation of acetyl (CH_3CO) radicals is consistent with the absence of PAN formation in O_3-NO_2-propene-air mixtures [152].

trans-2-Butene

No experimental data comparable to that obtained for ethene and propene by Herron and Huie [301,302] are available, but since the only biradical formed can be the $CH_3\dot{C}HO\dot{O}$ radical, the mechanism recommended is:

$$O_3 + CH_3CH = CHCH_3 \rightarrow CH_3\dot{C}H\text{—}\dot{C}HCH_3 \rightarrow CH_3CHO + [CH_3\dot{C}HO\dot{O}]$$

followed by the above reactions of the $[CH_3\dot{C}HO\dot{O}]$ radical.

1-Butene

For this system, we must estimate, based on the above alkene systems, the decomposition pathways of the $[C_2H_5\dot{C}HO\dot{O}]$ biradical. By analogy with the propene system, we assume that the initial reaction is

$$O_3 + CH_2 = CHCH_2CH_3 \rightarrow CH_2\text{—}CHCH_2CH_3$$

50% → $HCHO + [CH_3CH_2\dot{C}HO\dot{O}]$; 50% → $[H\dot{C}HO\dot{O}] + CH_3CH_2CHO$

The reactions of the energy-rich $[H\dot{C}HO\dot{O}]$ biradical have been discussed above. For $[CH_3CH_2\dot{C}HO\dot{O}]$, we postulate:

$$[CH_3CH_2\dot{C}HO\dot{O}] \rightarrow CH_3CH_2\dot{C}HO\dot{O}\ \text{(thermalized)}\quad 40\%$$

$$[CH_3CH_2\dot{C}HO\dot{O}] \rightarrow [C_2H_5COOH] \rightarrow C_2H_5 + CO_2 + H \quad 70\%$$

$$[CH_3CH_2\dot{C}HO\dot{O}] \rightarrow C_2H_5 + CO + OH \quad 50\%$$

$$[CH_3CH_2\dot{C}HO\dot{O}] \rightarrow [HCOOC_2H_5] \rightarrow H + CO_2 + C_2H_5 \quad 10\%$$

$$[CH_3CH_2\dot{C}HO\dot{O}] \rightarrow HCO + C_2H_5O \quad 50\%$$

$$[CH_3CH_2\dot{C}HO\dot{O}] \rightarrow C_2H_6 + CO_2 \quad 20\%$$

We have based the relative reaction pathway percentages on (a) thermalization of the biradical has been assumed to be the same as for $CH_2O\dot{O}$ and $CH_3\dot{C}HO\dot{O}$ and consistent with the data of Cox and Penkett [299], and (b) the decomposition pathways of the biradical are consistent with those proposed by Herron and Huie [302] and Dodge and Arnts [307] for $CH_3\dot{C}HO\dot{O}$, allowing for the fact that the H atom migration pathway yielding the "hot" acid will be progressively favored over migration of the alkyl group as the size of the alkyl group increases.

This scheme then predicts that, under atmospheric conditions, the $[C_2H_5\dot{C}HO\dot{O}]$ biradical initially formed will yield:

$$[C_2H_5\dot{C}HO\dot{O}] \rightarrow 0.40\ C_2H_5\dot{C}HO\dot{O}\ \text{(thermalized)} + 0.12\ C_2H_6 + 0.36\ CO_2 + 0.24\ CO + 0.45\ C_2H_5O_2 + 0.27\ HO_2 + 0.21\ OH + 0.03\ C_2H_5O$$

and hence, for radical production, the O_3 + 1-butene reaction is postulated to yield:

$$O_3 + \text{1-butene} \rightarrow 0.20\ \dot{C}H_2O\dot{O} + 0.20\ C_2H_5\dot{C}HO\dot{O} + 0.225\ C_2H_5O_2 + 0.195\ HO_2 + 0.105\ OH + 0.015\ C_2H_5O$$

Table 28 summarizes the products obtained (in the presence of O_2) from these O_3-alkene reactions.

The products/radicals shown in table 28 will react further under atmospheric conditions - many have been dealt with earlier in this report, the remainder are dealt with below:

Reactions of thermalized biradicals $R\dot{C}HO\dot{O}$ under atmospheric conditions (69-74)

As has been discussed above in the elucidation of the reaction pathways of the initially energy rich biradicals $R\dot{C}HO\dot{O}$, several bimolecular reactions of the thermalized biradicals have been observed with aldehydes

Table 27. Intercepts From Plots of $-d[O_3]/dt/d[SO_3]/dt$ Against $1/[SO_2]$ Obtained by Cox and Penkett [299] for a Variety of Alkenes at 295 ± 2 K

Alkene	Relative Humidity (%)	Intercept (1/α)
cis-2-Butene	≤10	2.32 ± 0.08
	40	2.31 ± 0.15
	75	3.38 ± 0.58
trans-2-Butene	40	2.20 ± 0.13
cis-2-Pentene	40	2.72 ± 0.44
1-Hexene	40	1.24 ± 0.08
2-Methyl-1-pentene	40	2.7 ± 0.5

Table 28. Postulated Initial Products and Their Fractional Yields From the Reaction of O_3 With Ethene, Propene, 1-Butene and trans-2-Butene in the Presence of O_2

	Alkene			
Product	Ethene	Propene	1-Butene	trans-2-Butene
HCHO	1.00	0.50	0.50	
CH_3CHO		0.50		1.00
C_2H_5CHO			0.50	
$\dot{C}H_2\dot{O}O$	0.40	0.20	0.20	
$CH_3\dot{C}H\dot{O}O$		0.20		0.40
$C_2H_5\dot{C}H\dot{O}O$			0.20	
CH_4		0.06		0.12
C_2H_6			0.06	
CO	0.42	0.33	0.33	0.24
CO_2	0.18	0.27	0.27	0.36
HO_2	0.12	0.205	0.195	0.29
OH		0.095	0.105	0.19
CH_3O		0.025		0.05
CH_3O_2		0.215		0.43
C_2H_5O			0.015	
$C_2H_5O_2$			0.225	
H_2O	0.42	0.21	0.21	
H_2	0.12	0.06	0.06	

[288,295,296,303-305], with SO_2 [295,299,304, 314], and with H_2O [299,314,316,317]. The recent study of Hatakeyama et al. [317] is of great interest in that the $CH_2\dot{O}\dot{O}$ radical was produced by the addition of O_2 to $CH_2(^3B_1)$, formed by photolysis of ketene. Addition of H_2O to photolysed ketene-air mixtures led to an increase in the HCO_2H yield, and the use of $H_2{}^{18}O$ led to the formation of $HC^{18}OOH$ and $HCO^{18}OH$. However, few kinetic data are available for these reactions of $R\dot{C}HO\dot{O}$ radicals. Su et al. [295] have, from an analysis of their FT-IR product data, for the reactions,

$$CH_2\dot{O}\dot{O} + HCHO \rightarrow \text{product} \qquad (a)$$

$$CH_2\dot{O}\dot{O} + SO_2 \rightarrow \text{product} \qquad (69)$$

$$CH_2\dot{O}\dot{O} + CO \rightarrow (HCO)_2O \qquad (b)$$

obtained $k_a : k_{69} : k_b = 140 : 560 : 1$

The only other reported data allowing an evaluation of the fates of $R\dot{C}HO\dot{O}$ biradicals are those of Cox and Penkett [299] from studies of O_3-alkene-SO_2-H_2O-air systems. As has already been noted above, it was observed by Cox and Penkett [299] that an intermediate was capable of oxidizing SO_2 to (ultimately) H_2SO_4 aerosol. It was also observed that aldehyde yields were increased in the presence of SO_2, showing that the intermediate reacts with SO_2 to yield the aldehyde and (presumably) SO_3. A substantial effect of relative humidity was noted, with the conversion of SO_2 to H_2SO_4 aerosol (relative to the O_3 + alkene reaction rate) decreasing with increasing relative humidity (at constant temperature). Calvert et al. [314] have reviewed and reevaluated this data of Cox and Penkett [299], and, by a slight extension of Cox and Penkett's [299] suggested mechanism, postulated that (taking cis-2-butene as an example and simplifying the mechanism of Calvert et al. [314] somewhat and taking into account the recent analysis of Martinez and Herron [315]):

$$O_3 + CH_3CH=CHCH_3 \rightarrow CH_3CH\underset{O}{\overset{O}{\diagdown\!\diagup}}CHCH_3 \rightarrow \alpha\ CH_3\dot{C}HO\dot{O} + \text{other products}$$

where α is the fraction of thermalized $CH_3CHO\dot{O}$ radicals formed, with the subsequent reactions of the thermalized $CH_3\dot{C}HO\dot{O}$ biradical being:

$$CH_3\dot{C}HO\dot{O} + SO_2 \xrightarrow{H_2O} CH_3CHO + H_2SO_4 \qquad (69)$$

$$CH_3\dot{C}HO\dot{O} + H_2O \rightarrow CH_3COOH + H_2O \qquad (70)$$

$$CH_3\dot{C}HO\dot{O} \rightarrow \text{other products} \qquad (c)$$

Then,

$$\frac{-d[O_3]}{dt} \Big/ \frac{d[SO_3]}{dt} = \frac{1}{\alpha}\left\{1 + \frac{(k_{70}[H_2O]+k_c)}{k_{69}[SO_2]}\right\}$$

Hence, as observed by Cox and Penkett [299] and Calvert et al. [314], a plot of $-d[O_3]/dt/d[SO_3]/dt$ against $1/[SO_2]$ yields a straight line, with the above kinetic scheme, with an intercept of $1/\alpha$ and a slope/intercept of $(k_{70}[H_2O]+k_c)/k_{69}$.

Table 29 gives the slope/intercept ratios obtained by Cox and Penkett [299] for cis-2-butene at various relative humidities and, for comparison, since the same biradical is involved, for trans-2-butene at 40% relative humidity. For cis-2-butene, the slope/intercept ratios increase markedly with relative humidity (being the same at 40% relative humidity for the two 2-butene isomers). On the basis of the above reaction scheme, a plot of slope/intercept ratio versus $[H_2O]$ should yield a straight line of slope k_{70}/k_{69} and intercept k_c/k_{69}. Figure 13 shows such a plot; within the rather substantial scatter and limited data, they support a linear increase of the slope/intercept ratio with H_2O concentration. From the approximately "best-fit" line drawn, $k_c/k_{69} \sim 0.3 \pm 0.13$ ppm and $k_{70}/k_{69} \sim (5\pm2) \times 10^{-5}$.

However, since the reaction

$$R\dot{C}HO\dot{O} + SO_2 \xrightarrow{H_2O} RCHO + H_2SO_4 \qquad (69)$$

probably occurs, then it is expected that the reactions

$$R\dot{C}HO\dot{O} + NO \rightarrow RCHO + NO_2, \text{ and} \qquad (71)$$

$$R\dot{C}HO\dot{O} + NO_2 \rightarrow RCHO + NO_3 \qquad (72)$$

will also occur.

Under atmospheric conditions at ~50% relative humidity at 300 K, the H_2O concentration is $\gtrsim 2 \times 10^4$ ppm, and hence $k_{70}[H_2O]/k_{69} \gtrsim 1$ ppm. Since NO and NO_2 are expected to react much more rapidly than SO_2 with $RR'C\dot{O}\dot{O}$ radicals (by analogy with HO_2, RO_2 and O_3 reactions with NO_2 and SO_2), then we expect that the reactions

$$RR'C\dot{O}\dot{O} + \begin{Bmatrix} NO \\ NO_2 \end{Bmatrix} \rightarrow RR'CO + \begin{Bmatrix} NO_2 \\ NO_3 \end{Bmatrix}$$

may predominate over any reactions with H_2O for $NO_x \gtrsim 10$ ppb (but see below).

Thus, under atmospheric conditions, we should initially consider the reactions:

Table 29. Slope/Intercept Ratios From Plots of $-d[O_3]/dt/d[SO_3]/dt$ Against $1/[SO_2]$ Obtained by Cox and Penkett [299] for the O_3-2-Butene SO_2 Reactions at 295 ± 2 K

Alkene	Relative Humidity (%)	Slope/Intercept = $([k_{70}(H_2O)+k_c]/k_{69}$ ppm
cis-2-Butene	≤10	0.30 ± 0.03
	40	0.63 ± 0.10[a]
	75	1.44 ± 0.50
trans-2-Butene	40	0.64 ± 0.13

[a]The quoted value of R_{O_3}/R_{SO_3} for cis-2-butene at $[SO_2]$ = 2.12 ppm in table 2 of Cox and Penkett [299] of 2.0 is apparently in error. It should be 3.0 as derived from the quoted values of $-d[O_3]/dt$ and $d[SO_3]/dt$ and as given in their Figure 12. This will modify the plots shown by Calvert et al. [314] slightly (their Figures 7 and 8) and the slope of their Figure 8. See text here.

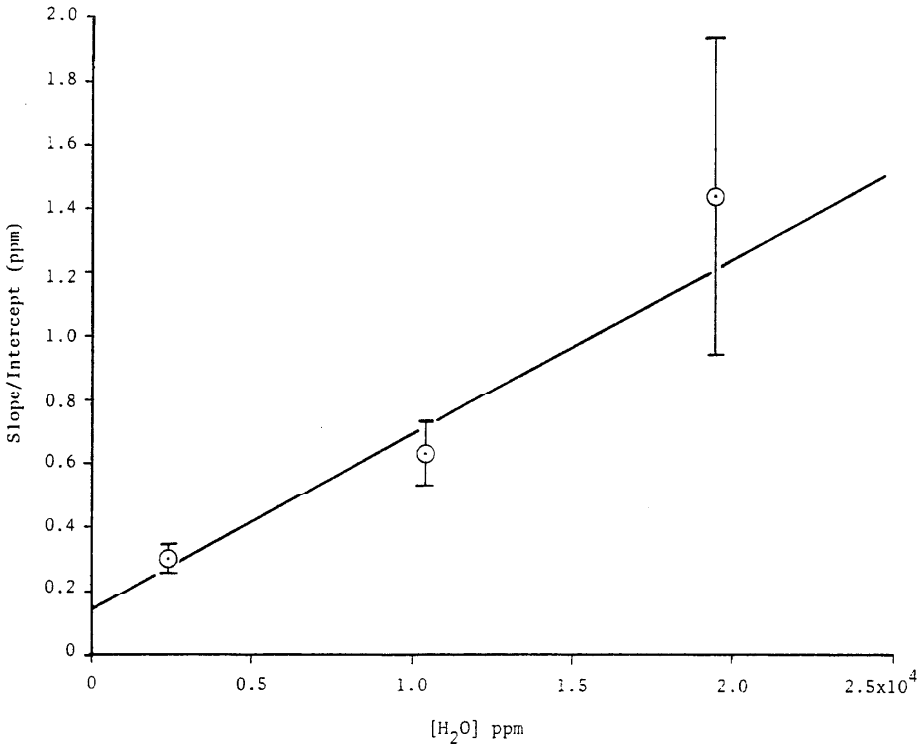

Figure 13. Plot of $(k_{70}[H_2O] + k_c)/k_{69}$ = slope/intercept against $[H_2O]$ for the $O_3 + SO_2$ + cis-2-butene + H_2O system of Cox and Penkett [299].

$$\dot{R}CH\dot{O}O + NO \rightarrow RCHO + NO_2 \quad (71)$$

$$\dot{R}CH\dot{O}O + NO_2 \rightarrow RCHO + NO_3 \quad (72)$$

$$\dot{R}CH\dot{O}O + SO_2 \rightarrow RCHO + SO_3 \text{ (or other products)} \quad (69)$$

$$\dot{R}CH\dot{O}O + H_2O \rightarrow RCOOH + H_2O \quad (70)$$

$$\dot{R}CH\dot{O}O + CO \rightarrow \text{products} \quad (73)$$

$$\dot{R}CH\dot{O}O + R'CHO \rightarrow RCH\langle{}^{O}_{O}\rangle CHR' \quad (74)$$

Making the, perhaps gross, assumption that the kinetic data from Su et al. [295] for $C\dot{H}_2O\dot{O}$ and that obtained from the data of Cox and Penkett [299] for $\dot{C}H_3CH\dot{O}O$ can be amalgamated, and estimating from the data of Akimoto et al. [316] that $k_{71} \sim 10k_{72} \sim 100\ k_{69}$, (see below) the rates shown in table 30 are obtained for two sets of conditions, smog chamber runs and ambient atmospheric conditions. In the smog chamber NO_x-propene-air irradiations of Akimoto et al. [316,318], the major effect of added H_2O on the product distribution was to increase markedly the HCOOH yield. After ~200 mins irradiation of run 2, NIES-78070 [316,318], -d[HCOOH]/d[propene] ~0.3 which is certainly comparable to, if not greater than, our recommended yield of thermalised $\dot{C}H_2O\dot{O}$ species (20%) in the O_3-propene reaction. This then implies that, if reaction of $\dot{C}H_2O\dot{O}$ with H_2O is the major source of HCOOH under these conditions, then the majority of $\dot{C}H_2O\dot{O}$ radicals react with H_2O. Since there are obviously other sources of HCOOH (e.g., HO_2 + HCHO, heterogeneous processes, etc.), the relative rate constants given in table 30 have been adjusted to give an appreciable HCOOH formation rate under conditions pertaining to the observations of Akimoto et al. [316,318]. It is obvious that reaction with CO may be neglected but the other reactions should be considered.

We recommend that, in the absence of experimental data, the reaction of $\dot{R}CH\dot{O}O$ biradicals with NO has a similar rate constant to its reaction with alkylperoxy radicals,

$$k_{71} = 7 \times 10^{-12} \text{ cm}^3 \text{ molecule}^{-1} \text{ s}^{-1}$$

at 298 K with an uncertainty of at least a factor of 10.

Any temperature dependence is expected to be small for these values of k_{71}. This value of k_{71}, coupled with the (extremely uncertain) relative rate constants given in table 30 yield (at ~298 K):

$$k_{72}\ (\dot{R}CH\dot{O}O + NO_2) \sim 7 \times 10^{-13} \text{ cm}^3 \text{ molecule}^{-1} \text{ s}^{-1}$$

$$k_{69}\ (\dot{R}CH\dot{O}O + SO_2) \sim 7 \times 10^{-14} \text{ cm}^3 \text{ molecule}^{-1} \text{ s}^{-1}$$

$$k_{70}\ (\dot{R}CH\dot{O}O + H_2O) \sim 4 \times 10^{-18} \text{ cm}^3 \text{ molecule}^{-1} \text{ s}^{-1}$$

and $k_{74}\ (\dot{R}CH\dot{O}O + R_1CHO \text{ or } R_1R_2CO) \sim 2 \times 10^{-14} \text{ cm}^3 \text{ molecule}^{-1} \text{ s}^{-1}$

The uncertainties in these constants must be at least a factor of 100, although some of the rate constant ratios, i.e., k_{70}/k_{69} and k_{74}/k_{69} are probably good to within a factor of 10. The comprehensive article by Herron et al. [309] dealing with the reactions of $\dot{R}CH\dot{O}O$ radicals in ozone-alkene reactions should also be consulted. Specifically, based upon the data of Martinez et al. [319] on the effect of NO_2 on ozonide yields in the reaction of O_3 with trans-2-butene, Herron et al. [309] derive $k_{72}/k_{74} \sim 14$ and the rate constants (at 300 K)

$$k_{72} \sim 1 \times 10^{-17} \text{ to } 7 \times 10^{-14} \text{ cm}^3 \text{ molecule}^{-1} \text{ s}^{-1}$$

$$k_{69} \sim 3 \times 10^{-15} \text{ to } 2 \times 10^{-11} \text{ cm}^3 \text{ molecule}^{-1} \text{ s}^{-1}$$

$$k_{70} \sim 2 \times 10^{-19} \text{ to } 1 \times 10^{-15} \text{ cm}^3 \text{ molecule}^{-1} \text{ s}^{-1}$$

$$k_{74} \sim 2 \times 10^{-16} \text{ to } 8 \times 10^{-13} \text{ cm}^3 \text{ molecule}^{-1} \text{ s}^{-1}$$

together with

$$k\ (\dot{R}CH\dot{O}O + O_2) < 8 \times 10^{-22} \text{ cm}^3 \text{ molecule}^{-1} \text{ s}^{-1}$$

These estimated values of k_{69}, k_{70} and k_{74} are consistent with the above estimations, while that for k_{72} is lower by a factor of ≥ 10. Obviously much more experimental data are necessary in order to allow further elucidation of these reaction pathways.

Reactions of the $C_2H_5O_2$ and C_2H_5O radicals

As discussed previously in this report for RO_2 and RO radicals, the reaction sequence for the ethylperoxy (and ethoxy) radicals are:

$$C_2H_5O_2 + NO_2 \rightleftarrows C_2H_5OONO_2 \quad (51,52)$$

$$C_2H_5O_2 + NO \rightarrow C_2H_5O + NO_2 \quad (50)$$

$$C_2H_5O + NO_2 \rightarrow C_2H_5ONO_2 \quad (56)$$

$$C_2H_5O + NO \rightarrow C_2H_5ONO \quad (55)$$

$$C_2H_5O + O_2 \rightarrow CH_3CHO + HO_2 \quad (57)$$

The atmospheric reactions of C_2H_5CHO will be considered later.

6. Alkane Chemistry

In the following section the atmospheric chemistry of the two alkanes n-butane ($CH_3CH_2CH_2CH_3$) and 2,3-dimethylbutane [$(CH_3)_2CHCH(CH_3)_2$] are evaluated. Because of similarities, their reactions are treated as a group with differing rate constants/products noted.

$$O(^3P) + \text{alkanes} \rightarrow \text{products} \quad (75)$$

Surprisingly, relatively few absolute rate constant studies have been carried out for the reaction of $O(^3P)$ atoms with n-butane and 2,3-dimethylbutane. The absolute rate constant data available, which should be free from stoichiometric corrections, etc., are:

Alkane	$10^{14} \times k_{75}$(298 K)	E cal mol^{-1}	Reference
n-butane	4.1	4200	[320]
	2.1[a]	5200[a]	[321]
	2.2 ± 0.4	4170 ± 300	[322]
2,3-dimethylbutane	21	3260[a]	[321]

[a] Based on a least squares treatment of the rate constant data over the temperature range 307-441 K.

In view of the proven reliability of the flash photolysis - NO_2 chemiluminescence technique used by Atkinson et al. [322] (see for instance, [233]) and the fact that Herron and Huie [321] stated that their n-butane data was the least reliable of all of their data on the alkanes, we recommend for n-butane:

$$k_{75} = 2.5 \times 10^{-11} e^{-2099/T} \text{ cm}^3 \text{ molecule}^{-1} \text{ s}^{-1}$$

$$= 2.2 \times 10^{-14} \text{ cm}^3 \text{ molecule}^{-1} \text{ s}^{-1}$$

at 298 K, with an uncertainty of a factor of 1.5.

For 2,3-dimethylbutane the sole data are those of Herron and Huie [321]. However, in view of the discrepancy for n-butane with their data, we hesitate to recommend their data for 2,3-dimethylbutane, but propose, based on a lower effective Arrhenius pre-exponential factor than for n-butane over the same temperature range, that for 2,3-dimethylbutane:

$$k_{75} = 1.4 \times 10^{-11} e^{-1250/T} \text{ cm}^3 \text{ molecule}^{-1} \text{ s}^{-1}$$

$$= 2.1 \times 10^{-13} \text{ cm}^3 \text{ molecule}^{-1} \text{ s}^{-1}$$

at 298 K, with an uncertainty of a factor of 2 at 298 K, increasing rapidly with temperature.

These reactions can proceed via:

$$O(^3P) + CH_3CH_2CH_2CH_3 \rightarrow CH_3CH_2CH_2\dot{C}H_2 + OH \quad (a)$$

$$\rightarrow CH_3CH_2\dot{C}HCH_3 + OH \quad (b)$$

$$O(^3P) + (CH_3)_2CHCH(CH_3)_2 \rightarrow (CH_3)_2CHCH\langle^{CH_2\cdot}_{CH_3} + OH \quad (c)$$

$$\rightarrow (CH_3)_2C\dot{H}C(CH_3)_2 + OH \quad (d)$$

The data of Herron and Huie [321] and their review [323] show that for 2,3-dimethylbutane:

$$k_c/(k_c + k_d) \simeq 0.03 \text{ at } 298 \text{ K},$$

increasing slowly with temperature, while for n-butane,

$$k_a/(k_a + k_b) \simeq 0.12 \text{ at } 298 \text{ K},$$

again increasing with temperature. Since for typical alkane levels in environmental chamber

studies the $O(^3P)$ atom reactions are of minor significance, we recommend:

n-butane - formation of $CH_3CH_2CH_2\dot{C}H_2$ occurs 12% of the time, independent of temperature over the small ranges typical of smog chamber modelling (273-323 K), with the radical $CH_3CH_2\dot{C}HCH_3$ being formed the rest (88%) of the time.

2,3-dimethylbutane - to a good approximation, sole production of the radical $(CH_3)_2CHC(CH_3)_2$ over a small temperature range around 298 K.

$$NO_3 + \text{alkanes} \rightarrow \text{products} \qquad (76)$$

The sole data reported to date concerning these reactions are from Atkinson et al. [324]. From the increased N_2O_5 decay rates upon the addition of the alkanes to N_2O_5 NO_2 air mixtures and from relative rate measurements, rate constants of

$$k_{76}\ (\text{n-butane}) = (2.0 \pm 1.0) \times 10^{-17}\ \text{cm}^3\ \text{molecule}^{-1}\ \text{s}^{-1}$$

at 298 ± 1 K and

$$k_{76}\ (\text{2,3-dimethylbutane}) = (1.2 \pm 0.5) \times 10^{-16}\ \text{cm}^3\ \text{molecule}^{-1}\ \text{s}^{-1}$$

at 298 ± 1 K were obtained [324]. These rate constants are linearly dependent on the value of $K_{7,8}$ used [27]. We recommend these rate constants, i.e.,

$$k_{76}\ (\text{n-butane}) = 2.0 \times 10^{-17}\ \text{cm}^3\ \text{molecule}^{-1}\ \text{s}^{-1},$$

$$k_{76}\ (\text{2,3-dimethylbutane}) = 1.2 \times 10^{-16}\ \text{cm}^3\ \text{molecule}^{-1}\ \text{s}^{-1}$$

at 298 K, with an estimated uncertainty of a factor of 2. The data obtained by Atkinson et al. [324] indicate that these reactions proceed predominantly via H-atom abstraction from the secondary or tertiary C-H bonds.

$$OH + \text{alkanes} \rightarrow \text{products} \qquad (77)$$

The relevant rate constant and mechanistic data for n-butane and 2,3-dimethylbutane are those of Greiner [325], Stuhl [326], Perry et al. [327], Paraskevopoulos and Nip [328] and Atkinson et al. [262]. For n-butane the room temperature rate constants obtained from absolute rate constant studies are ($\times 10^{12}$ cm^3 molecule^{-1} s^{-1}):

2.57 [325], 2.35 ± 0.35 [326], 2.72 ± 0.27 [327] and 2.67 ± 0.22 [328], with a mean value of

$$2.58 \times 10^{-12}\ \text{cm}^3\ \text{molecule}^{-1}\ \text{s}^{-1}$$

The Arrhenius activation energies obtained by Greiner [325] and Perry et al. [327] of (1041 ± 185) cal mol^{-1} and (1110 ± 300) cal mol^{-1}, respectively, are in excellent agreement. We recommend the Arrhenius activation energy of Perry et al. [327], combined with a rate constant of

$$2.58 \times 10^{-12}\ \text{cm}^3\ \text{molecule}^{-1}\ \text{s}^{-1}$$

at 298 K, i.e.,

$$k_{77}\ (\text{n-butane}) = 1.68 \times 10^{-11}\ e^{-559/T}\ \text{cm}^3\ \text{molecule}^{-1}\ \text{s}^{-1} = 2.58 \times 10^{-12}\ \text{cm}^3\ \text{molecule}^{-1}\ \text{s}^{-1}$$

at 298 K, with an uncertainty of ± 15% at 298 K.

For 2,3-dimethylbutane the sole absolute rate constant determination is that of Greiner [325], with

$$k_{77} = 4.8 \times 10^{-12}\ e^{(129\pm67)/T}\ \text{cm}^3\ \text{molecule}^{-1}\ \text{s}^{-1},$$

i.e., a negative temperature dependence. As discussed by Darnall et al. [329] and Atkinson et al. [116,262], the rate constant obtained by Greiner [325] at 300 K of

$$k_{77} = 7.45 \times 10^{-12}\ \text{cm}^3\ \text{molecule}^{-1}\ \text{s}^{-1}$$

appears to be somewhat high.

We recommend, based on the room temperature rate constant of Atkinson et al. [262]

$$k_{77} = 6.26 \times 10^{-12}\ \text{cm}^3\ \text{molecule}^{-1}\ \text{s}^{-1}$$

at 299 ± 2 K, which is based on the above recommendation for n-butane, and the higher temperature (493-498 K) data of Greiner [325] that

$$k_{77}(\text{2,3-dimethylbutane}) = 6.3 \times 10^{-12}\ \text{cm}^3\ \text{molecule}^{-1}\ \text{s}^{-1},$$

independent of temperature, with an estimated uncertainty of ± 15% at 298 K.

As discussed by Darnall et al. [329] and Atkinson et al. [116], the literature data for ≥ C_3 alkanes (apart from cyclopropane and cyclobutane) can be reasonably well fit over the temperature range 300-500 K (within ± 20% or better) by the modified Greiner [325] formula:

$$k_{77} = 1.01 \times 10^{-12} N_1 e^{-823/T} + 2.41 \times 10^{-12} N_2 e^{-428/T} + 2.10 \times 10^{-12} N_3 \text{ cm}^3 \text{ molecule}^{-1} \text{ s}^{-1}$$

where N_1, N_2 and N_3 are the number of primary, secondary and tertiary C-H bonds, respectively. Recent work by Atkinson et al. [330,331] has shown that this formula and approach is an oversimplification. However, these more recent data yield an essentially identical conclusion as to the reaction pathways at 299 ± 2 K as the above formula.

Use of this formula to derive the rate constant for H-atom abstraction from the primary C-H bonds indicates that over the temperature range 270-330 K; for n-butane formation of the primary radical $CH_3CH_2CH_2CH_2$ occurs ∿14% of the time, while for 2,3-dimethylbutane formation of the primary radical $(CH_3)_2CHCH(CH_3)CH_2$ accounts for 10-17% of the reaction, depending on the temperature. Figure 14 shows the calculated fractions, $k_a/(k_a + k_b)$, for the reactions:

$$\text{OH + alkane} \rightarrow H_2O + \text{primary alkyl radical} \quad \text{(a)}$$

$$\rightarrow H_2O + \text{secondary (n-butane) or tertiary (2,3-dimethylbutane) alkyl radical} \quad \text{(b)}$$

$\underline{CH_3CH_2CH_2CH_2^{\cdot}}$ reactions

The reactions under atmospheric conditions of this alkyl radical have been covered above in the various reaction classes. The specific reactions are given below, with brief discussion where necessary:

$$CH_3CH_2CH_2CH_2^{\cdot} + O_2 \rightarrow CH_3CH_2CH_2CH_2OO. \quad (54)$$

This reaction is fast,

$$k_{54} = (7.5 \pm 1.4) \times 10^{-12} \text{ cm}^3 \text{ molecule}^{-1} \text{ s}^{-1}$$

at room temperature [185], and hence, because of the high atmospheric O_2 concentration, is the sole reaction of this, and other, alkyl radicals (see reaction 54).

$$CH_3CH_2CH_2CH_2OO. + NO \xrightarrow{a} CH_3CH_2CH_2CH_2ONO_2 \quad (50)$$

$$\xrightarrow{b} CH_3CH_2CH_2CH_2O + NO_2$$

where $k_a/(k_a + k_b) \simeq 0.08$ [7,169,170] at atmospheric pressure (but see [170] for the possibility of lower nitrate yields for 1-alkylperoxy radicals)

and

$$(k_a + k_b) = 7 \times 10^{-12} \text{ cm}^3 \text{ molecule}^{-1} \text{ s}^{-1}$$

at 298 K (see reaction (50) above in section 4).

This alkoxy radical can isomerise,

$$CH_3CH_2CH_2CH_2O. \rightarrow .CH_2CH_2CH_2CH_2OH \quad (65)$$

react with O_2, or decompose. Based upon the data of Gutman et al. [222] for the reactions of O_2 with CH_3O and C_2H_5O, Gutman et al. [222] have estimated that the reaction

$$CH_3CH_2CH_2CH_2O. + O_2 \rightarrow CH_3CH_2CH_2CHO + HO_2 \quad (57)$$

has a rate constant of

$$k_{57} = 7 \times 10^{-14} e^{-690/T} \text{ cm}^3 \text{ molecule}^{-1} \text{ s}^{-1} = 7 \times 10^{-15} \text{ cm}^3 \text{ molecule}^{-1} \text{ s}^{-1}$$

at 298 K.

In an atmosphere of air, this leads to a first order rate constant for the reaction with O_2 of

$$3.6 \times 10^4 \text{ s}^{-1}$$

at 298 K. The decomposition reaction

$$CH_3CH_2CH_2CH_2O \rightarrow CH_3CH_2CH_2. + HCHO \quad (64)$$

is estimated [224] to have a rate constant at 298 K of ≃ 0.3 s^{-1}, i.e., to be negligible with respect to the reaction with O_2. The isomerization

$$CH_3CH_2CH_2CH_2O. \rightarrow {}^{\cdot}CH_2CH_2CH_2CH_2OH \quad (65)$$

is estimated (table 25) to have a rate constant at 298 K of ∿ 2×10^5 - 6×10^5 s^{-1} [224,269] and is hence expected to dominate

Table 30. Estimated Reaction Rates for $R\dot{C}HO\dot{O}$ Biradicals

Reactant	Relative[a] Rate Constant	"Smog Chamber" Concentration[b] (ppm)	"Smog Chamber" Relative Rate	"Ambient" Concentration[c] (ppm)	"Ambient" Relative Rate
NO	∿100	0.002	0.2	0.01	1.0
NO_2	∿10	0.09	0.9	0.1	1.0
SO_2	1			0.05	0.05
H_2O	5×10^{-5}	2×10^4	1.0	1×10^4	0.5
CO	2×10^{-3}	1.0	2×10^{-3}	10.0	0.02
RCHO	0.25	3.0	0.75	0.02	0.005

[a]Based upon relative rate data discussed in text.

[b]Based on smog chamber data of Akimoto et al. [316], photooxidation of the propene-NO_x-air system at 40% relative humidity (Run 2, 200 mins.).

[c]Reasonable values from the Los Angeles air basin.

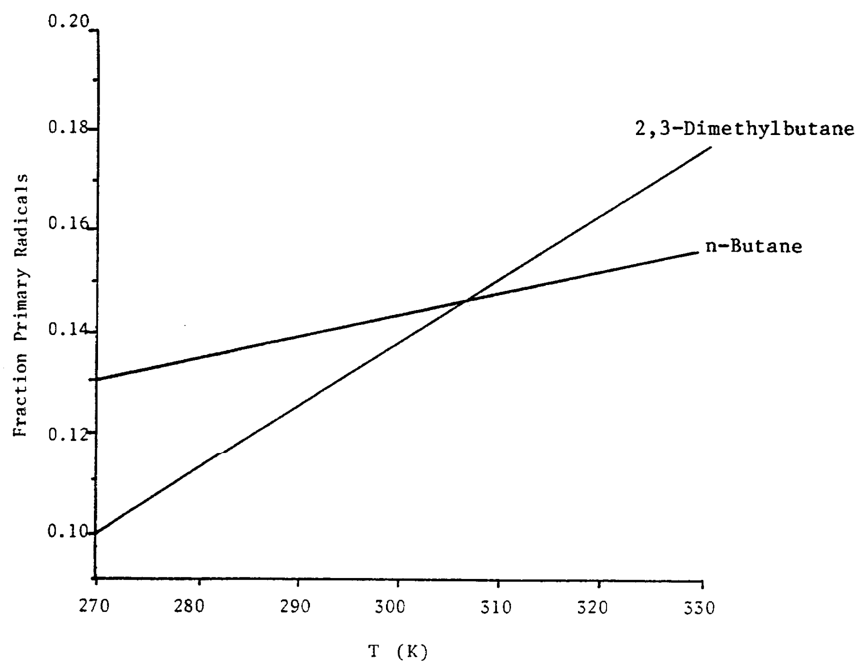

Figure 14. Calculated fractions of the reaction of $O(^3P)$ atoms with n-butane and 2,3-dimethylbutane yielding the primary alkyl radicals $CH_3CH_2CH_2CH_2$ and $(CH_3)_2CHCH(CH_3)CH_2$, respectively.

over the reaction with O_2, the activation energy for reaction (65) being ≃ 8 kcal mol^{-1} [224,269].

A priori, no more precise estimate of the isomerisation rate constant is available and it may be adjusted to fit the experimental data. The room temperature (296-303 K) experimental data of Carter et al. [7], Cox et al. [271] and Niki et al. [272], obtained from irradiations of NO_x-n-butane-air [7], HONO-n-butane-air [271] or n-C_4H_9ONO-air [272] mixtures, show that, based upon the above rate constant for the reaction of n-butoxy radicals with O_2, i.e.

$$k_{57} = 7 \times 10^{-15} \text{ cm}^3 \text{ molecule}^{-1} \text{ s}^{-1}$$

at ∿ 300 K, then

$$k_{65} = (1.0 - 1.4) \times 10^5 \text{ s}^{-1} \text{ at} \sim 300 \text{ K}.$$

Based upon this data, we recommend that

$$k_{65} = 1.1 \times 10^5 \text{ s}^{-1}$$

at 298 K, with an uncertainty of a factor of ∿ 1.5, and

$$k_{65} = 1.5 \times 10^{11} e^{-4200/T} \text{ s}^{-1}$$

Note that (a) the split between reaction with O_2 and isomerisation is temperature dependent, with a temperature dependence of ≃ $e^{-3500/T}$, and (b) this isomerisation rate derived from the experimental data is in remarkably good agreement with the thermochemical estimates [224,269] given in table 25.

Butyraldehyde chemistry is discussed along with that for propionaldehyde in section 7.

The hydroxyalkyl radical resulting from the isomerisation will undergo the sequence of reactions:

$$\cdot CH_2CH_2CH_2CH_2OH + O_2 \rightarrow \cdot OOCH_2CH_2CH_2CH_2OH$$

$$\cdot OOCH_2CH_2CH_2CH_2OH + NO \xrightarrow{a} O_2NOCH_2CH_2CH_2CH_2OH$$

$$\xrightarrow{b} \cdot OCH_2CH_2CH_2CH_2OH + NO_2$$

with

$$k_a/(k_a + k_b) \sim 0.08$$

at atmospheric pressure and

$$(k_a + k_b) = 7 \times 10^{-12} \text{ cm}^3 \text{ molecule}^{-1} \text{ s}^{-1}$$

at 298 K, followed almost exclusively by another alkoxy radical isomerisation,

$$\cdot OCH_2CH_2CH_2CH_2OH \rightarrow HOCH_2CH_2CH_2\dot{C}HOH \quad (65)$$

since this isomerisation is estimated [224] to be ≃ 1.2 kcal mol^{-1} more facile, i.e., a factor of ≃ 5 faster at 298 K (when the number of abstractable H atoms are taken into account), than the first isomerisation of the $CH_3CH_2CH_2CH_2O\cdot$ radical. This α-hydroxy radical will then [7,275-277] (see discussion under reaction 66) react rapidly with O_2 to form 4-hydroxy-butanal:

$$HOCH_2CH_2CH_2\dot{C}HOH + O_2 \rightarrow HOCH_2CH_2CH_2CHO + HO_2 \quad (66)$$

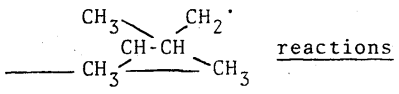

reactions

Similar reaction sequences occur here, since the alkoxy radical isomerisations are expected to be facile. Hence:

$$(CH_3)_2CHCH(CH_3)\dot{C}H_2 + O_2 \rightarrow (CH_3)_2CHCH(CH_3)CH_2OO\cdot$$

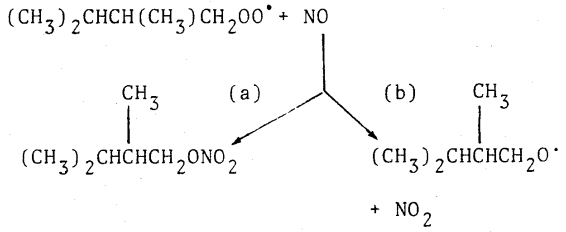

with $k_a/(k_a + k_b) \sim 0.1$

at atmospheric pressure [332] and

$$(k_a + k_b) = 7 \times 10^{-12} \text{ cm}^3 \text{ molecule}^{-1} \text{ s}^{-1}$$

at 298 K, followed by either isomerisation or reaction of the alkoxy radical with O_2. The reaction with O_2:

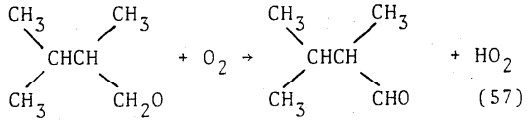

(57)

may be assumed [222] to have a rate constant of:

$$k_{57} = 7 \times 10^{-14} e^{-690/T} \text{ cm}^3 \text{ molecule}^{-1} \text{ s}^{-1}$$

equivalent to a first order rate at 298 K and 1 atmosphere air of 3.6×10^4 s^{-1}. Since there are twice as many abstractable H atoms

for the isomerisation reaction as in the corresponding n-butane reaction, its rate constant may be estimated, by analogy with the n-butane system, to be

$$k_{65} \approx 3 \times 10^{11} e^{-4200/T} s^{-1}$$

$$\approx 2.2 \times 10^{5} s^{-1}$$

at 298 K. Hence the isomerisation reaction is expected to predominate over reaction with O_2 by a factor of ~6

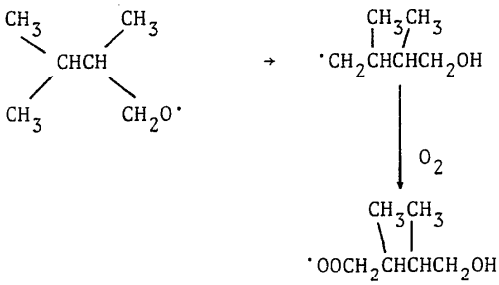

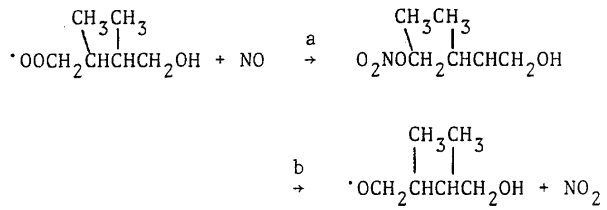

with (in the absence of firm data)

$$k_a/(k_a + k_b) \sim 0.1$$

at atmospheric pressure and 298 K. The next isomerisation can proceed in two ways:

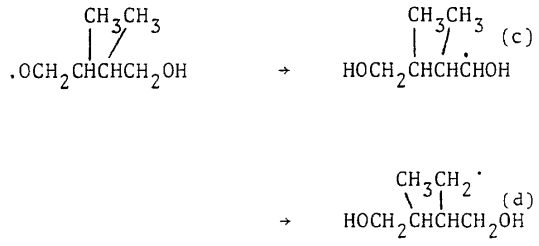

As estimated by Baldwin et al. [224] and discussed above, reaction (c) should predominate over (d) by a factor of ≈ 5, i.e.,

$$k_c/(k_c + k_d) \approx 0.8$$

in agreement with the expectation that the H-CH(OH) bond energy is significantly less than the H-CH_2 bond energy.

The subsequent reactions are expected to be:

and

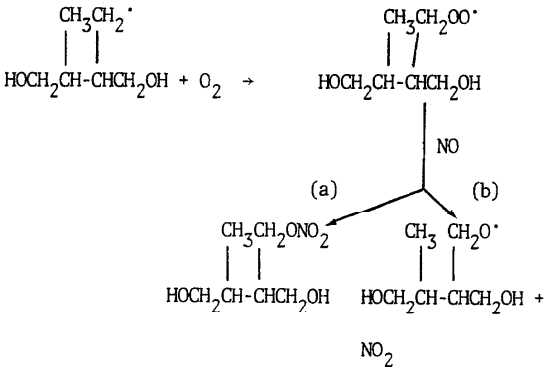

with, in the absence of firm data,

$$k_a/(k_a + k_b) \sim 0.1$$

at atmospheric pressure and 298 K, followed by

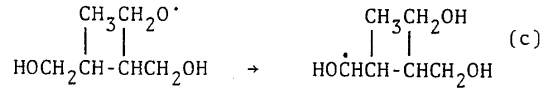

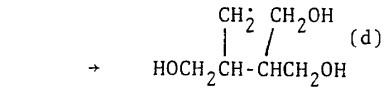

again with

$$k_c/(k_c + k_d) \approx 0.8.$$

These radicals then react:

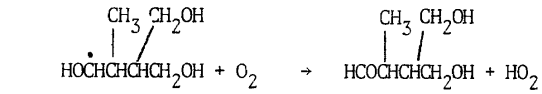

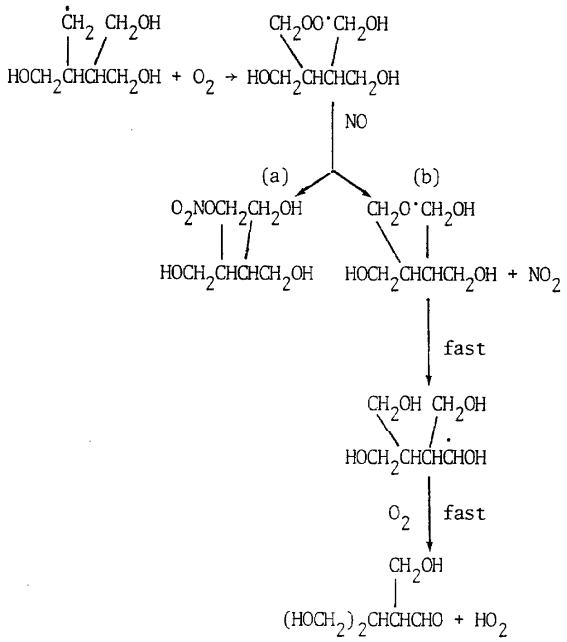

With the reaction pathway rate constant ratios used here, this leads to the following product pattern shown in figure 15 (NO_2 + RO combination has been neglected since the isomerisation rates of > 10^5 s^{-1} are $\gtrsim 10^3$ faster than nitrate formation even at 1 ppm NO_2 concentrations).

$CH_3\dot{C}H_2CHCH_3$ Radical Reactions

As discussed under the various reaction classes the atmospheric reactions of this radical will be

$$CH_3\dot{C}H_2CHCH_3 + O_2 \rightarrow CH_3CH_2\overset{OO\cdot}{C}HCH_3 \qquad (54)$$

with [184,185]

$$k_{54} = 1.7 \times 10^{-11} \text{ cm}^3 \text{ molecule}^{-1} \text{ s}^{-1}$$

at 298 K.

$$CH_3CH_2\overset{OO}{C}HCH_3 + NO \rightarrow CH_3CH_2\overset{ONO_2}{C}HCH_3 \qquad (a)$$

$$\rightarrow CH_3CH_2\overset{O\cdot}{C}HCH_3 + NO_2 \qquad (b)$$

where

$$k_a/(k_a + k_b) \simeq 0.08$$

at atmospheric pressure [7,169,170] and

$$(k_a + k_b) = 7 \times 10^{-12} \text{ cm}^3 \text{ molecule}^{-1} \text{ s}^{-1}$$

at 298 K.

The 2-butoxy radical can either react with O_2 or decompose; isomerisation is estimated ([7,224] and table 25) to be unimportant:

$$CH_3CH_2\overset{O\cdot}{C}HCH_3 \rightarrow C_2H_5^{\cdot} + CH_3CHO \qquad (64)$$

$$CH_3CH_2\overset{O\cdot}{C}HCH_3 + O_2 \rightarrow CH_3CH_2COCH_3 + HO_2 \qquad (57)$$

Smog chamber data [7,271] show that at ~300 K and atmospheric pressure these two reaction pathways are of comparable importance. For reaction (64) the experimental data of Batt and McCulloch [194] over the temperature range 440-470 K yields

$$k_{64} = 8 \times 10^{14} e^{-7700/T} \text{ s}^{-1}$$

at one atmosphere of NO. Even though this decomposition may be in the fall-off region, NO is expected to have a similar third-body efficiency to N_2 + O_2, and hence this expression should be approximately applicable to atmosphere conditions.

For reaction (57), the estimates of Gutman et al. [22] lead to

$$k_{57} = 5 \times 10^{-14} \text{ cm}^3 \text{ molecule}^{-1} \text{ s}^{-1}$$

at 300 K for the 2-butoxy radical, independent of temperature.

(We have recommended

$$k_{57} = 3 \times 10^{-14} \text{ cm}^3 \text{ molecule}^{-1} \text{ s}^{-1}$$

independent of temperature, for secondary alkoxy radicals in general.)

These rate constant expressions for k_{57} and k_{64} lead to values of k_{64}/k_{57} of

$$2.5 \times 10^{17} \text{ molecule cm}^{-3} \text{ at 303 K and}$$

$$1.3 \times 10^{17} \text{ molecule cm}^{-3} \text{ at 296 K.}$$

However, the experimental values are

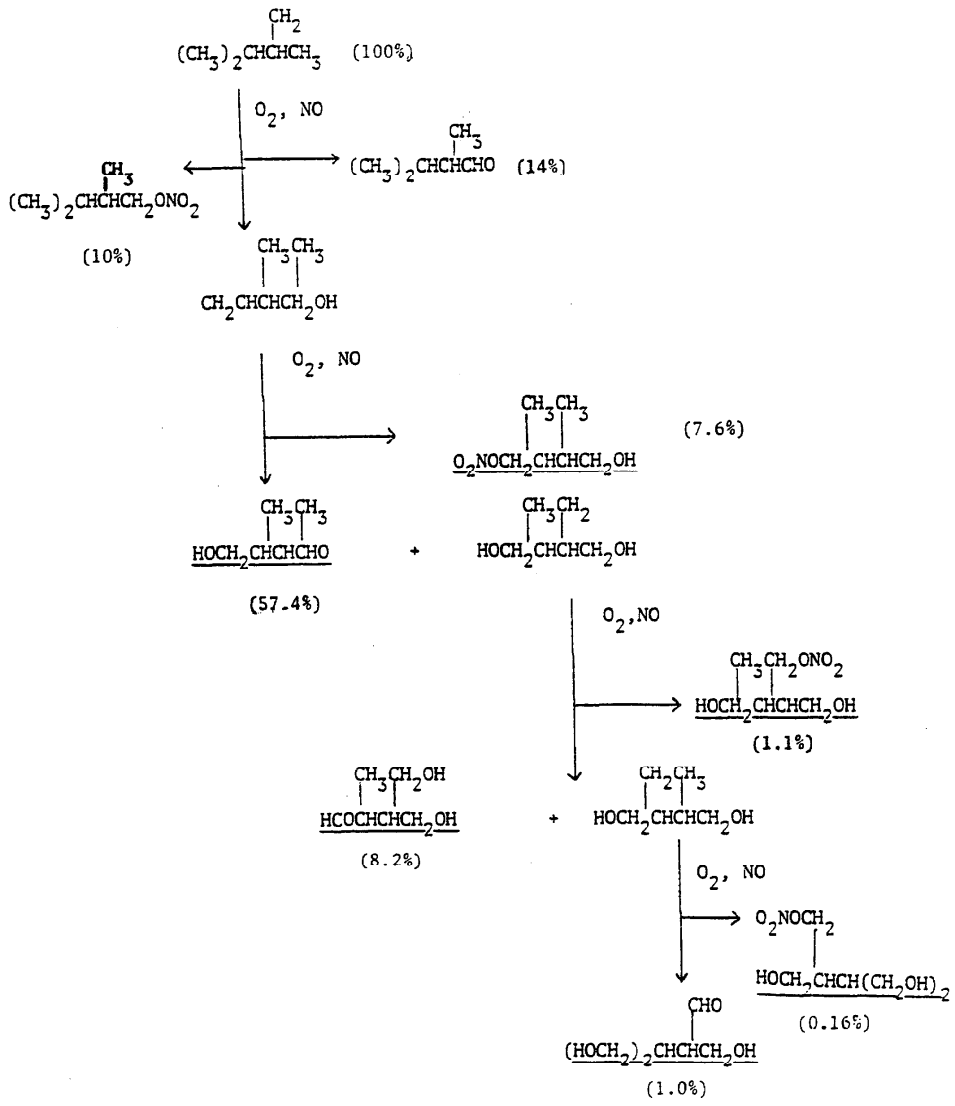

Figure 15. Reaction pathway for 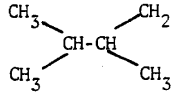 radicals at 298 K and atmospheric pressure.

3.1×10^{18} molecule cm^{-3} at 303 K [7] and $(2.60 \pm 0.35) \times 10^{18}$ molecule cm^{-3} at 296 K [271].

Hence the experimental data from smog chamber data are, using our recommended rate constants k_{57} for the reaction of 2-butoxy radicals with O_2, an order of magnitude higher than the extrapolation of experimental 2-butoxy decomposition data. These inconsistencies imply that either our recommendation of k_{64} is incorrect, or that the 2-butoxy radical decomposition rate constant is higher than estimated by extrapolation of the data of Batt and McCulloch [194]. We thus make no firm recommendation for k_{64} (2-butoxy) at this time, but note that the rate constant ratio k_{64}/k_{57} is temperature dependent, with a temperature dependence of the order of $\sim e^{-7000/T}$, i.e.

$$k_{64}/k_{57} \sim 4 \times 10^{28}\ e^{-7000/T}\ \text{molecule cm}^{-3}$$

at 300 K.

Further work on the general reactions of alkoxy radicals (i.e., decomposition, isomerisation and reaction with O_2) are obviously necessary.

The reactions of methyl ethyl ketone ($CH_3CH_2COCH_3$) under atmospheric conditions will be dealt with in a later section (7), while those for ethyl radicals have been dealt with above in section 5.

$(CH_3)_2\dot{C}H(CH_3)_2$ Radical Reactions

These radicals will react with O_2 and NO:

$$(CH_3)_2\dot{C}H(CH_3)_2 + O_2 \rightarrow (CH_3)_2CH(CH_3)_2 \quad (54)$$

$$(CH_3)_2CH(CH_3)_2 + NO \rightarrow (CH_3)_2CH(CH_3)_2 \quad (a)$$

$$\rightarrow (CH_3)_2CH(CH_3)_2 \quad (b)$$

with [332] $k_a/(k_a + k_b) \sim 0.1$ at atmospheric pressure and, as discussed previously,

$$(k_a + k_b) = 7 \times 10^{-12}\ \text{cm}^3\ \text{molecule}^{-1}\ \text{s}^{-1}$$

at 298 K.

The $(CH_3)_2CH(CH_3)_2$ radical cannot react with O_2 (no appropriate abstractable hydrogen atom) and [224,269] isomerisation will be very slow, so the sole reaction pathways will be

$$(CH_3)_2CH(CH_3)_2 + NO_2 \rightarrow (CH_3)_2CH(CH_3)_2 \quad (56)$$

with (section 4)

$$k_{56} = 1.5 \times 10^{-11}\ \text{cm}^3\ \text{molecule}^{-1}\ \text{s}^{-1}$$

independent of temperature, and

$$(CH_3)_2CH(CH_3)_2 \rightarrow CH_3\dot{C}HCH_3 + CH_3COCH_3 \quad (64)$$

Hendry et al. [6] estimate from thermochemical considerations that

$$k_{64} = 6.3 \times 10^{5}\ \text{s}^{-1}$$

at 303 K

$$(1.3 \times 10^{15}\ e^{-6440/T}\ \text{s}^{-1})$$

Since this rapid decomposition means that reactions with NO or NO_2 (reactions 55 and 56) will be essentially negligible at sub-ppm levels of NO_x, the precise value of k_{64} is somewhat immaterial, we then recommend this estimate of Hendry et al. [6], that

$$k_{64} = 1.3 \times 10^{15}\ e^{-6440/T}\ \text{s}^{-1}$$

$$= 5.4 \times 10^{5}\ \text{s}^{-1}$$

at 298 K with an uncertainty of a factor of $\gtrsim 20$ [224].

The atmospheric chemistry of acetone will be dealt with in a later section, while the isopropyl radical will react as follows:

$$CH_3\dot{C}HCH_3 + O_2 \rightarrow (CH_3)_2CHO_2 \quad (54)$$

$$(CH_3)_2CHO_2 + NO \rightarrow (CH_3)_2CHONO_2 \quad (a)$$

$$\rightarrow (CH_3)_2\dot{C}HO + NO_2 \quad (b)$$

with [7,170], $k_a/(k_a + k_b) = 0.04$ at atmospheric pressure and, as discussed above, (section 4),

$$(k_a + k_b) = 7 \times 10^{-12}\ \text{cm}^3\ \text{molecule}^{-1}\ \text{s}^{-1}$$

at 298 K.

The 2-propoxy radical can react via (isomerisation will be negligibly slow [224, 269]):

$$(CH_3)_2CHO^{\cdot} \rightarrow CH_3^{\cdot} + CH_3CHO \quad (64)$$

$$(CH_3)_2CHO^{\cdot} + O_2 \rightarrow CH_3COCH_3 + HO_2 \quad (57)$$

together with the previously discussed reactions with NO (reaction 55) and NO_2 (reaction 56).

Experimental or estimated data are available for these two pathways:

$$k_{64} = 4 \times 10^{14} e^{-8656/T} s^{-1}$$

at the high pressure limit [195,200-202] and

$$k_{57} \approx 3 \times 10^{-14} \text{ cm}^3 \text{ molecule}^{-1} \text{ s}^{-1},$$

independent of temperature [222].

The decomposition pathway (reaction 64) will be in the fall-off region at atmospheric temperature and pressure [195,200-202,224], and hence at 298 K

$$k_{64} < 100 \text{ s}^{-1}$$

Baldwin et al. [224] estimate, with a correction for fall-off, that

$$k_{64} = 18 \text{ s}^{-1},$$

to be compared with

$$k_{57}[O_2] \approx 1.5 \times 10^5 \text{ s}^{-1}$$

(table 25). Hence, reaction with O_2 will completely dominate over decomposition. We thus recommend the expression:

$$k_{57} = 3 \times 10^{-14} \text{ cm}^3 \text{ molecule}^{-1} \text{ s}^{-1},$$

independent of temperature with an uncertainty of at least a factor of 2 at 298 K.

7. Atmospheric Chemistry of Various Carbonyls

In this section, the atmospheric chemistry of various carbonyl compounds produced as products of the NO_x photooxidations of alkenes (section 5) and alkanes (section 6) are discussed. The carbonyls considered here are propionaldehyde (CH_3CH_2CHO), butyraldehyde ($CH_3CH_2CH_2CHO$), methyl ethyl ketone ($CH_3CH_2COCH_3$), and acetone (CH_3COCH_3).

The atmospheric chemistry of the various hydroxy-substituted aldehydes (such as $HOCH_2CH_2CHO$, etc.) formed from the alkanes are, in the absence of experimental data, expected to behave essentially identically to the corresponding aldehyde. However, the 1,4-hydroxyaldehydes may undergo cyclization:

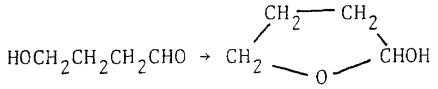

which would, after H atom abstraction by OH radicals lead to difunctional compounds containing carboxylic acid and carbonyl groups ($CHOCH_2CH_2CO_2H$). While for the above example, the cyclic form is calculated to be ≈ 4 kcal mol^{-1} more stable than the 1,4-hydroxyaldehyde, the activation energy for cyclization is expected to be high.

For the aldehydes such as $(CH_3)_2CHCH(CH_3)CHO$, little information is available.

Propionaldehyde

Under atmospheric conditions, the reactions of any importance are expected to be those with NO_3 and OH radicals and photolysis. Reaction of $O(^3P)$ atoms with propionaldehyde

$$O(^3P) + CH_3CH_2CHO \rightarrow CH_3CH_2CO + OH$$

$$k = 1.3 \times 10^{-11} e^{-(869 \pm 33)/T} \text{ cm}^3 \text{ molecule}^{-1} \text{ s}^{-1}$$

$$= 7.0 \times 10^{-13} \text{ cm}^3 \text{ molecule}^{-1} \text{ s}^{-1}$$

at 298 K [138] will be of minor importance. Reaction with NO_3 (reaction 61) has been discussed in section 4.

$$OH + C_2H_5CHO \rightarrow \text{Products} \quad (78)$$

The rate constant for this reaction has been determined from relative rate studies [118,259,333] at room temperature.

Relative to our recommended rate constant for the reaction of OH radicals with ethene, the mean of the data of Niki et al. [118] and Kerr and Sheppard [333] leads to the recommended value of:

$$k_{78} = 1.9 \times 10^{-11} \text{ cm}^3 \text{ molecule}^{-1} \text{ s}^{-1}$$

at 298 ± 2 K, with an estimated uncertainty of a factor of 1.5.

This recommended value is consistent with the rate constant of

$$k_{78} = 1.8 \times 10^{-11} \text{ cm}^3 \text{ molecule}^{-1} \text{ s}^{-1}$$

at 298 K obtained by Audley et al. [334] relative to the rate constant for the reaction of OH radicals with CH_3CHO of

$$1.6 \times 10^{-11} \text{ cm}^3 \text{ molecule}^{-1} \text{ s}^{-1}$$

By analogy with the reaction of OH radicals with CH_3CHO (reaction 47) we anticipate a similar negative temperature dependence, and hence:

$$k_{78} = 9.0 \times 10^{-12} e^{250/T} \text{ cm}^3 \text{ molecule}^{-1} \text{ s}^{-1}$$

This reaction is expected to proceed via H atom abstraction to yield

$$H_2O + C_2H_5\dot{C}O, \text{ or } H_2O + CH_3\dot{C}HCHO; \text{ i.e.,}$$

$$OH + CH_3CH_2CHO \rightarrow H_2O + CH_3CH_2\dot{C}O \quad (a)$$

$$\rightarrow H_2O + CH_3\dot{C}HCHO \quad (b)$$

Based upon the data for methyl ethyl ketone and other ketones [335] and acetaldehyde, path (b) is expected to be essentially negligible.

The behavior of the $C_2H_5\dot{C}O$ radical will be totally analogous to the $CH_3\dot{C}O$ radical, as evidenced by the formation of peroxypropionyl nitrate (PPN) from irradiated NO_x/1-butene/air systems [336,337].

$$CH_3CH_2CHO + h\nu \xrightarrow{O_2} C_2H_5O_2 + HO_2 + CO \quad \phi_a \quad (79)$$

$$\rightarrow C_2H_6 + CO \quad \phi_b$$

The recent data of Shepson and Heicklen [338,339] yield a quantum yield at atmosphere pressure of

$$\phi_a \approx 0.20 \pm 0.08$$

from 254-334 nm. The quantum yield ϕ_b was determined to be essentially zero for $\lambda \geq 313$ nm. While this data are the only information available, further work on the photolysis of propionaldehyde is obviously necessary. Absorption cross-sections are given by Calvert and Pitts [230].

Butyraldehyde, $CH_3CH_2CH_2CHO$

As with propionaldehyde, the reactions of importance are expected to be those with NO_3 and OH radicals and photolysis. Reaction with $O(^3P)$ atoms

$$O(^3P) + CH_3CH_2CH_2CHO \rightarrow OH + CH_3CH_2CH_2\dot{C}O$$

with

$$k = 1.66 \times 10^{-11} e^{-(857 \pm 20)/T} \text{ cm}^3 \text{ molecule}^{-1} \text{ s}^{-1}$$

$$= 9.5 \times 10^{-13} \text{ cm}^3 \text{ molecule}^{-1} \text{ s}^{-1}$$

at 298 K [138] will be of minor importance.

The reaction with NO_3 radicals (reaction 61) has been dealt with in section 4.

$$OH + CH_3CH_2CH_2CHO \rightarrow H_2O + CH_3CH_2CH_2\dot{C}O \quad a \quad (80)$$

$$\rightarrow H_2O + CH_3CH_2\dot{C}HCHO \quad b$$

$$\rightarrow H_2O + CH_3\dot{C}HCH_2CHO \quad c$$

Two recent relative rate constant studies have been carried out by Kerr and Sheppard [333] and by Audley et al. [334]. Relative to the rate constants for the reactions of OH radicals with ethene of

$$8.1 \times 10^{-12} \text{ cm}^3 \text{ molecule}^{-1} \text{ s}^{-1} \text{ at 298 K}$$

and with acetaldehyde of

$$1.6 \times 10^{-11} \text{ cm}^3 \text{ molecule}^{-1} \text{ s}^{-1} \text{ at 298 K}$$

(our recommended values), values of

$$k_{80} = (2.4 \pm 0.1) \times 10^{-11} \text{ cm}^3 \text{ molecule}^{-1} \text{ s}^{-1}$$

[333] and

$$= (2.6 \pm 0.3) \times 10^{-11} \text{ cm}^3 \text{ molecule}^{-1} \text{ s}^{-1}$$

[334] were obtained at 298 K.

Hence we recommend the rate constant

$$k_{80} = 2.5 \times 10^{-11} \text{ cm}^3 \text{ molecule}^{-1} \text{ s}^{-1}$$

at 298 K, with an uncertainty of a factor of ~1.5. The temperature dependence is expected to be close to zero by analogy with HCHO and CH_3CHO, and it is expected (see reaction (78) above) that the major reaction pathway will be via (80a) to yield the $CH_3CH_2CH_2\dot{C}O$ radical.

This radical will behave analogously to $CH_3\dot{C}O$ and $CH_3CH_2\dot{C}O$.

$$CH_3CH_2CH_2CHO + h\nu \rightarrow \text{Products} \qquad (81)$$

The absorption cross-sections are as given by Calvert and Pitts [230]. The gas phase photolysis of n-butyraldehyde at 313 nm has recently been studied for Forgeteg et al. [340]. At 100 torr of n-butyraldehyde and room temperature, the following quantum yields were obtained:

$$CH_3CH_2CH_2CHO + h\nu\ (\lambda = 313\ nm) \rightarrow C_3H_7 + HCO \qquad \phi = 0.34 \pm 0.02$$

$$\rightarrow C_2H_4 + CH_3CHO \qquad \phi = 0.17 \pm 0.01$$

with other photodecomposition pathways being essentially negligible (quantum yields ≤ 0.025). The quantum yield for formation of C_3H_7 + HCO is in excellent agreement with the previous value of 0.36 using the iodine trapping technique [341].

The effect of added O_2 is unknown, but we recommend using the above quantum yields at 313 nm.

Acetone

$$OH + CH_3COCH_3 \rightarrow H_2O + CH_3COCH_2^{\cdot} \qquad (82)$$

The sole rate constant obtained for this reaction is a value of

$$k_{82} \lesssim 5 \times 10^{-13}\ cm^3\ molecule^{-1}\ s^{-1}$$

at room temperature [342]. By analogy with ethane and biacetyl [116,343] for which the C-H bond strengths are equal to those in acetone [344], a rate constant of:

$$k_{82} \sim 1.7 \times 10^{11}\ e^{-1230/T}\ cm^3\ molecule^{-1}\ s^{-1}$$

$$\sim 2.8 \times 10^{-13}\ cm^3\ molecule^{-1}\ s^{-1}$$

at 298 K is estimated [116,343] and recommended.

The $CH_3COCH_2^{\cdot}$ radical is expected to react via:

$$CH_3COCH_2^{\cdot} + O_2 \rightarrow CH_3COCH_2O_2^{\cdot} \qquad (54)$$

$$CH_3COCH_2O_2 + NO \rightarrow CH_3COCH_2ONO_2 \quad a$$

$$\rightarrow CH_3COCH_2O^{\cdot} + NO_2 \quad b$$

with

$$k_a/(k_a + k_b) \sim 0.04$$

at atmospheric pressure [7,170] and

$$(k_a + k_b) = 7 \times 10^{-12}\ cm^3\ molecule^{-1}\ s^{-1}$$

at 298 K. The CH_3COCH_2O radical can decompose or react with O_2 (besides reactions (55) and (56) discussed previously):

$$CH_3COCH_2O^{\cdot} \rightarrow CH_3\dot{C}O + HCHO \qquad (64)$$

$$CH_3COCH_2O^{\cdot} + O_2 \rightarrow CH_3COCHO + HO_2 \qquad (57)$$

Based on a calculated endothermicity of $\sim$ 4 kcal mol^{-1} for the decomposition, it can be estimated, using the procedure of Baldwin et al. [224], that at 298 K,

$$k_{64} \simeq 1 \times 10^3\ s^{-1}$$

$$(k_{64} \simeq 4 \times 10^{14}\ e^{-7850/T}\ s^{-1})$$

at the high pressure limit. This should be compared with an estimate, based on the data of Gutman et al. [222] for other $RCH_2O^{\cdot}$ radical reactions with O_2, of

$$k_{57}\ (O_2) \simeq 3.6 \times 10^4\ s^{-1}$$

at 298 K. Thus we recommend that reaction with O_2 predominates to yield methylglyoxal.

$$CH_3COCH_3 + h\nu \rightarrow CH_3 + CH_3CO \qquad (83)$$

Absorption cross sections are given by Calvert and Pitts [230]. Detailed quantum yield information as a function of wavelength under atmospheric conditions is not available, but recently Cox et al. [345] have reported an average photodissociation quantum yield of 0.33 + 0.06 over the 280-350 nm region, i.e. significantly lower than unity. Photodissociation will, however, because of the slowness of the OH radical reaction, be the major loss process of acetone under atmospheric conditions.

Methyl ethyl ketone

The loss processes for this carbonyl under atmosperhic conditions will be via photolysis and OH radical reaction:

$$OH + CH_3CH_2COCH_3 \rightarrow H_2O + CH_3\dot{C}HCOCH_3 \quad a \qquad (84)$$

$$\rightarrow H_2O + {}^{\cdot}CH_2CH_2COCH_3 \text{ or}$$

$$CH_3CH_2COCH_2^{\cdot} \quad b$$

Rate constants k_{84} have been determined by Winer et al. [346], and Cox et al. [271, 342]. Although the values obtained vary by a factor of ∿4, the latest, and lowest, value of k_{84} determined by Cox et al. [271] is totally consistent with the recent work of Atkinson et al. [335] on the higher ketones.

Thus we recommend the rate constant of Cox et al. [271], i.e.,

$$k_{84} = 8.8 \times 10^{-13} \text{ cm}^3 \text{ molecule}^{-1} \text{ s}^{-1}$$

at 298 K with an uncertainty of a factor of 1.5. The data of Cox et al. [271] further show that reaction (84a) accounts for ∿62% of the overall reaction at 296 K, i.e.,

$$k_{84a} \sim 5.5 \times 10^{-13} \text{ cm}^3 \text{ molecule}^{-1} \text{ s}^{-1}$$

$$k_{84b} \sim 3.3 \times 10^{-13} \text{ cm}^3 \text{ molecule}^{-1} \text{ s}^{-1}$$

The subsequent reactions are expected to be (see also [271]):

$$CH_3\dot{C}HCOCH_3 + O_2 \rightarrow CH_3\underset{\displaystyle OO^{\cdot}}{\underset{|}{C}}HCOCH_3 \qquad (54)$$

$$CH_3\underset{\displaystyle OO^{\cdot}}{\underset{|}{C}}HCOCH_3 + NO \rightarrow CH_3\underset{\displaystyle ONO_2}{\underset{|}{C}}HCOCH_3 \quad a$$

$$\rightarrow CH_3\underset{\displaystyle O^{\cdot}}{\underset{|}{C}}HCOCH_3 + NO_2 \quad b$$

with

$$k_a/(k_a + k_b) \sim 0.08$$

at atmospheric pressure and

$$(k_a + k_b) = 7 \times 10^{-12} \text{ cm}^3 \text{ molecule}^{-1} \text{ s}^{-1}$$

at 298 K.

The $CH_3\underset{\displaystyle O.}{\underset{|}{C}}HCOCH_3$ radical is, from thermochemical estimates, expected to decompose rapidly [7,224]

$$CH_3\underset{\displaystyle O.}{\underset{|}{C}}HCOCH_3 \rightarrow CH_3CHO + CH_3CO \qquad (64)$$

with [224]

$$k_{64} \simeq 3.2 \times 10^{14} e^{-6440/T} \text{ s}^{-1}$$

$$\simeq 1.3 \times 10^5 \text{ s}^{-1} \text{ at 298 K.}$$

Reaction with O_2:

$$CH_3\underset{\displaystyle O}{\underset{|}{C}}HCOCH_3 + O_2 \rightarrow CH_3COCOCH_3 + HO_2 \qquad (57)$$

is expected to have a rate constant similar to those for other secondary alkoxy radicals of [222]:

$$k_{57} \sim 3 \times 10^{-14} \text{ cm}^3 \text{ molecule}^{-1} \text{ s}^{-1}$$

at 298 K, with a first order rate of

$$\sim 1.6 \times 10^5 \text{ s}^{-1}$$

at 298 K and atmospheric pressure. However, the lack of observation of biacetyl [271] shows that these estimates of k_{57} and/or k_{64} are in error, since Cox et al. [271] derived k_{64}/k_{57} $[O_2] \gtrsim 100$. Further work on reactions (57) and (64) are obviously necessary. The radicals ${}^{\cdot}CH_2CH_2COCH_3$ and $CH_3CH_2COCH_2^{\cdot}$ (of which the former is more likely to be formed [335]) will react with O_2 and NO to yield $OCH_2CH_2COCH_3$ and $CH_3CH_2COCH_2O$ respectively. The reactions of these alkoxy radicals are not known with any certainty, but due to the low rate constant for reaction (84) they can probably be neglected to a first approximation

$$CH_3CH_2COCH_3 + h\nu \rightarrow \text{products} \qquad (85)$$

The photodissociation pathways and quantum yields are not known. However, it is expected that photodissociation to $C_2H_5 + CH_3CO$ will predominate [7].

8. Atmospheric Reactions of Toluene and m-Xylene

In this section, the available evidence pertaining to the atmospheric reactions of toluene and m-xylene is discussed. Much of the discussion must, at the present time, be of a speculative nature because of the low carbon balance obtained in smog chamber experiments and the lack of experimental data as to the fates of the organic radicals initially derived from the aromatics [11,116].

The only significant chemical loss process of the aromatic hydrocarbons (not phenolics) under atmospheric conditions is via reaction with the OH radical [11,116,250,347-349]. Thus, reactions with NO_3 radicals,

$O(^3P)$ atoms and O_3 are negligible under atmospheric conditions; data for these reactions are summarized as follows:

NO_3 + Aromatic Hydrocarbons

For the NO_3 radical reactions with toluene and m-xylene, rate constants of

$$(2.0 \pm 1.1) \times 10^{-17} \text{ cm}^3 \text{ molecule}^{-1} \text{ s}^{-1}$$

for toluene and

$$(7.6 \pm 3.5) \times 10^{-17} \text{ cm}^3 \text{ molecule}^{-1} \text{ s}^{-1}$$

for m-xylene have been determined at 298 ± 1 K [130].

O_3 + Aromatic Hydrocarbons

Rate constants for the gas phase reactions of O_3 with a series of aromatic hydrocarbons have been determined at 297 ± 2 K [349]; rate constants (in cm^3 $molecule^{-1}$ s^{-1} units) obtained ranged from

$\sim (7 \pm 4) \times 10^{-23}$ for benzene,

$(1.5 \pm 0.8) \times 10^{-22}$ for toluene,

$\sim 6 \times 10^{-22}$ for the xylenes to

$(2.2 \pm 0.6) \times 10^{-21}$ for 1,3,5-trimethylbenzene.

The products observed were the α-dicarbonyls expected from breakup of the aromatic ring. These reactions are totally negligible under atmospheric conditions.

$O(^3P)$ + Aromatic Hydrocarbons → Products (86)

Absolute rate constants, free from stoichiometry corrections, for the reaction of $O(^3P)$ atoms with the aromatic hydrocarbons have been determined recently by Atkinson and Pitts [350-352], by Colussi et al. [353] and by Ravishankara and coworkers [234,354]. The rate constants recommended for toluene and m-xylene are those of Nicovich et al. [234,354]:

Toluene

$$k_{86} = 4.26 \times 10^{-11} e^{-1910/T} \text{ cm}^3 \text{ molecule}^{-1} \text{ s}^{-1}$$

$$= 7.1 \times 10^{-14} \text{ cm}^3 \text{ molecule}^{-1} \text{ s}^{-1}$$

at 298 K [234] with, based on the data from [350-353], an estimated uncertainty at 298 K of ∼ ± 30%.

m-Xylene

$$k_{86} = 3.78 \times 10^{-11} e^{-1350/T} \text{ cm}^3 \text{ molecule}^{-1} \text{ s}^{-1}$$

$$= 3.9 \times 10^{-13} \text{ cm}^3 \text{ molecule}^{-1} \text{ s}^{-1}$$

at 298 K [354], with an estimated uncertainty at 298 K of ± 30%.

Products of the reaction of $O(^3P)$ atom with toluene have been investigated [355]. However, the reaction pathways under atmospheric conditions have not been well established, and we recommend neglecting all the above reactions for computer modeling purposes.

OH + Aromatic Hydrocarbons → Products (87)

The reaction of OH radicals with the aromatic hydrocarbons proceeds via two pathways: H atom abstraction from the substituent methyl group(s), and OH radical addition to the ring [116,356-360].

The rate constants recommended for the overall OH radical reaction pathways are taken from Atkinson et al. [116], Perry et al. [356] and Ravishankara and coworkers [358,359], while the rate constant ratios for the abstraction/addition pathways are those of Atkinson et al. [360] for toluene and of Perry et al. [356] and Nicovich at al. [359] for m-xylene.

Toluene:

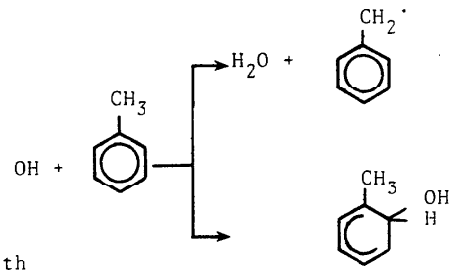

(87a)

(87b)

with

$$k_{87} = (k_{87a} + k_{87b}) = 6.4 \times 10^{-12} \text{ cm}^3 \text{ molecule}^{-1} \text{ s}^{-1}$$

at 298 K [356,358], with an estimated uncertainty of ± 20%. This overall rate constant has a small negative temperature dependence equivalent to an Arrhenius activation energy of $E_{87} \simeq -(1 \pm 1)$ kcal mol^{-1} below ∼320 K [356,358]. At temperatures significantly above 300 K the OH-aromatic adduct thermally decomposes increasingly rapidly [116,356,358], and in the absence of other reactions of the OH-aromatic adduct the addition reaction will become significantly less important. However, fortunately, under atmospheric conditions the

above expression for k_{87} will hold for temperatures $\lesssim$ 325 K.

The rate constant ratio k_{87a}/k_{87b} is more uncertain, but the recent work of Atkinson et al. [360] indicates that at ~300 K,

$$k_{87a}/k_{87} = 0.08 \pm 0.03,$$

with this ratio increasing with temperature [356,358]. Hence at 298 K we recommend:

$$k_{87a} = 5.1 \times 10^{-13} \text{ cm}^3 \text{ molecule}^{-1} \text{ s}^{-1},$$

with an estimated uncertainty of ± 50%,

$$k_{87b} = 5.9 \times 10^{-12} \text{ cm}^3 \text{ molecule}^{-1} \text{ s}^{-1},$$

with an estimated uncertainty of ± 25%.

Over a small temperature range around 298 K, i.e., 325 $\lesssim$ T $\lesssim$ 270 K, we would also recommend using these values, i.e., assuming essentially no temperature dependence.

Further work is obviously necessary concerning the kinetics of reaction 87a (or the rate constant ratio k_{87a}/k_{87}).

OH radical addition is expected [11,116, 356,357] to occur mainly at the ortho position, as shown.

m-Xylene:

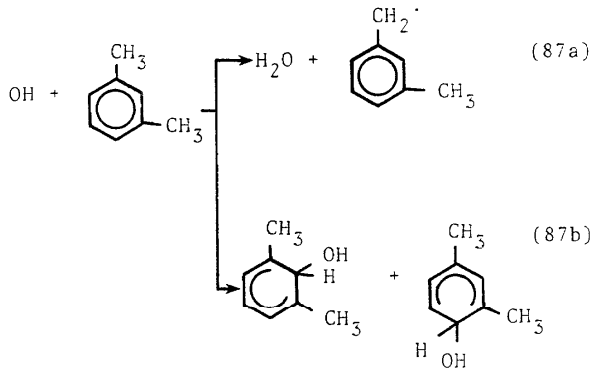

with

$$k_{87} = k_{87a} + k_{87b} = 2.4 \times 10^{-11} \text{ cm}^3 \text{ molecule}^{-1} \text{ s}^{-1}$$

at 298 K [116,356,359], with an estimated uncertainty of ± 20%. This overall rate constant is essentially temperature independent [356,359].

From kinetic studies, k_{87a}/k_{87} ~0.05 at 298 K, with an uncertainty of at least a factor of 2 [356,359].

OH radical addition is expected to occur at the two positions shown, with, estimated from the $O(^3P)$ atom distribution obtained by Grovenstein and Mosher [361], an approximately equal distribution between the two isomers shown.

The fates of these initially formed radicals under atmospheric conditions will be discussed in the following sections.

Atmospheric Reactions of Benzyl Type Radicals

The reactions of the benzyl radicals under atmospheric conditions have been discussed previously [11,116,357,360] and are expected to be:

Toluene

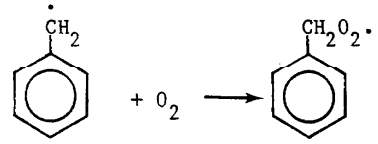

(54)

with

$$k_{54} \text{ (benzyl)} \sim 1.0 \times 10^{-12} \text{ cm}^3 \text{ molecule}^{-1} \text{ s}^{-1}$$

at room temperature [362,363], independent of temperature [363] over the range 292-372 K.

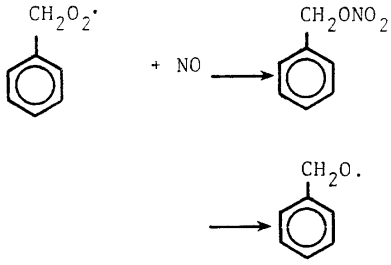

where the ratio $k_a/(k_a + k_b)$ is not known with any certainty. However, the data of Hoshino et al. [364] indicate that at atmospheric pressure the benzyl nitrate yields are ~12% of the benzaldehyde yields. In the absence of further data, the overall rate constant $(k_a + k_b)$ is recommended to be

$$(k_a + k_b) = 7 \times 10^{-12} \text{ cm}^3 \text{ molecule}^{-1} \text{ s}^{-1}$$

at 298 K, i.e., identical to that for the analogous reaction (50), with $k_a/(k_a + k_b)$ ~ 0.1 at atmospheric pressure. Reaction of $C_6H_5CH_2O_2$ radicals with NO_2 to yield a benzyl peroxynitrate should also occur (reaction 51), but by analogy the lifetime of this RO_2NO_2 species is expected to be short enough that it may be neglected.

The $C_6H_5CH_2O$ radical will then react with NO, NO_2 and O_2:

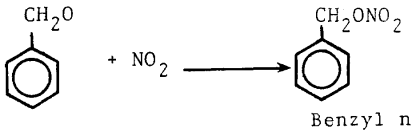

Benzyl nitrate

$k = 1.5 \times 10^{-11}$ cm^3 molecule^{-1} s^{-1},

based on an analogy to the alkoxy radical reaction (56)

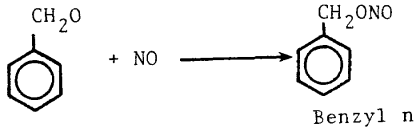

Benzyl nitrite

$k = 3 \times 10^{-11}$ cm^3 molecule^{-1} s^{-1},

by analogy to the alkoxy radical reaction (55)

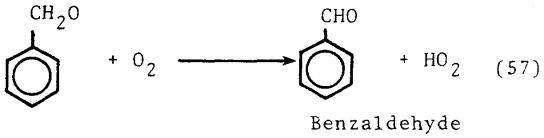

Benzaldehyde (57)

We recommend the use of a rate constant for the reaction with O_2 (reaction 57) of

$$k_{57} = 7 \times 10^{-14} e^{-690/T} \text{ cm}^3 \text{ molecule}^{-1} \text{ s}^{-1}$$

by analogy with simple primary alkoxy radicals (section 4) i.e.,

$$k_{57} = 7 \times 10^{-15} \text{ cm}^3 \text{ molecule}^{-1} \text{ s}^{-1}$$

at 298 K (equivalent to a first order rate of 3.6×10^4 s^{-1} at 298 K and 1 atmosphere of air).

The reactions of the 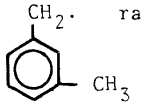 radical

should be totally analogous to these of the benzyl radical shown above, with essentially identical rate constants. However, because of its small yield (~3%) this reaction pathway will be of very minor importance under atmospheric conditions.

Hence, the initial products formed from the H-atom abstraction are:

Toluene: benzaldehyde, benzyl nitrate and benzyl nitrite

m-Xylene: m-tolualdehyde, m-methylbenzyl nitrate and m-methylbenzyl nitrite.

The nitrites are expected [230] to photolyse rapidly, and hence their formation should be of little consequence (see methyl nitrite, section 4). However, the aldehydes and nitrates will accumulate and react primarily with OH radicals, or photolyse [11, 357].

At sub-ppm levels of NO_x, the benzyl nitrates will be formed in very low yield, especially so from m-xylene (because of the small amount of H atom abstraction (reaction (87a)). Under atmospheric conditions these nitrates are expected to react predominantly with the OH radical, but no experimental data are available on this point. At this time, we expect that these nitrates will react with OH radicals with somewhat lower rate constants than the parent aromatic hydrocarbons. However, because of their low concentrations under simulated atmospheric conditions and the lack of experimental data, we suggest that the subsequent reactions be neglected.

Atmospheric Reactions of the Aromatic Aldehydes

The aromatic aldehydes react rapidly with the OH radical [116,118,333] and also photolyse [11]. The rate constant for the reaction of OH radicals with benzaldehyde at 298 ± 2 K has been determined relative to that for the reaction of OH radicals with ethene [118,333]. Using our recommended rate constant for that reaction, these data yield:

$$k_{88} \text{ (OH + benzaldehyde)} = 1.2 \times 10^{-11} \text{ cm}^3 \text{ molecule}^{-1} \text{ s}^{-1}$$

at 298 K.

Since the magnitude of this rate constant is essentially identical with those for the alphatic aldehydes [116,118,333], and is much higher than would be expected for OH radical addition to the aromatic ring, the reaction of OH radicals with benzaldehyde must proceed almost exclusively via H atom abstraction from the -CHO substituent group [11,116].

$$OH + C_6H_5CHO \rightarrow H_2O + C_6H_5\dot{C}O \qquad (88a)$$

By analogy with the alphatic aldehydes [119, 120], the temperature dependence of this rate constant, k_{88}, where

$$k_{88} = (k_{88a} + k_{88b}),$$

and k_{88b} is the rate constant for the addition reaction of OH radicals to benzaldehyde, is

expected to be zero or near zero, and we recommend:

$$k_{88} = 1.2 \times 10^{-11} \text{ cm}^3 \text{ molecule}^{-1} \text{ s}^{-1},$$

independent of temperature, with an estimated uncertainty of a factor of approximately 1.5 at 298 K.

Although a certain amount of OH radical addition to the aromatic ring must occur, since the -CHO group is electron withdrawing, the rate constant for OH radical addition to the ring is expected to be less or equal to that for the reaction of OH radicals with benzene, i.e.,

$$k_{88b} \leq 1.2 \times 10^{-12} \text{ cm}^3 \text{ molecule}^{-1} \text{ s}^{-1},$$

approximately independent of temperature. Hence as a first approximation reaction pathway (88b) can be neglected.

For the case of 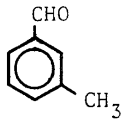

the OH radical addition pathway is then, by analogous arguments, expected to have a rate constant less or equal to that for OH radical addition to toluene

$$(k_{88b} \lesssim 6 \times 10^{-12} \text{ cm}^3 \text{ molecule}^{-1} \text{ s}^{-1},$$

independent of temperature) while the H-atom abstraction route will have a rate constant of

$$k_{88a} \sim 1.3 \times 10^{-11} \text{ cm}^3 \text{ molecule}^{-1} \text{ s}^{-1},$$

independent of temperature.

Thus, the atmospheric reaction pathways expected are as follows (taking benzaldehyde as an example):

OH Radical Reaction:

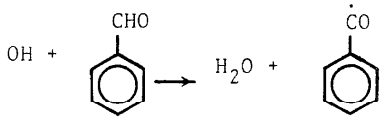

$$k_{88a} = 1.2 \times 10^{-11} \text{ cm}^3 \text{ molecule}^{-1} \text{ s}^{-1},$$

independent of temperature

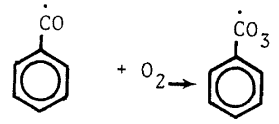

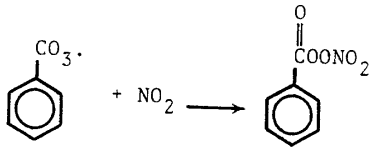

Peroxybenzoyl nitrate (PBzN) (51)

As previously discussed (section 4), we recommend using

$$k_{51} = 4.7 \times 10^{-12} \text{ cm}^3 \text{ molecule}^{-1} \text{ s}^{-1}$$

at 298 K, since

$$k_{50} = 7 \times 10^{-12} \text{ cm}^3 \text{ molecule}^{-1} \text{ s}^{-1}$$

at 298 K and

$$k_{50}/k_{51} = 1.52 \pm 0.12$$

at 303 K [174].

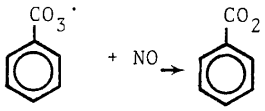

(50)

PBzN thermal decomposition:

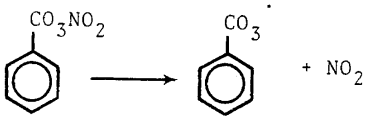

(89)

Rate constants of

$$k_{89} = 1.6 \times 10^{15} \, e^{-(13035 \pm 458)/T} \text{ s}^{-1}$$

$$= 1.6 \times 10^{-4} \text{ s}^{-1}$$

at 298 K [174], and

$$k_{89} = 8.5 \times 10^{14} \, e^{-(12682 \pm 1509)/T} \text{ s}^{-1}$$

$$= 2.8 \times 10^{-4} \text{ s}^{-1}$$

at 298 K [365] have been determined. Although clearly further work is required concerning the kinetics of this reaction, in view of the more detailed study of Kenley and Hendry [174] we recommend the use of their Arrhenius expression of [174]:

$$k_{89} = 1.6 \times 10^{15}\ e^{-13035/T}\ s^{-1}$$

$$= 1.6 \times 10^{-4}\ s^{-1}$$

at 298 K with an estimated uncertainty of a factor of 2.

The $C_6H_5CO_2$ radical formed is expected [11,177] to decompose rapidly (see reaction 53).

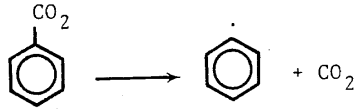

The phenyl radical ($C_6H_5^{\cdot}$) will then react with O_2 and NO or NO_2:

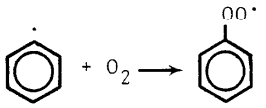

this being the sole reaction of phenyl radicals under atmospheric conditions, followed by:

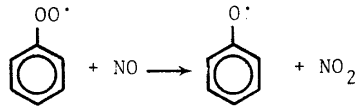

(50)

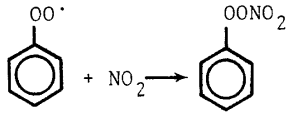

(51)

with rate constants of approximately

$$7 \times 10^{-12}\ cm^3\ molecule^{-1}\ s^{-1}$$

at 298 K for both reactions (section 4). The decomposition of the peroxyphenyl nitrate ($C_6H_5OONO_2$) is expected, according to Hendry and Kenley [178], to occur via:

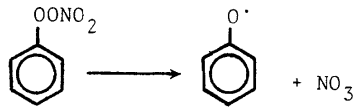

because of the weakened O-O bond strength (because of interaction with the aromatic ring), with a very short lifetime (of the order of μsec at room temperature [178]). Hence this peroxynitrate itself can be neglected, and the reaction written as:

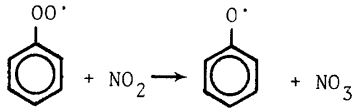

The fates of phenoxy radicals under atmospheric conditions are not known with any certainty but Niki et al. [177] have observed the formation of o- and p-nitrophenols in irradiated Cl_2-NO-benzaldehyde-air systems, presumably via the reaction of phenoxy radicals (formed from C_6H_5CO radicals as shown above) with NO_2

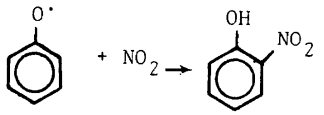

(90a)

o-nitrophenol

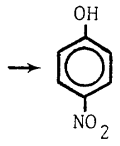

(90b)

p-nitrophenol

In the presence of NO_x, this appears, because of the inherent stability of the phenoxy radical, to be the predominant sink for phenoxy radicals. The rate constant for the reaction

$$k_{90} = (k_{90a} + k_{90b})$$

is not known, but is presumably fast, of the same order as for other RO + NO_2 reactions (i.e., approximately

$$1.5 \times 10^{-11}\ cm^3\ molecule^{-1}\ s^{-1}$$

at 298 K). In the absence of NO_2, reaction with HO_2 is also likely:

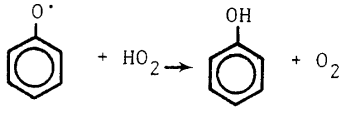

with a rate constant at 298 K of approximately

$$5 \times 10^{-12}\ cm^3\ molecule^{-1}\ s^{-1},$$

by analogy with the reaction of CH_3O_2 with HO_2 [3] [since CH_3OOH has a very similar O-H bond strength (∿90 kcal mol^{-1} [366]) to phenol (∿87 kcal mol^{-1} [367])].

The nitrophenols have low vapor pressures and are likely [177] to go to the chamber walls (dry deposition) or accumulate in the aerosol phase.

For the 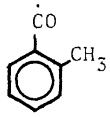

radical a totally analogous series of reactions can be written. At this stage, we recommend the above reaction sequence for benzaldehyde with the substituent $-CH_3$ group having no effect on the reaction rate constants or products. Of course, the products formed are different, i.e.:

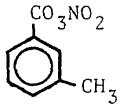

instead of

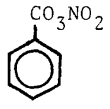

(PBzN)

and

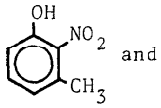

and

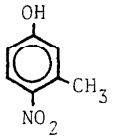

instead of o- and p-nitrophenol

However, a small, but probably significant portion of the

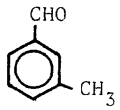

will react with OH radicals via OH radical addition to the ring. We estimate the rate constant for this pathway to be

$$\lesssim 6 \times 10^{-12} \text{ cm}^3 \text{ molecule}^{-1} \text{ s}^{-1}$$

at 298 K, approximately independent of temperature (i.e., ≲35% of the total OH radical rate constant for this aldehyde). Since the formation of this aldehyde is minor (<4% of the total OH + m-xylene reaction) and this reaction pathway is also minor, to a first approximation we feel it could be neglected.

NO_3 Radical Reaction

An upper limit of

$$\lesssim 6 \times 10^{-15} \text{ cm}^3 \text{ molecule}^{-1} \text{ s}^{-1}$$

at 300 ± 1 K has been derived for the reaction of NO_3 radicals with benzaldehyde by Carter et al. [368] using the equilibrium constant $K_{7,8}$ of Malko and Troe [27]. It is expected, consistent with this datum, that these reaction rate constants will be similar to those for the aliphatic aldehydes (reaction 61), i.e.,

$$k_{61} = 1.4 \times 10^{-15} \text{ cm}^3 \text{ molecule}^{-1} \text{ s}^{-1}$$

at 298 K, with an estimated uncertainty of a factor of ∿3.

The reaction is also expected to proceed via:

$$NO_3 + C_6H_5CHO \rightarrow HNO_3 + C_6H_5\dot{C}O$$

followed by the reactions of the $C_6H_5\dot{C}O$ (or $C_6H_4(CH_3)\dot{C}O$) radical discussed above.

Photolysis

The aromatic aldehydes absorb in the near UV [230] and at 366 nm an efficient (near unity) intersystem crossing from the initially formed singlet to the triplet state of benzaldehyde occurs [369,370]. Although the photodissociation quantum yield, in the absence of O_2, is very low [230], interaction of O_2 with triplet benzaldehyde leading to dissociation is possible.

In order to fit the benzaldehyde time-concentration profiles in irradiated NO_x-toluene-air and NO_x-benzaldehyde-toluene-air systems (the most sensitive being obviously the NO_x-benzaldehyde-toluene-air system), Atkinson et al. [11] and Killus and Whitten [371] have found it necessary to include a photolysis reaction of benzaldehyde (as well as OH radical reaction and dilution). There is, however, no agreement as to the photolysis products. Atkinson et al. [11] concluded, based upon computer model calculations, that photodissolution into non-radical products is necessary. While the most likely pathway would be to benzene + CO, the small yields of benzene observed (∿0.5-1 ppb) in the NO_x-toluene-benzaldehyde-air irradiations were much less than the amounts expected if it were the major product of benzaldehyde photolysis. However, Killus and Whitten [371], also on the basis of computer modeling calculations, concluded that radical production from benzaldehyde photodissociation must occur, and assumed the other obvious pathway of phenyl radical + HCO formation. It is hence obvious that elucidation of the photodissociation pathways and their quantum yields for benzaldehyde and the methyl substituted benzaldehydes are needed before any firm recommendations can be made.

Atmospheric Reactions of the OH-Aromatic Adducts

As discussed above, the initially formed OH-aromatic adducts are expected to be:

from toluene:

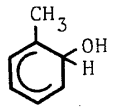

from m-xylene:

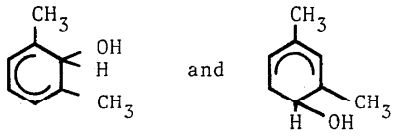

These addition adducts initially contain ∿18 kcal mol^{-1} internal energy due to the exothermicity of the reaction [116,356], but at atmospheric pressure these initially energy rich radicals will be rapidly thermalised [356]. While these thermalised OH-aromatic adducts can thermally decompose back to the reactants (i.e., an OH radical and the aromatic hydrocarbon) with a rate constant of

$$\sim 3 \times 10^{13} e^{-9000/T} s^{-1},$$

corresponding to half lives of ∿0.37 sec at 298 K and 0.03 sec at 325 K [116,356], the reaction with O_2 (see below) of $\gtrsim 10^4$ s^{-1} at atmospheric pressure and 298 K means that this back decomposition can be totally neglected under atmospheric conditions.

Taking the toluene case as an example, the thermalised adduct (A) can react under atmospheric conditions with O_2 via two reaction pathways [11,116,360,372]: H atom abstraction to form the cresol (reaction 91), or reversible addition to form the peroxy radical (B) (reaction 92,-92):

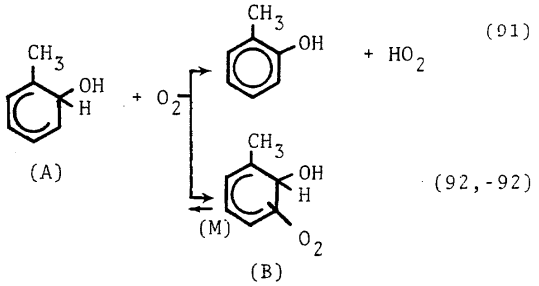

(91)

(92,-92)

(A) (B)

or it can react with NO_2 to form the nitrotoluene:

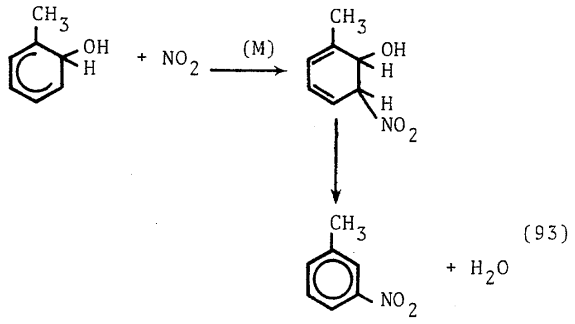

(93)

Kenley et al. [357] have concluded from a discharge flow study of the reaction of OH radicals with toluene, carried out at ∿6-15 torr total pressure of (Ar + O_2), that the cresol isomers and m-nitrotoluene are the sole initial products of the OH radical addition pathway, and that

$$k_{93}/k_{91} = (4.4 \pm 0.5) \times 10^3.$$

If these discharge flow results were applicable to atmospheric pressure, then for sub-ppm concentrations of NO_2, the initial products would be ∿85% cresols (mainly o-cresol [357]) and ∿15% benzaldehyde. However, smog chamber experiments have shown that:

a) While there is still a significant uncertainty in the absolute yield of o-cresol (the predominant cresol isomer) from toluene, the most recent direct determination of Atkinson et al. [360] has obtained an o-cresol yield of 13.1 ± 7.2%, independent of total pressure from 62-740 torr. This o-cresol yield is in reasonably good agreement with that used (21%) to give a fit of calculated to experimental data in the modeling study of Atkinson et al. [11]. Assuming that the isomeric cresol distribution obtained by Kenley et al. [357], although incorrect on an absolute basis, is correct on a relative basis (o-cresol/total cresols = 0.806 ± 0.022 [357]), then, based upon the o-cresol yield of Atkinson et al. [360] the overall cresol (o- , m- , and p-) yield becomes 16 ± 9% (13% o-cresol, 1% m-cresol and 2% p-cresol).

b) In irradiated NO_x-o-xylene-air systems, α-dicarbonyls have been observed in significant yields [343,360,373]. In all of these studies, the concentration-time profiles for biacetyl showed that the rate determining step for its formation was the reaction of OH radicals with o-xylene, since the initial formation of an hydroxyxlene followed by reaction of this hydroxyxylene with OH radicals and/or O_3 would have resulted in incorrect time-concentration profiles [343].

The biacetyl yields obtained from o-xylene are 18 ± 4% [343], 26 ± 10% [373] and 13.7 ± 1.6% [360], while Takagi et al. [373] reported methylglyoxal and glyoxal yields of 85 ± 47 and 14 ± 10% respectively. These studies, together with the observations of unsaturated 1,4-dicarbonyls from toluene [374] and 1,2,4-trimethylbenzene [375] lead to the conclusion that the OH-aromatic adducts react with O_2 under atmospheric conditions to form ring cleavage products, and not cresols, most of the time, and that this ring cleavage is rapid, not involving OH radical or O_3 reaction with the adduct.

Unfortunately, there is almost no definitive data on which to unambiguously delineate a reaction sequence subsequent to the reaction of O_2 with an OH-toluene or other OH-aromatic adduct, apart from the fact that any reaction scheme must predict the rapid formation of the α-dicarbonyls glyoxal, methylglyoxal and biacetyl from the o-xylene system [343,360, 373,376], methylglyoxal and/or glyoxal from the benzene, toluene, m- or p-xylene systems [376], and the occurrence of unsaturated 1,4-dicarbonyls [374,375]. Hence, much of the following discussion is speculative and is based upon thermochemical arguments and the NO_x-toluene-air and NO_x-cresol-air photooxidation modeling study of Atkinson et al. [11], which was based on recent experimental data.

For the toluene system at atmospheric pressure and ∿303 K, we recommend for the OH radical addition pathway the following reactions, based on the o-cresol yield data of Atkinson et al. [360]:

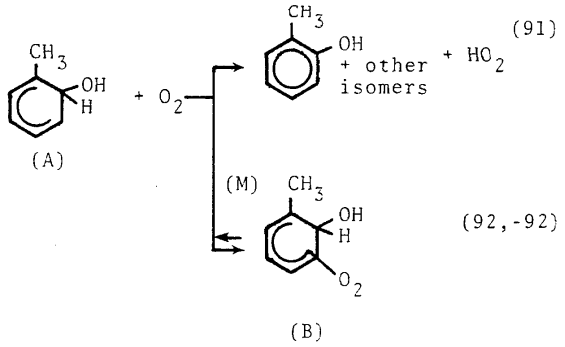

with

$$k_{91}/k_{92}^{\ eff} \simeq 0.21$$

and

$$k_{91} = 7 \times 10^{-14} e^{-690/T} \text{ cm}^3 \text{ molecule}^{-1} \text{ s}^{-1}$$

$$(7 \times 10^{-15} \text{ cm}^3 \text{ molecule}^{-1} \text{ s}^{-1} \text{ at } 303 \text{ K}).$$

The cresol isomeric distribution is based upon the data of Kenley et al. [357], and is o- :m- :p-cresol = 1.0 : 0.06 : 0.18. $k_{92}^{\ eff}$ is an overall observed rate constant including reactions (92) and (-92) and will be discussed later. The rate constant k_{91} for the reaction of O_2 with the OH-toluene adduct to form cresol has been assumed to be the same as that for the reaction of primary alkoxy radicals with O_2 (reaction 57). Hence at ∿303 K,

$$k_{92}^{\ eff} \simeq 3.3 \times 10^{-15} \text{ cm}^3 \text{ molecule}^{-1} \text{ s}^{-1}.$$

The uncertainty in the ratio $k_{91}/k_{92}^{\ eff}$ (the parameter which is of importance) is difficult to estimate, but ± 60% is a reasonable estimate based on the currently available data [360].

Using this value of k_{91} leads, from the data of Kenley et al. [357], to

$$k_{93} = 3.1 \times 10^{-11} \text{ cm}^3 \text{ molecule}^{-1} \text{ s}^{-1},$$

with a large uncertainty, including the possibility of a pressure dependence for reaction (93) (see reference [11]).

For the m-xylene system, we recommend analogous reactions:

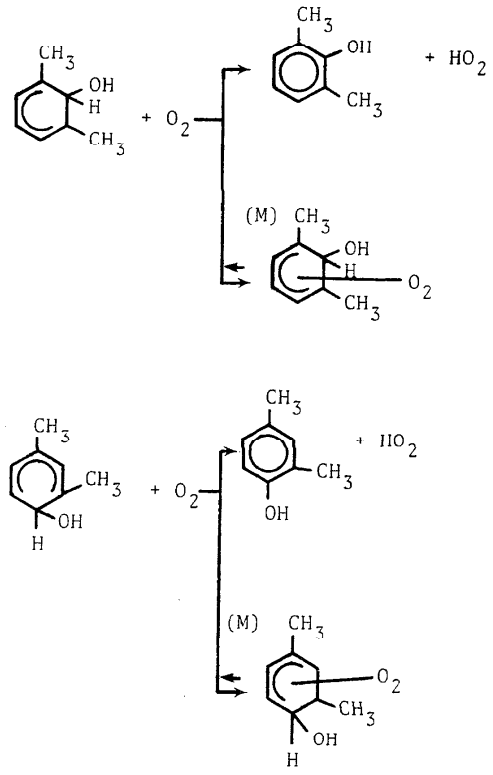

and, in the absence of further information, we recommend using the same rate constants and rate constant ratios as for the toluene system.

Structure and Reactions of the OH-Aromatic-O_2 Adducts

In the following section we will focus primarily on the OH-toluene-O_2 adduct (B), with totally analogous reactions and rate constants being assumed to apply to the corresponding adducts in the m-xylene system. Thus for the m-xylene case, there is a $-CH_3$ substituent at the 3- or 5- position in the discussion below.

The structure of the radical (B) is not known; addition of O_2 to (A) could occur at the 1- , 3- , or 5- positions:

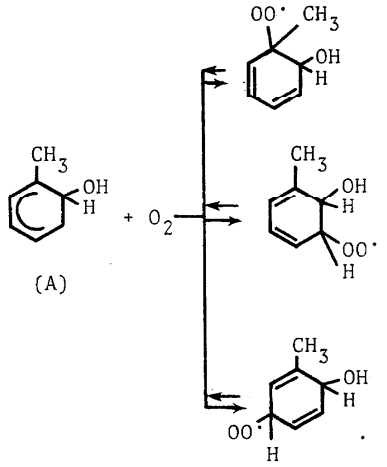

O_2 addition at the 5- position should be the least thermodynamically favored, since the double bonds are non-conjugated. For the toluene case shown above, addition at the 1- position is estimated to be slightly more favored thermodynamically over addition to the 3- position, although the resulting radical (B1) also has the most steric hindrance.

Based on thermochemical estimates (using group additivity principles [366] and the heat of formation of radical (A) [356], O_2 addition to radical (A) is $\sim$10 kcal mol^{-1} exothermic. This means that significant back-decomposition of (B) to (A) may be occurring (see later). No definitive information is available concerning the reactions of radicals (B1) or (B2), possible alternatives being (taking (B2) as an example):

a) Reaction with NO analogous to other peroxy radicals:

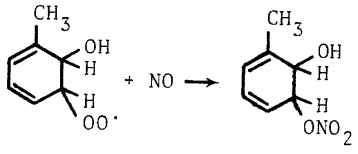

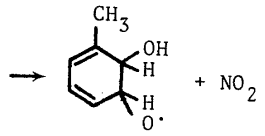

followed by reaction of the alkoxy radical with O_2:

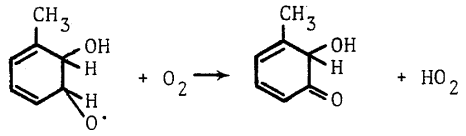

or ring opening:

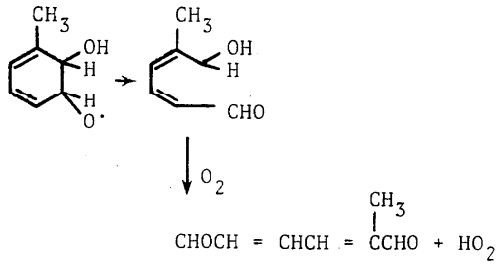

However, this scheme is inconsistent with the prompt formation of biacetyl and other α-dicarbonyls from o-xylene [343,360,373,376]. Furthermore, for a 1 ppm level of NO, the reaction of (B) with NO will have a rate of $\sim$180 s^{-1}, much less than the calculated rate of back decomposition of (B) to (A) of

$$\sim 3 \times 10^{13}\ e^{-5000/T}\ s^{-1}$$

$$\sim 2 \times 10^{6}\ s^{-1} \text{ at } 303\ K.$$

It is thus assumed [11] that the OH-aromatic-O_2 radicals (B) undergo cyclization:

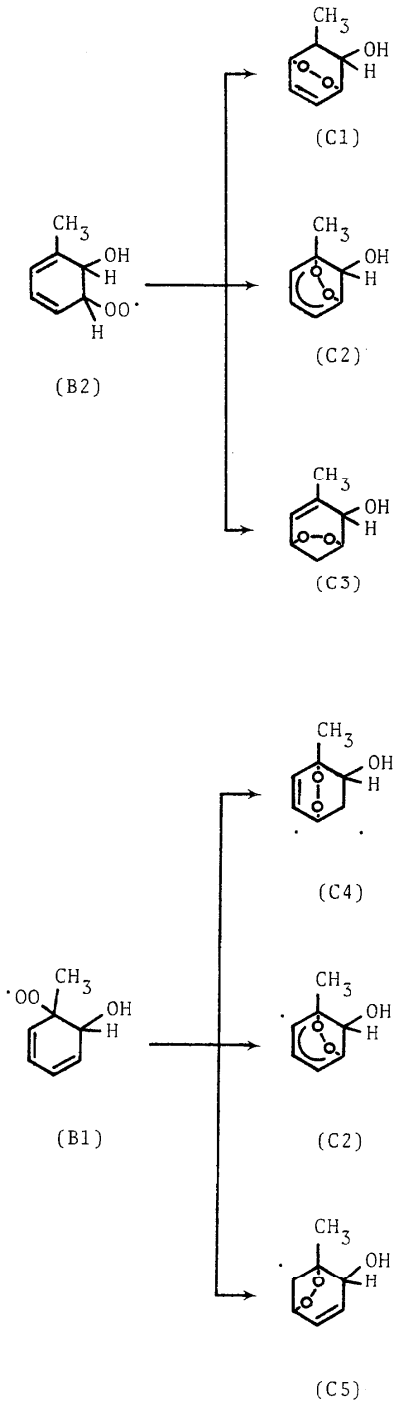

In addition to accounting for the ring cleavage products observed [343,360,373,374-376], these reactions are expected to dominate on the basis of thermochemical and kinetic estimates. Assuming [11] that for cyclization the preexponential factor A > 10^{10} s^{-1} [366] and that the activation energy is ($\lesssim$9 kcal mol^{-1} [based on radical double bond additions] + the reaction endothermicity) and that ΔH cyclization $\simeq$ (ring strain - 14) kcal mol^{-1} (based on thermochemical calculations), then cyclization of (B) should dominate reaction of (B) with NO at 1 ppm if the ring strain of the cyclic radicals is less than $\sim$16 kcal mol^{-1}. Especially for the 2.2.2-bicyclic forms (C1 and C4) this is expected to be so, since the ring strain of multicyclic structures appears [366] to be approximately the sum of the individual ring strains (so the 2.2.2-bicyclics with 6 membered rings should have low, $\lesssim$5 kcal mol^{-1}, ring strains).

The overall reaction sequence is complex:

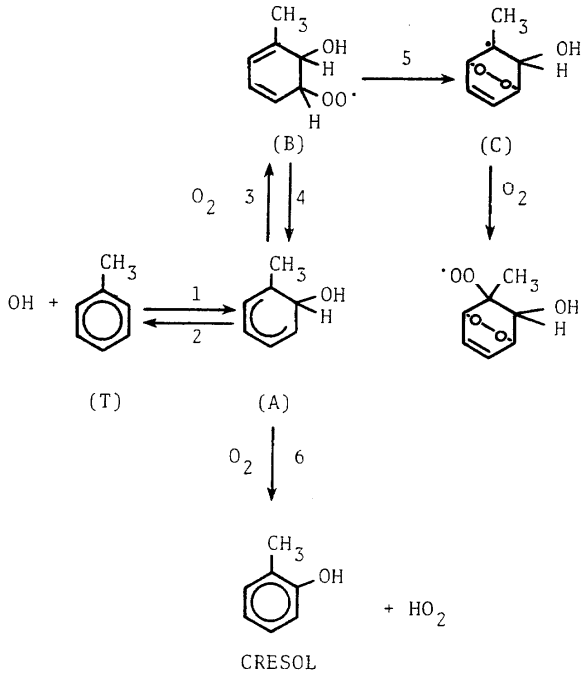

Radicals (C) (C1 is shown as an example) are calculated to be stable with respect to back reaction to (B) since they are expected to be rapidly removed by reaction with O_2 at a rate of

$$\sim 5 \times 10^{6}\ s^{-1}$$

to form bicyclic peroxy radicals (see below). Also, as noted above, back decomposition of (A) to OH + toluene can be neglected, since the lifetime of (A) with respect to reaction with O_2 to form cresol is

$$\sim 3 \times 10^{-5}\ s$$

at 303 K, against $\sim$1 s for back decomposition.

Using the steady state approximation leads to:

$$\frac{d(C)}{d(CRESOL)} = \frac{k_3}{k_6} \times \frac{k_5}{(k_4 + k_5)}$$

Since O_2 addition to (A) should have (by analogy with alkyl radical + O_2 reactions) a rate constant of

$$\sim 10^{-12} \text{ cm}^3 \text{ molecule}^{-1} \text{ s}^{-1}$$

and

$$k_6 \sim 7 \times 10^{-15} \text{ cm}^3 \text{ molecule}^{-1} \text{ s}^{-1}$$

at 303 K (see above) then $k_3/k_6 \sim 140$. For d(C)/d(CRESOL) ~ 6 as observed at atmospheric pressure [11,360],

$$k_5/k_4 \sim 4 \times 10^{-2}$$

is then calculated. Hence radicals (A) and (B) are essentially in equilibrium at room temperature, and using the estimate of k_4 above leads to

$$k_5 \sim 8 \times 10^4 \text{ s}^{-1}$$

which is greatly in excess of the rate of reaction of (B) with NO (~ 180 s^{-1} at 1 ppm of NO).

Hence, this cyclisation scheme appears to be self-consistent, and the rapid back decomposition of (B) to ((A) + O_2) is manifested by a greatly reduced effective rate constant for O_2 addition to (A) to form (C). The effect of changing the temperature is of interest; the temperature dependence being exp -((E3+E5-E6-E4)/RT). It is expected that $E_3 \sim 0$, $E_6 \sim 1.4$ kcal mol^{-1}, $E_4 \sim 10$ kcal mol^{-1} and $E_5 \sim 12$ kcal mol^{-1} based on the very approximate above estimate of k_5 and $A_5 \sim 3 \times 10^{13}$ s^{-1}.

Hence, the formation of (C) versus cresol is expected to be approximately independent of temperature, within the uncertainties of E_3 through E_6. Darnall et al. [343] observed no change, within the experimental error limits, of the biacetyl yield on varying the temperature from 283-323 K, which is in excellent agreement with this prediction, further strengthening the above arguments.

Of the radicals C1-C5, C3 and C5 will be the least thermochemically favored, C1 and C4 will have the least ring strain, while the ring strain in C2 will be somewhat offset by resonance stabilization by virtue of its allylic character. Since it cannot be determined, a-priori, which of these structures will predominate, C1, C2, and C4 must be considered.

For m-xylene, the corresponding radicals are:

from:

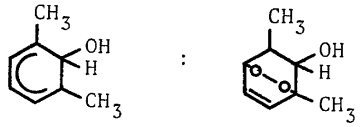

and

(C_m1)

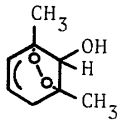

(C_m2)

from:

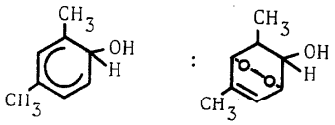

(C_m3)

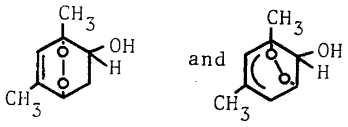

(C_m4) (C_m5)

These cyclised radicals are then expected to add O_2 to form peroxy radicals of the type (taking C1 as an example)

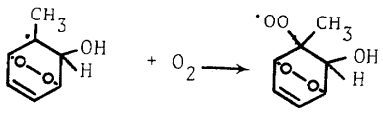

(C1) (D1)

with a rate constant of

$\sim 10^{-12}$ cm^3 molecule^{-1} s^{-1} at room temperature.

These bicyclic peroxy radicals are expected to react with NO to form an alkoxy radical or yield a stable nitrate (analogous to the $\geq C_3$ alkylperoxy case [169,170] (see also section 4).

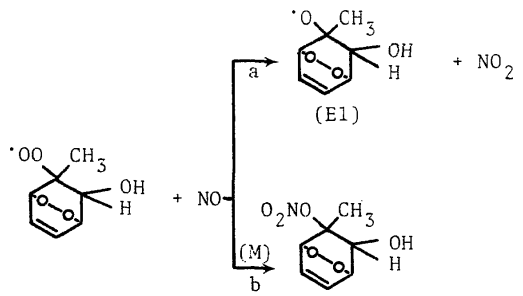

The overall rate constant is expected to be

$$\sim 7 \times 10^{-12} \text{ cm}^3 \text{ molecule}^{-1} \text{ s}^{-1}$$

at 298 K (reaction 50). The ratio $k_b/(k_a + k_b)$ is obviously not known--Atkinson et al. [11] obtained a best fit of experimental versus calculated data for $k_b/(k_a + k_b) = 0.25$ at atmospheric pressure, though obviously in such a complex reaction sequence this must be regarded as little more than an arbitrary adjustable parameter. Changes elsewhere in the model gave rise to large compensating changes in $k_b/(k_a + k_b)$ [11], and Killus and Whitten [371] neglect nitrate formation.

A further reaction to be considered is recyclisation of D1, as, for instance:

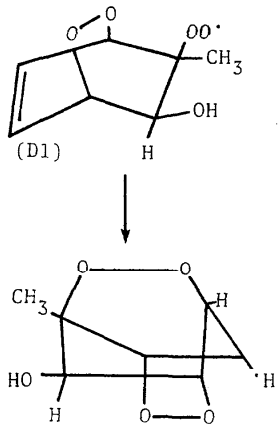

The thermochemistry of such highly bridged radicals is, needless to say, obscure and the modeling study of Atkinson et al. [11] concluded that such recyclisations could not be involved in the NO_x-toluene-air or NO_x-cresol-air photo-oxidations, since no mechanistic options subsequent to such recyclisations could fit both the toluene and o-cresol systems. For a further discussion of this particular point, see Atkinson et al. [11].

Thus it appears that the ring cleavage proceeds via the alkoxy bicyclic radicals (E); which should undergo a series of favorable β-scission fragmentations: (taking E1 as an example):

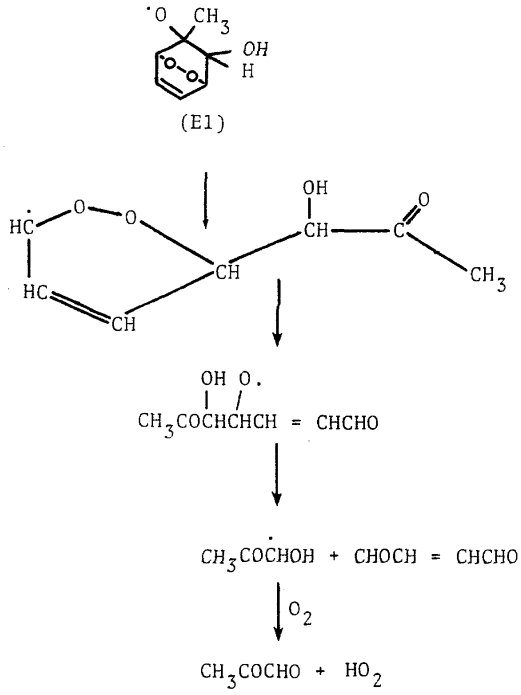

(reaction of an α-hydroxy radical with O_2 [275,276])

While there is only one mode of decomposition for radicals C1 via D1 and E1, radical C2 can react with O_2 via two modes to form:

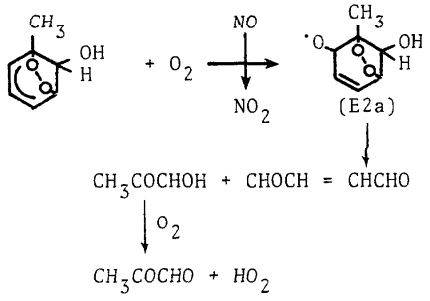

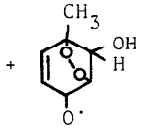

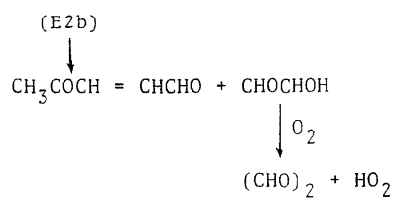

While formation of E2a is favored thermochemically, the relative formation rates of E2a and E2b are not known. Table 31 shows, by analogous reaction sequences, the carbonyls formed from the various radicals (C).

There is, a priori, no way of assessing the importance of these modes of reaction. However, Atkinson et al. [11] found that, regardless of the subsequent chemistry, exclusive 1-addition of O_2 to the OH-toluene adduct and 2.2.2-cyclisation to form radical (C4), and its analogy in the o-cresol system, was calculated to significantly underpredict O_3 and PAN in the toluene system, and overpredict them in the o-cresol system, and hence that this pathway was not exclusively operative. The data could be fitted by either exclusive formation of

$$CH_3COCHO + CHOCH = CHCHO + HO_2$$

or a combination of

$$CH_3COCHO + CHOCH = CHCHO + HO_2$$

and

$$(CHO)_2 + CH_3COCH = CHCHO + HO_2.$$

More recently Killus and Whitten [371] have used exclusive formation of

$$CH_3COCHO + CHOCH = CHCHO + HO_2$$

in their modeling study. Obviously only further experimental evidence as to the initial dicarbonyl production will help elucidate these uncertainties.

However, the alternatives cannot always be distinguished; thus a combination of C1 and C4 cannot be distinguished from C2(a) + C2(b) etc.--only if there is exclusive formation of CH_3COCHO or of $(CHO)_2$ as the α-dicarbonyls could unambiguous choices be made. The data of Nojima et al. [376] from the irradiation of NO-aromatic mixtures (presumably in air) at high concentrations (1000 ppm of aromatic, 50, 100 or 200 ppm of NO) show that methylglyoxal is the major dicarbonyl product from both toluene and m-xylene, indicating reaction mainly via C1 or C2a for toluene, and Cm1, Cm2, Cm3 or Cm5a for m-xylene. Of course, to some extent the precise structure of the various intermediates is immaterial, since all that is necessary are the coefficients such as α and β:

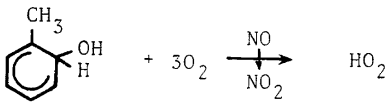

$$+ \alpha(CH_3COCHO + CHOCH = CHCHO)$$

$$+ \beta((CHO)_2 + CH_3COCH = CHCHO)$$

In the following sections, the subsequent atmospheric chemistry of the cresols, α-dicarbonyls, γ-unsaturated dicarbonyls and ketoacids is discussed.

Atmospheric Reactions of Cresols and Dimethylphenols

The cresols are known to react rapidly with OH [116,377,378] and NO_3 [11,368] radicals, these reactions being the major loss process of the cresols under atmospheric conditions. Reaction of the cresols with O_3 is much slower, but is nevertheless a minor contributor to cresol consumption at O_3 levels of $\lesssim$ 0.1 ppm [298].

$$O_3 + \text{cresols} \rightarrow \text{products} \qquad (94)$$

The products of these reactions are not known, but by analogy with the aromatic hydrocarbons [349], ring cleavage to α-dicarbonyls and ketoacids is likely. Rate constants have been determined at room temperature for all three cresol isomers, the most recent and (presumably) accurate values being [298]:

o-cresol,

$$k_{94} = (2.55 \pm 0.39) \times 10^{-19} \text{ cm}^3 \text{ molecule}^{-1} \text{ s}^{-1}$$

m-cresol,

$$k_{94} = (1.94 \pm 0.35) \times 10^{-19} \text{ cm}^3 \text{ molecule}^{-1} \text{ s}^{-1}$$

p-cresol,

$$k_{94} = (4.71 \pm 0.66) \times 10^{-19} \text{ cm}^3 \text{ molecule}^{-1} \text{ s}^{-1},$$

all at 296 ± 2 K.

We recommend these values, with error limits of ± 50% instead of those indicated.

As noted above, under atmospheric conditions with $O_3 \lesssim 0.1$ ppm these reactions contribute < 5-10% of the cresol loss rates at 298 K, and with the current state of knowledge can probably be neglected as a first approximation.

No rate constants are available for the reaction of O_3 with the dimethyl phenols formed in the m-xylene system. We recommend,

in the absence of further information, using the above rate constants.

$$NO_3 + \text{cresols} \rightarrow \text{products} \qquad (95)$$

It has been observed by O'Brien [379] and by Carter et al. [368] that the cresols are "stable" in the presence of O_3 or NO_x, but disappear rapidly in $O_3 + NO_2$ mixtures, suggesting a rapid reaction with NO_3 radicals. In the modeling study of Atkinson et al. [11] a rapid reaction of NO_3 radicals with the cresols was found to be necessary in order to fit the observed cresol time-concentration profiles, with a rate constant at 298 K in the range

$$(5\text{-}20) \times 10^{-12} \text{ cm}^3 \text{ molecule}^{-1} \text{ s}^{-1}$$

at 303 K. More recently, Carter et al. [368], using a relative rate technique, have derived rate constants for the reaction of NO_3 radicals with the three cresol isomers, the rate constants being approximately

$$k_{95} = 1 \times 10^{-11} \text{ cm}^3 \text{ molecule}^{-1} \text{ s}^{-1}$$

for all three isomers. Uncertainty limits are likely to be at least a factor of 2. In view of the high values of the rate constants at approximately 300 K, any temperature dependence should be zero or near zero, and we recommend:

$$k_{95} = 1 \times 10^{-11} \text{ cm}^3 \text{ molecule}^{-1} \text{ s}^{-1}$$

independent of temperature, with an uncertainty at 298 K of a factor of $\sim$3. While products of these reactions have not been determined, the variation of the NO_3 radical rate constants with substituent groups on the aromatic ring (very slow for toluene [279,368] and methoxybenzene [368], and increasing from phenol to the cresols [368]) indicates that H atom abstraction from the weak phenolic O-H group (bond strength $\sim$87 kcal mol^{-1} in phenol [367]) is the operative reaction pathway:

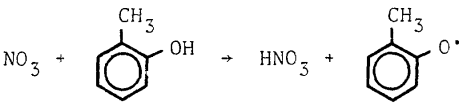

This is in agreement with the computer modeling study of Atkinson et al. [11] and with the essential lack of a dependence of the NO_3 radical rate constants on the position of alkyl substituents in the cresol (if addition to the ring was the reaction pathway, then the m- isomer would, analogous to $O(^3P)$ atom [350,351,354] and OH radical [116] reactions, be expected to react faster than the o- and p- isomers, contrary to the observation of Carter et al. [368]).

No information is available for the reaction of NO_3 radicals with the dimethylphenols, but on the basis of the data of Carter et al. [368] for the cresols we suggest a rate constant, independent of temperature, of

$$1.5 \times 10^{-11} \text{ cm}^3 \text{ molecule}^{-1} \text{ s}^{-1},$$

uncertain by a factor of at least 5.

$$OH + \text{cresols} \rightarrow \text{products} \qquad (96)$$

Rate constants have been obtained for o-cresol by a flash photolysis-resonance fluorescence technique over a range of temperature [377] and for the three cresol isomers by a relative rate technique [378]. The rate constants obtained are given in table 32. The rate constant obtained by Perry et al. [377] may have been somewhat low due to wall losses of the o- cresol, especially in the UV absorption calibration cell, while the rate constants of Atkinson et al. [378] may have been high due to a small contribution to the cresol disappearance rate at the longer irradiation times due to NO_3 radical reaction, which was not known at that time.

In view of these points, we recommend:

$$k_{96}(OH + \text{o-cresol}) = 4.1 \times 10^{-11} \text{ cm}^3 \text{ molecule}^{-1} \text{ s}^{-1}$$

at 298 K with an uncertainty of $\pm$ 30%.

$$k_{96}(OH + \text{m-cresol}) = 5.9 \times 10^{-11} \text{ cm}^3 \text{ molecule}^{-1} \text{ s}^{-1}$$

at 298 K with an uncertainty of $\pm$ 40%.

$$k_{96}(OH + \text{p-cresol}) = 4.5 \times 10^{-11} \text{ cm}^3 \text{ molecule}^{-1} \text{ s}^{-1}$$

at 298 K with an uncertainty of $\pm$ 40%.

Perry et al. [377], from their temperature dependent kinetic study, derived the amount of H-atom abstraction occurring in the reaction of OH radicals with o-cresol to be 8% (with an uncertainty of a factor of $\sim$2) at 298 K. The H-atom abstraction rate constant was given by

$$k_{96}(\text{abstraction}) = 5 \times 10^{-11} e^{-900/T} \text{ cm}^3 \text{ molecule}^{-1} \text{ s}^{-1}$$

Upon reevaluation to be consistent with the above recommendation, this becomes:

$$k_{96}(\text{abstraction}) = 6.8 \times 10^{-11} e^{-900/T} \text{ cm}^3 \text{ molecule}^{-1} \text{ s}^{-1}$$

Table 31. Carbonyls Anticipated From the Ring Cleavage Pathway From the Bicyclic Radicals (C)

Toluene	$(CHO)_2$	CH_3COCHO	CHOCH=CHCHO	$CH_3COCH=CHCHO$	$CHOCH=C(CH_3)CHO$	$CH_3COCH=C(CH_3)CHO$
C1		√	√			
C2[a]		√	√			
C2[b]	√			√		
C4	√			√		
m-xylene						
Cm1		√		√		
Cm2		√		√		
Cm3		√			√	
Cm4	√					√
Cm5[a]		√			√	
Cm5[b]	√					√

a≡ 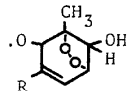

b≡ 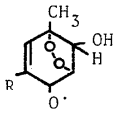

Where R = H (toluene) or CH_3 (m-xylene), as the final alkoxy radicals (Ė).

Table 32. Rate Constants for the Reaction of OH Radicals With the Cresols at Room Temperature

Cresol Isomer	$10^{11} \times k_{96}$ cm^3 $molecule^{-1}$ s^{-1}	T K	Reference
o-cresol	3.4 ± 0.7	299	[377]
	4.5 ± 0.4[a]	300 ± 1	[378]
m-cresol	6.5 ± 0.7[b]	300 ± 1	[378]
p-cresol	5.0 ± 0.5[b]	300 ± 1	[378]

[a] Relative to [k (OH + n-butane) - k(OH + neopentane)] = 1.81×10^{-12} cm^3 $molecule^{-1}$ s^{-1} at 300 K [262], consistent with our recommendation for k(OH + n-butane).

[b] Rate constants of m- and p-cresol, relative to that for o-cresol, of 1.42 ± 0.08 and 1.10 ± 0.05 were obtained.

$= 3.3 \times 10^{-12}$ cm^3 molecule^{-1} s^{-1}

at 298 K with an uncertainty of a factor of 2.

In the absence of further information, this is also suggested for the m- and p-cresol isomers. Since at ∿400 K the H-atom abstraction rate constant for o-cresol is [356,377] approximately a factor of 4 higher than that for toluene, and is ∿50% higher than those for the trimethylbenzenes, this indicates (analogous to the NO_3 radical reaction, see above) that the H-atom abstraction occurs primarily from the -OH substituent group:

followed by reaction of these methyl phenoxy radicals with NO_2 to form hydroxynitrotoluenes:

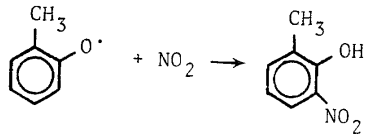

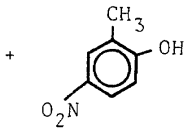

as discussed above for the phenoxy radical. The OH radical reaction rate constant with o-cresol was observed [377] to exhibit a small temperature dependence in the range of ∿298-320 K, but within the error limits may be assumed to be temperature independent. The OH radical addition rate constants then become for o-cresol,

$$k_{96}^{add}(\text{o-cresol}) = 3.8 \times 10^{-11} \text{ cm}^3 \text{ molecule}^{-1} \text{ s}^{-1}$$

and, by inference:

$$k_{96}^{add}(\text{m-cresol}) = 5.6 \times 10^{-11} \text{ cm}^3 \text{ molecule}^{-1} \text{ s}^{-1}$$

$$k_{96}^{add}(\text{p-cresol}) = 4.2 \times 10^{-11} \text{ cm}^3 \text{ molecule}^{-1} \text{ s}^{-1}$$

all approximately independent of temperature over the range ∿270-320 K.

Rate constants are not available for the dimethylphenols, but they may be estimated to be:

for 2,6-dimethylphenol:

$$k_{96} \simeq (7 \pm 3) \times 10^{-11} \text{ cm}^3 \text{ molecule}^{-1} \text{ s}^{-1}$$

for 2,4-dimethylphenol:

$$k_{96} \simeq (8 \pm 3) \times 10^{-11} \text{ cm}^3 \text{ molecule}^{-1} \text{ s}^{-1}$$

again independent of temperature over the range ∿270-320 K.

Since the H-atom abstraction pathway should have a very similar rate constant to that for o-cresol, then these OH + dimethylphenol reactions will proceed almost entirely via OH radical addition to the ring.

Thermochemical calculations show that for OH radical addition to o- and p-cresol, the isomers:

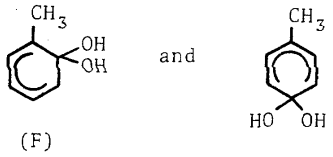

(F)

are the most favorable by ∿5.7 kcal mol^{-1}. For the case of m-cresol, formation of:

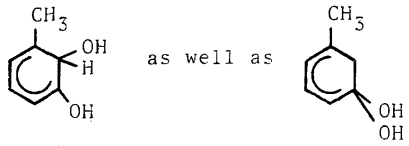

would appear to be also favorable, since both the CH_3 and OH substituent groups are o- , p- directing.

Presumably a similar situation exists for the addition reaction of OH radicals with the dimethylphenols.

In the following discussion, attention will be focused on o-cresol, which is the most studied of the three cresol isomers [11]. The reaction sequence for the other cresols and the dimethylphenols should be assumed,

in the absence of further information, to be totally analogous.

The radical (F) can react with NO_2 to yield hydroxynitrotoluenes:

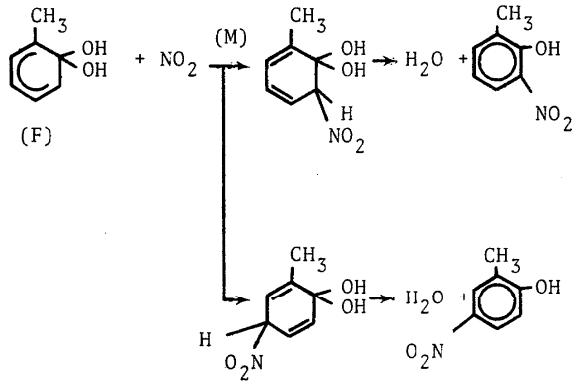

and these reactions, with the initial OH radical addition at the site of the substituent OH group, account, at least in part, for the hydroxynitrotoluene isomers observed in the NO_x-air photooxidations of o- , m- , and p-cresol [11]. It should be noted that the observed hydroxynitrotoluene isomers can also be formed from the reaction of NO_2 with the methylphenoxy radicals formed by H-atom abstraction from the cresol OH group by OH radicals or NO_3 radicals, as noted above, and so at this time the reaction pathways leading to hydroxynitrotoluene production cannot be unambiguously ascertained. However, the observed hydroxynitrotoluene yields are small ($\lesssim$3% of the o-cresol reacted in NO_x-cresol-air photooxidations [11]), and the dominant reaction of the radicals such as (F) is expected to be with O_2:

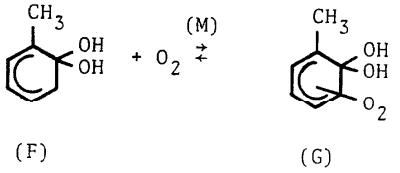

The subsequent reactions of radicals (G) are then assumed, again in the absence of any definitive information, to be analogous to those of radical (B) in the toluene system, i.e.,

for example:

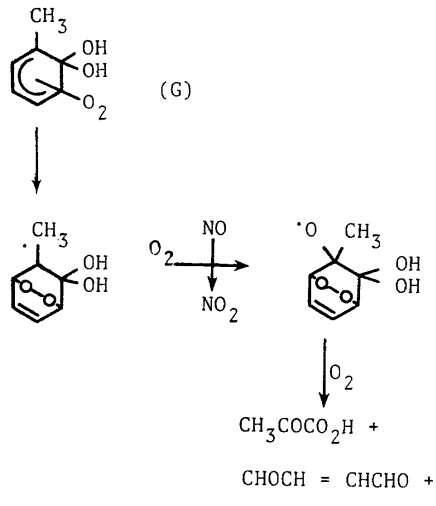

Hence, in general, $CHOCO_2H$ is formed instead of $(CHO)_2$, and CH_3COCO_2H instead of CH_3COCHO in the schemes in table 31. This reaction scheme for the cresols then explains their low reactivity in terms of NO to NO_2 conversion and O_3 forming potential [11], since CH_3COCO_2H can be considered, at least as a first approximation, to be of low reactivity, when compared with the high reactivity towards OH radicals and photolysis of CH_3COCHO (see below).

Subsequent Reactions of α-Dicarbonyls

For the toluene and m-xylene systems the α-dicarbonyls involved are glyoxal and methylglyoxal; biacetyl will be involved only in the o-xylene and 1,2,3- and 1,2,4-trimethylbenzene systems. These species can react under atmospheric conditions with OH radicals and can undergo photolysis:

$$OH + \alpha\text{-Dicarbonyls} \rightarrow \text{products} \qquad (97)$$

Biacetyl, as anticipated, reacts slowly with OH radicals. Darnall et al. [343] using a flash photolysis-resonance fluorescence technique obtained a rate constant of

$$(2.4\ ^{+0.8}_{-0.6}) \times 10^{-13}\ cm^3\ molecule^{-1}\ s^{-1}$$

at 298 ± 2 K, showing that under atmospheric conditions the reaction of OH radicals with biacetyl is negligible. Glyoxal and methylglyoxal, however, will react rapidly with OH radicals:

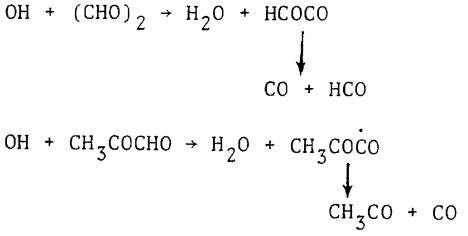

Rate constants for these reactions have been recently determined in two studies. Kleindienst et al. [380] obtained a rate constant for the reaction of OH radicals with methylglyoxal of

$$(7.1 \pm 1.6) \times 10^{-12} \text{ cm}^3 \text{ molecule}^{-1} \text{ s}^{-1}$$

at 297 K using a flash photolysis-resonance fluorescence technique. More recently, using a relative rate technique, Plum et al. [381] have obtained rate constants for both glyoxal and methylglyoxal (relative to that for cyclohexane) of

$$1.15 \times 10^{-11} \text{ cm}^3 \text{ molecule}^{-1} \text{ s}^{-1}$$

and

$$1.73 \times 10^{-11} \text{ cm}^3 \text{ molecule}^{-1} \text{ s}^{-1},$$

respectively, at 298 ± 2 K.

While there is a discrepancy of over a factor of 2 between these two studies for methylglyoxal, since the investigation of Plum et al. [381] also determined photolysis rates, and yielded the only OH radical rate constant data for glyoxal, we recommend the data from this study, i.e.,

Glyoxal:

$$k_{97} = 1.15 \times 10^{-11} \text{ cm}^3 \text{ molecule}^{-1} \text{ s}^{-1},$$

assumed to be independent of temperature, with an estimated uncertainty at 298 K of ± 40%.

Methylglyoxal:

$$k_{97} = 1.7 \times 10^{-11} \text{ cm}^3 \text{ molecule}^{-1} \text{ s}^{-1},$$

assumed to be independent of temperature, with an estimated uncertainty at 298 K of ± 40%. It may be noted that these rate constants are very similar to those for HCHO and CH_3CHO, respectively.

$$NO_3 + \alpha\text{-Dicarbonyls} \rightarrow \text{products} \qquad (98)$$

These reactions are presumed, by analogy with the other aldehydes, to have rate constants of:

Glyoxal:

$$k_{98} \simeq 2 \times 10^{-15} \text{ cm}^3 \text{ molecule}^{-1} \text{ s}^{-1}$$

at 298 K with an uncertainty of a factor of ∿3-5.

Methylglyoxal:

$$k_{98} \simeq 2 \times 10^{-15} \text{ cm}^3 \text{ molecule}^{-1} \text{ s}^{-1}$$

at 298 K with an estimated uncertainty of a factor of ∿3-5. These reactions should hence be negligible under atmospheric conditions.

$$\alpha\text{-Dicarbonyl} + h\nu \rightarrow \text{products} \qquad (99)$$

These α-dicarbonyls absorb radiation up to ∿470 nm [381] where the light intensity in outdoor and indoor smog chambers, and in the ambient atmospheres, is usually much more intense than at wavelengths of ∿300 nm.

However, quantum yields and photodissociation pathways for their photodissociation as a function of wavelength under atmospheric conditions are not known at the present time.

The most relevant information regarding photolysis of these α-dicarbonyls under simulated atmospheric conditions comes from the work of Darnall et al. [343] and Plum et al. [381]. While these photolysis rates are only applicable to the spectral distribution used, this spectral distribution was approximately that of sunlight in the lower troposphere [381]. Thus the ratio of these photolysis rates to that for NO_2 (k_1) measured in the same experimental system can be used in the absence of detailed quantum yield data for the particular environmental chamber or for the ambient atmosphere. For biacetyl, Darnall et al. [343] obtained $k_{99}/k_1 \simeq 0.032$-0.040, while Plum et al. [381] determined this photolysis rate ratio to be 0.036 ± 0.004, in excellent agreement. For glyoxal and methylglyoxal, Plum et al. [381] obtained ratios of k_{99}/k_1 of 0.008 ± 0.005 and 0.019 ± 0.005, respectively. We recommend, in the absence of experimental data for the particular application, the use of these rate constant ratios determined by Plum et al. [381], i.e.,

Glyoxal:

$$k_{99} = (0.008 \pm 0.005)k_1$$

Methylglyoxal:

$$k_{99} = (0.019 \pm 0.005)k_1$$

Biacetyl:

$$k_{99} = (0.036 \pm 0.004)k_1$$

Plum et al. [381] further showed that for the spectral distribution used the observed photodissociation must occur essentially totally from the 340-470 nm absorption band and that the average quantum yields are significantly less than unity, being 0.029 ± 0.018 for glyoxal, 0.107 ± 0.030 for methylglyoxal and 0.158 ± 0.024 for biacetyl for $\lambda \gtrsim 325$ nm. For the 280-350 nm region, Cox

et al. [345] derived an average photodissociation quantum yield of 0.98 ± 0.15.

The photolysis products are not known quantitatively. Glyoxal photolysis apparently does not lead to radical formation [230], leading instead to HCHO + CO or H_2 + 2 CO [382]:

$$(CHO)_2 + h\nu \rightarrow HCHO + CO \qquad a$$

$$\rightarrow H_2 + 2\ CO \qquad b$$

Plum et al. [381] observed formaldehyde formation corresponding to 13% of the glyoxal photolysis by pathway (a); presumably pathway (b) accounts for the remainder of glyoxal photodissociation.

The observation of PAN formation from photolysis of methylgloxal and biacetyl-NO_x-air mixtures shows that the processes:

$$CH_3COCHO + h\nu \rightarrow CH_3CO + HCO$$

$$CH_3COCOCH_3 + h\nu \rightarrow 2\ CH_3CO$$

occur, with CH_3CO and HCO radicals reacting rapidly with O_2 to yield CH_3CO_3 radicals and HO_2 + CO, respectively. This is in agreement with the observation of the absorption spectrum of the CH_3CO_3 radical by Cox and coworkers [148,345] from the photolysis of biacetyl-O_2 mixtures.

Obviously, further work is needed to determine the photodissociation pathways and their quantum yields as a function of wavelength for these α-dicarbonyls.

Subsequent Reactions of Keto Acids (100,101)

The keto acids $CHOCO_2H$ and CH_3COCO_2H are expected to be formed in the NO_x photooxidation of toluene and m-xylene, from the initially formed cresols and dimethylphenols [11]. The atmospheric chemistry of these compounds is, to say the least, incompletely understood at the present time.

Photolysis (reaction 100) of CH_3COCO_2H is reported [230] to be efficient in the gas phase with a photodissociation quantum yield to CH_3CHO of approximately unity at 353 K [230]. This formation of CH_3CHO could well explain the acetaldehyde yields observed in NO_x-aromatic irradiations [5,373]. Photodissociation quantum yields and absorption cross-section data for these carbonyl acids are obviously needed.

By analogy with CH_3CHO and CH_3COCHO CH_3COCO_2H should react only very slowly at 298 K with OH radicals, with

$$k_{101} \sim 1.5 \times 10^{-13}\ cm^3\ molecule^{-1}\ s^{-1}$$

while $CHOCO_2H$ is expected to react rapidly with OH radicals:

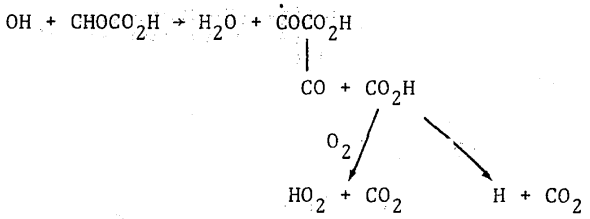

with an estimated rate constant of:

$$k_{101} \sim 1.5 \times 10^{-11}\ cm^3\ molecule^{-1}\ s^{-1}$$

independent of temperature, with estimated uncertainties of a factor of approximately 2.

Subsequent Reactions of γ-Unsaturated Dicarbonyls

The possible γ-unsaturated dicarbonyls formed in the toluene and m-xylene systems are:

$$CHOCH = CHCHO$$

$$CH_3COCH = CHCHO$$

$$CHOCH = \underset{\displaystyle CH_3}{\overset{\displaystyle |}{CCHO}}$$

$$\text{and } CH_3COCH = \overset{CH_3}{\overset{|}{C}}CHO$$

and reaction with NO_3 and OH radicals and O_3, and photolysis must be considered.

Photolysis (102)

By analogy with acrolein (CH_2 = CHCHO) and crotonaldehyde (CH_3CH = CHCHO), which are apparently photochemically stable under atmospheric conditions [230], photolysis of the above γ-unsaturated dicarbonyls is expected to be slow. However, data are urgently needed to confirm this expectation.

NO_3 Reactions (103)

NO_3 radicals are expected to react analogously to their reaction with aldehydes, i.e., by H-atom abstraction from the -CHO group with an estimated rate constant of

$$k_{103} \sim 1.4 \times 10^{-15}\ cm^3\ molecule^{-1}\ s^{-1}$$

(uncertain to a factor of ≥5) per CHO group at 298 K (i.e., an overall rate constant of

$$k_{103} \sim 3 \times 10^{-11}\ cm^3\ molecule^{-1}\ s^{-1}$$

at 298 K for the reaction of NO_3 radicals with CHOCH = CHCHO). The subsequent reactions of the products are discussed below in the OH radical section.

O_3 Reactions (104)

No data are available for the reaction of O_3 with such γ-unsaturated dicarbonyls.

However, by analogy with the literature rate constants for the reactions of $O(^3P)$ atoms, OH radicals and O_3 with acrolein, crotonaldehyde and other selected carbonyls and alkenes (table 33), it can be seen that

a) replacement of -H by -CHO decreases the O_3 rate constant (acrolein versus ethene and crotonaldehyde or meth-acrolein versus propene)

b) the effect of the CH_3CO- group is intermediate between the H- and CH_3- substituents (see OH radical and O_3 rate constants for $CH_2=CH_2$, $CH_3CH=CH_2$, and $CH_3COCH=CH_2$).

Thus, the data indicate that

$$k_{104}(O_3 + CHOCH{=}CHCHO) < k_{104}(O_3 + \text{acrolein}) < k(O_3 + \text{ethene})$$

and

$$k_{104}(O_3 + CH_3COCH{=}CHCHO) < k_{104}(O_3 + \text{crotonaldehyde}).$$

The rate constants for the reactions of O_3 with the various γ-unsaturated dicarbonyls are estimated, on the basis of the data shown in table 33, to be:

	k_{104} cm^3 molecule^{-1} s^{-1}
CHOCH = CHCHO	$< 3 \times 10^{-19}$
CH_3COCH = CHCHO	$\sim 5 \times 10^{-19}$
CHOCH = C(CHO)(CH_3)	$\lesssim 3 \times 10^{-19}$
CH_3COCH = C(CHO)(CH_3)	$\sim 4 \times 10^{-18}$

Since the OH radical rate constants, (see below) are estimated to be

$$k_{105} \gtrsim 1.5 \times 10^{-11} \text{ cm}^3 \text{ molecule}^{-1} \text{ s}^{-1},$$

we recommend that, possibly apart from $CH_3COCH = C(CH_3)CHO$, their reaction with O_3 be considered to be negligible under most atmospheric conditions; obviously experimental work is necessary to substantiate this recommendation.

OH Radical Reactions (105)

OH radicals can react with these γ-unsaturated dicarbonyls via H-atom abstraction from the -CHO group or via OH radical addition to the double bond:

$$OH + CHOCH{=}CHCHO \rightarrow H_2O + CHOCH{=}\dot{C}HCO$$

$$\rightarrow CHOCH(OH)\text{-}CHCHO$$

The OH radical addition rate constants may be estimated by a method analogous to that used for the estimation of the O_3 reaction rate constants (see above); the rate constants for OH radical addition so estimated at 298 K are (see also [385]):

	$10^{12} \times k_{105}$ cm^3 molecule^{-1} s^{-1}
CHOCH = CHCHO	< 5
CH_3COCH = CHCHO	$\lesssim 5$
CHOCH = C(CH_3)CHO	$\lesssim 5$
CH_3COCH = C(CH_3)CHO	∼20

For the H atom abstraction pathway, the rate constants are estimated, by analogy with other aldehydes [116,381], to be approximately

1.5×10^{-11} cm^3 molecule^{-1} s^{-1} per -CHO group.

The H-atom abstraction rate constants are expected to be essentially temperature independent while the OH radical addition rate constants will, by analogy with the alkenes [116], have a negative temperature dependence of $\sim e^{500/T}$.

Hence at 298 K, we estimate the following OH radical rate constants:

	$10^{11} \times k_{105}$ cm^3 molecule^{-1} s^{-1}	
	H-Atom Abstraction	OH Radical Addition
CHOCH = CHCHO	3.0	<0.5
CH_3COCH = CHCHO	1.5	$\lesssim$0.5
CHOCH = $C(CH_3)$CHO	3.0	$\lesssim$0.5
CH_3COCH = $C(CH_3)$CHO	1.5	$\sim$2.0

For OH radical addition, by reaction schemes analogous to those for the alkenes (section 5), the reactions subsequent to the initial addition will be (R,R'=H or CH_3),

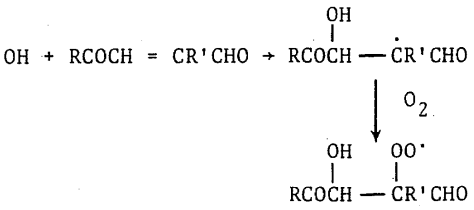

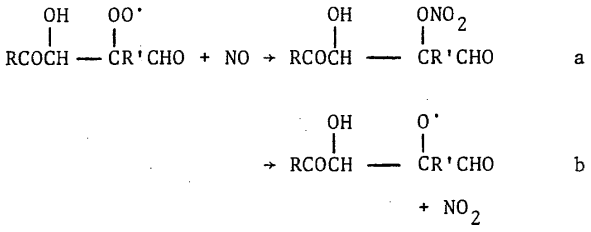

with $(k_a + k_b)$ approximately equal to

$$7 \times 10^{-12} \text{ cm}^3 \text{ molecule}^{-1} \text{ s}^{-1}$$

at 298 K, and, at atmospheric pressure and 298 K, $k_a/(k_a + k_b)$ possibly $\sim$0.08 (R, R'=H), $\sim$0.12 (R = CH_3, R' = H or R = H, R' = CH_3) or $\sim$0.2 (R, R' = CH_3).

By analogy to the β-hydroxy alkoxy radicals formed in the alkene systems, the above β-hydroxy alkoxy radicals are assumed to undergo rapid decomposition.

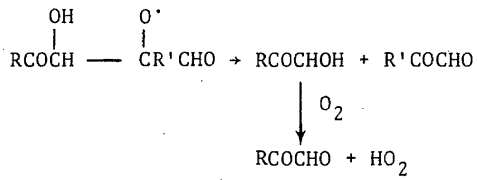

Hence the products are (exactly the same products are formed from OH radical addition to the other carbon atom):

γ-Dicarbonyl	Products
CHOCH = CHCHO	2 $(CHO)_2$ + HO_2
CH_3COCH = CHCHO	CH_3COCHO + $(CHO)_2$ + HO_2
CHOCH = $C(CH_3)$CHO	$(CHO)_2$ + CH_3COCHO + HO_2
CH_3COCH = $C(CH_3)$CHO	2 CH_3COCHO + HO_2

The subsequent reactions of these α-di-carbonyls have been dealt with above.

For H-atom abstraction, the initially formed acyl radical will rapidly add O_2.

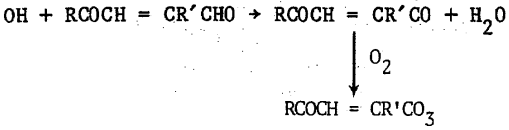

This acylperoxy radical can undergo three reactions; reaction with NO, reaction with NO_2, or cyclisation:

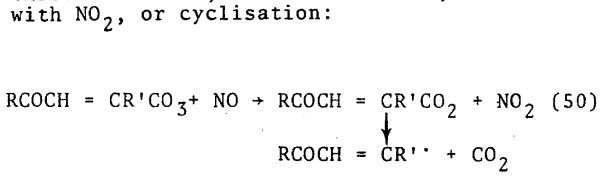

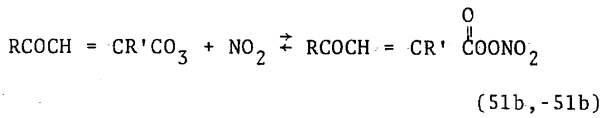

(51b,-51b)

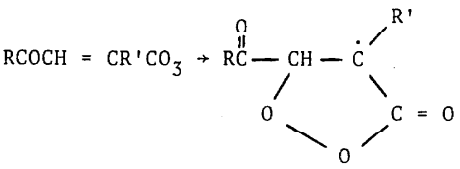

As with the case of peroxyacetyl nitrate (PAN), we assume that at 298 K:

$$k_{51b} \sim 4.7 \times 10^{-12} \text{ cm}^3 \text{ molecule}^{-1} \text{ s}^{-1},$$

$$k_{51b} \sim 4.7 \times 10^{-12} \text{ cm}^3 \text{ molecule}^{-1} \text{ s}^{-1}$$

$$k_{-51b} \sim 1.95 \times 10^{16} \, e^{-13543/T} \text{ s}^{-1}$$

$$= 3.6 \times 10^{-4} \text{ s}^{-1}$$

at 298 K, with an uncertainty of at least a factor of 2 at 298 K.

The rate of cyclisation of RCOCH = CR'CO_3 radicals is not at present known. The cyclisation reaction appears to be, based on thermochemical calculations, slightly exothermic. If the estimates of Demerjian et al. [267] are correct, then

$$k \simeq 3 \times 10^{11} e^{-5500/T}$$

$$\simeq 3 \times 10^{3} \text{ s}^{-1}$$

at 298 K, and cyclisation should dominate over reaction with NO or NO_2 (120-180 s^{-1} at 1 ppm of NO_2 or NO respectively). However, if the activation energy is higher by $\gtrsim$5 kcal mol^{-1}, then cyclisation will be unimportant. However, until further information becomes available for the RCOCH = CR'CO_3 radicals, both mechanistic routes should be considered.

The recent product study of Arnts and Gay [268] on the NO_x-photooxidation of isoprene has shown that, before significant amounts of O_3 are formed, methyl vinyl ketone and methacrolein are formed from the reaction of OH radicals with isoprene, and hence, for radicals of the type

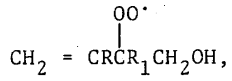

where R, R_1 = H and CH_3, or CH_3 and H,

reaction with NO dominates (see also [384] and references therein).

Cyclisation Dominates

The subsequent reactions of the

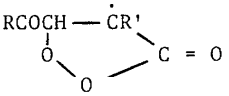

radicals are expected to be:

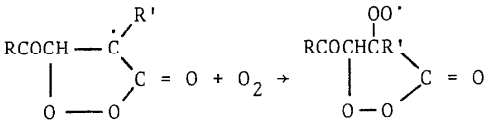

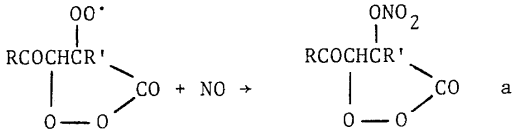

with

$$(k_a + k_b) \sim 7 \times 10^{-12} \text{ cm}^3 \text{ molecule}^{-1} \text{ s}^{-1}$$

at 298 K and $k_a/(k_a + k_b) \sim 0.1$ at atmospheric pressure and 298 K.

These cyclic alkoxy radicals are then expected to rapidly decompose (they must do so if R' = CH_3), although isomerisation could possibly compete for the cases where R = CH_3. At the present time we assume that the energetically highly favorable decompositions will be the exclusive pathway--obviously experimental data to confirm or disprove this postulate would be useful. The decompositions and subsequent reactions for the specific γ-unsaturated dicarbonyls are:

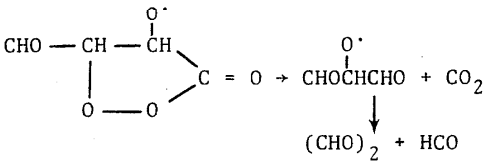

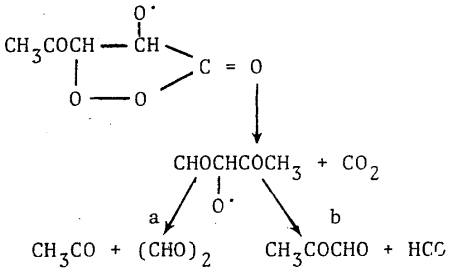

Since the decompositions

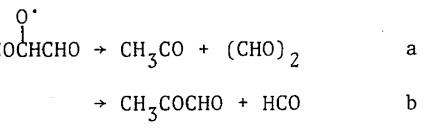

have almost identical calculated exothermicities the two pathways probably have similar rates, hence $k_a \sim k_b$.

3a) 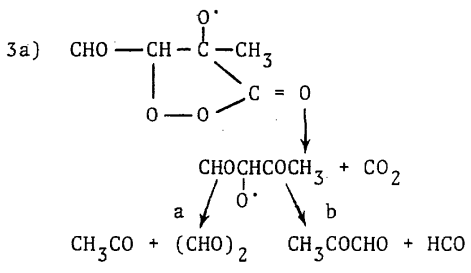

as above.

3b) 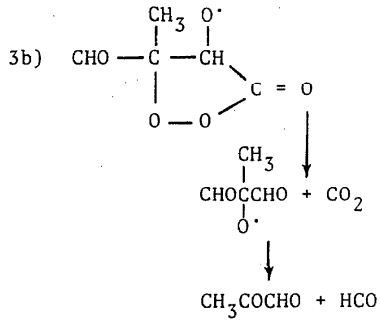

Radicals shown in (3a) and (3b) both can occur from:

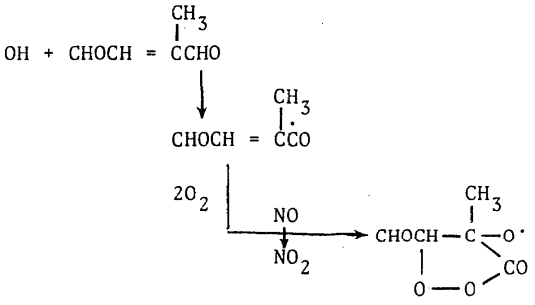

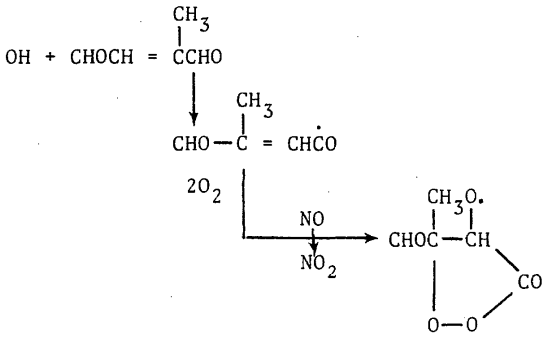

and these two OH radical reaction pathways are expected to have similar rate constants.

4) 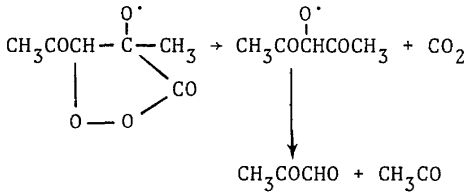

The products expected from the reaction of OH radicals with these dicarbonyls, proceeding via H-atom abstraction with cyclization, are shown in table 34.

Cyclisation Negligible

As noted above, the initial peroxyacyl radical can in this scheme react with NO or NO_2, the latter reaction forming an unsaturated peroxyacyl nitrate, RCOCH = CR'CO_3NO_2. This peroxyacyl nitrate, if formed (as appears likely [384]) is assumed to have an equivalent stability to that of PAN, and is responsible in NO_x-aromatic photooxidations as a sink (albeit temporary) of NO_x [11]. Reaction of the peroxyacyl radical with NO leads to:

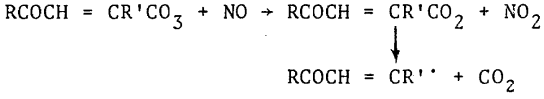

The RCOCH = CR'· radical should react with O_2 and then NO or NO_2:

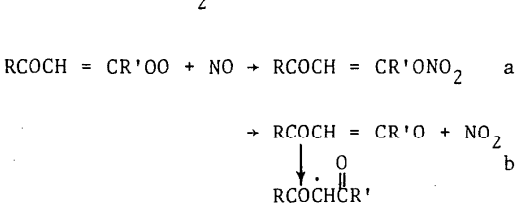

with

$$(k_a + k_b) \sim 7 \times 10^{-12} \text{ cm}^3 \text{ molecule}^{-1} \text{ s}^{-1}$$

at 298 K and, at atmospheric pressure,

$k_a/(k_a + k_b) \sim 0.04$ (R, R' - H);

~ 0.08 (R = H or CH_3, R' = CH_3 or H);

~ 0.12 (R, R' = CH_3),

based upon the data for the n-alkane series [170,172] (though this analogy may not hold).

Table 33. Rate Constants at Room Temperature for the Reactions of $O(^3P)$ Atoms OH Radicals and O_3 With Selected Carbonyls and Alkenes

Organic	$k(cm^3$ molecule^{-1} $s^{-1})^a$		
	$O(^3P)$	OH	O_3
HCHO	1.6×10^{-13}	1.0×10^{-11}	-
CH_3CHO	4.3×10^{-13}	1.6×10^{-11}	$<6 \times 10^{-21}$[d]
CH_2=CHCHO	4.4×10^{-13}[b]	1.8×10^{-11}[c]	2.8×10^{-19}[d]
CH_3CH=CHCHO	1.0×10^{-12}[b]	3.5×10^{-11}[c]	9.0×10^{-19}[d]
$CH_2 = C(CH_3)CHO$	-	2.9×10^{-11}[c]	1.1×10^{-18}[d]
$CH_3COCH=CH_2$		1.9×10^{-11}[c]	4.8×10^{-18}[d]
$CH_2=CH_2$	7.3×10^{-13}	8.1×10^{-12}	1.8×10^{-18}
$CH_3CH=CH_2$	4.0×10^{-12}	2.5×10^{-11}	1.1×10^{-17}

[a] Recommendations from this work, except as noted.
[b] [383], relative to k[$O(^3P)$ + propene].
[c] [384].
[d] [385].

Table 34. Products Formed From the H Atom Abstraction Route in the Reaction of OH Radicals With γ-Unsaturated Dicarbonyls, Assuming Ring Cyclisation (see text) Predominates

γ-Dicarbonyl	Estimated Product Yield			
	HCO	CH_3CO	CH_3COCHO	$(CHO)_2$
CHOCH = CHCHO	1.0			1.0
CH_3COCH = CHCHO	0.5	0.5	0.5	0.5
CHOCH = $C(CH_3)CHO$	0.75	0.25	0.75	0.25
CH_3COCH = $C(CH_3)CHO$		1.0	1.0	

$$RCOCH = CR'OO^{\bullet} + NO_2 \rightarrow RCOCH = CR'OONO_2 \quad (51)$$

$$k \sim 7 \times 10^{-12}\ cm^3\ molecule^{-1}\ s^{-1}$$

at 298 K.

This particular type of peroxynitrate decomposes very rapidly to the NO_3 and the alkoxy radical rather than back to reactants [178],

$$RCOCH = CR'OONO_2 \rightarrow RCOCH = CR'O^{\bullet} + NO_3$$

$$\downarrow$$

$$RCOCH\dot{C}R' \quad (O)$$

and hence the reaction effectively proceeds as a single step for modeling purposes:

$$RCOCH = CR'OO^{\bullet} + NO_2 \rightarrow ROCH\dot{C}R' + NO_3 \quad (O)$$

This latter radical is then expected to react in a manner typical of alkyl radicals with O_2 and then NO or NO_2.

The radicals formed at the stage for the various γ-dicarbonyls are then:

γ-Dicarbonyl	Radical
CHOCH = CHCHO	$\dot{C}HOCHCHO$
CH_3COCH = CHCHO	$CH_3\dot{C}OCHCHO$
CHOCH = $C(CH_3)CHO$	$\dot{C}HOCHCOCH_3$ [a] and $CH_3\dot{C}(CHO)_2$ [b]
$CH_3COCH = C(CH_3)CHO$	$CH_3\dot{C}OCHCOCH_3$

with (a) formed from the CHOCH = $\dot{C}CO$ radical, (b) from the $CH_3\underset{CHO}{\underset{|}{C}} = CH\dot{C}O$ radical.

The subsequent reactions are then:

$$RR'R''C + O_2 \rightarrow RR'R''CO_2\cdot$$

$$RR'R''CO_2 + NO \rightarrow RR'R''CONO_2 \quad a$$

$$\rightarrow RR'R''CO^{\bullet} + NO_2 \quad b$$

with

$$(k_a + k_b) \sim 7 \times 10^{-12}\ cm^3\ molecule^{-1}\ s^{-1}$$

at 298 K and

$$k_a/(k_a + k_b) \sim 0.04 \text{ to } \sim 0.12$$

at atmospheric pressure, depending on the number of carbon atoms (C_3 to C_5). At this stage the radicals are then:

γ-Dicarbonyl	Alkoxy Radical
CHOCH = CHCHO	$CHOCHCHO$ (O)
CH_3COCH = CHCHO	$CH_3COCHCHO$ (O)
CHOCH = $C(CH_3)CHO$	$CH_3COCHCHO$ (O) and $CH_3C(CHO)_2$ (O)
$CH_3COCH = C(CH_3)CHO$	$CH_3COCHCOCH_3$ (O)

These radicals are expected to undergo rapid decomposition:

$$CHOCHCHO\ (O) \rightarrow (CHO)_2 + HCO$$

$$CH_3COCHCHO\ (O) \xrightarrow{a} CH_3CO + (CHO)_2$$

$$\xrightarrow{b} CH_3COCHO + CHO$$

with $k_a \sim k_b$

$$CH_3C(CHO)_2\ (O) \rightarrow CH_3COCHO + HCO$$

and $$CH_3COCHCOCH_3\ (O) \rightarrow CH_3COCHO + CH_3CO$$

to yield α-dicarbonyls, which have been discussed above.

At the present time, the meager data [384 and references therein] indicate that a peroxyacyl nitrate, assumed to be

$$CH_2 = C(CH_3)C(=O)OONO_2,$$

is formed from the NO_x-air photooxidation of methacrolein. This, if confirmed, indicates that cyclisation of the RCH = $CHCO_3$ radical does not occur. Further work to identify such peroxynitrates and to study their thermal decompositions and other reactions operable under atmospheric conditions is obviously needed.

9. Combination Reactions of Peroxy Radicals

In this section, the available data for the combination reactions of peroxy radicals are discussed along with other miscellaneous reactions not covered in the earlier sections.

Obviously, the number of different peroxy radicals present in any (even in a single simple organic) NO_x photooxidation can be large. However, in the presence of NO_x (for NO levels $\geq$1 ppb, certainly) the reactions with NO will predominate over combination and under such conditions, peroxy radical combination reactions can be neglected [7].

In the following sections, the available rate constant data are given together with the product distributions.

$$CH_3O_2 + CH_3O_2 \rightarrow \text{products} \qquad (106)$$

Rate constants for this reaction have been obtained from numerous studies [155,158, 159,161,187,188,386-391] and the data obtained (absorption cross-sections and rate constants at room temperature) are given in table 35.

Since the rate constant is derived from measurements of k/σ and σ, and most studies were carried out at different wavelengths, comparison of the reported data is somewhat difficult. Absorption spectra and cross-sections have been reported from several studies (table 35). The data of Parkes [188, 387], Parkes et al. [187] and Adachi et al. [390] are in agreement, but disagree with those of Hochanadel et al. [386], Kan et al. [388] and Sander and Watson [391], being a factor of 1.5-2 higher in cross-section. Table 35 gives the absorption cross-sections and values of k/σ. The very recent absorption cross-section determined by Sander and Watson [391] at 250 nm is in excellent agreement with the values of Hochanadel et al. [386] and Kan et al. [388] at that wavelength, and we hence recommend the use of the absorption cross-section data of Hochanadel et al. [386]. Using these absorption cross-section data of Hochanadel et al. [386], reevaluated rate constants k_{106}^{obs} are also given in table 35. The agreement is reasonable, with the total spread being some 50% of the mean value of

$$3.4 \times 10^{-13} \text{ cm}^3 \text{ molecule}^{-1} \text{ s}^{-1}$$

at room temperature. Kan and Calvert [392] have shown that, different from the combination reaction of HO_2 radicals, H_2O vapor has no effect on the measured rate constant for combination of CH_3O_2 radicals at room temperature.

Both Parkes [387] and Anastasi et al. [155] reported that the rate constant for this reaction has little, if any, temperature dependence, although the small temperature ranges used (288-298 K and 300-325 K, respectively) did not rule out a positive or negative temperature dependence equivalent to an activation energy of a few kcal mol^{-1}. Very recently Sander and Watson [391] have determined rate constants for this reaction over the temperature range 248-417 K, and have obtained the Arrhenius expression

$$k_{106}^{obs} = 1.4 \times 10^{-13} e^{223/T} \text{ cm}^3 \text{ molecule}^{-1} \text{ s}^{-1}$$

$$= (3.0 \pm 0.5) \times 10^{-13} \text{ cm}^3 \text{ molecule}^{-1} \text{ s}^{-1}$$

at 298 K. NASA [3] have, based upon the data of references [155,161,386-389] and the absorption cross-section data of Hochanadel [386] recommended

$$k_{106}^{obs} = 3.4 \times 10^{-13} \text{ cm}^3 \text{ molecule}^{-1} \text{ s}^{-1}$$

at 298 K with an estimated uncertainty of a factor of 1.25 and, using the temperature dependence obtained by Sander and Watson [391], recommended:

$$k_{106}^{obs} = 1.6 \times 10^{-13} e^{(220\pm220)/T} \text{ cm}^3 \text{ molecule}^{-1} \text{ s}^{-1}.$$

However, this recommendation at 298 K, which is identical with that derived from the mean of the data in table 35, is based upon the measured rate constants. Secondary reactions of the products of this reaction will result in these measured values being upper limits to the true elementary rate constant k_{106}.

The reaction can proceed via the pathways [387,393-395]

$$CH_3O_2 + CH_3O_2 \rightarrow 2\ CH_3O + O_2 \qquad a$$

$$\rightarrow HCHO + CH_3OH + O_2 \qquad b$$

$$\rightarrow CH_3O_2CH_3 + O_2 \qquad c$$

$$\rightarrow \dot{C}H_2O\dot{O} + CH_3O_2H \qquad d$$

Quantitative data for these reaction pathways have been obtained by Parkes [188], using molecular modulation spectroscopy, and more recently by Kan et al. [393] and Niki et al.

Table 35. Literature Room Temperature Absorption Cross-Sections (σ) and Combination Rate Constants k_{106}^{obs} For Methylperoxy Radical Combination

$10^{18} \times \sigma$ cm^2 [a] at λ nm		$10^{-4} \times k_{106}^{obs}/\sigma$ cm molecule^{-1} s^{-1}	$10^{13} \times k_{106}^{obs}$ cm^3 molecule^{-1} s^{-1} [b]	$10^{13} \times k_{106}^{obs}$ cm^3 molecule^{-1} s^{-1} [c]	Technique[d]	Reference
4.4	240	10	4.4	3.1	MMS	[187, 188]
5.5 ± 1.0	238	10	5.5 ± 1.0	3.3 ± 0.6	MMS	[387]
3.3	235	11 ± 2	3.8 ± 0.7	3.8 ± 0.7	FP	[386]
	235-240	8 ± 2		2.6 ± 0.6	FP	[155]
2.0 ± 0.1	265	20.5	4.2 ± 0.5	3.7 ± 0.4	FP	[388]
3.1	239					
	253.7	15	3.7 ± 0.3	3.7 ± 0.3	FP	[389]
	245	11		3.2 ± 0.2	FP	[161]
	270	28		4.3 ± 0.5	FP	[161]
6.0	240	10.8 ± 0.8	5.8 ± 0.5[e]	3.2 ± 0.3	FP	[390]
3.9	250	13.3	5.2 ± 0.9	3.7 ± 0.7	MMS	[158, 159]
2.5 ± 0.4	250	12 ± 1	3.0 ± 0.5	3.3	FP	[391]

[a] To base e.
[b] As reported.
[c] Using the absorption cross-sections of Hochanadel et al. [386].
[d] MMS - molecular modulation spectroscopy; FP - flash photolysis-kinetic spectroscopy.
[e] Corrected for secondary reactions.

[394] using FT-IR absorption spectroscopy. The rate constant ratios obtained are:

Parkes [188]

$$k_a/k_{106} = 0.33 \pm 0.05$$

Kan et al. [393]

$$k_b/k_a = 1.32 \pm 0.16$$

$$k_c/k_b \leq 0.14$$

and $k_d << k_b$

Hence $k_a/k_{106} = 0.42 \pm 0.07$

$$k_b/k_{106} \simeq 0.53 \pm 0.10$$

$$k_c/k_{106} \leq 0.08$$

Niki et al. [394]

$$k_a/k_{106} = 0.32$$

$$k_b/k_{106} = 0.60$$

$$k_c/k_{106} \leq 0.08$$

with no evidence for channel (d)

These data are in good agreement and we recommend

$$k_a/k_{106} = 0.35$$

$$k_b/k_{106} = 0.57$$

and $k_c/k_{106} = 0.08$

with the ratios k_a/k_{106} and k_c/k_{106} being uncertain by ± 30%. Hence, secondary reactions of CH_3O radicals:

$$CH_3O + CH_3O_2 \rightarrow CH_3OOH + HCHO$$

$$CH_3O + O_2 \rightarrow HCHO + HO_2$$

$$CH_3O_2 + HO_2 \rightarrow \text{products}$$

lead to the observed rate constant being an upper limit to the "true" rate constant k_{106}. Kan et al. [388] have assessed the influence of secondary reactions in this system and estimate that the value of k_{106} is some 12% lower than the observed value of k_{106}^{obs}. We thus recommend

$$k_{106} = 3.1 \times 10^{-13} \text{ cm}^3 \text{ molecule}^{-1} \text{ s}^{-1}$$

at 298 K, with an uncertainty of a factor of 1.3, and:

$$k_{106} = 1.5 \times 10^{-13} e^{-220/T} \text{ cm}^3 \text{ molecule}^{-1} \text{ s}^{-1}$$

$$CH_3O_2 + HO_2 \rightarrow \text{products} \quad (107)$$

(presumably $CH_3OOH + O_2$)

Rate constants for this reaction have been obtained recently by Cox and Tyndall [158, 159] using molecular modulation spectroscopy over the temperature range 274-337 K, with

$$k_{107} = (6.0 \pm 0.9) \times 10^{-12} \text{ cm}^3 \text{ molecule}^{-1} \text{ s}^{-1}$$

at 298 K,

$$= (8.5 \pm 1.2) \times 10^{-12} \text{ cm}^3 \text{ molecule}^{-1} \text{ s}^{-1}$$

at 274 K,

$$= (3.5 \pm 0.5) \times 10^{-12} \text{ cm}^3 \text{ molecule}^{-1} \text{ s}^{-1}$$

at 338 K, assuming the CH_3O_2 absorption cross-section to be independent of temperature (as since confirmed by Sander and Watson [391]).

A strongly absorbing (210-280 nm range) product was observed and was attributed to CH_3OOH. The spectrum of this product is reasonably similar, at wavelengths $\lesssim$250 nm, to that reported by Molina and Arguello [396], supporting the postulate that the reaction proceeds via formation of $CH_3OOH + O_2$.

While, based upon these data, NASA [3] recommends:

$$k_{107} = 7.7 \times 10^{-14} e^{1300/T} \text{ cm}^3 \text{ molecule}^{-1} \text{ s}^{-1}$$

$$= 6 \times 10^{-12} \text{ cm}^3 \text{ molecule}^{-1} \text{ s}^{-1}$$

at 298 K with an estimated uncertainty of a factor of 3 at 298 K, Kan et al. [393] derive, from their data for the $CH_3O_2 + CH_3O_2$ system, a value of

$$k_{107} = 1.3 \times 10^{-12} \text{ cm}^3 \text{ molecule}^{-1} \text{ s}^{-1},$$

and Niki et al. [397] deduced a similar value of

$$(1.5 \pm 0.5) \times 10^{-12} \text{ cm}^3 \text{ molecule}^{-1} \text{ s}^{-1}$$

for the $C_2H_5O_2 + HO_2$ reaction. Obviously further work is necessary before a firm recommendation can be made.

$$C_2H_5O_2 + C_2H_5O_2 \rightarrow 2\ C_2H_5O + O_2 \quad a \quad (108)$$

$$\rightarrow C_2H_5OH + CH_3CHO + O_2 \quad b$$

$$\rightarrow C_2H_5OOC_2H_5 + O_2 \quad c$$

Adachi et al. [398] have, using a flash photolysis technique, determined the rate constant for the combination of ethylperoxy radicals to be:

$$k_{108}^{obs} = (1.10 \pm 0.09) \times 10^{-13}\ cm^3\ molecule^{-1}\ s^{-1}$$

at room temperature. Assuming a rate constant ratio of

$$k_{108a}/(k_{108a} + k_{108b} + k_{108c})$$

approximately equal to 0.3 to 0.5 Adachi and Basco [398] derived a rate constant, corrected for secondary reactions of the ethoxy radicals formed in reaction pathway (108a), of

$$k_{108} = (1.0 \pm 0.1) \times 10^{-13}\ cm^3\ molecule^{-1}\ s^{-1}$$

at room temperature.

More recently Niki et al. [397] have obtained the rate constant ratios

$$k_a/k_b = 1.3 \pm 0.16 \text{ and}$$

$$k_c/k_b \leq 0.22$$

which lead to

$$k_a/k_{107} = 0.52 - 0.56$$

$$k_b/k_{107} = 0.40 - 0.44$$

$$k_c/k_{107} \leq 0.09$$

Anastasi et al. [399] have determined that

$$k_{108}^{obs} = (9.48 \pm 1.30) \times 10^{-14}\ cm^3\ molecule^{-1}\ s^{-1}$$

at 303 K, increasing with temperature, and that

$$k_a/k_b = 1.75 \pm 0.05 \text{ at } 302 \text{ K},$$

$$2.12 \pm 0.10 \text{ at } 333 \text{ K and}$$

$$2.45 \pm 0.15 \text{ at } 373 \text{ K},$$

with channel (c) contributing $\lesssim$5% of the overall reaction. From these data Anastasi et al. [399] derived:

$$k_{108a} = 3.2 \times 10^{-13}\ e^{-683/T}\ cm^3\ molecule^{-1}\ s^{-1}$$

$$= 3.2 \times 10^{-14}\ cm^3\ molecule^{-1}\ s^{-1}$$

at 298 K,

$$k_{108b} = 5.8 \times 10^{-14}\ e^{-316/T}\ cm^3\ molecule^{-1}\ s^{-1}$$

$$= 2.0 \times 10^{-14}\ cm^3\ molecule^{-1}\ s^{-1}$$

at 298 K.

Since the experimental data of these three studies [397-399] are in reasonable agreement, we recommend the data of Anastasi et al. [399] (the most comprehensive study), which yield

$$k_{108} = 5.2 \times 10^{-14}\ cm^3\ molecule^{-1}\ s^{-1}$$

at 298 K.

$$CH_3CH_2CH_2CH_2O_2 + CH_3CH_2CH_2CH_2O_2 \rightarrow \text{products} \quad (109)$$

The sole reported data concerning this reaction are those of Adachi and Basco [400], who obtained a value of

$$k_{109}^{obs} = (3.8 \pm 0.3) \times 10^{-13}\ cm^3\ molecule^{-1}\ s^{-1}$$

at room temperature. No determination of the products formed were made, and this rate constant is an upper limit to the "true" rate constant for reaction (109).

$$(CH_3)_2CHO_2\cdot + (CH_3)_2CHO_2\cdot \rightarrow \quad (110)$$

$$(CH_3)_2CHOH + (CH_3)_2CO + O_2 \quad a$$

$$\rightarrow 2\ (CH_3)_2CHO\cdot + O_2 \quad b$$

This reaction has been investigated by Kirsch et al. [401,402], Cowley et al. [403] and Adachi and Basco [400]. The observed overall

rate constants for this combination reaction of isopropylperoxy radicals were determined by Kirsch et al. [401] over the temperature range 300-373 K, using molecular modulation spectroscopy. The observed rate constants were [401]

$$k_{110}^{obs} = 1.3 \times 10^{-15} \text{ cm}^3 \text{ molecule}^{-1} \text{ s}^{-1}$$

at 298 K

$$= 2.4 \times 10^{-12} e^{-2243/T} \text{ cm}^3 \text{ molecule}^{-1} \text{ s}^{-1}.$$

More recently, Adachi and Basco [400] have determined, using a flash photolysis technique, an observed rate constant of

$$k_{110}^{obs} = (2.0 \pm 0.6) \times 10^{-15} \text{ cm}^3 \text{ molecule}^{-1} \text{ s}^{-1}$$

at room temperature, in reasonable agreement with the data of Kirsch et al. [401].

These observed rate constants are again expected to be upper limits to the "true" rate constant because of the influence of secondary reactions of the isopropoxy radicals formed in reaction (b), and Kirsch et al. [402] and Cowley et al. [403] obtained, from a product analysis study, the rate constant ratios

$$k_{110b}/k_{110a} = 1.39 \pm 0.04 \text{ at } 302 \text{ K}$$

$$= 1.84 \pm 0.04 \text{ at } 333 \text{ K}$$

$$= 2.80 \pm 0.08 \text{ at } 373 \text{ K}$$

From these data and the observed rate constants of Kirsch et al. [401], the Arrhenius expressions for reaction pathways (110a) and (110b) were derived [403]

$$k_{110a} = 4.1 \times 10^{-14} e^{-1440/T} \text{ cm}^3 \text{ molecule}^{-1} \text{ s}^{-1}$$

$$= 3.3 \times 10^{-16} \text{ cm}^3 \text{ molecule}^{-1} \text{ s}^{-1}$$

at 298 K, with an estimated uncertainty of ± 25% at 298 K.

$$k_{110b} = 2.3 \times 10^{-12} e^{-2560/T} \text{ cm}^3 \text{ molecule}^{-1} \text{ s}^{-1}$$

$$= 4.3 \times 10^{-16} \text{ cm}^3 \text{ molecule}^{-1} \text{ s}^{-1}$$

at 298 K with an estimated uncertainty of ± 30% at 298 K. We recommend the use of these expressions of Cowley et al. [403].

$$(CH_3)_3CO_2\cdot + (CH_3)_3CO_2\cdot \rightarrow \quad (111)$$

$$2\ (CH_3)_3CO\cdot + O_2 \quad \text{a}$$

$$\rightarrow (CH_3)_3COO(CH_3)_3 + O_2 \quad \text{b}$$

$$\rightarrow \text{other products} \quad \text{c}$$

Rate constants for the combination of t-butylperoxy radicals have been obtained by Parkes [188] and Anastasi et al. [155] using molecular modulation and flash photolysis techniques.

These data of Parkes [188] and of Anastasi et al. [155] are in excellent agreement and, using an absorption cross-section for the t-butylperoxy radical of

$$4.0 \times 10^{-18} \text{ cm}^2 \text{ at } 240 \text{ nm [155]},$$

yield an observed rate constant at 298 K of

$$k_{111}^{obs} = (2.6 \pm 0.8) \times 10^{-17} \text{ cm}^3 \text{ molecule}^{-1} \text{ s}^{-1},$$

with an activation energy of ∿8.8 kcal mol^{-1} [155] over the narrow temperature range of 298-325 K. This temperature dependence is consistent with the Arrhenius expression obtained by Kirsch et al. [401] of

$$k_{111}^{obs} = 1.7 \times 10^{-10} e^{-4775/T} \text{ cm}^3 \text{ molecule}^{-1} \text{ s}^{-1}$$

Kirsch and Parkes [404] have shown that the initial reaction leads predominantly to t-butoxy radicals, pathway (a), with pathway (b) being ∿14% of the overall reaction at 298 K, decreasing rapidly with temperature.

$$CH_3O_2 + (CH_3)_3CO_2 \rightarrow \text{products} \quad (112)$$

Parkes [188], from a complex system, has derived a rate constant for the cross-combination reaction of methylperoxy radicals with t-butylperoxy radicals of

$$k_{112} \sim 1 \times 10^{-13} \text{ cm}^3 \text{ molecule}^{-1} \text{ s}^{-1}$$

at room temperature. However, in view of the inherent complexity of the system, we do not make any recommendation.

$$CH_3CO_3 + CH_3CO_3 \rightarrow \text{products} \quad (113)$$

This combination reaction has recently been studied by Addison et al. [148] using molecular modulation absorption spectroscopy.

By monitoring the acetylperoxy radical in absorption, a recombination rate constant of

$$k_{113} = 2.5 \times 10^{-12} \text{ cm}^3 \text{ molecule}^{-1} \text{ s}^{-1},$$

with an estimated uncertainty of a factor of 2, was obtained. CH_3O_2 radicals were also observed in absorption in this system, implying that the acetylperoxy radical combination proceeds, at least partly, via

$$CH_3CO_3 + CH_3CO_3 \rightarrow 2\ CH_3CO_2 + O_2$$

$$CH_3CO_2 \rightarrow CH_3 + CO_2 \text{ (fast)}$$

$$CH_3 + O_2 \rightarrow CH_3O_2$$

although a minor channel producing O_3 was reported:

$$CH_3CO_3 + CH_3CO_3 \rightarrow (CH_3CO)_2O + O_3$$

A rate constant for the reaction of CH_3O_2 radicals with CH_3CO_3 radicals of

$$3 \times 10^{-12} \text{ cm}^3 \text{ molecule}^{-1} \text{ s}^{-1}$$

was also deduced from this system [148]. In the absence of further detailed experimental data on this system, we make no recommendations.

In the absence of more experimental data, we recommend the rate constants and product ratios obtained for the $C_2H_5O_2$, $(CH_3)_2CHO_2$ and $(CH_3)_3CO_2$ radicals as being reasonably representative of other primary, secondary and tertiary alkylperoxy radicals, and similary with CH_3CO_3 radicals. Furthermore, we would recommend the use of a rate constant at 298 K of

$$3 \times 10^{-12} \text{ cm}^3 \text{ molecule}^{-1} \text{ s}^{-1},$$

uncertain by a factor of 3, for the reaction of HO_2 radicals with all peroxy radicals (this being the major cross-combination reaction occurring).

Miscellaneous Reactions

$$CH_3O_2 + O_3 \rightarrow \text{products} \qquad (114)$$

Two investigations of this reaction have been carried out by Simonaitis and Heicklen [405] and by Sander and DeMore [406]. Both these investigations showed this reaction to be slow at room temperature, with upper limits of

$$k_{114} < 2.4 \times 10^{-17} \text{ cm}^3 \text{ molecule}^{-1} \text{ s}^{-1}$$

[405] and

$$< 5 \times 10^{-17} \text{ cm}^3 \text{ molecule}^{-1} \text{ s}^{-1}$$

[406]. This is not unexpected, since the "supposedly" analogous reaction

$$HO_2 + O_3 \rightarrow OH + 2O_2$$

presumably involves the breakage of the weak ($\sim$50 kcal mol^{-1} [366]) H-OO bond, while any similar reaction of CH_3O_2 (or RO_2 in general) with O_3 would involve breakage of a very much stronger C-H bond. Hence, the reaction of O_3 with CH_3O_2, and presumably other RO_2 species, can be totally neglected for lower tropospheric modeling purposes.

OH Radical Reactions

For any OH radical reactions not covered in this report, i.e., with alcohols or hydroperoxides, the OH radical review article of Atkinson et al. [116] should be consulted.

10. Homogeneous Gas Phase SO_2 Reactions Under Atmospheric Conditions

The gas phase homogeneous reactions of SO_2 under atmospheric conditions have been extensively reviewed by Calvert et al. [314], and in this section their review article will be used as a basis for our recommendations, although in certain reactions, more recent experimental data causes modifications to the conclusions of Calvert et al. [314]. As discussed by Calvert et al. [314], the reaction pathways which are potential sinks for SO_2 under atmospheric conditions are the reactions of SO_2 with OH, HO_2, and RO_2 radicals and the intermediate in O_3-alkene reactions. In fossil fuel fired power plant plumes, SO_2 oxidation can also possibly be influenced, for a short time period after the time of emission, by the kinetically third order reaction of SO_2 with $O(^3P)$ atoms (this is in addition to possible heterogeneous reactions catalyzed by particulates and by metal ions). In the following discussion, the rate constants and mechanisms of these reactions will be evaluated.

$$O(^3P) + SO_2 + M(M = \text{air}) \rightarrow SO_3 + M \qquad (115)$$

This reaction is of minimal importance as an oxidative reaction of SO_2 under ambient atmospheric conditions, although it may be of importance in power plant plume chemistry [314]. The most recent study of Atkinson and Pitts [407], using a flash photolysis technique, obtained rate constants for this reaction for M = Ar, N_2, SO_2 at 299 K and for M = Ar over the temperature range 299-440 K.

The data obtained by Atkinson and Pitts [407] were reasonably consistent with previous studies, and based on that work, we recommend for M = air, with O_2 having the same third body efficiency as N_2 [408]:

$$k_{113} = 4.0 \times 10^{-32} e^{-1009/T} \text{ cm}^6 \text{ molecule}^{-2} \text{ s}^{-1}$$

$$= 1.35 \times 10^{-33} \text{ cm}^6 \text{ molecule}^{-2} \text{ s}^{-1}$$

at 298 K, with an estimated uncertainty of ± 30%.

The temperature dependence recommended is good only for relatively small temperature variations around 300-440 K, since the Arrhenius activation energy for this reaction is a strong function of temperature [409].

The SO_3 formed in this reaction reacts rapidly with H_2O to form either an initial hydrate or H_2SO_4:

$$SO_3 + H_2O \overset{(M)}{\rightleftharpoons} SO_3.H_2O \quad \text{a} \qquad (116)$$

$$\rightarrow H_2SO_4 \quad \text{b}$$

with

$$k_{116} = (9.1 \pm 2.0) \times 10^{-13} \text{ cm}^3 \text{ molecule}^{-1} \text{ s}^{-1}$$

at room temperature [410]. Under atmospheric conditions, where H_2O concentrations are typically $\gtrsim 10^{17}$ molecule cm^{-3}, this reaction can be considered to be essentially instanteous. Even if the initial product is a hydrated SO_3 molecule, this will presumably ultimately end up as H_2SO_4 in various stages of hydration. Hence the initial formation of SO_3 appears to be the rate determining step in this particular reaction sequence.

$$OH + SO_2 + M(M = \text{air}) \rightarrow HSO_3 + M \qquad (117)$$

This reaction is in the fall-off region between second and third order kinetics at the pressures encountered in the atmosphere [411]. From a review and evaluation of the literature data, Calvert et al. [314] recommended a bimolecular rate constant at 1 atmosphere of air and 298 K of:

$$k_{117} = (1.1 \pm 0.3) \times 10^{-12} \text{ cm}^3 \text{ molecule}^{-1} \text{ s}^{-1}$$

while Davis et al. [412] have estimated, from a long extrapolation of absolute rate constant data, that at 1 atmosphere of N_2 and at 298 K,

$$k_{117} \sim 9 \times 10^{-13} \text{ cm}^3 \text{ molecule}^{-1} \text{ s}^{-1}$$

with an estimated uncertainty of a factor of -1.5, +2.5. (This data of Davis et al. [412] was included in the review and evaluation of Calvert et al. [314].) The most recent kinetic studies of this reaction have been carried out by Harris et al. [413] and Wine and Ravishankara [414], using flash photolysis-resonance fluorescence techniques. Rate constants were obtained by Harris et al. [413] for M = Ar and SF_6 over the temperature range 298-424 K at total pressures of 98-653 torr. At approximately 650 torr total pressure the Arrhenius expressions:

$$k_{117}(M = Ar) = 1.16 \times 10^{-14} e^{(1193 \pm 150)/T} \text{ cm}^3 \text{ molecule}^{-1} \text{ s}^{-1}$$

and

$$k_{117}(M = SF_6) = 1.27 \times 10^{-13} e^{(752 \pm 150)/T} \text{ cm}^3 \text{ molecule}^{-1} \text{ s}^{-1}$$

were obtained [413], with bimolecular rate constants at 298 K and approximately 650 torr of:

$$k_{117}(M = Ar) = (6.5 \pm 0.8) \times 10^{-13} \text{ cm}^3 \text{ molecule}^{-1} \text{ s}^{-1}$$

(in excellent agreement with previous data of Atkinson et al. [411]); and

$$k_{117}(M = SF_6) = (1.6 \pm 0.2) \times 10^{-12} \text{ cm}^3 \text{ molecule}^{-1} \text{ s}^{-1}$$

By assuming that air has a third body efficiency intermediate between those for Ar and SF_6, a rate constant of:

$$k_{117}(M = \text{air}) = 4 \times 10^{-14} e^{956/T} \text{ cm}^3 \text{ molecule}^{-1} \text{ s}^{-1}$$

at approximately atmospheric pressure was estimated [413], with

$$k_{117}(M = \text{air}) = 1.0 \times 10^{-12} \text{ cm}^3 \text{ molecule}^{-1} \text{ s}^{-1}$$

at 298 K and approximately 650 torr [413].

The data of Wine and Ravishankara [414] for M = SF_6 are ∿20% lower than these reported by Harris et al. [413], and thus suggest a value of

$$\sim 8 \times 10^{-13} \text{ cm}^3 \text{ molecule}^{-1} \text{ s}^{-1}$$

at atmospheric pressure for M = air.

In view of the surprisingly good agreement between these various estimates, we recommend that at atmospheric pressure

$$k_{117}(M = \text{air}) = 9 \times 10^{-13} \text{ cm}^3 \text{ molecule}^{-1} \text{ s}^{-1}$$

at 298 K with an uncertainty of a factor of 1.5, and

$$k_{117}(M = \text{air}) = 9 \times 10^{-13} (T/298)^{-2.5} \text{ cm}^3 \text{ molecule}^{-1} \text{ s}^{-1}$$

based upon the temperature dependence reported by Harris et al. [413] for $M = SF_6$.

The subsequent fate of the HSO_3 radicals has recently been discussed by Davis et al. [412], and investigated, using long-path FT-IR spectroscopy, by Niki et al. [415].

Davis et al. [412] suggest the following sequence of reactions of HSO_3:

$$HSO_3 + O_2 \overset{M}{\rightleftharpoons} HSO_5$$

$$HSO_5 + H_2O \rightarrow HSO_5 \cdot (H_2O) \xrightarrow{H_2O} HSO_5 \cdot (H_2O)_x$$

followed by possible reaction with NO, SO_2, etc.; these reactions being probably of a gas-aerosol nature. The recent FT-IR spectroscopic study of Niki et al. [415] is consistent with such a sequence of reactions. In irradiated Cl_2-H_2-NO-SO_2-air mixtures, where the dominant reactive species is the OH radical, SO_2 was observed to disappear, with the appearance of infrared absorption bands attributable to H_2SO_4 (dry and ∿20% hydrated) in the aerosol phase. It was suggested [415] that formation of H_2SO_4 from the H_2SO_5 radical could occur via the reaction sequence:

$$HSO_5 + NO \rightarrow HSO_4 + NO_2$$

$$HSO_4 + HO_2 \rightarrow H_2SO_4 + O_2$$

However, the study of Niki et al. [415] was carried out at ppm (∿10^{14} molecule cm^{-3}) concentrations of H_2O vapor, and under ambient atmospheric conditions, where H_2O concentrations are $\geq 10^{17}$ molecule cm^{-3}, the fate of the HSO_5 radical is probably as suggested by Davis et al. [412], in that hydration may predominate over reaction with NO. Thus it appears that the rate determining step in the conversion of SO_2 to sulfate by reaction with OH is the initial step, i.e., the addition of OH radicals to SO_2, and that, on a phenomenological basis, the necessary information is the number, if any, of NO to NO_2 conversions or subsequent reactions of SO_2 with hydrated HSO_5 species--these of course may also be construed as not being in the realm of homogeneous gas phase chemistry but of gas-liquid or gas-aerosol chemistry.

For modeling studies, we recommend that the rate determining step is the addition of OH radicals to SO_2 to form an HSO_3 radical which rapidly reacts with O_2 and hydrates to (ultimately) form sulfate aerosol: i.e.,

$$OH + SO_2 \overset{(M)}{\rightleftharpoons} HSO_3 \xrightarrow[\text{fast}]{O_2} SO_4^=$$

$$HO_2 + SO_2 \rightarrow \text{products} \qquad (118)$$

At the time of the Calvert et al. [314] review article, the sole study of the reaction of HO_2 radicals with SO_2 was that of Payne et al. [416], who obtained, using an isotope labeling relative rate technique, a rate constant of:

$$k_{118} = (8.4 \pm 1.8) \times 10^{-16} \text{ cm}^3 \text{ molecule}^{-1} \text{ s}^{-1}$$

at 300 K (relative to

$$k(HO_2 + HO_2) = 3.1 \times 10^{-12} \text{ cm}^3 \text{ molecule}^{-1} \text{ s}^{-1}).$$

More recently, Thrush and coworkers [417] have obtained, using a discharge flow system with laser magnetic resonance (LMR) spectroscopic detection of HO_2, upper limits of

$$k_{118}^{bi} \leq 2 \times 10^{-17} \text{ cm}^3 \text{ molecule}^{-1} \text{ s}^{-1}$$

at 298 K

$$k_{118}^{tri}(M = He + SO_2) \leq 4 \times 10^{-34} \text{ cm}^6 \text{ molecule}^{-2} \text{ s}^{-1}$$

at 298 K while Graham et al. [418], from the rates of dissappearance of HO_2NO_2 in the presence and absence of SO_2, obtained:

$$k_{118}^{bi} \leq 1 \times 10^{-18} \text{ cm}^3 \text{ molecule}^{-1} \text{ s}^{-1}$$

at 300 K and 760 torr total pressure (mainly N_2). We recommend, as does NASA [3], this upper limit of Graham et al. [418]. Thus, it appears that this reaction can be neglected under atmospheric conditions [418]. Niki [419] has also reported experimental evidence which indicates that the reaction of HO_2 radicals with SO_2 is very slow.

It is likely that any reaction would proceed via the sequence:

$$HO_2 + SO_2 \rightleftarrows HO_2SO_2^* \rightarrow OH + SO_3$$
$$\downarrow M$$
$$HO_2SO_2$$

Benson [420] estimates that

$$\Delta H_f(HO_2SO_2) \simeq -73 \pm 4 \text{ kcal mol}^{-1}$$

so that formation of HO_2SO_2 is approximately 3 ± 6 kcal mol^{-1} exothermic. Hence, this intermediate adduct (HO_2SO_2) should not be stable (even when thermalized) and should either redissociate to $HO_2 + SO_2$ or form $OH + SO_3$. The low upper limit observed for the rate constant then implies either a substantial energy barrier (of the order of $\gtrsim 8$ kcal mol^{-1}) in the exit channel from HO_2SO_2 to $OH + SO_3$ or that redissociation to $HO_2 + SO_2$ is much favored over formation of $SO_3 + OH$ (as is somewhat expected on the basis of the respective entropy changes).

$$RO_2 + SO_2 \rightarrow \text{products} \qquad (119)$$

Rate constants have been determined only for R = CH_3 and $(CH_3)_3C$. Whitbeck et al. [421] (quoted in [314]) derived, from a flash photolysis study, an upper limit of

$$k_{119} < 7.3 \times 10^{-19} \text{ cm}^3 \text{ molecule}^{-1} \text{ s}^{-1}$$

at room temperature for R = $(CH_3)_3C$. Hence, this particular reaction appears to be negligible under atmospheric conditions.

However, both Kan et al. [388] and Sanhueza et al. [389], both using flash photolysis techniques, have obtained rate constants of

$$1.06 \times 10^{-14} \text{ cm}^3 \text{ molecule}^{-1} \text{ s}^{-1}$$

and

$$8.2 \times 10^{-15} \text{ cm}^3 \text{ molecule}^{-1} \text{ s}^{-1},$$

respectively, at room temperature for the reaction of methylperoxy radicals with SO_2.

Kan et al. [388] monitored the time dependence of CH_3O_2 radicals after flash photolysis of $CH_3N_2CH_3$-O_2-SO_2 mixtures, and ascribed the suppression of the CH_3O_2 absorbance in the presence of SO_2 to reaction of CH_3O_2 radicals with SO_2. Because of the onset of aerosol formation, the range of SO_2 pressures studied was small ($\leq$0.20 torr), resulting in an effective observed extra first order rate of removal of CH_3O_2 radicals of $\sim$40 s^{-1}, which was a relatively small perturbation of the "average" pseudo-first order decay rate of CH_3O_2 radicals due to self-combination of $\sim$400 s^{-1} over the first half-life ([CH_3O_2] initial $\sim 10^{15}$ molecule cm^{-3}). The rate constant for reaction of CH_3O_2 radicals with SO_2, if any, was determined from the CH_3O_2 decay rates at longish times after the flash.

The experimental system of Sanhueza et al. [389] was potentially more direct involving the flash photolysis of Cl_2-CH_4-O_2-SO_2 mixtures. Experiments were carried out with and without added SO_2, and the CH_3O_2 decays

$$(\text{initial } [CH_3O_2] \sim \{3\text{-}4\} \times 10^{15} \text{ molecule cm}^{-3})$$

were observed to change from second order to first order kinetics when $\gtrsim$ 6 torr SO_2 was added. However a first order plot of their data with and without SO_2 shows that the increased CH_3O_2 decay occurs after approximately one half-life (figure 14) and no allowance seems to have been made for the concurrent self-combination of CH_3O_2 radicals in the systems with added SO_2. It is possible that the increased decay of CH_3O_2 radicals after $\sim$0.3 ms (figure 14) is caused by secondary reactions such as:

$$CH_3O_2 + CH_3O_2 \rightarrow \alpha A + B$$

$$A + SO_2 \rightarrow Y \text{ (fast)}$$

$$Y + CH_3O_2 \rightarrow \text{products (fast)}$$

The Sanhueza et al. [389] data could apparently be fitted with an $\sim$30% yield of A, i.e.,

$$CH_3O_2 + CH_3O_2 \rightarrow 0.30\ A + \text{other products}$$

$$A + SO_2 \rightarrow Y \text{ (fast)}$$

$$Y + CH_3O_2 \rightarrow \text{products (fast)}$$

More recently Sander and Watson [422], from the flash photolysis of Cl_2-CH_4-O_2-SO_2 mixtures (but with much reduced initial CH_3O_2 concentrations), observed no reaction, such that

$$k_{119}(R=CH_3) \lesssim 5 \times 10^{-17} \text{ cm}^3 \text{ molecule}^{-1} \text{ s}^{-1}$$

at room temperature. Since, totally analogous to the HO_2 case, any reaction sequence is expected to be:

$$RO_2 + SO_2 \rightleftarrows RO_2SO_2^* \rightarrow RO + SO_2$$
$$\downarrow M$$
$$RO_2SO_2$$

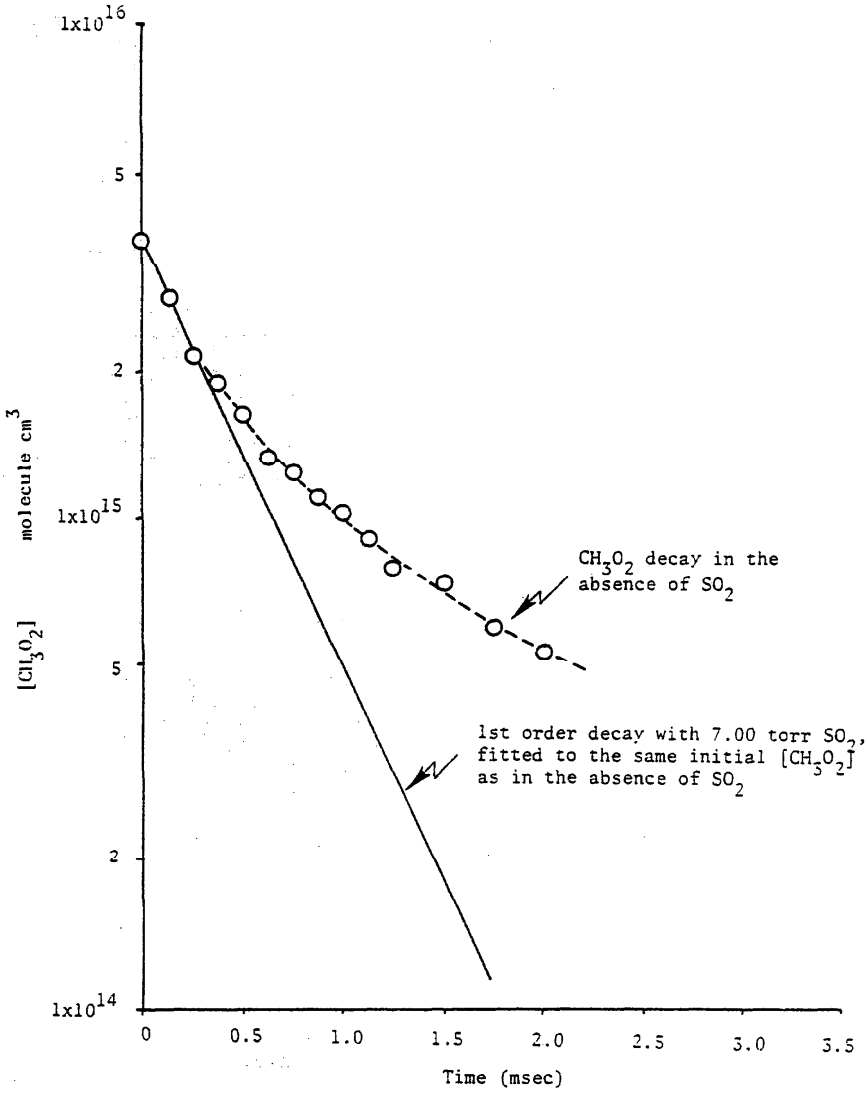

Figure 16. CH_3O_2 Decay Data of Sanhueza et al. [389].

with [420] the formation of RO_2SO_2 being 4 ± 4 kcal mol^{-1} exothermic, and hence, not stable under ambient conditions. Kan et al. [423] have recently reinvestigated the CH_3O_2-SO_2 system, and postulate, in order to explain their observations, that the $CH_3O_2 + SO_2$ reaction is reversible, with the primary reaction

$$CH_3O_2 + SO_2 \rightarrow CH_3O_2SO_2$$

having a rate constant of

$$\sim 1.4 \times 10^{-14} \text{ cm}^3 \text{ molecule}^{-1} \text{ s}^{-1}.$$

However, in the absence of high concentrations of CH_3O_2 or of NO, the reversibility of this reaction leads to no net loss of CH_3O_2 or SO_2. In the presence of added NO a metastable product, tentatively identified as $CH_3O_2SO_2ONO_2$, was observed. Kan et al. [423] postulated the reaction scheme

$$CH_3O_2 + SO_2 \rightleftarrows CH_3O_2SO_2$$

$$CH_3O_2SO_2 + O_2 \rightleftarrows CH_3O_2SO_2O_2$$

$$CH_3O_2SO_2O_2 + CH_3O_2 \rightarrow \text{products}$$

$$CH_3O_2SO_2O_2 + NO \rightarrow CH_3O_2SO_2O + NO_2$$

$$CH_3O_2SO_2O + NO_2 \rightarrow CH_3O_2SO_2ONO_2$$

However, based upon this data and, by analogy with lack of observed reaction of SO_2 with HO_2, $(CH_3)_3CO_2$ and

radicals [314], the reaction of CH_3O_2 and other RO_2 radicals with SO_2 is expected to be slow under atmospheric conditions.

Hence, we recommend that the reactions of RO_2 radical reactions with SO_2 be neglected, and that at room temperature their rate constants are

$$\lesssim 5 \times 10^{-17} \text{ cm}^3 \text{ molecule}^{-1} \text{ s}^{-1}.$$

NASA [3] also recommends the use of this upper limit for the $CH_3O_2 + SO_2$ reaction, based upon the data [388,389,422,423] discussed above.

O_3-Alkene-SO_2 Mixtures

The oxidation of SO_2 by intermediates in O_3-alkene reaction mixtures has been discussed in section 5. Specifically, it appears that SO_2 oxidation occurs via

$$\dot{R}C\dot{R}'OO + SO_2 \rightarrow RCHO + SO_3 \qquad (69)$$

However, as pointed out in section 5, other competing reactions of $\dot{R}C\dot{R}'OO$ radicals are, taking $CH_3\dot{C}HOO$ as an example:

$$CH_3CHOO + H_2O \rightarrow CH_3CO_2H + H_2O \qquad (70)$$

$$CH_3CHOO + NO \rightarrow CH_3CHO + NO_2 \qquad (71)$$

$$CH_3CHOO + NO_2 \rightarrow CH_3CHO + NO_3 \qquad (72)$$

and it is not totally clear as to the importance of this SO_2 oxidation reaction under atmospheric conditions. Calvert et al. [314], neglecting any reactions of this Creigee biradical with NO or NO_2, concluded that this route for SO_2 oxidation is minor. Inclusion of the RR'COO + NO_x reactions will further decrease the importance of this pathway. This reaction has been discussed in detail in section 5.

$$NO_3 + SO_2 \rightarrow \text{products} \qquad (120)$$

$$N_2O_5 + SO_2 \rightarrow \text{products} \qquad (121)$$

These reactions have been studied by Daubendiek and Calvert [424] using infrared absorption spectroscopy to follow the rates of chemical changes in N_2O_5-SO_2 and N_2O_5-SO_2-O_3 mixtures. No significant SO_2 removal was observed and upper limits of

$$k_{120} \leq 7 \times 10^{-21} \text{ cm}^3 \text{ molecule}^{-1} \text{ s}^{-1}$$

at 303 K and

$$k_{121} \leq 4.2 \times 10^{-23} \text{ cm}^3 \text{ molecule}^{-1} \text{ s}^{-1}$$

at 303 K were obtained. Thus these reactions are also of negligible importance under atmospheric conditions.

Acknowledgments

The authors gratefully thank the U. S. Environmental Protection Agency for financial support under Contract No. 68-02-3280 and Order No. 2D5409NA5A to Environmental Research & Technology, Inc., and thank the Project Officer, Dr. Marcia C. Dodge, for helpful discussions.

References

[1] Herron, J. T., Huie, R. E., and Hodgeson, J. A., (Editors), "Chemical Kinetic Data Needs for Modeling the Lower Troposphere", Nat. Bur. Stand. Special Publication 557 (August 1979).

[2] Hampson, R. F., Jr., and Garvin, D. (Editors), "Reaction Rate and Photochemical Data for Atmospheric Chemistry - 1977", Nat. Bur. Stand. Special Publication 513 (May 1978).

[3] "Chemical Kinetic and Photochemical Data for Use in Stratospheric Modeling". Evaluation No. 5, July 15 (1982), J.P.L. Publication 82-57.

[4] Baulch, D. L., Cox, R. A., Hampson, R. F., Jr., Kerr, J. A., Troe, J., and Watson, R. T., J. Phys. Chem. Ref. Data 9, 295 (1980); 11, 327 (1982).

[5] Pitts, J. N., Jr., Darnall, K., Carter, W. P. L., Winer, A. M., and Atkinson, R., "Mechanisms of Photochemical Reactions in Urban Air", EPA-600/3-79-110 (1979).

[6] Hendry, D. G., Baldwin, A. C., Barker, J. R., and Golden, D. M., "Computer Modeling of Simulated Photochemical Smog", EPA-600/3-78-059 (1978).

[7] Carter, W. P. L., Lloyd, A. C., Sprung, J. L., and Pitts, J. N., Jr., Int. J. Chem. Kinet. 11, 45 (1979).

[8] Whitten, G. Z., Hogo, H., Meldgin, M. J., Killus, J. P., and Bekowies, P. J., "Modeling of Simulated Photochemical Smog with Kinetic Mechanisms", Vol. 1, Interim Report, EPA-600/3-79-001a (1979).

[9] Whitten, G. Z., Killus, J. P., and Hogo, H., "Modeling of Simulated Photochemical Smog with Kinetic Mechanisms", Vol. 1, Final Report, EPA-600/3-80-028a (1980).

[10] Hendry, D. G., Baldwin, A. C., and Golden, D. M., "Computer Modeling of Simulated Photochemical Smog", EPA-600/3-80-029 (1980).

[11] Atkinson, R., Carter, W. P. L., Darnall, K. R., Winer, A. M., and Pitts, J. N., Jr., Int. J. Chem. Kinet. 12, 779 (1980).

[12] Atkinson, R., Lloyd, A. C., and Winges, L., Atmos. Environ. 16, 1341 (1982).

[13] Bass, A. M., Ledford, A. E., and Laufer, A. H., J. Research Nat. Bur. Stand. 80A, 143 (1976).

[14] Harker, A. B., Ho, W., and Ratto, J. J., Chem. Phys. Lett. 50, 394 (1977).

[15] Pitts, J. N., Jr., Sharp, J. H., and Chan, S. I., J. Chem. Phys 40, 3655 (1964).

[16] Gaedtke, H., and Troe, J., Ber. Bunsenges Phys. Chem. 79, 184 (1975).

[17] Davenport, J. E., "Determination of NO_2 Photolysis Parameters for Stratospheric Modeling", Report No. FAA-EQ-78-14 (1978).

[18] Jones, I. T. N., and Bayes, K. D., J. Chem. Phys. 59, 4836 (1973).

[19] Klais, O., Anderson, P. C., and Kurylo, M. J., Int. J. Chem. Kinet. 12, 469 (1980).

[20] Lin, C. L., and Leu, M. T., Int. J. Chem. Kinet. 14, 417 (1982).

[21] Davis, D. D., Herron, J. T., and Huie, R. E., J. Chem. Phys. 58, 530 (1973).

[22] Graham, R. A., and Johnston, H. S., J. Phys. Chem. 82, 254 (1978).

[23] Leu, M. T., J. Chem. Phys. 70, 1662 (1979).

[24] Howard, C. J., J. Chem. Phys. 71, 2352 (1979).

[25] Connell, P., and Johnston, H. S., Geophys. Res. Lett. 6, 553 (1979).

[26] Viggiano, A. A., Davidson, J. A., Fehsenfeld, F. C., and Ferguson, E. E., J. Chem. Phys. 74, 6113 (1981).

[27] Malko, M. W., and Troe, J., Int. J. Chem. Kinet. 14, 399 (1982).

[28] Johnston, H. S., and Graham, R., Can. J. Chem. 52, 1415 (1974).

[29] Mitchell, D. N., Wayne, R. P., Allen, P. J., Harrison, R. P., and Twin, R. J., J. Soc. Faraday Trans II 76, 785 (1980).

[30] Marinelli, W. J., Swanson, D. M., and Johnston, H. S., J. Chem. Phys. 76, 2864 (1982).

[31] Magnotta, F., and Johnston, H. S., Geophys. Res. Lett. 7, 769 (1980).

[32] Inn, E. C. Y., and Tanaka, Y., J. Opt. Soc. Amer. 43, 870 (1953).

[33] Griggs, M., J. Chem. Phys. 49, 857 (1968).

[34] Moortgat, G. K., and Warneck, P., Z. Naturforsch. 30A, 835 (1975).

[35] Arnold, I., Comes, F. J., and Moortgat, G. K., Chem. Phys. 24, 211 (1977).

[36] Amimoto, S. T., Force, A. P., and Wiesenfeld, J. R., Chem. Phys. Lett. 60, 40 (1978).

[37] Kajimoto, O., and Cvetanovic, R. J., Int. J. Chem. Kinet. 11, 605 (1979).

[38] Fairchild, C. E., Stone, E. J., and Lawrence, G. M., J. Chem. Phys. 69, 3632 (1978).

[39] Sparks, R. K., Carlson, L. R., Shobatake, K., Kowalczyk, M. L., and Lee, Y. T., J. Chem. Phys. 72, 1401 (1980).

[40] Brock, J. C., and Watson, R. T., Chem. Phys. Lett. 71, 371 (1980).

[41] Amimoto, S. T., Force, A. P., Wiesenfeld, J. R., and Young, R. H., J. Chem. Phys. 73, 1244 (1980).

[42] Wine, P. H., and Ravishankara, A. R., Chem. Phys. 69, 365 (1982).

[43] Greenblatt, G. D., and Wiesenfeld, J. R., J. Chem. Phys. 78, 4924 (1983).

[44] Brock, J. C., and Watson, R. T., Chem. Phys. 46, 477 (1980).

[45] Moortgat, G. K., Kudszus, E., and Warneck, P., J. Chem. Soc. Faraday Trans II 73, 1216 (1977).

[46] Moortgat, G. K., and Kudszus, E., Geophys. Res. Lett. 5, 191 (1978).

[47] Paraskevopoulos, G., and Cvetanovic, R. J., J. Amer. Chem. Soc. 91, 7572 (1969).

[48] Paraskevopoulos, G., and Cvetanovic, R. J., Chem. Phys. Lett. 9, 603 (1971).

[49] Overend, R., Paraskevopoulos, G., and Black, C., J. Chem. Phys. 64, 4149 (1976).

[50] Anastasi, C., and Smith, I. W. M., J. Chem. Soc. Faraday Trans II 74, 1056 (1978).

[51] Atkinson, R., Hansen, D. A., and Pitts, J. N., Jr., J. Chem. Phys. 62, 3284 (1975).

[52] "Chemical Kinetic and Photochemical Data for Use in Stratospheric Modeling", Evaluation No. 2, April 15, J. P. L. Publication 79-27, and revisions and additions therein, cited in Upper Atmosphere Programs Bulletin 79-4 (1979).

[53] Anastasi, C., and Smith, I. W. M., J. Chem. Soc. Faraday Trans II 72, 1459 (1976).

[54] Wine, P. H., Kreutter, N. M., and Ravishankara, A. R., J. Phys. Chem. 83, 3191 (1979).

[55] Cox, R. A., Int. J. Chem. Kinet. Symp. 1, 379 (1975).

[56] Cox, R. A., and Derwent, R. G., J. Photochem. 6, 23 (1976/77).

[57] Stockwell, W. R., and Calvert, J. G., J. Photochem. 8, 193 (1978).

[58] Molina, L. T., and Molina, M. J., J. Photochem. 15, 97 (1981).

[59] Johnston, H., and Graham, R., J. Phys. Chem. 77, 62 (1973).

[60] Biaume, F., J. Photochem. 2, 139 (1973/74).

[61] Johnston, H. S., Chang, S. G., and Whitten, G., J. Phys. Chem. 78, 1 (1974).

[62] Nelson, H. H., Marinelli, W. J., and Johnston, H. S., Chem. Phys. Lett. 78, 495 (1981).

[63] Poulet, G., Jourdain, J. L., and Le Bras, G., C. R. Acad. Sc. Paris 293, 899 (1981).

[64] Ravishankara, A. R., Eisele, F. L., and Wine, P. H., J. Phys. Chem. 86, 1854 (1982).

[65] Cox, R. A., Derwent, R. G., and Holt, P. M., J. Chem. Soc. Faraday Trans I 72, 2031 (1976).

[66] Cohen, N., and Westberg, K., J. Phys. Chem. 83, 46 (1979).

[67] Chan, W. H., Nordstrom, R. J., Calvert, J. G., and Shaw, J. H., Chem. Phys. Lett. 37, 441 (1976).

[68] Chan, W. H., Nordstrom, R. J., Calvert, J. G., and Shaw, J. H., Environ. Sci. Technol. 10, 674 (1976).

[69] Kaiser, E. W., and Wu, C. H., J. Phys. Chem. 81, 1701 (1977).

[70] Ashmore, P. G., and Tyler, B. J., J. Chem. Soc. 1017 (1961).

[71] Morris, E. D., Jr., and Niki, H., J. Phys. Chem. 77, 1929 (1973).

[72] Niki, H., Daby, E. E., and Weinstock, B., Adv. Chem. Ser. 113, 16 (1972).

[73] Tuazon, E. C., Atkinson, R., Plum, C. N., Winer, A. M., and Pitts, J. N., Jr., Geophys. Res. Lett. 10, 953 (1983).

[74] Sie, B. K. T., Simonaitis, R., and Heicklen, J., Int. J. Chem. Kinet. 8, 85 (1976).

[75] Chan, W. H., Uselman, W. M., Calvert, J. G., and Shaw, J. H., Chem. Phys. Lett. 45, 240 (1977).

[76] Overend, R., and Paraskevopoulos, G., Chem. Phys. Lett. 49, 109 (1977).

[77] Perry, R. A., Atkinson, R., and Pitts, J. N., Jr., J. Chem. Phys. 67, 5577 (1977).

[78] Butler, R., Solomon, I. J., and Snelson, A., Chem. Phys. Lett. 54, 19 (1978).

[79] Paraskevopoulos, G., and Irwin, R. S., Chem. Phys. Lett. 93, 138 (1982).

[80] Niki, H., Maker, P. D., Savage, C. M., and Breitenbach, L. P., Chem. Phys. Lett. 45, 564 (1977).

[81] Graham, R. A., Winer, A. M., and Pitts, J. N., Jr., Chem. Phys. Lett. 51, 215 (1977).

[82] Howard, C. J., J. Chem. Phys. 67, 5258 (1977).

[83] Graham, R. A., Winer, A. M., and Pitts, J. N., Jr., J. Chem. Phys. 68, 4505 (1978).

[84] Simonaitis, R., and Heicklen, J., Int. J. Chem. Kinet. 10, 67 (1978).

[85] Cox, R. A., and Patrick, K., Int. J. Chem. Kinet. 11, 635 (1979).

[86] Cox, R. A., Derwent, R. G., and Hutton, A. J. L., Nature 270, 328 (1977).

[87] Zahniser, M. S., and Howard, C. J., J. Chem. Phys. 73, 1620 (1980).

[88] Cox, R. A., and Burrows, J. P., J. Phys. Chem. 83, 2560 (1979).

[89] Lii, R. R., Gorse, R. A., Jr., Sauer, M. C., Jr., and Gordon, S., J. Phys. Chem. 83, 1803 (1979).

[90] Lii, R. R., Sauer, M. C., Jr., and Gordon, S., J. Phys. Chem. 85, 2833 (1981).

[91] Thrush, B. A., and Wilkinson, J. P. T., Chem. Phys. Lett. 66, 441 (1979).

[92] Sander, S. P., Peterson, M., Watson, R. T., and Patrick, R., J. Phys. Chem. 86, 1236 (1982).

[93] Simonaitis, R., and Heicklen, J., J. Phys. Chem. 86, 3416 (1982).

[94] Thrush, B. A., and Tyndall, G. S., J. Chem. Soc. Faraday Trans II 78, 1469 (1982).

[95] Thrush, B. A., and Tyndall, G. S., Chem. Phys. Lett. 92, 232 (1982).

[96] Patrick, R., and Pilling, M. J., Chem. Phys. Lett. 91, 343 (1982).

[97] Hamilton, E. J., Jr., and Lii, R. R., Int. J. Chem. Kinet. 9, 875 (1977).

[98] Lin, C. L., Rohatgi, N. K., and DeMore, W. B., Geophys. Res. Lett. 5, 113 (1978).

[99] Sridharan, U. C., Reimann, B., and Kaufman, F., J. Chem. Phys. 73, 1286 (1980).

[100] Keyser, L. F., J. Phys. Chem. 84, 1659 (1980).

[101] Wine, P. H., Semmes, D. H., and Ravishankara, A. R., J. Chem. Phys. 75, 4390 (1981).

[102] Kurylo, M. J., Murphy, J. L., Haller, G. S., and Cornett, K. D., Int. J. Chem. Kinet. 14, 1149 (1982).

[103] Chang, J. S., and Barker, J. R., J. Phys. Chem. 83, 3059 (1979).

[104] Klemm, R. B., J. Chem. Phys. 71, 1987 (1979).

[105] Klemm, R. B., Skolnik, E. G., and Michael, J. V., J. Chem. Phys. 72, 1256 (1980).

[106] Niki, H., J. Chem. Phys. 45, 2330 (1966).

[107] Herron, J. T., and Penzhorn, R. D., J. Phys. Chem. 73, 191 (1969).

[108] Mack, G. P. R., and Thrush, B. A., J. Chem. Soc. Faraday Trans I 69, 208 (1973).

[109] Bass, A. M., Glasgow, L. C., Miller, C., Jesson, J. P., and Filken, D. L., Planet. Space Sci. 28, 675 (1980).

[110] Moortgat, G. K., Klippel, W., Mobus, K. H., Seiler, W., and Warneck, P., "Laboratory Measurements of Photolytic Parameters for Formaldehyde", FAA-EE-80-47 (1980).

[111] Horowitz, A., and Calvert, J. G., Int. J. Chem. Kinet. 10, 805 (1978).

[112] Clark, J. H., Moore, C. B., and Nogar, N. S., J. Chem. Phys. 68, 1264 (1978).

[113] Moortgat, G. K., and Warneck, P., J. Chem. Phys. 70, 3639 (1979).

[114] Tang, K. Y., Fairchild, P. W., and Lee, E. K. C., J. Phys. Chem. 83, 569 (1979).

[115] Moortgat, G. K., Seiler, W., and Warneck, P., J. Chem. Phys. 78, 1185 (1983).

[116] Atkinson, R., Darnall, K. R., Lloyd, A. C. Winer, A. M., and Pitts, J. N., Jr., Adv. Photochem. 11, 375 (1979).

[117] Morris, E. D., Jr., and Niki, H., J. Chem. Phys. 55, 1991 (1971).

[118] Niki, H., Maker, P. D., Savage, C. M., and Breitenbach, L. P., J. Phys. Chem. 82, 132 (1978).

[119] Atkinson, R., and Pitts, J. N., Jr., J. Chem. Phys. 68, 3581 (1978).

[120] Stief, L. J., Nava, D. F., Payne, W. A., and Michael, J. V., J. Chem. Phys. 73, 2254 (1980).

[121] Smith, R. H., Int. J. Chem. Kinet. 10, 519 (1978).

[122] Horowitz, A., Su, F., and Calvert, J. G., Int. J. Chem. Kinet. 10, 1099 (1978).

[123] Niki, H., (1979), p. 46 in [1].

[124] Morrison, B. M., Jr., and Heicklen, J., J. Photochem. 13, 189 (1980).

[125] Su, F., Calvert, J. G., Shaw, J. H., Niki, H., Maker, P. D., Savage, C. M., and Breitenbach, L. P., Chem. Phys. Lett. 65, 221 (1979).

[126] Su, F., Calvert, J. G., and Shaw, J. H., J. Phys. Chem. 83, 3185 (1979).

[127] Veyret, B., Rayez, J. C., and Lesclaux, R., J. Phys. Chem. 86, 3424 (1982).

[128] Niki, H., Maker, P. D., Savage, C. M., and Breitenbach, L. P., Chem. Phys. Lett. 75, 533 (1980).

[129] Niki, H., Maker, P. D., Savage, C. M., and Breitenbach, L. P., Chem. Phys. Lett. 72, 71 (1980).

[130] Atkinson, R., Plum, C. N., Carter, W. P. L., Winer, A. M., and Pitts, J. N., Jr., J. Phys. Chem. 88, 1210 (1984).

[131] Hunziker, H. E., and Wendt, H. R., 12th Int. Symp. Free Radicals, Laguna Beach, CA (1976).

[132] Hanst, P. L., and Gay, B. W., Jr., Environ. Sci. Technol. 11, 1105 (1977).

[133] Shibuya, K., Ebata, T., Obi, K., and Tanaka, I., J. Phys. Chem. 81, 2292 (1977).

[134] Radford, H. E., Evenson, K. M., and Howard, C. J., J. Chem. Phys. 60, 3178 (1974).

[135] Osif, T. L., and Heicklen, J., J. Phys. Chem. 80, 1526 (1976).

[136] Niki, H., Maker, P. D., Savage, C. M., and Breitenbach, L. P., 173rd Amer. Chem. Soc. Meeting, New Orleans, LA (1977).

[137] Veyret, B., and Lesclaux, R., J. Phys. Chem. 85, 1918 (1981).

[138] Singleton, D. L., Irwin, R. S., and Cvetanovic, R. J., Can. J. Chem. 55, 3321 (1977).

[139] Mack, G. P. R., and Thrush, B. A., J. Chem. Soc. Faraday Trans I 70, 178 (1974).

[140] Cadle, R. D., and Powers, J. W., J. Phys. Chem. 71, 1702 (1967).

[141] Cvetanovic, R. J., Can. J. Chem. 34, 775 (1956).

[142] Avery, H. E., and Cvetanovic, R. J., J. Chem. Phys. 43, 3727 (1965).

[143] Horowitz, A., Kershner, C. J., and Calvert, J. G., J. Phys. Chem. 86, 3094 (1982).

[144] Horowitz, A., and Calvert, J. G., J. Phys. Chem. 86, 3105 (1982).

[145] Meyrahn, H., Moortgat, G. K., and Warneck, P., 15th Inf. Conf. on Photochem., Stanford, CA (1982).

[146] Morris, E. D., Jr., Stedman, D. H., and Niki, H., J. Amer. Chem. Soc. 93, 3570 (1971).

[147] Hunziker, H. E., and Wendt, H. R., J. Chem. Phys. 64, 3488 (1976).

[148] Addison, M. C., Burrows, J. P., Cox, R. A., and Patrick, R., Chem. Phys. Lett. 73, 283 (1980).

[149] Pate, C. T., Atkinson, R., and Pitts, J. N., Jr., J. Environ. Sci. Health A11, 19 (1976).

[150] Hendry, D. G., and Kenley, R. A., J. Amer. Chem. Soc. 99, 3198 (1977).

[151] Cox, R. A., and Roffey, M. J., Environ. Sci. Technol. 11, 900 (1977).

[152] Nieboer, H., and Duyzer, J. H., "Photochemical Smog Formation in the Netherlands", TNO, P89-, (1978).

[153] Cox, R. A., Derwent, R. G., Holt, P. M., and Kerr, J. A., J. Chem. Soc. Faraday Trans I 72, 2061 (1976).

[154] Cox, R. A., Derwent, R. G., Holt, P. M., and Kerr, J. A., J. Chem. Soc. Faraday Trans I 72, 2044 (1976).

[155] Anastasi, C., Smith, I. W. M., and Parkes, D. A., J. Chem. Soc. Faraday Trans I 74, 1693 (1978).

[156] Plumb, I. C., Ryan, K. R., Steven, J. R., and Mulcahy, M. F. R., Chem. Phys. Lett. 63, 255 (1979).

[157] Adachi, H., and Basco, N., Chem. Phys. Lett. 63, 490 (1979).

[158] Cox, R. A., and Tyndall, G. S., Chem. Phys. Lett. 65, 357 (1979).

[159] Cox, R. A., and Tyndall, G. S., J. Chem. Soc. Faraday Trans II 76, 153 (1980).

[160] Simonaitis, R., and Heicklen, J., Chem. Phys. Lett. 65, 361 (1979).

[161] Sander, S. P., and Watson, R. T., J. Phys. Chem. 84, 1664 (1980).

[162] Ravishankara, A. R., Eisele, F. L., Kreutter, N. M., and Wine, P. H., J. Chem. Phys. 74, 2267 (1981).

[163] Simonaitis, R., and Heicklen, J., J. Phys. Chem. 85, 2946 (1981).

[164] Plumb, I. C., Ryan, K. R., Steven, J. R., and Mulcahy, M. F. R., J. Phys. Chem. 85, 3136 (1981).

[165] Adachi, H., and Basco, N., Chem. Phys. Lett. 64, 431 (1979).

[166] Plumb, I. C., Ryan, K. R., Steven, J. R., and Mulcahy, M. F. R., Int. J. Chem. Kinet. 14, 183 (1982).

[167] Pate, C. T., Finlayson, B. J., and Pitts, J. N., Jr., J. Amer. Chem. Soc. 96, 6554 (1974).

[168] Simonaitis, R., and Heicklen, J., J. Phys. Chem. 78, 2417 (1974).

[169] Darnall, K. R., Carter, W. P. L., Winer, A. M., Lloyd, A. C., and Pitts, J. N., Jr., J. Phys. Chem. 80, 1948 (1976).

[170] Atkinson, R., Aschmann, S. M., Carter, W. P. L., Winer, A. M., and Pitts, J. N., Jr., J. Phys. Chem. 86, 4563 (1982).

[171] Takagi, H., Washida, N., Bandow, H., Akimoto, H., and Okuda, M., J. Phys. Chem. 85, 2701 (1981).

[172] Atkinson, R., Carter, W. P. L., and Winer, A. M., J. Phys. Chem. 87, 2012 (1983).

[173] Ravishankara, A. R., Eisele, F. L., and Wine, P. H., J. Chem. Phys. 73, 3743 (1980).

[174] Kenley, R. A., and Hendry, D. G., J. Amer. Chem. Soc. 104, 220 (1982).

[175] Gay, B. W., Jr., Noonan, R. C., Bufalini, J. J., and Hanst, P. L., Environ. Sci. Technol. 10, 82 (1976).

[176] Niki, H., Maker, P. D., Savage, C. M., and Breitenbach, L. P., Chem. Phys. Lett. 55, 289 (1978).

[177] Niki, H., Maker, P. D., Savage, C. M., and Breitenbach, L. P., in "Nitrogeneous Air Pollutants", D. Grosjean, ed., Ann Arbor Press, Ann Arbor, MI (1979).

[178] Hendry, D. G., and Kenley, R. A., in "Nitrogeneous Air Pollutants", D. Grosjean, ed. Ann Arbor Press, Ann Arbor, MI (1979).

[179] Edney, E. O., Spence, J. W., and Hanst, P. L., in "Nitrogeneous Air Pollutants", D. Grosjean, ed., Ann Arbor Press, Ann Arbor, MI (1979).

[180] Edney, E. O., Spence, J. W., and Hanst, P. L., J. Air Poll. Contr. Assoc. 29, 741 (1979).

[181] Bahta, A., Simonaitis, R., and Heicklen, J., J. Phys. Chem. 86, 1849 (1982).

[182] Baldwin, A. C., and Golden, D. M., J. Phys. Chem. 82, 644 (1978).

[183] Hendry, D. G., private communication (1979).

[184] Ruiz, R. P., and Bayes, K. D., 14th Int. Conf. Photochem., Newport Beach, CA (1980).

[185] Lenhardt, T. M., McDade, C. E., and Bayes, K. D., J. Chem. Phys. 72, 304 (1980).

[186] Plumb, I. C., and Ryan, K. R., Int. J. Chem. Kinet. 13, 1011 (1981).

[187] Parkes, D. A., Paul, D. M., Quinn, C. P., and Robson, R. C., Chem. Phys. Lett. 23, 425 (1973).

[188] Parkes, D. A., 15th Int. Symp. Combust., Tokyo, 1974, The Combustion Institute, 795 (1975).

[189] Kirsch, L. J., Parkes, D. A., Waddington, D. J., and Woolley, A., J. Chem. Soc. Faraday Trans I 74, 2293 (1978).

[190] Sanders, N., Butler, J. E., Pasternack, L. R., and McDonald, J. R., Chem. Phys. 48, 203 (1980).

[191] Mendenhall, G. D., Golden, D. M., and Benson, S. W., Int. J. Chem. Kinet. 7, 725 (1975).

[192] Batt, L., McCulloch, R. D., and Milne, R. T., Int. J. Chem. Kinet. Symp. 1, 441 (1975).

[193] Batt, L., and Milne, R. T., Int. J. Chem. Kinet. 8, 59 (1976).

[194] Batt, L., and McCulloch, R. D., Int. J. Chem. Kinet. 8, 911 (1976).

[195] Batt, L., and Milne, R. T., Int. J. Chem. Kinet. 9, 141 (1977).

[196] Batt, L., and Milne, R. T., Int. J. Chem. Kinet. 9, 549 (1977).

[197] Batt, L., Milne, R. T., and McCulloch, R. D., Int. J. Chem. Kinet. 9, 567 (1977).

[198] Batt, L., Islam, T. S. A., and Rattray, G. N., Int. J. Chem. Kinet. 10, 931 (1978).

[199] Baldwin, A. C., and Golden, D. M., Chem. Phys. Lett. 60, 108 (1978)

[200] Batt, L., (1979), pp. 62-64 in [1].

[201] Batt, L., Int. J. Chem. Kinet. 11, 977 (1979).

[202] Batt, L., "Reactions of Alkoxy Radicals Relevant to Atmospheric Chemistry", 1st European Symp. on Physico-Chemical Behavior of Atmos. Pollutants, Ispra, Italy 1979, B. Verdino and H. Ott, eds., Commission of the European Communities (1980).

[203] Batt, L., and Rattray, G. N., Int. J. Chem. Kinet. 11, 1183 (1979).

[204] Gray, P., and Pratt, M. W. T., J. Chem. Soc. 3403 (1958).

[205] Wiebe, H. A., Villa, A., Hellman, T. M., and Heicklen, J., J. Amer. Chem. Soc. 95, 7 (1973).

[206] Rebbert, R. E., J. Phys. Chem. 67, 1923 (1963).

[207] Arden, E. A., Phillips, L., and Shaw, R., J. Chem. Soc. 5126 (1964).

[208] Livermore, R. A., and Phillips, L., J. Chem. Soc. (B), 640 (1966).

[209] East, R. L., Gilbert, J. R., and Phillips, L., J. Chem. Soc. (A), 1673 (1968).

[210] East, R. L., and Phillips, L., J. Chem. Soc. (A), 331 (1970).

[211] McMillan, G. R., J. Amer. Chem. Soc. 83, 3018 (1961).

[212] Hughes, G. A., and Phillips, L., J. Chem. Soc. (A), 894 (1967).

[213] Ludwig, B. E., and McMillan, G. R., J. Phys. Chem. 71, 762 (1967).

[214] Yee Quee, M. J., and Thynne, J. C. J., Trans. Faraday Soc. 64, 1296 (1968).

[215] East, R. L., and Phillips, L., J. Chem. Soc. (A), 1939 (1967).

[216] Walker, R. F., and Phillips, L., J. Chem. Soc. (A), 2103 (1968).

[217] Baker, G., and Shaw, R., J. Chem. Soc., 6965 (1965).

[218] Phillips, L., and Shaw, R., 10th Int. Symp. Combust. 1964, The Combustion Institute, 453 (1965).

[219] Barker, J. R., Benson, S. W., and Golden, D. M., Int. J. Chem. Kinet. 9, 31 (1977).

[220] Batt, L., and Alvarado-Salinas, G., (1979), cited in [203].

[221] Batt, L., and Robinson, G. N., Int. J. Chem. Kinet. 11, 1045 (1979).

[222] Gutman, D., Sanders, N., and Butler, J. E., J. Phys. Chem. 86, 66 (1982).

[223] Cox, R. A., Derwent, R. G., Kearsey, S. V., Batt, L., and Patrick, K. G., J. Photochem. 13, 149 (1980).

[224] Baldwin, A. C., Barker, J. R., Golden, D. M., and Hendry, D. G., J. Phys. Chem. 81, 2483 (1977).

[225] Atkinson, R., Aschmann, S. M., Carter, W. P. L., and Winer, A. M., Int. J. Chem. Kinet. 14, 919 (1982).

[226] Campbell, I. M., and Goodman, K., Chem. Phys. Lett. 36, 382 (1975).

[227] Audley, G. J., Baulch, D. L., Campbell, I. M., Waters, D. J., and Watling, G., J. Chem. Soc. Faraday Trans I 78, 611 (1982).

[228] Tuazon, E. C., Carter, W. P. L., Atkinson, R., and Pitts, J. N., Jr., Int. J. Chem. Kinet. 15, 619 (1983).

[229] Taylor, W. D., Allston, T. D., Moscato, M. J., Fazekas, G. B., Kozlowski, R., and Takacs, G. A., Int. J. Chem. Kinet. 12, 231 (1980).

[230] Calvert, J. G., and Pitts, J. N., Jr., "Photochemistry", Wiley, New York, NY (1966).

[231] Morris, E. D., Jr., and Niki, H., J. Phys. Chem. 78, 1337 (1974).

[232] Singleton, D. L., and Cvetanovic, R. J., J. Amer. Chem. Soc. 98, 6812 (1976).

[233] Atkinson, R., and Pitts, J. N., Jr., J. Chem. Phys. 67, 38 (1977).

[234] Nicovich, J. M., Gump, C. A., and Ravishankara, A. R., J. Phys. Chem. 86, 1684 (1982).

[235] Sugawara, K., Ishikawa, Y., and Sato, S., Bull. Chem. Soc. Japan 53, 1344 (1980).

[236] Sato, S., Int. Symp. Chemical Kinetics Related to Atmospheric Chemistry, Tsukuba, Ibaraki, Japan (July 1982).

[237] Cvetanovic, R. J., Adv. Photochem. 1, 115 (1963).

[238] Cvetanovic, R. J., Can. J. Chem. 36, 623 (1958).

[239] Kanofsky, J. R., Lucas, D., and Gutman, D., 14th Int. Symp. Combust. 1972, The Combustion Institute, 285 (1973).

[240] Pruss, F. J., Jr., Slagle, I. R., and Gutman, D., J. Phys. Chem. 78, 663 (1974).

[241] Inoue, G., and Akimoto, H., J. Chem. Phys. 74, 425 (1981).

[242] Kleinermanns, K., and Luntz, A. C., J. Phys. Chem. 85, 1966 (1981).

[243] Hunziker, H. E., Kneppe, H., and Wendt, H. R., J. Photochem. 17, 377 (1981).

[244] Buss, R. J., Baseman, R. J., He, G., and Lee, Y. T., J. Photochem. 17, 389 (1981).

[245] Cvetanovic, R. J., Can. J. Chem. 33, 1684 (1955).

[246] Blumenberg, B., Hoyermann, K., and Sievert, R., 16th Int. Symp. on Combust. 1976, The Combustion Institute, 841 (1977).

[247] Luria, M., Simonaitis, R., and Heicklen, J., Int. J. Chem. Kinet. 5, 715 (1973).

[248] Gutman, D., and Nelson, H. H., J. Phys. Chem. 87, 3902 (1983).

[249] Winer, A. M., Darnall, K. R., Atkinson, R., and Pitts, J. N., Jr., (1978) unpublished data cited in [116].

[250] Ravishankara, A. R., Wagner, S., Fischer, S., Smith, G., Schiff, R., Watson, R. T., Tesi, G., and Davis, D. D., Int. J. Chem. Kinet. 10, 783 (1978).

[251] Atkinson, R., Perry, R. A., and Pitts, J. N., Jr., J. Chem. Phys. 66, 1197 (1977).

[252] Overend, R., and Paraskevopoulos, G., J. Chem. Phys. 67, 674 (1977).

[253] Tully, F. P., Chem. Phys. Lett. 96, 148 (1983).

[254] Bradley, J. N., Hack, W., Hoyermann, K., and Wagner, H. Gg., J. Chem. Soc. Faraday Trans I 69, 1889 (1973).

[255] Stuhl, F., Ber. Bunsenges Phys. Chem. 77, 674 (1973).

[256] Pastrana, A. V., and Carr, R. W., Jr., J. Phys. Chem. 79, 765 (1975).

[257] Atkinson, R., and Pitts, J. N., Jr., J. Chem. Phys. 63, 3591 (1975).

[258] Nip, W. S., and Paraskevopoulos, G., J. Chem. Phys. 71, 2170 (1979).

[259] Morris, E. D., Jr., and Niki, H., J. Phys. Chem. 75, 3640 (1971).

[260] Wu, C. H., Japar, S. M., and Niki, H., J. Environ. Sci. Health A11, 191 (1976).

[261] Lloyd, A. C., Darnall, K. R., Winer, A. M., and Pitts, J. N., Jr., J. Phys. Chem. 80, 789 (1976).

[262] Atkinson, R., Aschmann, S. M., Winer, A. M., and Pitts, J. N., Jr., Int. J. Chem. Kinet. 14, 507 (1982).

[263] Hoyermann, K., and Sievert, R., Ber. Bunsenges Phys. Chem. 83, 933 (1979).

[264] Biermann, H. W., Harris, G. W., and Pitts, J. N., Jr., J. Phys. Chem. 86, 2958 (1982).

[265] Cvetanovic, R. J., 12th Int. Symp. Free Radicals, Laguna Beach, CA (1976).

[266] Atkinson, R., Perry, R. A., and Pitts, J. N., Jr., J. Chem. Phys. 67, 3170 (1977).

[267] Demerjian, K. L., Kerr, J. A., and Calvert, J. G., Adv. Environ. Sci. Technol. 4, 1 (1974).

[268] Arnts, R. R., and Gay, B. W., Jr., "Photochemistry of Some Naturally Emitted Hydrocarbons", EPA-600/3-79-081 (1979).

[269] Carter, W. P. L., Darnall, K. R., Lloyd, A. C., Winer, A. M., and Pitts, J. N., Jr., Chem. Phys. Lett. 42, 22 (1976); NSF-RANN Grant ENV73-02904 A03 Annual Report (1976).

[270] Golden, D. M., (1979), pp. 51-61 in [1].

[271] Cox, R. A., Patrick, K. F., and Chant, S. A., Environ. Sci. Technol. 15, 587 (1981).

[272] Niki, H., Maker, P. D., Savage, C. M., and Breitenbach, L. P., J. Phys. Chem. 85, 2698 (1981).

[273] Niki, H., Maker, P. D., Savage, C. M., and Breitenbach, L. P., J. Phys. Chem. 82, 135 (1978).

[274] Niki, H., Maker, P. D., Savage, C. M., and Breitenbach, L. P., Chem. Phys. Lett. 80, 499 (1981).

[275] Carter, W. P. L., Darnall, K. R., Graham, R. A., Winer, A. M., and Pitts, J. N., Jr., J. Phys. Chem. 83, 2305 (1979).

[276] Ohta, T., Bandow, H., and Akimoto, H., Int. J. Chem. Kinet. 14, 173 (1982).

[277] Radford, H. E., Chem. Phys. Lett. 71, 195 (1980).

[278] Michael, J. V., Nava, D. F., Payne, W. A., and Stief, L. J., J. Chem. Phys. 70, 3652 (1979).

[279] Japar, S. M., and Niki, H., J. Phys. Chem. 79, 1629 (1975).

[280] Hoshino, M., Ogata, T., Akimoto, H., Inoue, G., Sakamaki, F., and Okuda, M., Chem. Lett. 1367 (1978).

[281] Akimoto, H., Hoshino, M., Inoue, G., Sakamaki, F., Bandow, H., and Okuda, M., J. Environ. Sci. Health A13, 677 (1978).

[282] Bandow, H., Okuda, M., and Akimoto, H., J. Phys. Chem. 84, 3604 (1980); Bandow, H., Hoshino, M., Inoue, G., Sakamaki, F., Ogata, T., Tezuka, T., Okuda, M., and Akimoto, H., Research Report No. 9, R-9-79, Nat. Inst. for Environ. Studies, Japan (1979).

[283] Niki, H., (1979), pp. 7-14 in [1].

[284] Japar, S. M., Wu, C. H., and Niki, H., J. Phys. Chem. 78, 2318 (1974).

[285] Herron, J. T., and Huie, R. E., J. Phys. Chem. 78, 2085 (1974).

[286] Huie, R. E., and Herron, J. T., Int. J. Chem. Kinet. Symp. 1, 165 (1975).

[287] Cadle, R. D., and Schadt, C., J. Amer. Chem. Soc. 74, 6002 (1952).

[288] Hanst, P. L., Stephens, E. R., Scott, W. E., and Doerr, R. C., "Atmospheric Ozone-Olefin Reactions", The Franklin Institute, Philadelphia, PA (1958).

[289] Bufalini, J. J., and Altshuller, A. P., Can. J. Chem. 43, 2243 (1965).

[290] DeMore, W. B., Int. J. Chem. Kinet. 1, 209 (1969).

[291] Stedman, D. H., Wu, C. H., and Niki, H., J. Phys. Chem. 77, 2511 (1973).

[292] Becker, K. H., Schurath, U., and Seitz, H., Int. J. Chem. Kinet. 6, 725 (1974).

[293] Japar, S. M., Wu, C. H., and Niki, H., J. Phys. Chem. 80, 2057 (1976).

[294] Toby, F. S., Toby, S., and O'Neal, H. E., Int. J. Chem. Kinet. 8, 25 (1976).

[295] Su, F., Calvert, J. G., and Shaw, J. H., J. Phys. Chem. 84, 239 (1980).

[296] Kan, C. S., Su, F., Calvert, J. G., and Shaw, J. H., J. Phys. Chem. 85, 2359 (1981).

[297] Adeniji, S. A., Kerr, J. A., and Williams, M. R., Int. J. Chem. Kinet. 13, 209 (1981).

[298] Atkinson, R., Aschmann, S. M., Fitz, D. R., Winer, A. M., and Pitts, J. N., Jr., Int. J. Chem. Kinet. 14, 13 (1982).

[299] Cox, R. A., and Penkett, S. A., J. Chem. Soc. Faraday Trans I 68, 1735 (1972).

[300] Atkinson, R., Aschmann, S. M., Carter, W. P. L., and Pitts, J. N., Jr., Int. J. Chem. Kinet. 15, 721 (1983).

[301] Herron, J. T., and Huie, R. E., J. Amer. Chem. Soc. 99, 5430 (1977).

[302] Herron, J. T., and Huie, R. E., Int. J. Chem. Kinet. 10, 1019 (1978).

[303] Niki, H., Maker, P. D., Savage, C. M., and Breitenbach, L. P., Int. Conf. Environ. Sensing and Assessment, Las Vegas, NV, Vol. 2, 24-4 (1975).

[304] Niki, H., Maker, P. D., Savage, C. M., and Breitenbach, L. P., Chem. Phys. Lett. 46, 327 (1977).

[305] Niki, H., Maker, P. D., Savage, C. M., and Breitenbach, L. P., J. Phys. Chem. 85, 1024 (1981).

[306] Martinez, R. I., Herron, J. T., and Huie, R. E., J. Amer. Chem. Soc. 103, 3807 (1981).

[307] Dodge, M. C., and Arnts, R. R., Int. J. Chem. Kinet. 11, 399 (1979).

[308] Harding, L. B., and Goddard, W. A., III, J. Amer. Chem. Soc. 100, 7180 (1978).

[309] Herron, J. T., Martinez, R. I., and Huie, R. E., Int. J. Chem. Kinet. 14, 201 (1982).

[310] Lovas, F. J., and Suenram, R. D., Chem. Phys. Lett. 51, 453 (1977).

[311] Martinez, R. I., Huie, R. E., and Herron, J. T., Chem. Phys. Lett. 51, 457 (1977).

[312] Wadt, W. R., and Goddard, W. A., III, J. Amer. Chem. Soc. 97, 3004 (1975).

[313] Kuhne, H., Vaccini, S., Ha, T. K., Bandes, A., and Gunthard, H. H., Chem. Phys. Lett. 38, 449 (1976).

[314] Calvert, J. G., Su, F., Bottenheim, J. W., and Strausz, O. P., Atmos. Environ. 12, 197 (1978).

[315] Martinez, R. I., and Herron, J. T., J. Environ. Sci. Health A16, 623 (1981).

[316] Akimoto, H., Bandow, H., Sakamaki, F., Inoue, G., Hoshino, M., and Okuda, M., Research Report No. 9, R-9-79, Nat. Inst. for Environ. Studies, Japan (1979).

[317] Hatakeyama, S., Bandow, H., Okuda, M., and Akimoto, H., J. Phys. Chem. 85, 2249 (1981).

[318] Akimoto, H., Bandow, H., Sakamaki, F., Inoue, G., Hoshino, M., and Okuda, M., Environ. Sci. Technol. 14, 172 (1980).

[319] Martinez, R. I., Huie, R. E., and Herron, J. T., Chem. Phys. Lett. 72, 443 (1980).

[320] Elias, L., and Schiff, H. I., Can. J. Chem. 38, 1657 (1960).

[321] Herron, J. T., and Huie, R. E., J. Phys. Chem. 73, 3327 (1969).

[322] Atkinson, R., Perry, R. A., and Pitts, J. N., Jr., Chem. Phys. Lett. 47, 197 (1977).

[323] Herron, J. T., and Huie, R. E., J. Phys. Chem. Ref. Data 2, 467 (1973).

[324] Atkinson, R., Plum, C. N., Carter, W. P. L., Winer, A. M., and Pitts, J. N., Jr., J. Phys. Chem. 88, 2361 (1984).

[325] Greiner, N. R., J. Chem. Phys. 53, 1070 (1970).

[326] Stuhl, F., Z. Naturforsch. 28A, 1383 (1973).

[327] Perry, R. A., Atkinson, R., and Pitts, J. N., Jr., J. Chem. Phys. 64, 5314 (1976).

[328] Paraskevopoulos, G., and Nip, W. S., Can. J. Chem. 58, 2146 (1980).

[329] Darnall, K. R., Atkinson, R., and Pitts, J. N., Jr., J. Phys. Chem. 82, 1581 (1978).

[330] Atkinson, R., Aschmann, S. M., Carter, W. P. L., Winer, A. M., and Pitts, J. N., Jr., Int. J. Chem. Kinet. 14, 781 (1982).

[331] Atkinson, R., Carter, W. P. L., Aschmann, S. M., Winer, A. M., and Pitts, J. N., Jr., Int. J. Chem. Kinet. 16, 469 (1984).

[332] Carter, W. P. L., Atkinson, R., Winer, A. M., and Pitts, J. N., Jr., 28th Congress Int. Union Pure Appl. Chem., Vancouver, Canada (1981).

[333] Kerr, J. A., and Sheppard, D. W., Environ. Sci. Technol. 15, 960 (1981).

[334] Audley, G. J., Baulch, D. L., and Campbell, I. M., J. Chem. Soc. Faraday Trans I 77, 2541 (1981).

[335] Atkinson, R., Aschmann, S. M., Carter, W. P. L., and Pitts, J. N., Jr., Int. J. Chem. Kinet. 14, 839 (1982).

[336] Heuss, J. M., and Glasson, W. A., Environ. Sci. Technol. 2, 1109 (1968).

[337] Winer, A. M., Darnall, K. R., Atkinson, R., and Pitts, J. N., Jr., Environ. Sci. Technol. 13, 822 (1979).

[338] Shepson, P. B., and Heicklen, J., J. Photochem. 18, 169 (1982).

[339] Shepson, P. B., and Heicklen, J., J. Photochem. 19, 215 (1982).

[340] Forgeteg, S., Berces, T., and Dobe, S., Int. J. Chem. Kinet. 11, 219 (1979).

[341] Blacet, F. E., and Calvert, J. G., J. Amer. Chem. Soc. 73, 667 (1951).

[342] Cox, R. A., Derwent, R. G., and Williams, M. R., Environ. Sci. Technol. 14, 57 (1980).

[343] Darnall, K. R., Atkinson, R., and Pitts, J. N., Jr., J. Phys. Chem. 83, 1943 (1979).

[344] Kerr, J. A., Parsonage, M. J., and Trotman-Dickenson, A. F., "Strengths of Chemical Bonds", in Handbook of Chemistry and Physics, 56th ed., CRC Press, Cleveland, OH (1975).

[345] Cox, R. A., Addison, M. C., Burrows, J. P., and Patrick, R., 14th Inf. Conf. Photochem., Newport Beach, CA (1980).

[346] Winer, A. M., Lloyd, A. C., Darnall, K. R., and Pitts, J. N., Jr., J. Phys. Chem. 80, 1635 (1976).

[347] Davis, D. D., Bollinger, W., and Fischer, S., J. Phys. Chem. 79, 293 (1975).

[348] Doyle, G. J., Lloyd, A. C., Darnall, K. R., Winer, A. M., and Pitts, J. N., Jr., Environ. Sci. Technol. 9, 237 (1975).

[349] Pate, C. T., Atkinson, R., and Pitts, J. N., Jr., J. Environ. Sci. Health A11, 1 (1976).

[350] Atkinson, R., and Pitts, J. N., Jr., J. Phys. Chem. 78, 1780 (1974).

[351] Atkinson, R., and Pitts, J. N., Jr., J. Phys. Chem. 79, 295 (1975).

[352] Atkinson, R., and Pitts, J. N., Jr., Chem. Phys. Lett. 63, 485 (1979).

[353] Colussi, A. J., Singleton, D. L., Irwin, R. S., and Cvetanovic, R. J., J. Phys. Chem. 79, 1900 (1975).

[354] Nicovich, J. M., Gump, C. A., and Ravishankara, A. R., J. Phys. Chem. 86, 1690 (1982).

[355] Gaffney, J. S., Atkinson, R., and Pitts, J. N., Jr., J. Amer. Chem. Soc. 98, 1828 (1976).

[356] Perry, R. A., Atkinson, R., and Pitts, J. N., Jr., J. Phys. Chem. 81, 296 (1977).

[357] Kenley, R. A., Davenport, J. E., and Hendry, D. G., J. Phys. Chem. 85, 2740 (1981).

[358] Tully, F. P., Ravishankara, A. R., Thompson, R. L., Nicovich, J. M., Shah, R. C., Kreutter, N. M., and Wine, P. H., J. Phys. Chem. 85, 2262 (1981).

[359] Nicovich, J. M., Thompson, R. L., and Ravishankara, A. R., J. Phys. Chem. 85, 2913 (1981).

[360] Atkinson, R., Carter, W. P. L., and Winer, A. M., J. Phys. Chem. 87, 1605 (1983).

[361] Grovenstein, E., Jr., and Mosher, A. J., J. Amer. Chem. Soc. 92, 3810 (1970).

[362] Ebata, T., Obi, K., and Tanaka, I., Chem. Phys. Lett. 77, 480 (1981).

[363] Nelson, H. H., and McDonald, J. R., J. Phys. Chem. 86. 1242 (1982).

[364] Hoshino, M., Akimoto, H., and Okuda, M., Bull. Chem. Soc. Japan 51, 718 (1978).

[365] Ohta, T., and Mizoguchi, I., Environ. Sci. Technol. 15, 1229 (1981).

[366] Benson, S. W., "Thermochemical Kinetics", 2nd ed., Wiley, New York, NY (1976).

[367] DeFrees, D. J., McIver, R. T., Jr., and Hehre, W. J., J. Amer. Chem. Soc. 102, 3334 (1980).

[368] Carter, W. P. L., Winer, A. M., and Pitts, J. N., Jr., Environ. Sci. Technol. 15, 829 (1981).

[369] DeMare, G. R., Fontaine, M. C., Huybrechts, G., and Termonia, M., J. Photochem. 1, 289 (1972/73).

[370] Yarwood, G. R., DeMore, W. B., and Termonia, M., 12th Informal Conf. on Photochem., Nat. Bur. Stand. Special Publication 526 (1978).

[371] Killus, J. P., and Whitten, G. Z., Atmos. Environ. 16, 1973 (1982).

[372] O'Brien, R. J., Green, P. J., Doty, R. A., Vanderzanden, J. W., Easton, R. R., and Irwin, R. P., in "Nitrogeneous Air Pollutants", D. Grosjean, ed., Ann Arbor Press, Ann Arbor, MI (1979).

[373] Takagi, H., Washida, N., Akimoto, H., Nagasawa, K., Usui, Y., and Okuda, M., J. Phys. Chem. 84, 478 (1980).

[374] Besemer, A. C., Atmos. Environ. 16, 1599 (1982).

[375] Takagi, H., Washida, N., Akimoto, H., and Okuda, M., Spectros. Lett. 15, 145 (1982).

[376] Nojima, K., Fukaya, K., Fukui, S., and Kanno, S., Chemosphere 5, 247 (1974).

[377] Perry, R. A., Atkinson, R., and Pitts, J. N., Jr., J. Phys. Chem. 81, 1607 (1977).

[378] Atkinson, R., Darnall, K. R., and Pitts, J. N., Jr., J. Phys. Chem. 82, 2759 (1978).

[379] O'Brien, R. J., Private Communication (1979).

[380] Kleindienst, T. E., Harris, G. W., and Pitts, J. N., Jr., Environ. Sci. Technol. 16, 844 (1982).

[381] Plum, C. N., Sanhueza, E., Atkinson, R., Carter, W. P. L., and Pitts, J. N., Jr., Environ. Sci. Technol. 17, 479 (1983).

[382] Osamura, Y., Schaefer, H. F., III, Dupruis, M., and Lester, W. A., Jr., J. Chem. Phys. 75, 5828 (1981).

[383] Gaffney, J. S., Atkinson, R., and Pitts, J. N., Jr., J. Amer. Chem. Soc. 97, 5049 (1975).

[384] Atkinson, R., Aschmann, S. M., and Pitts, J. N., Jr., Int. J. Chem. Kinet. 15, 75 (1983).

[385] Atkinson, R., Aschmann, S. M., Winer, A. M., and Pitts, J. N., Jr., Int. J. Chem. Kinet. 13, 1133 (1981).

[386] Hochanadel, C. J., Ghormley, J. A., Boyle, J. W., and Ogren, P. J., J. Phys. Chem. 81, 3 (1977).

[387] Parkes, D. A., Int. J. Chem. Kinet. 9, 451 (1977).

[388] Kan, C. S., McQuigg, R. D., Whitbeck, M. R., and Calvert, J. G., Int. J. Chem. Kinet. 11, 921 (1979).

[389] Sanhueza, E., Simonaitis, R., and Heicklen, J., Int. J. Chem. Kinet. 11, 907 (1979).

[390] Adachi, H., Basco, N., and James, D. G. L., Int. J. Chem. Kinet. 12, 949 (1980).

[391] Sander, S. P., and Watson, R. T., J. Phys. Chem. 85, 2960 (1981).

[392] Kan, C. S., and Calvert, J. G., Chem. Phys. Lett. 63, 111 (1979).

[393] Kan, C. S., Calvert, J. G., and Shaw, J. H., J. Phys. Chem. 84, 3411 (1980).

[394] Niki, H., Maker, P. D., Savage, C. M., and Breitenbach, L. P., J. Phys. Chem. 85, 877 (1981).

[395] Nangia, P. S., and Benson, S. W., Int. J. Chem. Kinet. 12, 43 (1980).

[396] Molina, M. J., and Arguello, G., Geophys. Res. Lett. 4, 580 (1979).

[397] Niki, H., Maker, P. D., Savage, C. M., and Breitenbach, L. P., J. Phys. Chem. 86, 3825 (1982).

[398] Adachi, H., Basco, N., and James, D. G. L., Int. J. Chem. Kinet. 11, 1211 (1979).

[399] Anastasi, C., Waddington, D. J., and Woolley, A., J. Chem. Soc. Faraday Trans. I 79, 505 (1983).

[400] Adachi, H., and Basco, N., Int. J. Chem. Kinet. 14, 1125 (1982).

[401] Kirsch, L. J., and Parkes, D. A. (1978) unpublished data cited in [189].

[402] Kirsch, L. J., Parkes, D. A., Waddington, D. J., and Woolley, A., J. Chem. Soc. Faraday Trans I 75, 2678 (1979).

[403] Cowley, L. T., Waddington, D. J., and Woolley, A., J. Chem. Soc. Faraday Trans I 78, 2535 (1982).

[404] Kirsch, L. J., and Parkes, D. A., J. Chem. Soc. Faraday Trans I 77, 293 (1981).

[405] Simonaitis, R., and Heicklen, J., J. Phys. Chem. 79, 298 (1975).

[406] Sander, S., and DeMore, W. B., Pacific Conf. on Chem. and Spectroscopy (1975).

[407] Atkinson, R., and Pitts, J. N., Jr., Int. J. Chem. Kinet. 10, 1081 (1978).

[408] Mulcahy, M. F. R., Steven, J. R., and Ward, J. C., J. Phys. Chem. 71, 2124 (1967).

[409] Astholz, D. C., Glanzer, K., and Troe, J., J. Chem. Phys. 70, 2409 (1979).

[410] Castleman, A. W., Jr., Davis, R. E., Munkelwitz, H. R., Tang, I. N., and Wood, W. P., Int. J. Chem. Kinet. Symp. 1, 629 (1975).

[411] Atkinson, R., Perry, R. A., and Pitts, J. N., Jr., J. Chem. Phys. 65, 306 (1976).

[412] Davis, D. D., Ravishankara, A. R., and Fischer, S., Geophys. Res. Lett. 6, 113 (1979).

[413] Harris, G. W., Atkinson, R., and Pitts, J. N., Jr., Chem. Phys. Lett. 69, 378 (1980).

[414] Wine, P. H., and Ravishankara, A. R., 2nd Symp. on the Composition of the Nonurban Troposphere, Williamsburg, VA (1982).

[415] Niki, H., Maker, P. D., Savage, C. M., and Breitenbach, L. P., J. Phys. Chem. 84, 14 (1980).

[416] Payne, W. A., Stief, L. J., and Davis, D. D., J. Amer. Chem. Soc. 95, 7614 (1973).

[417] Burrows, J. P., Cliff, D. I., Harris, G. W., Thrush, B. A., and Wilkinson, J. P. T., Proc. Roy. Soc. A368, 463 (1979).

[418] Graham, R. A., Winer, A. M., Atkinson, R., and Pitts, J. N., Jr., J. Phys. Chem. 83, 1563 (1979).

[419] Niki, H., (1979), p. 100 in [1].

[420] Benson, S. W., Chem. Rev. 78, 23 (1978).

[421] Whitbeck, M. R., Bottenheim, J. W., Levine, S. Z., and Calvert, J. G., (1978), in [314].

[422] Sander, S. P., and Watson, R. T., Chem. Phys. Lett. 77, 473 (1981).

[423] Kan, C. S., Calvert, J. G., and Shaw, J. H., J. Phys. Chem. 85, 1126 (1981).

[424] Daubendiek, R. L., and Calvert, J. G., Environ. Lett. 8, 103 (1975).

[425] "Chemical Kinetic and Photochemical Data for Use in Stratospheric Modeling", Evaluation No. 6, September 15 (1983), J. P. L. Publication 83-62.

[426] Kircher, C. C., Margitan, J. J., and Sander, S. P., J. Phys. Chem., in press (1984).

[427] Tuazon, E. C., Sanhueza, E., Atkinson, R., Carter, W. P. L., Winer, A. M., and Pitts, J. N., Jr., J. Phys. Chem., in press (1984).

[428] Paraskevopoulos, G., and Irwin, R. S., J. Chem. Phys., 80, 259 (1984).

[429] Niki, H., Maker, P. D., Savage, C. M., and Breitenbach, L. P., J. Phys. Chem., 88, 2116 (1984).

[430] Sander, S. P., and Peterson, M. E., J. Phys. Chem., in press (1984).

[431] Kircher, C. C., and Sander, S. P., J. Phys. Chem., 88, 2082 (1984).

[432] Atkinson, R., Aschmann, S. M., Carter, W. P. L., Winer, A. M., and Pitts, J. N., Jr., Int. J. Chem. Kinet., in press (1984).

[433] Hoyermann, K., and Sievert, R., Ber. Bunsenges Phys. Chem., 87, 1027 (1983).

[434] Bandow, H., Washida, N., and Akimoto, H., 11th Int. Conf. on Photochem., Univ. of Maryland, College Park, MD, August 21-26 (1983).

[435] Tuazon, E. C., Atkinson, R., Mac Leod, H., Biermann, H. W., Winer, A. M., Carter, W. P. L., and Pitts, J. N., Jr., Environ. Sci. Technol., submitted for publication (1984).

[436] Leone, J. A., and Seinfeld, J. H., Int. J. Chem. Kinet., 16, 159 (1984).

[437] Atkinson, R., Carter, W. P. L., Plum, C. N., Winer, A. M., and Pitts, J. N., Jr., Int. J. Chem. Kinet., in press (1984).

[438] Wine, P. H., Thompson, R. J., Ravishankara, A. R., Semmes, D. H., Gump, C. A., Torabi, A., and Nicovich, J. M., J. Phys. Chem., 88, 2095 (1984).

[439] Izumi, K., Mizuochi, M., Yoshioka, M., Murano, K., and Fukuyama, T., Environ. Sci. Technol., 18, 116 (1984).

[440] Stockwell, W. R., and Calvert, J. G., Atmos. Environ., 17, 2231 (1983).

11. ADDENDUM

Data obtained recently which cause changes in the recommendations or conclusions given in Sections 2-10 above are briefly discussed, by section number, below.

Section 2 - Inorganic Reactions

The 1982 NASA evaluation [3] has been superceded by the 1983 NASA evaluation [425]. For most of the reactions dealt with in Sections 2 and 3, the 1983 NASA evaluations [425] are identical to those in the 1982 evaluation [3]. Minor changes, not affecting the 298 K rate constants, occur for reactions (4), (17) and (34) [425]. However, more substantial changes occur for reactions (25) and (31). The latest literature data for these and other reactions are discussed below, and in fact the following discussion generally supercedes this latest NASA evaluation [425]

$$NO_2 + NO_3 \xrightarrow{M} N_2O_5 \qquad (7)$$

and

$$N_2O_5 \xrightarrow{M} NO_2 + NO_3 \qquad (8)$$

Kircher et al. [426] have determined, using a flash photolysis-ultraviolet absorption technique, rate constants for reaction (7) over the temperature and pressure ranges 236-358 K and 20-700 torr, respectively, for He and N_2 as the diluent gases.

The resulting data were fitted to the "fall-off" equation

$$k = \left\{ \frac{k_o(T)[M]}{1 + \frac{k_o(T)[M]}{k_\infty(T)}} \right\} F \left\{ 1 + \left[\frac{1}{N} \log\left(\frac{k_o(T)[M]}{k_\infty(T)} \right) \right]^2 \right\}^{-1} \qquad (I)$$

where $N = 0.75 - \log F$.

For $M=N_2$, and using a value of $F = 0.6$, values of

$$k_o(T) = 2.0 \times 10^{-30} (T/300)^{-4.3} \text{ cm}^6 \text{ molecule}^{-2} \text{ s}^{-1}$$

and

$$k_\infty(T) = 1.4 \times 10^{-12} (T/300)^{-0.5} \text{ cm}^3 \text{ molecule}^{-1} \text{ s}^{-1}$$

were obtained [426]. Making the reasonable assumption that O_2 and N_2 have the same third body efficiencies, then at 298 K and 760 torr total pressure of air,

$$k_7 = 1.2 \times 10^{-12} \text{ cm}^3 \text{ molecule}^{-1} \text{ s}^{-1}$$

a factor of ~1.2 higher than our recommendation in Section 2 based upon the evaluation of Malko and Troe [27]. We recommend the above expression derived by Kircher et al. [426].

Furthermore, based upon their data for k_7 and literature data for k_8 [25,26], Kircher et al. [426] derived the equilibrium constant

$$K_{8,7} = 3.17 \times 10^{29} T^{-1} e^{-11350/T} \text{ molecule cm}^{-3}$$

$$= 3.07 \times 10^{10} \text{ molecule cm}^{-3} \text{ at 298 K}$$

While this is in good agreement with

$$K_{8,7} = (2.91 \pm 0.69) \times 10^{10} \text{ molecule cm}^{-3}$$

determined directly by Tuazon et al. [427] at 298 K using long pathlength spectroscopic techniques, it is a factor of ~1.7 lower than those given by NASA [3,425] and Malko and Troe [27].

Obviously further experimental work on this reaction system is necessary before final recommendations can be made. This uncertainty in the equilibrium constant translates directly into added uncertainties in the NO_3 radical rate constants recommended in Sections 3, 4, 5, 6 and 8 above.

$$OH + CO \xrightarrow{O_2} HO_2 + CO \qquad (25)$$

The recent studies of Paraskevopoulos and Irwin [428] and Niki et al. [429] have shown that the rate constant k_{25} at 298 K and atmospheric pressure is ~20% lower than our recommendation. Paraskevopoulos and Irwin [428] used a flash photolysis-resonance absorption technique to determine rate constants k_{25} for $M=N_2$ over the pressure range 20-700 torr at 298 K, and derived

$$k_{25} = 1.50 \times 10^{13} \left(\frac{1 + 9.19 \times 10^{-4} P}{1 + 2.24 \times 10^{-4} P} \right) \text{ cm}^3 \text{ molecule}^{-1} \text{ s}^{-1} \text{ at 298 K,}$$

where P is the pressure of N_2 in torr. This expression is expected to be applicable to M=air, and yields

$$k_{25} = 2.18 \times 10^{-13} \text{ cm}^3 \text{ molecule}^{-1} \text{ s}^{-1}$$

at 760 torr of air and 298 K.

Niki et al. [429] have obtained rate constants for the reactions of OH radicals with $^{12}C^{18}O$ and $^{13}C^{16}O$ at 299 ± 2 K and 700 torr total pressure of air, relative to that for the reaction of OH radicals with ethene. Using our recommended rate constant for the reaction of OH radicals with ethene of 8.1×10^{-12} cm^3 molecule^{-1} s^{-1}, a value of

$$k_{25} = (2.24 \pm 0.13) \times 10^{-13} \text{ cm}^3 \text{ molecule}^{-1} \text{ s}^{-1}$$

is derived, in excellent agreement with the data of Paraskevopoulos and Irwin [426]. Hence we recommend the use of the expression of Paraskevopoulos and Irwin [428] given above, resulting in

$$k_{25} = 2.2 \times 10^{-13} \text{ cm}^3 \text{ molecule}^{-1} \text{ s}^{-1} \text{ at}$$

298 K and 760 torr total pressure of air.

$$\underline{HO_2 + NO_2} \xrightarrow{M} \underline{HO_2NO_2} \qquad (28)$$

Sander and Peterson [430] have determined, using a flash photolysis-ultraviolet absorption technique, rate constants for reaction (28) over the pressure and temperature ranges 50-700 torr and 229-362 K, respectively, for M=He, N_2 and O_2. The data obtained were fitted to the fall-off equation (I) given above.

For $M=N_2$, values of

$$F = 0.56$$

$$k_o(T) = 2.3 \times 10^{-31}(T/300)^{-4.6} \text{ cm}^6 \text{ molecule}^{-2} \text{ s}^{-1}$$

and

$$k_\infty(T) = 4.2 \times 10^{-12}(T/300)^{0.2} \text{ cm}^3 \text{ molecule}^{-1} \text{ s}^{-1}$$

were derived. Since essentially identical rate constants were obtained for $M=N_2$ and $M=O_2$ [430], this yields

$$k_{28} = 1.4 \times 10^{-12} \text{ cm}^3 \text{ molecule}^{-1} \text{ s}^{-1}$$

at 298 K and 760 torr of air.

These values of $k_o(T)$ and $k_\infty(T)$ are identical to those recommended by the 1982 and 1983 NASA evaluations [3,425], and we now recommend the use of this fall-off expression. In addition, an effect of H_2O vapor, separate from its effect as a purely third body, has been observed [430], and reference 430 should be consulted for further details.

$$\underline{HO_2 + HO_2} \rightarrow \underline{H_2O_2 + O_2} \qquad (31)$$

and

$$\underline{HO_2 + HO_2 + H_2O} \rightarrow \underline{H_2O_2 + O_2 + H_2O} \qquad (32)$$

Kircher and Sander [431] have determined, again using a flash photolysis-ultraviolet absorption technique, rate constants for the combination of HO_2 radicals. For $M=N_2$ data were obtained over the pressure and temperature ranges 100-700 torr and 241-417 K, respectively, and also in the presence of water vapor. The rate constant data obtained were fit by the expression

$$k_{(31+32)} = [2.2 \times 10^{-13} e^{620/T} + 1.9 \times 10^{-33} [M] e^{980/T}] \times [1 + 1.4 \times 10^{-21} [H_2O] e^{2200/T}] \text{ cm}^3 \text{ molecule}^{-1} \text{ s}^{-1}$$

where the second term is due to the effect of water vapor on the $HO_2 + HO_2$ reaction. Since the third body efficiencies of N_2 and O_2 are expected to be essentially identical, this expression is applicable to M=air. The rate constants k_{31} obtained at room temperature [431] in the absence of water vapor are in excellent agreement with previous literature data [92-95], and we recommend the use of the above expression for the combination of HO_2 radicals under atmospheric conditions.

Section 3

$$\underline{HO_2 + HCHO} \rightleftarrows \underline{HOOCH_2O} \rightleftarrows \underline{OOCH_2OH} \qquad (39,-39)$$

While the experimental data of Su et al. [125, 126] indicates that O_2CH_2OH can thermally decompose back to the reactants, this reaction (-39) appears unlikely on thermochemical grounds. Thus O_2CH_2OH is calculated to be ~17 kcal mol^{-1} more stable than $HOOCH_2O$ [366], and a barrier height of ≳6 kcal mol^{-1} is anticipated for the isomerization of $HOOCH_2O$ to $OOCH_2OH$ [224,269]. This leads to a minimum activation energy of ~23 kcal mol^{-1} for isomerization of thermalized $OOCH_2OH$ to $HOOCH_2O$, resulting in a $OOCH_2OH$ lifetime of ~2 x 10^3 sec with respect to this isomerization at 298 K. Obviously further experimental data on the HO_2 + HCHO reaction system are required before firm recommendations concerning reaction (39) and the subsequent fates of the $OOCH_2OH$ radical can be made.

Section 4

$$\underline{RO_2 + NO} \xrightarrow{M} \underline{RONO_2} \qquad (50a)$$

Further studies of alkyl nitrate formation from the reaction of alkyl peroxy radicals with NO have been carried out by Atkinson et al. [432] for a series of branched and cyclic alkyl peroxy radicals. The rate constant ratios $k_a/(k_a + k_b)$, where k_a and k_b are the rate constants for the reactions,

$$RO_2 + NO \xrightarrow{M} RONO_2 \qquad (a)$$

$$\rightarrow RO + NO_2 \qquad (b)$$

are summarized in table 36 for the individual RO_2 radicals involved. This table also contains the data for the individual C_2-C_8 alkyl peroxy radicals previously studied [170,172].

It can be seen that for the secondary alkyl peroxy radicals these rate constant ratios increase monotonically with the carbon number of the RO_2 radical (from ~0.04 for C_3 to ~0.33 for C_8), and to a first approximation are reasonably constant for a given set of alkyl peroxy radicals of the same carbon number. This is most apparent for the secondary C_6 alkyl peroxy radicals generated from n-hexane, cyclohexane, 2-methylpentane and 3-methylpentane, for which the rate constant ratios $k_a/(k_a + k_b)$ range from 0.14 to 0.22. However, there do appear to be differences in the $k_a/(k_a + k_b)$ ratios within these various secondary C_6 alkyl peroxy radicals, with the most branched radicals having the lower rate constant ratios.

It is also apparent, as concluded previously [170], that the rate constant ratios for primary alkyl peroxy radicals are at least a factor of 2 lower than those for secondary alkyl peroxy radicals of the same carbon number (compare the rate constant ratios for 1-propyl peroxy vs that for 2-propyl peroxy, and that for neopentyl peroxy vs those for the secondary C_5 alkyl peroxy radicals). In a similar manner the rate constant ratios $k_a/(k_a + k_b)$ for tertiary alkyl peroxy radicals are also markedly lower, by factors of ~3-5, than those for the corresponding secondary alkyl peroxy radicals.

While the reasons for these differences in the rate constant ratios $k_a/(k_a + k_b)$ for primary, secondary and tertiary alkyl peroxy radicals of the same carbon number are not yet known, the data given in table 36, together with the fall-off expression given in Section 4 (which is now seen to be applicable to secondary alkyl peroxy radicals), allow approximate a-priori estimates to be made for alkyl nitrate formation yields from the various alkyl peroxy radicals involved in alkane degradation pathways under atmospheric conditions.

Section 5

$OH + 1\text{-butene} \rightarrow \text{products}$ (63)

Hoyerman and Sievert [433], using a discharge flow system with mass spectrometric detection, have investigated the mechanisms for the reactions of OH radicals with a series of butenes at 0.9-10 torr total pressure and 295-298 K. In contradiction to the results of Biermann et al. [264], the amount of H-atom abstraction from 1-butene was determined to be <10%, i.e., $k_{63a}/k_{63} < 0.10$. Confirmation that reaction k_{63a} is negligible further arises from product studies carried out at atmospheric pressure using FT-IR absorption spectroscopy and gas chromatography (Atkinson, R., Tuazon, E. C., and Carter, W. P. L., unpublished data, 1984).

Based on these data, we now recommend that H-atom abstraction from 1-butene (and, by analogy, from other alkenes with $\geq C_2$ side chains) by OH radicals be neglected.

Section 8

α-Dicarbonyl Yields from Aromatic Hydrocarbons

Two recent product studies using long path-length spectroscopic techniques [434,435] have determined the yields of α-dicarbonyls from a series of aromatic hydrocarbons at room temperature and atmospheric pressure.

Bandow et al. [434] studied the aromatic hydrocarbons benzene, toluene, the xylenes and the trimethylbenzenes, while Tuazon et al. [435] have investigated toluene and m- and p-xylene. In all cases the sum of the α-dicarbonyl yields are significantly less than unity [434,435]. The data obtained by both groups for toluene and m- and p-xylene are given in table 37. These yields are in good agreement, with the only significant discrepancy being that for the methylglyoxal yield from m-xylene. Clearly, these data define reasonably closely the yields of these α-dicarbonyls from these three aromatic hydrocarbons.

As discussed in Section 8, for toluene the abstraction pathway accounts for ~8% of the overall OH radical reaction [360], and cresol formation accounts for ~16 ± 8% of the overall reaction [360]. Hence, the inclusion of reaction pathways resulting in the formation of ~28% of glyoxal and methylglyoxal [together with the corresponding co-products] account for only ~50 (±15)% of the overall reaction pathways. Clearly, the products and mechanisms of a major portion of the OH-aromatic reactions under atmospheric conditions are presently not identified.

These data obviously have major implications for the validity and predictions of present chemical kinetic computer models of aromatic hydrocarbons, since these chemical computer models [11,371,436] assume that the reactions subsequent to reaction (92) yield exclusively α-dicarbonyls (together with the corresponding co-products). Further studies are urgently needed to identify the remaining products and reaction pathways involved under atmospheric conditions following the initial OH radical reaction with the aromatic hydrocarbons.

$NO_3 + \text{Cresols} \rightarrow \text{products}$ (95)

Atkinson et al. [437] have recently determined rate constants k_{95} for the reactions of the NO_3 radical with phenol and the three cresol isomers. Using the equilibrium constant $K_{7,8}$ of Malko and Troe [27] (which is uncertain to at least a factor of ~2 [427]) rate constants k_{95} at 296 ± 2 K and atmospheric pressure of:

$$k_{95}\ (\text{phenol}) = (2.1 \pm 0.5) \times 10^{-12}\ \text{cm}^3\ \text{molecule}^{-1}\ \text{s}^{-1}$$

$$k_{95}\ (\text{o-cresol}) = (1.20 \pm 0.34) \times 10^{-11}\ \text{cm}^3\ \text{molecule}^{-1}\ \text{s}^{-1}$$

$$k_{95}\ (\text{m-cresol}) = (9.2 \pm 2.4) \times 10^{-12}\ \text{cm}^3\ \text{molecule}^{-1}\ \text{s}^{-1}$$

Table 36. Rate Constant Ratios $k_a/(k_a + k_b)$ for the Reaction of Individual Alkyl Peroxy (RO_2) Radicals with NO at 299 ± 2 K and 735-740 Torr Total Pressure

	Primary		Secondary		Tertiary	
Alkane	RO_2	$k_a/(k_a + k_b)$	RO_2	$k_a/(k_a + k_b)$	RO_2	$k_a/(k_a + k_b)$
Ethane	ethyl	≤0.014				
Propane	1-propyl	0.020±0.009	2-propyl	0.043±0.003	-	-
n-Butane	1-butyl	≤0.040	2-butyl	0.090±0.009	-	-
n-Pentane	-		2-pentyl	0.129±0.014	-	-
			3-pentyl	0.118±0.014	-	-
Neopentane	neopentyl	0.0513±0.0053				
2-Methylbutane			2-methyl-3-butyl	0.109±0.003	2-methyl-2-butyl	0.0533±0.0022
n-Hexane			2-hexyl	0.220±0.034		
			3-hexyl	0.219±0.029		
Cyclohexane			cyclohexyl	0.160±0.015		
2-Methylpentane			2-methyl-3-pentyl +2-methyl-4-pentyl	0.165±0.016	2-methyl-2-pentyl	0.0350±0.0096
3-Methylpentane			3-methyl-2-pentyl	0.140±0.014		
n-Heptane			2-heptyl	0.324±0.044		
			3-heptyl	0.312±0.041		
			4-heptyl	0.290±0.037		
n-Octane			2-octyl	0.353±0.027		
			3-octyl	0.343±0.031		
			4-octyl	0.324±0.032		

Table 37. Glyoxal and Methylglyoxal Yields from the NO_x-Air Photooxidations of Toluene, m-Xylene and p-Xylene at Room Temperature and Atmospheric Pressure

	Yield[a]			
	Glyoxal		Methylglyoxal	
Aromatic Hydrocarbon	Bandow et al. [434]	Tuazon et al. [435]	Bandow et al. [434]	Tuazon et al. [435]
Toluene	0.15 ± 0.04	0.173 ± 0.029	0.14 ± 0.04	0.105 ± 0.016
m-Xylene	0.13 ± 0.03	0.104 ± 0.020	0.42 ± 0.05	0.265 ± 0.035
p-Xylene	0.24 ± 0.02	0.200 ± 0.032	0.12 ± 0.02	0.178 ± 0.021

[a]The indicated errors are two least squares standard deviations.

and

$$k_{95}\ (p\text{-cresol}) = (1.27 \pm 0.36) \times 10^{-11}\ cm^3\ molecule^{-1}\ s^{-1}$$

were obtained. We recommend that these rate constants supersede those given in Section 8 above, and that the error limits should be realistically judged (in view of the uncertainties in $K_{7,8}$) to be a factor of ~3. Similar error limits should apply to all NO_3 radical reaction rate constants given in Sections 3, 4, 5, 6 and 8.

Section 10

$$OH + SO_2 \xrightarrow{M} HSO_3 \qquad (117)$$

The study of Wine et al. [438] concerning the kinetics of this reaction has recently been published (their preliminary data [414] were discussed in Section 10). Rate constants k_{117} were determined for M=He, Ar, N_2 and SF_6 over the temperature and pressure ranges 260-420 K and 13-696 torr total pressure, respectively. Fitting the data for M=N_2 to the equation

$$k_{117} = \left(\frac{k_o(T)[M]}{1 + \frac{k_o(T)[M]}{k_\infty(T)}}\right) F^{\left\{1 + \left[\log\left(k_o(T)[M]/k_\infty(T)\right)\right]^2\right\}^{-1}}$$

with F held constant led to

$$F = 0.525$$

$$k_o(T) = 4.5 \times 10^{-31}(T/300)^{-3.9}\ cm^6\ molecule^{-2}\ s^{-1}$$

$$k_\infty(T) = 1.26 \times 10^{-12}(T/300)^{-0.7}\ cm^3\ molecule^{-1}\ s^{-1}$$

This yields (assuming, as expected, that N_2 and O_2 have essentially identical third body efficiencies)

$$k_{117} = 8.1 \times 10^{-13}\ cm^3\ molecule^{-1}\ s^{-1}$$

at 298 K and 760 torr of air, identical to the value given by [414] and used in Section 10.

Another recent study [439] has determined a rate constant for reaction (117) relative to that for the reaction of OH radicals with n-butane [reaction (77)] at 303 ± 1 K and 780-820 torr total pressure of air. Using our recommended rate constant for k_{77} (n-butane) of 2.66×10^{-12} cm^3 $molecule^{-1}$ s^{-1} at 303 K, a value of

$$k_{117} = (1.16 \pm 0.06) \times 10^{-12}\ cm^3\ molecule^{-1}\ s^{-1}$$

is derived, in good agreement with the other recent data discussed in Section 10. Thus we do not change our recommendation for k_{117} at 298 K and 760 torr of air as given in Section 10. For temperatures and pressures other than 298 K and 760 torr, we recommend the use of the fall-off equation of Wine et al. [438] given above.

Stockwell and Calvert [440] have shown from kinetic studies of reaction (117), using long path-length FT-IR spectroscopy to monitor the reactants and products in irradiated HONO-CO-SO_2-NO_x-O_2-N_2 mixtures, that the OH radical reaction with SO_2 leads to chain propagation. Stockwell and Calvert [440] conclude that the reaction proceeds via:

$$OH + SO_2 \xrightarrow{M} HSO_3$$

$$HSO_3 + O_2 \rightarrow SO_3 + HO_2$$

followed by hydration of SO_3 [reaction (116)] to ultimately form H_2SO_4.

Hence this reaction sequence can be considered for computer modeling purposes as a single step:

$$OH + SO_2 \xrightarrow{O_2,\ H_2O} H_2SO_4 + HO_2$$